Dynamique de l'albédo de surface et bénéfice climatique de l'agriculture de conservation au Zimbabwe sub-humide

Souleymane Diop

THÈSE DE DOCTORAT

NNT : 2024UPASB066

université PARIS-SACLAY

Impact of albedo change on the climate benefit of conservation agriculture in sub-humid Zimbabwe

Dynamique de l'albédo de surface et bénéfice climatique de l'agriculture de conservation au Zimbabwe sub-humide

Thèse de doctorat de l'université Paris-Saclay

École doctorale n°581, Agriculture, Alimentation, Biologie, Environnement, Santé (ABIES)
Spécialité de doctorat : Sciences de l'environnement
Graduate School : Biosphera. Référent : AgroParisTech

Thèse préparée dans l'UMR **ECOSYS** (Université Paris-Saclay, INRAE, AgroParisTech), sous la direction de **Eric CESCHIA**, Directeur de recherche, la co-direction de **Rémi CARDINAEL**, Chercheur (HDR) et le co-encadrement de **Ronny LAUERWALD**, Chercheur

Thèse soutenue à Paris-Saclay, le 28 novembre 2024, par

Souleymane DIOP

Composition du Jury

Membres du jury avec voix délibérative

Claire CHENU Professeure, AgroParisTech (Université Paris-Saclay)	Présidente
Dominique CARRER Ingénieur divisionnaire (HDR), Météo-France (Université de Toulouse)	Rapporteur & Examinateur
Bernard LONGDOZ Professeur, Université de Liège (Belgique)	Rapporteur & Examinateur
Philippe PEYLIN Directeur de recherche, CNRS (Université Paris-Saclay)	Examinateur

université PARIS-SACLAY
ÉCOLE DOCTORALE
Agriculture, alimentation, biologie, environnement, santé (ABIES)

Titre : Dynamique de l'albédo de surface et bénéfice climatique de l'agriculture de conservation au Zimbabwe sub-humide

Mots clés : atténuation du changement climatique, effets biogéophysiques, effets biogéochimiques, Afrique subsaharienne, modélisation, agroécologie

Résumé : L'agriculture de conservation (AC) est une des solutions basées sur la nature offrant des perspectives intéressantes en termes de leviers d'atténuation et de stratégies d'adaptation au changement climatique. En Afrique subsaharienne, les études des potentiels d'atténuation des changements climatiques par l'AC se concentrent sur les effets biogéochimiques (stockage C, emissions de GES) tandis que les effets biogéophysiques (effets albédo, flux d'énergie) sont souvent ignorés. Dans ce contexte, il est très pertinent d'approfondir les effets de l'AC sur les contributions biogéophysiques de l'agriculture sur le climat afin d'identifier les potentiels leviers d'atténuation associés aux changements de pratiques et les possibles synergies avec les effets biogéochimiques. Nous avons mené des études de quantification des effets biogéophysiques à travers des mesures d'albédo de surface, de rayonnement thermique, de température de surface, de contenu en eau dans le sol, et de dynamiques de croissance des cultures durant deux années culturales au Zimbabwe sur deux types de sol contrasté : un Lixisol abruptique sableux et clair et un Ferralsol xanthique argileux et sombre. Trois pratiques culturales sont comparées dans cette études : le labour conventionnel (CT, pour Conventional Tillage en anglais), la suppression du labour (NT pour No-Tillage en anglais) et le maintien des résidus en surface (NTM pour No-Tillage with Mulch en anglais). Les résultats ont montré une augmentation d'albédo de surface suite à l'adoption de la pratique du NT comparé au CT quel que soit le type de sol. L'apport des résidus de culture en surface comparé au CT à des effets contrasté suivant les types de sol. En effet, les résidus contribuent à une augmentation de l'albédo de surface sur les sols argileux sombres et contribuent à sa diminution sur les sols sableux clairs. Ces changements d'albédo ont entraîné des forçages radiatifs négatifs associés à un effet refroidissant sur le climat du NT quel que soit le type de sol et des effets contrastés pour le NTM, avec un effet refroidissant sur les sols argileux foncés et un effet réchauffant sur les sols sableux clairs. Nous avons comparé ces forçages radiatifs induits par l'albédo de surface aux effets biogéochimiques du stockage de carbone (C) et des émissions de N_2O induits par ces mêmes pratiques. Les résultats obtenus ont montré que sur 30 ans de pratique d'AC, les changements d'albédo liés aux pratiques NT et NTM ont des effets climatiques allant de -1,27 à +1,15 t CO_2-éq ha^{-1} an^{-1}, comparables au potentiel de stockage de carbone dans les sols en Afrique subsaharienne. Sur les sols argileux sombres, ces pratiques renforcent l'effet de refroidissement, tandis que sur les sols sableux clairs, elles entraînent un effet réchauffant à court terme, annulant les bénéfices climatiques du C stocké à long terme. Pour mieux comprendre les déterminants des dynamiques d'albédo et être en capacité à les simuler en fonction des pratiques, le modèle STICS a été utilisé, révélant des limites dans la prise en compte de l'effet des tissus sénescents et de l'humidité de surface sur les dynamiques de l'albédo de surface. De nouveaux formalismes ont ensuite été proposés et testés, ce qui a permis d'améliorer les simulations de l'albédo de surface. Cette étude met en avant l'importance d'intégrer les effets biogéophysiques et biogéochimiques pour mieux évaluer les impacts climatiques des pratiques agricoles et optimiser les mesures d'adaptation et d'atténuation.

ÉCOLE DOCTORALE
Agriculture, alimentation, biologie, environnement, santé (ABIES)

Title: Impact of albedo change on the climate benefit of conservation agriculture in sub-humid Zimbabwe

Keywords: albedo, biogeophysical effects, biogeochemical effects, Sub-Saharan Africa, modelling, agroecology

Abstract: In Sub-Saharan Africa, studies of potential climate change mitigation levers by CA focus more on biogeochemical effects (C storage, GHG emissions) while biogeophysical effects (albedo effects, energy fluxes) are often ignored. In this context, it is very relevant to delve into the effects of CA on agriculture's biogeophysical contributions to climate in order to identify potential mitigation levers associated with changes in practices and possible synergies with the biogeochemical effects. We conducted studies to quantify the biogeophysical effects through measurements of surface albedo, heat radiation, surface temperature, water content in soil, and dynamics of crop growth during two growing years in Zimbabwe on two types of contrasting soil: a sandy, light-coloured abruptic Lixisol and a clayey, dark-coloured xanthic Ferralsol. Three cropping practices are compared in this study: conventional tillage (CT), no-tillage (NT) and no-tillage with mulch (NTM). The results showed an increase in surface albedo following the adoption of NT practice compared to CT regardless of soil type. The contribution of crop residues to surface albedo compared with CT lead to contrasting effects according to soil types. Indeed, the residues contribute to an increase in surface albedo on dark clay soils and contribute to its decrease on light sandy soils. These albedo changes have led to negative radiative forcing associated with a cooling climatic effect on the NT regardless of soil type and contrasting effects for the NTM, with a cooling effect on dark clay soils and a warming effect on light sandy soils. We compared these surface albedo-induced radiative forcings with the biogeochemical effects of carbon (C) storage and N_2O emissions induced by these same practices. The results obtained showed that over 30 years of CA practice, albedo changes related to NT and NTM practices have climatic effects ranging from -1.27 to +1.15 t CO_2-eq ha^{-1} $year^{-1}$, comparable to the potential for carbon storage in soils in Sub-Saharan Africa. On dark clay soils, these practices enhance the cooling effect, while on light sandy soils, they cause a warming effect in the short term, negating the climate benefits of long-term stored C. To better understand the determinants of albedo dynamics and to be able to simulate them according to practices, the STICS model was used, revealing limitations in the consideration of the effect of senescent tissues and surface moisture on the dynamics of surface albedo. New formalisms were then proposed and tested, which allowed to improve the simulations of the surface albedo. This study highlights the importance of integrating biogeophysical and biogeochemical effects to better assess climate impacts of agricultural practices and optimize adaptation and mitigation measures.

Remerciements

Une thèse est loin d'être un accomplissement individuel. Elle est faite de rencontres, d'expériences, de vécus, de découvertes et de collaborations. Au cours de ces années, j'ai croisé des personnes, des cultures, des usages et des coutumes diverses, ainsi que des idées qui se complètent, se renforcent ou parfois s'opposent. Durant ces trois années, j'ai eu l'opportunité de me former, de m'améliorer, et d'apprendre des choses que je ne saurais résumer en quelques mots. Cette "fin", qui n'en est pas vraiment une, marque le début d'un nouveau chapitre, rempli de défis, de nouvelles thématiques de recherche et d'autres perspectives à explorer.

À travers ces quelques lignes, je tiens à remercier toutes les personnes qui ont contribué à l'aboutissement de ce travail.

Tout d'abord, je remercie les membres du jury d'avoir accepté d'évaluer ce travail, malgré leurs emplois du temps chargés. Un immense merci aux rapporteurs **Dominique Carrer** et **Bernard Longdoz**, ainsi qu'à **Claire Chenu** et **Philippe Peylin**, pour avoir accepté d'examiner ce travail.

Ce travail n'aurait pu être réalisé sans l'appui exceptionnel de l'encadrement dont j'ai eu la chance de bénéficier pendant 36 mois. À cet égard, je remercie du fond du cœur **Eric Ceschia**, qui a dirigé brillamment ces travaux de thèse. Tout a commencé au CESBIO, lors de mon stage de Master 2. Malgré les conditions difficiles liées à la pandémie, Eric s'est toujours montré disponible. Il m'a pris sous son aile et m'a transmis la passion pour la recherche dans le domaine de la télédétection et de la modélisation. Au-delà de la transmission des connaissances scientifiques, il m'a inculqué des valeurs humaines telles que la générosité et la bienveillance, faisant de lui un modèle inspirant pour moi.

Je remercie également du fond du cœur **Rémi Cardinael**, co-directeur de cette thèse, pour tout ce qu'il m'a apporté durant ces trois années. Rémi m'a formé aux travaux de terrain et, à ses côtés, j'ai acquis de solides bases en collecte de données, analyse et suivi d'expérimentations sur le terrain. Il m'a également transmis des valeurs d'éthique et d'intégrité scientifique, le goût des grandes questions, et l'esprit du "plus ultra" 😉. Au-delà

de la recherche scientifique, merci pour tes valeurs humaines et pour la belle personne que tu es. Si aujourd'hui j'en suis là, c'est en grande partie grâce à toi ; tu es une source d'inspiration et de motivation pour les jeunes chercheurs.

Un immense merci à **Ronny Lauerwald**, co-encadrant de cette thèse, pour tout ce qu'il m'a appris. Ronny m'a permis de découvrir l'univers du modèle ORCHIDEE. Il m'a formé à son utilisation avec une grande rigueur. Sa patience et son "zen attitude" en toutes circonstances m'ont profondément marqué. Merci pour l'accueil au sein de l'unité ECOSYS, de l'encadrement dont j'ai pu bénéficier les dépannages en cas de blocages et les discussions toujours intéressantes sur beaucoup de sujets.

Un grand merci à **Morgan Ferlicoq** pour la mise en place du dispositif expérimental au Zimbabwe. Merci pour sa disponibilité le long de la thèse, les dépannages à distance à multi-reprises s'agissant du plan de câblage ou de la perturbation du signal des capteurs.

Un grand merci à toute l'équipe du CIRAD AIDA au Zimbabwe, pour les deux années passées sur le terrain. Merci aux chauffeurs, **Ngoni Chiweshe** et **Danmore Kativhu**, qui m'ont accompagné chaque fois que j'en avais besoin, ainsi qu'aux assistantes administratives, **Letween Mutasa** et **Yvonne Muambe**.

Merci à **Régis Chikowo** de l'Université du Zimbabwé, aux techniciens notamment à **M. Pari**, pour la pesée des échantillons de sol, de plantes et de paillis, ainsi qu'à l'ensemble des techniciens du CIMMYT, à Mazowe et Domboshawa, pour leur aide sur le terrain.

Un grand merci à **Petra Sieber** pour sa contribution et ses orientations sur l'utilisation des métriques climatiques, ses explications très claires sur la comparaison des effets biogéophysiques et biogéochimiques me sont particulièrement d'une grande aide au cours de cette thèse.

Je tiens également à remercier **Gatien Falconnier** et **Antoine Couëdel** pour la formation à la calibration du modèle STICS, ainsi que pour ses conseils avisés et ses contributions constructives lors des exercices de modélisation. Un grand merci à **François Affholder** pour son soutien tout au long de ces exercices, mais aussi pour m'avoir offert le livre d'Alan F.

Chalmers, ***"Qu'est-ce que la science ?"***, qui m'a grandement aidé à développer ma réflexion et à prendre du recul dans mon travail.

Merci à la famille **Prêt** — **Valentin, Mathilde** et **Sacha** — avec qui j'ai passé de très bons moments lors de mes travaux de terrain. Depuis, ils sont devenus des amis chers. Merci pour ma première randonnée, mon premier camping et ma première balade à cheval ; ce sont des souvenirs que je chéris profondément.

Un grand merci à mon collègue et colocataire, **Abderrahim Bouhenache**, excellent cuisinier et passionné de terrain. Merci pour ton soutien et pour nos soirées de discussions, principalement autour de nos thèses et, bien sûr, du football.

Je remercie également mes collègues de bureau du CIRAD au Zimbabwe, **Amandine Belard**, **Oriane Ploquin**, **Adrien Coquereau** et **Rejoice Nyoni**, pour leur gentillesse.

Un grand merci à toute l'UMR ECOSYS — chercheurs, doctorants et post-doctorants de l'unité — pour l'accueil chaleureux, les échanges fructueux et le soutien mutuel durant ces trois années. Merci à tous les collègues avec qui j'ai passé de bons moments au labo et avec qui j'ai apprécié échanger : **Yang Liu, Manuella, Bo, Frédéric, Yongping, Tristan, Shuaishuai, Siwar, Xianglin, Emilio, Solène, Pédro, Laura, Mohsen, Florent, Malick, Lan Anh.**

Merci infiniment à **Patrice Lecharpentier** pour la formation sur l'utilisation des branches de STICS pour le développement, ainsi qu'à toute l'équipe STICS qui m'a permis de travailler sur une branche du modèle.

Merci aux **"Gentlemen Lémuriens"**, une seconde famille pour moi, pour les moments où j'ai pu me confier et pour leurs encouragements.

L'individu n'est rien sans le groupe auquel il appartient. C'est pourquoi je remercie tous les membres de ma famille qui ont suivi de loin l'avancée de mes travaux, même s'ils ne comprenaient pas toujours ce que je faisais.

Enfin, je tiens à remercier ma douce chérie, **Rama Ndiaye**. Ce fut également une épreuve

pour elle, entre mes plaintes, mes sautes d'humeur et mes absences prolongées, parfois durant plusieurs mois. Merci de rester à mes côtés, de m'encourager à donner le meilleur de moi-même durant cette thèse. Je t'en serai éternellement reconnaissant. Merci pour tout ton soutien et ton amour.

Cette thèse a été financée par l'Union Européenne via le projet "The Resilience Building through Agroecological Intensification in Zimbabwe" (RAIZ, FOOD/2021/424-933, https://raiz.org.zw/) et par l'Institut de Convergence CLAND avec les contributions de l'Agence Nationale de la Recherche (ANR) à travers la subvention ANR-16-CT-0003. D'autres projets ont également permis d'acheter de l'équipement scientifique utilisé dans le cadre de la thèse, notamment à travers le projet Albedo, Conservation agriCUltuRe and climATe bEnefit (ACCURATE) financé par le Centre International Maize and Wheat Improvement Center (CIMMYT) et le programme MAIZE du CGIAR (www.maize.org), et par le CIRAD à travers le projet "aLbedo chANge and Climate bEnefit in Land-based mitigatiOn pracTices" (LANCELOT).

"*The life of the individual has meaning only in so far as it aids in making the life of every living thing nobler and more beautiful*" Albert Einstein

Valorisations

Publications (publiés)

Diop, S. Four-component net radiometers to quantify albedo and heat fluxes in conservation agriculture. Nature Reviews Earth & Environment 4, 678 (2023). https://doi.org/10.1038/s43017-023-00432-x

Publications (en cours)

Diop, S., Cardinael, R., Lauerwald, R., Ferlicoq, M., Thierfelder, C., Chikowo, R., Corbeels, M., Affholder, F., Baudron, F., Ceschia, E. Surface albedo and thermal radiation dynamics under conservation and conventional agriculture from two contrasting soils in sub-humid Zimbabwe. Under review.

Diop, S., Cardinael, R., Lauerwald, R., Sieber, P., Thierfelder, C., Chikowo, R., Corbeels, M., Ceschia, E. Balancing biogeochemical gains and surface albedo shifts: climate impacts of no-tillage and mulching in Southern Africa. In preparation.

Diop, S., Cardinael, R., Falconnier, G., Lauerwald, R., Felicoq, M., Thierfelder, C., Affholder, F., Chikowo, Regis., Ceschia, E. Simulating surface albedo dynamics under conservation agriculture using the STICS soil-crop model – Application to two Sub-Saharan sites. In preparation.

Communications

Diop, S., Cardinael, R., Lauerwald, R., Ferlicoq, M., Thierfelder, C., Chikowo, R., Corbeels, M., and Ceschia, E. Interaction between soil type and cropping system on albedo dynamics leads to contrasted impact on climate mitigation, EGU General Assembly 2024, Vienna, Austria, 14–19 April 2024, EGU24-6466, https://doi.org/10.5194/egusphere-egu24-6466, 2024.

Diop, S., Cardinael, R., Falconnier, G., Lauerwald, R., Felicoq, M., Thierfelder, C., Affholder, F., Chikowo, Regis., Ceschia, E. Modelling albedo and the energy budget using the STICS soil-crop model-Application to two Sub-Saharan sites.XIII STICS seminar, November 2023 INRAE, Latresnes, France.

Diop, S., Cardinael, R., Lauerwald, R., Ferlicoq, M., Thierfelder, C., Chikowo, R., Corbeels, M., and Ceschia, E. Climatic effect of no-tillage and mulch due to albedo change differs with soil type: a field study in Zimbabwe. Long Term Experiments: Meeting Future Challenges, June 2023, Rothamsted, United Kingdom.

Table des matières

Remerciements **1**

Table des matières **6**

Introduction générale **1**

1. Contexte 1

1.1 Le changement climatique 1

1.2 L'agriculture de conservation (AC) 5

1.3 Les effets climatiques de l'agriculture de conservation (AC) 6

2. Les effets biogéophysiques 8

2.1 Le bilan radiatif de la Terre 8

2.2 Le bilan d'énergie de la Terre 9

2.3 L'albédo de surface ($\boldsymbol{\alpha}$) 10

2.4 La notion de forçage radiatif 12

2.4.1 Forçage radiatif dû à la modification d'albédo de surface 12

2.4.2 Conversion RFα en équivalent CO2 14

2.5 Modélisation de l'albédo de surface 16

3. Justifications scientifiques et questions de recherches 18

Matériels et méthodes **21**

1. Description des sites 21

2. Mesure de la dynamique de la végétation 22

2.1 Dynamique d'indice foliaire (LAI) 22

2.2 Taux de couverture (GFCC) 23

3. Mesure des variables météorologiques 25

3.1 Mesure du rayonnement courtes et longues longueurs d'ondes 25

4. Approche de modélisation 26

4.1 Pourquoi STICS et quelles attentes ? 27

Chapitre I : Albédo de surface et rayonnement thermique en agriculture de conservation **29**

Résumé en français : **29**

Surface albedo and thermal radiation dynamics under conservation and conventional agriculture in subhumid Zimbabwe **31**

Abstract **31**

1. Introduction 33

2. Materials and methods 35
2.1 Experimental sites 35
2.2 Experimental treatments 37
2.3 Field measurements 38
2.3.1 Shortwave and longwave radiation sensors 38
2.3.2 Weather station and soil sensors 40
2.3.3 Crop measurements 41
2.4 Instantaneous radiative forcing 42
2.5 Statistical analyses 42
3. Results 43
3.1 Effects of treatments and soil type on the surface albedo 43
3.1.1 The surface albedo values during the growing season 43
3.1.2 Surface albedo values during fallow periods 44
3.2 Crop growth effect on surface albedo 47
3.3 Effect of topsoil moisture on daily surface albedo 49
3.4 Radiative forcing, thermal radiation and topsoil temperature 51
3.4.1 Daily instantaneous radiative forcing (iRF) 51
3.4.2 Daily outgoing longwave (LWout) radiation and topsoil temperature 53
4. Discussion 57
4.1 Interactive effects of soil type and cropping system on the dynamics of the surface albedo 57
4.2 Effects of maize growth on surface albedo dynamics 59
4.3 Changes in iRF and LWout caused by tillage and crop residue management 60
4.4 Limitations and perspectives 61
5. Conclusion 62
Supplementary materials 64
Chapitre II : Analyse des effets biogéophysiques et biogéochimiques des pratiques de l'AC en Afrique Subsaharienne 69
Résumé en français : 69
Balancing biogeochemical gains and surface albedo shifts: climate impacts of no-tillage and mulching in Southern Africa 70
Abstract 71
1. Introduction 72

2. Materials and methods 73
2.1 Experimental sites and treatments 73
2.2 Surface albedo measurements 74
2.3 Soil nitrous oxide emissions 75
2.4 Soil organic carbon stocks 75
2.5 Climate impact assessment 76
2.5.1 Instantaneous radiative forcing induced by albedo change 76
2.5.2 Metrics 76
2.5.3 Simulation of changes in soil organic carbon storage 77
3. Results 78
3.1 Effects of CA practices on SOC 78
3.2 Climate impact of CA practice 80
4. Discussion 83
4.1 Biogeochemical effect of CA 83
4.2 Soil type and management practices impacts on biogeophysical effect 84
4.3 Global and local climate effects 85
4.4 Climate metrics 85
4.5 Limits of our study 86
5. Conclusion 86
Supplementary materials 88
Chapitre III : Modélisation de l'albédo de surface avec le modèle de système de cultures STICS 93
Résumé en français : 93
Simulating surface albedo dynamics under conservation agriculture using the STICS soil-crop model – Application to two Sub-Saharan sites 95
Abstract 95
1. Introduction 97
2. Materials and methods 98
2.1 Experiments description and location 98
2.2 In situ data 99
2.2.1 SWin, Albedo and heat flux monitoring 99
2.2.2 Soil moisture monitoring 99
2.2.3 Leaf area index data 100

2.2.4 Weather data ... 100
2.3 Modelling methodology ... 101
2.3.1 STICS model ... 101
2.3.2 Calibration steps ... 101
2.3.3 Soil parametrization ... 101
2.3.4 Current soil evaporation formalism ... 102
2.3.5 New soil evaporation formalism ... 102
2.3.6 Surface albedo α ... 103
2.3.7 Including yellow leaves into α calculation ... 103
2.3.8 Model performance evaluation ... 104
3. Results ... 105
3.1 Crop development: Leaf Area index dynamics ... 105
3.2 Observations and simulations agreement of Leaf Area Index, biomass and yield ... 106
3.3 Soil water content dynamics ... 107
3.3.1 Soil water content over the soil profile ... 107
3.3.2 Topsoil moisture ... 108
3.4 Albedo dynamics ... 109
3.4.1 Simulating surface albedo considering the current surface albedo formalism ... 109
3.4.2 Simulating surface albedo considering senescent tissues ... 110
3.4.3 Simulating surface albedo considering senescent tissues and new soil evaporation formalism ... 113
4. Discussion ... 115
4.1 Crop development calibration in Zimbabwe ... 115
4.2 Drivers of surface albedo and their accounting in the STICS model ... 116
4.3 Limits and perspectives ... 117
5. Conclusion ... 118
Supplementary materials ... 119
Chapitre IV : Discussion générale et conclusion ... 122
1. Préambule ... 122
2. L'analyse des effets couplés : l'importance de considérer l'albédo ... 123
3. Qu'en est-il pour l'adaptation ? ... 125
4. L'albédo de surface dans les modèles ... 126

5. Approches spatialisées des effets couplés 127
5.1 ORCHIDEE-CROP : une potentielle perspective à l'analyse spatialisée des effets couplés 127
5.2 Intégration d'un modèle de culture dans un modèle de surface 128
5.3 L'apport du couplage des deux modèles dans notre étude 129
5.4 L'apport de la télédétection spatiale 130
Conclusion générale 131
Références bibliographiques 134
Annexes 153
Annexe 1 : Papier méthodologie 153
Annexe 2 : Liste des figures 155
Annexe 3 : Liste des tables 159

Listes des sigles et acronymes

α : albedo de surface

AC : Agriculture de conservation

AF : *Airborn Fraction*

APSIM : *Agricultural Production Systems sIMulator*

CIMMYT : *International Maize and Wheat Improvement Center*

CT : *Conventional tillage*

DSSAT : *Decision Support System for Agrotechnology Transfer*

DTC : *Domboshawa Training Center*

EESF : *emissions equivalent of shortwave forcing*

FAO : L'Organisation des Nations unies pour l'alimentation et l'agriculture

GIEC : Groupe d'experts intergouvernemental sur l'évolution du climat

GES : Gaz à effet de serre

GFCC : *Green Fractional Canopy Cover*

$GtCO_2$: Giga tonnes de CO_2

GWP : *Global Warming Potential* / Potentiel de Réchauffement Global

iRF : *Instantaneous radiative forcing* / Forçage radiatif instantané

LAI : *Leaf Area Index*

LWin : *Incoming Longwave radiation /* Rayonnement grandes longueurs d'onde entrant

LWout : *Outgoing Longwave radiation /* Rayonnement grandes longueurs d'onde sortant

NT : *No-tillage*

NTM : *No-tillage with mulch*

PAI : *Plant Area Index*

RF : *Radiative Forcing* / Forçage radiatif

Rn : Rayonnement net

SWin : *Shortwave incoming solar radiation* / Rayonnement solaire courtes longueurs d'onde incident

SWout : *Shortwave outgoing solar radiation* / Rayonnement solaire courtes longueurs d'onde réfléchi

STICS : Simulateur MulTIdisciplinaire pour les Cultures Standards

SOC : *Soil Organic Carbon*

Ta : *Atmospheric Transmittanc*e / Transmittance Atmosphérique

TDEE : *Time dependency emission equivalent*

UZF : *University of Zimbabwe Farm*

Introduction générale

Dans cette partie, le contexte général de la thèse ainsi que les notions clés en lien avec l'agriculture de conservation (AC), l'albédo, les effets biogéophysiques sur le climat, le forçage radiatif vont être abordés. L'état de l'art concernant le potentiel d'atténuation de l'AC face au changement climatique sera aussi rappelé.

1. Contexte

1.1 Le changement climatique

Les dernières mesures de concentration atmosphérique en CO_2 enregistrées à la station de Mauna Loa à Hawaï donnent une concentration moyenne de l'ordre de **425.55** ppm en Juillet 2024 (Figure 1 et 2). Cette mesure correspond à un peu plus de 1,5 fois la concentration en CO_2 atmosphérique avant l'ère préindustrielle où la concentration en CO_2 était d'environ **280 ppm** (IPCC, 2014). La concentration en CO_2 de l'atmosphère n'a donc cessé d'augmenter depuis la révolution industrielle jusqu'à aujourd'hui, et les émissions de gaz à effet de serre (GES) sont de plus en plus importantes et contribuent au réchauffement de la terre. Ce réchauffement est l'un des principaux facteurs du déséquilibre économique, écologique et socio-environnemental de la planète (Dellink et al., 2019). **Svante Arrhenius**, au 19ème siècle avait fait la démonstration de la relation directe entre concentration de CO_2 dans l'atmosphère et température de l'air (Figure 1). Cette hypothèse d'**Arrhenius** confirmée au cours du 20ème siècle a entraîné une prise de conscience collective menant à la création du Groupe d'Experts Intergouvernemental sur l'Evolution du Climat (**GIEC**) en 1988, et dont le but est d'étudier et de quantifier le réchauffement global en lien avec les activités humaines. Les travaux du GIEC ont démontré que les émissions de GES cumulées depuis 1850 sont environ de 2400 ± 240 $GtCO_2$ en 2019 dont plus 50% sont absorbées dans les puits naturels que sont les océans et les écosystèmes terrestres (IPCC, 2023). Le reste des émissions de GES se sont accumulées dans l'atmosphère, soit près de 1000 $GtCO_2$ (IPCC, 2023). Ce

réchauffement peut être évalué et quantifié à travers des concepts tels que le forçage radiatif (voir section 2.4).

Les agroécosystèmes ont des interactions avec l'atmosphère. Les échanges de gaz ou de flux d'énergie (ex. chaleur latente) à l'interface sol-atmosphère et les changements d'état de surface peuvent induire des perturbations du bilan d'énergie et donc du bilan radiatif terrestre quantifiable à travers le concept de forçage radiatif ou *"radiative forcing (**RF**)"* en anglais. Le RF est défini comme la *"Variation du rayonnement net (différence entre le flux radiatif reçu et le flux radiatif émis, exprimée en W m^{-2}) à la tropopause ou au sommet de l'atmosphère due à la variation d'un facteur du changement climatique, telle qu'une modification de la concentration de dioxyde de carbone ou du rayonnement solaire."* (IPCC, 2018). Le forçage radiatif induit par l'augmentation des gaz à effet de serre et d'autres activités humaines est entre 1750 et 2022 en moyenne de **2.91** $W.m^{-2}$ [2.19 - 3.63] selon Forster et al., (2024) (Figure 2) se traduisant par un réchauffement global de **1.09** °C [0.95 - 1.20] selon l'AR6 du GIEC (IPCC, 2023) ou de **1.15 °C** [1.00 to 1.25] selon Forster et al., (2024).

L'agriculture participe à près de 23% des émissions de GES (*i.e* CO_2, CH_4, N_2O) d'origine humaine (IPCC, 2019). Ces GES contribuent à l'absorption d'une portion du rayonnement infrarouge terrestre et participent de ce fait au réchauffement de l'atmosphère, d'où le nom d'effet de serre (Aydinalp and Cresser, 2008). Ce dernier est un phénomène naturel permettant de maintenir l'équilibre de la température moyenne de terre et il est perturbé aujourd'hui par les activités anthropiques. Nonobstant, les sols agricoles possèdent la capacité de capturer et de stocker le carbone atmosphérique à travers des pratiques dites stockantes. Les sols sont des réservoirs carbone contenant jusqu'à trois fois plus de carbone que l'atmosphère (Batjes, 1996). Certaines pratiques culturales comme la réduction du labour, la gestion des résidus de cultures et les couverts intermédiaires peuvent être bénéfiques pour le climat via le stockage de carbone et la réduction des émissions de GES (Beillouin et al., 2023; Blanco-Canqui and Lal, 2008; Gonzalez-Sanchez et al., 2019; Tribouillois et al., 2018).

Certaines de ces pratiques culturales peuvent également jouer sur certaines variables biogéophysiques (température de surface, albédo, flux de chaleur sensible et latente…)

pouvant contribuer au ou atténuer le réchauffement climatique (Ceschia et al., 2017; Davin et al., 2014; Irmak and Kukal, 2022).

L'agriculture de conservation peut contribuer à l'atténuation du changement climatique et à ses effets sur la production agricole (Corbeels et al., 2020) tout en apportant de nombreux autres services écosystémiques comme l'amélioration de la structure du sol et lutter contre l'érosion (Derpsch et al., 2010).

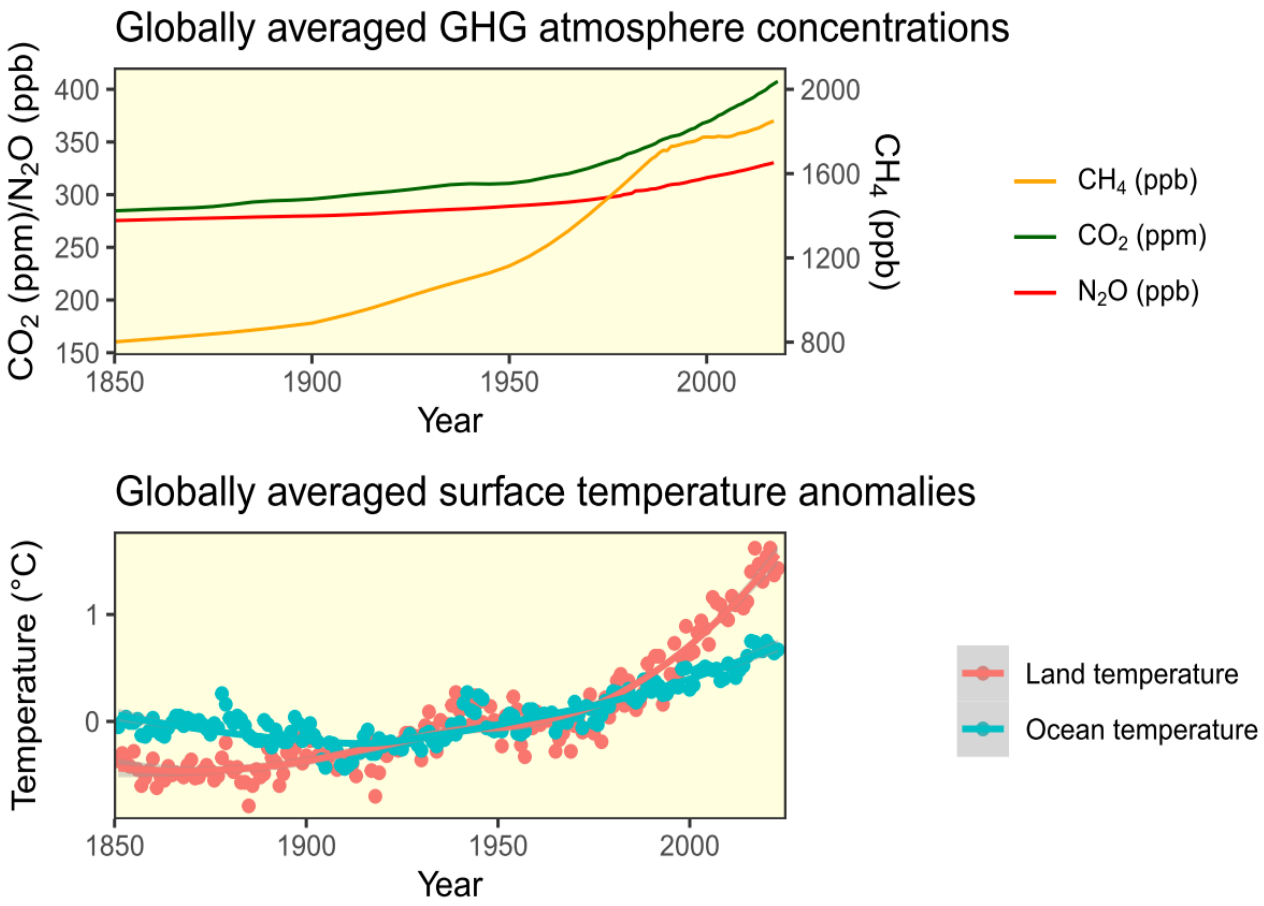

Figure 1. La figure en haut représente la moyenne globale de la concentration atmosphérique des gaz à effets de serres (CO2, CH4, N2O) (https://www.eea.europa.eu/). La figure en bas représente les anomalies de températures moyennes globales depuis 1850 (https://www.ncei.noaa.gov/)

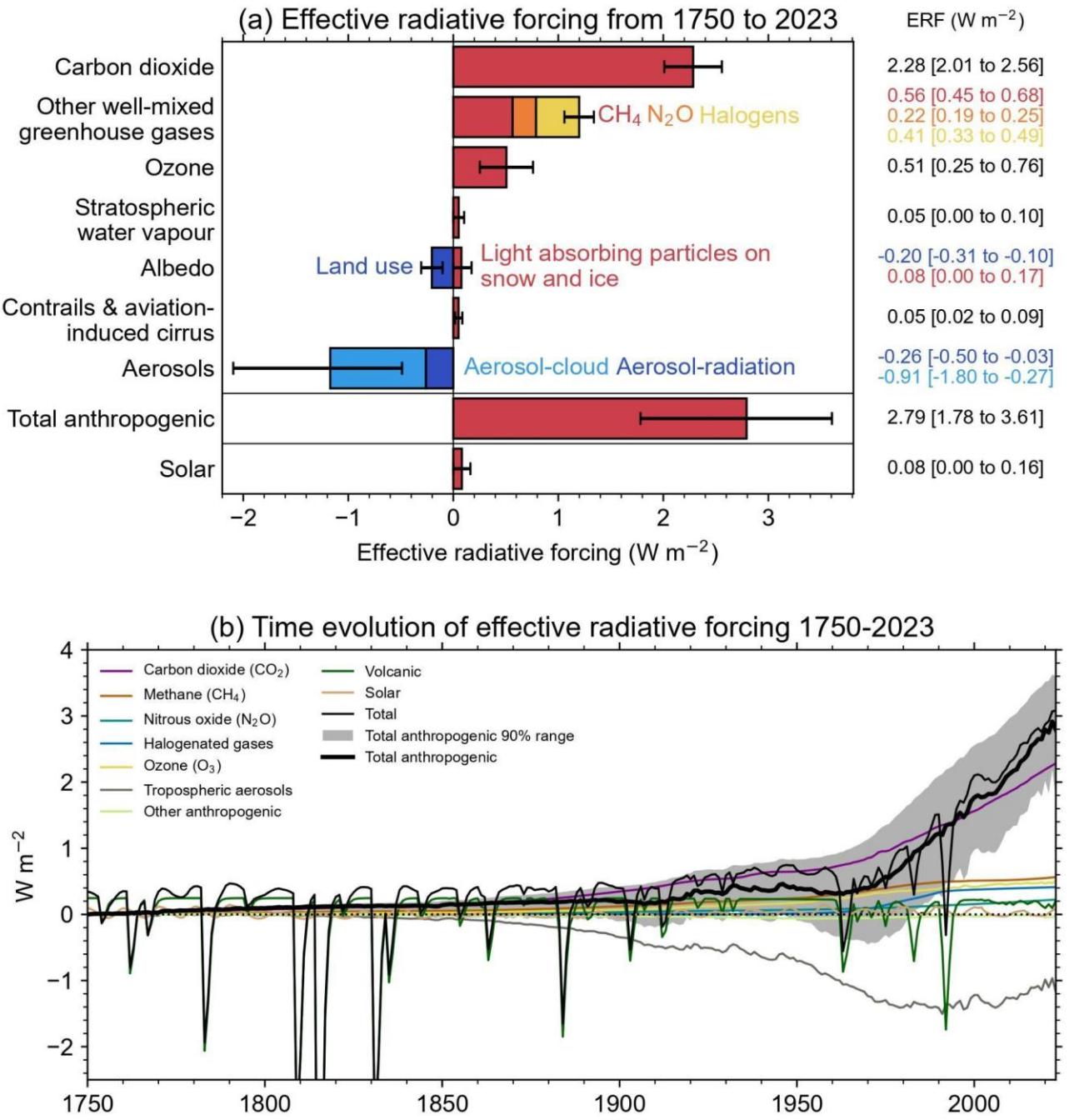

Figure 2. Contribution de 1750 à 2023 des principales composantes anthropiques et naturelles (solaire + volcans) au forçage radiatif effectif. Il est important de noter que les valeurs affichées pour chaque variable dans cette figure sont des moyennes globales pouvant masquer des différences très marquées au niveau local. Les effets albédo en moyennes globales sont faibles. Néanmoins, des effets albédo très forts ou ayant les mêmes magnitudes que les GES peuvent être observés localement selon les changements d'occupation et d'utilisation des sols (Forster et al., 2023).

1.2 L'agriculture de conservation (AC)

L'agriculture de conservation (AC) telle qu'elle est définie par la FAO consiste à réduire la perturbation du sol (ex. réduire le travail du sol, favoriser le semis direct), à avoir le sol couvert en permanence soit par des résidus de culture soit par des cultures intermédiaires et à favoriser la diversification des cultures en adoptant les systèmes de rotation de cultures, des intercultures ou des associations de cultures (Figure 3). Le type de pratique le plus répandu en agriculture de conservation dans le monde est le non-travail du sol couvrant 72 millions d'hectares dont plus de 80% en Amérique et les 20% restant étant réparti dans le reste du monde dont moins de 4% en Europe, en Asie et en Afrique entre 2002 et 2003 (Derpsch and Benites, 2003). La réduction du travail du sol, voire sa suppression, participe à la conservation de la matière organique en surface mais également à une meilleure structure du sol par le maintien des agrégats argilo-humiques et de la macro-porosité (Laurent, 2015). La couverture du sol par des résidus de cultures ou des couverts végétaux contribue à la réduction de l'érosion de l'horizon humifère, le protège contre l'effet splash engendré par les pluies, et les couverts végétaux jouent également le rôle de pompe biologique en faisant remonter les éléments nutritifs lessivés en profondeur (Séguy and Bouzinac, 1999). Les rotations de cultures ont pour but de réduire le cycle des maladies, la prolifération des plantes adventices et des parasites (Laurent, 2015). L'utilisation des résidus de cultures comme *mulch* enrichit le sol en carbone en se décomposant, protège aussi le sol contre l'érosion hydrique et éolienne (Corbeels et al., 2020; Powlson et al., 2016).

Les premiers mouvements qui ont révolutionné les pratiques agricoles traditionnelles vers des pratiques plus respectueuses de l'environnement comme l'AC ont vu le jour en Amérique du sud. Elle a ensuite été introduite en Afrique australe dans les années 1990 en réponse à des problèmes croissants d'érosion des sols, de baisse de fertilité et de faibles rendements agricoles. Cette approche promet une intensification durable des petites exploitations dans des environnements fragiles. Selon Derpsch et al. (2010), le système du "non travail du sol" est largement promu dans plusieurs pays d'Afrique de l'Est et du Sud à l'image du Zimbabwe, de la Zambie, du Kenya, du Mozambique, de la Tanzanie, de l'Eswatini et du Malawi. Malgré cette promotion, ces pratiques sont faiblement adoptées à cause du compromis à trouver pour les résidus de culture entre alimentation du bétail et leur utilisation comme mulch qui

permet de couvrir le sol (Baudron et al., 2014; Valbuena et al., 2012). Certains de ces pays ont incorporé l'agriculture de conservation dans les politiques agricoles à l'image du pfumvudza[1] au Zimbabwe, bien qu'il reste fragmentaire par rapport à l'agriculture conventionnelle et est surtout pratiquée en grande partie par les petits exploitants.

Des pratiques du CA comme le non-labour et la gestion des résidus présentent beaucoup d'avantages comme une possible l'augmentation des rendements (Rusinamhodzi et al., 2011) et l'amélioration des propriétés physico-chimiques du sol (Derpsch et al., 2010). L'agriculture de conservation peut ainsi dans certaines conditions avoir des effets bénéfiques pour le climat, notamment d'un point de vue séquestration de carbone (Corbeels et al., 2020) mais aussi potentiellement en contribuant à l'atténuation via d'autres effets biogéochimiques (ex. réduction des émissions liées à la production d'engrais) et biogéophysiques (ex. accroissement de l'albédo de surface, réduction du rayonnement infrarouge de surface) sur le climat.

Dans le cadre de mon travail de thèse, l'analyse des effets biogéophysiques de l'agriculture de conservation sur le climat occupe une place prépondérante.

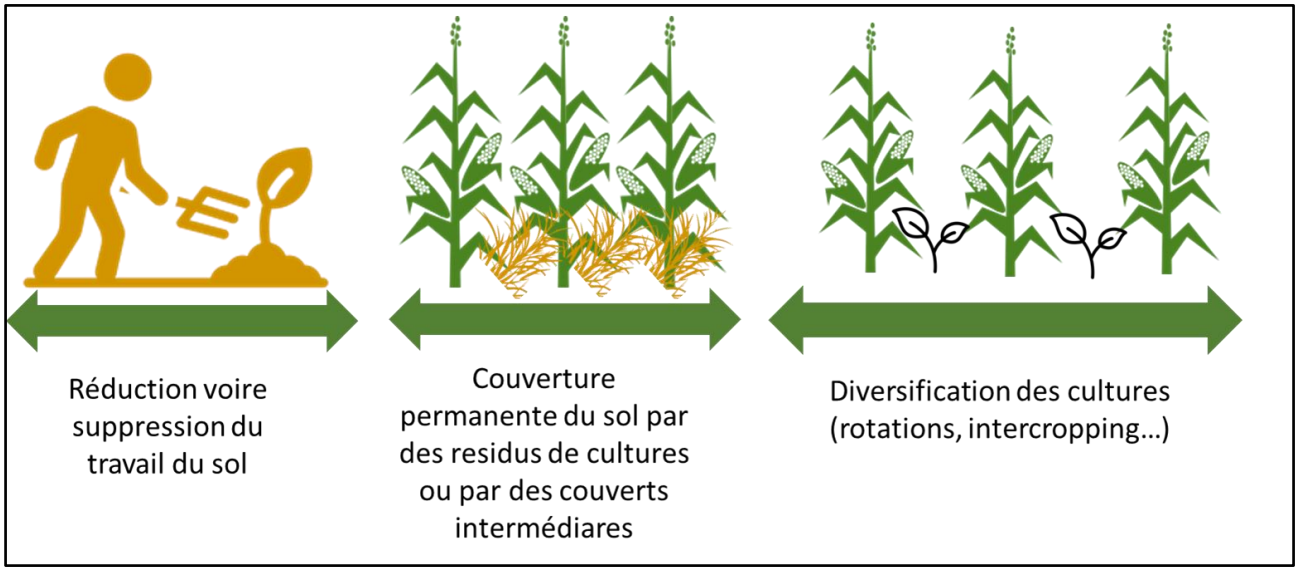

Figure 3. Les 3 principes de l'agriculture de conservation (FAO, 2015).

[1] Le pfumvudza (littérallement "Révolution des maitres agriculteurs") un programme du gouvernement Zimbabwéen visant à subventionner financièrement les jeunes agriculteurs. C'est une pratique de l'agriculture de conservation visant à réduire la perturbation du sol, s'assurant de la couverture permanente du sol et de la diversification des cultures à travers la rotation des cultures. Il est mis en œuvre pour avoir un meilleur rendement sur de petites surfaces. https://foundationsforfarming.org/?page_id=9384

1.3 Les effets climatiques de l'agriculture de conservation (AC)

L'étude de l'impact de l'agriculture et notamment de l'AC sur le changement climatique s'est principalement concentrée sur les effets biogéochimiques comme la séquestration de carbone dans le sol ou les émissions de gaz à effets de serre tandis que les effets biogéophysiques ont souvent été négligés (Figure 4). Or, les pratiques culturales ont aussi des effets sur les processus biogéophysiques du système en modifiant le bilan d'énergie local à travers 1) des changements d'albédo de surface et 2) des modifications de la répartition de l'énergie en surface entre évapotranspiration, flux de chaleurs sensibles, rayonnement infrarouge et stockage et flux de chaleur dans le sol et la végétation (Davin et al., 2014; Lobell et al., 2006). Des études récentes ont montré que les effets biogéophysiques liés aux changements de pratiques sont comparables à ceux liés aux changements d'occupation du sol (Luyssaert et al., 2014) et qu'ils sont comparables aussi aux effets biogéochimiques induits par les changements de pratiques (Kaye and Quemada, 2017; Lugato et al., 2020). Hirsch et al. (2018b) ont modélisé l'impact des pratiques de l'AC sur le climat local. Dans cette étude, les auteurs ont démontré que l'AC contribue généralement à un effet refroidissement du climat local d'environ 1°C durant les épisodes de chaleurs extrêmes dans les latitudes moyennes. Ils ajoutent que dans les régions tropicales la pratique de l'AC contribue à l'effet refroidissement d'environ 1°C en raison du changement d'évapotranspiration dominant l'effet albédo de surface. Lobell et al. (2006) ont montré à travers un exercice de modélisation que la réduction voire la suppression du travail du sol (un des piliers de l'agriculture de conservation) entraîne une augmentation de l'albédo de surface et par conséquent un effet de refroidissement global d'environ 0.2 °C. Les auteurs poursuivent en concluant que cet effet refroidissant global dû au changement d'albédo est comparable aux effets climatiques reportés pour les processus biogéochimiques comme la séquestration potentielle de carbone. Davin et al. (2014) ont démontré que l'absence de labour combiné avec un maintien du paillis en surface comparé au labour conventionnel pourrait entraîner localement un effet de refroidissement d'environ 2°C durant les vagues de chaleurs estivales. Kaye et Quemada (2017) ont comparé l'effet des changements d'albédo de surface dus à la présence de cultures intermédiaires sur le forçage radiatif (en

s'appuyant sur des données de la littérature) avec le stockage de carbone induit par ces couverts intermédiaires et les émissions de N_2O.

Pour évaluer l'effet climatique net des changements de pratiques, il est donc primordial de quantifier les forçages radiatifs induits à la fois par les effets biogéochimiques et biogéophysiques. A l'heure actuelle peu d'études se sont encore intéressées à l'analyse conjointe des effets biogéochimiques et des effets biogéophysiques.

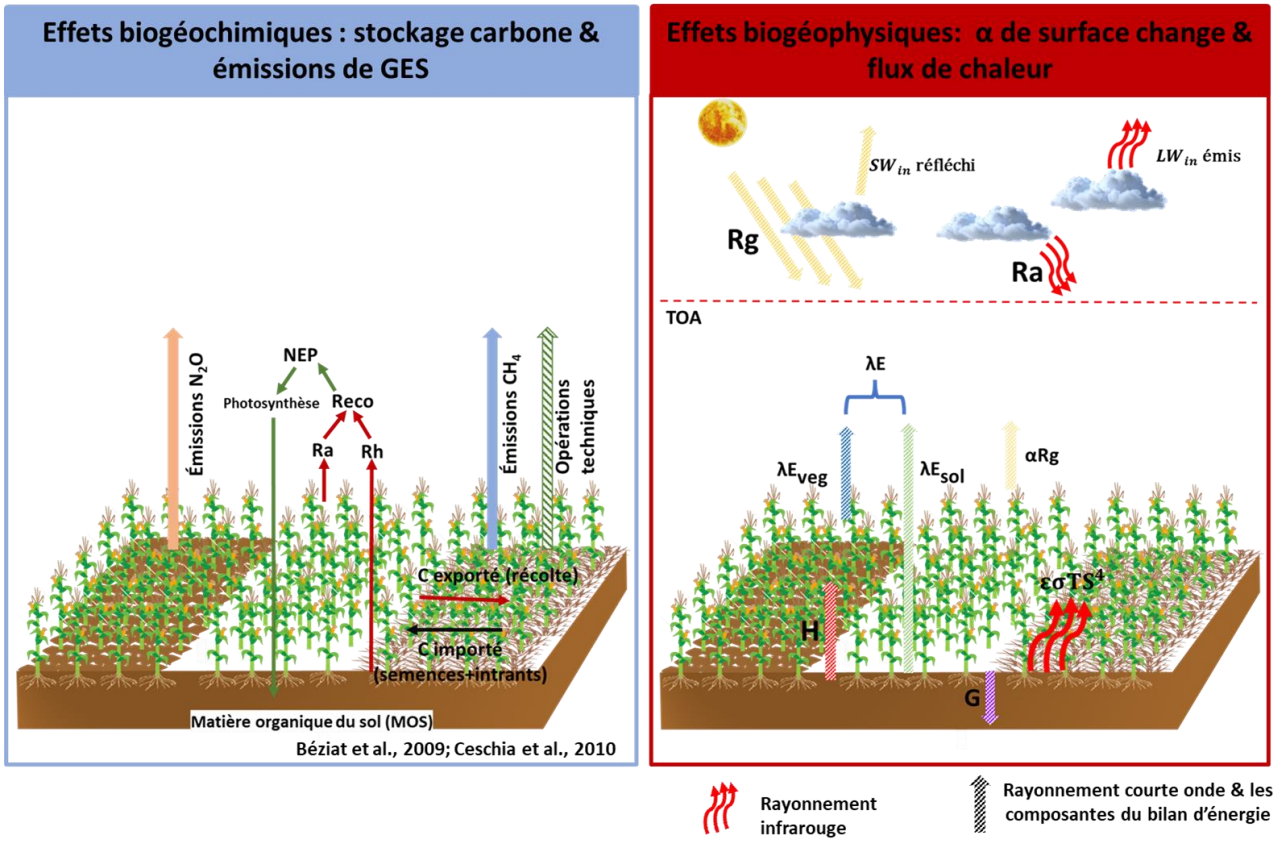

Figure 4. Le cadre de gauche montre les processus biogéochimiques impactant le climat qui correspondent aux composantes du bilan carbone et aux émissions de gaz à effet de serre. Dans le cadre de droite les processus biogéophysiques au sein et à l'interface avec les agroécosystèmes qui correspondent aux flux radiatifs de courte et longue longueur d'ondes et aux flux d'énergie non radiatifs avec **λ**E correspondant au flux de chaleur latente, H représente le flux de chaleur sensible, et G au flux de chaleur dans le sol par conduction (adapté de Ceschia et al., 2017).

2. Les effets biogéophysiques

2.1 Le bilan radiatif de la Terre

L'énergie disponible à la surface terrestre est avant tout conditionnée par le rayonnement provenant du soleil qui est sa principale source d'énergie et par l'albédo de surface qui représente la fraction du rayonnement solaire réfléchie par une surface (voir section 2.3 pour plus de détails). La terre reçoit en moyenne 340 $W.m^{-2}$ au sommet de l'atmosphère. Une partie de ce rayonnement environ 67 $W.m^{-2}$ interagit avec les particules de gaz dans l'atmosphère via les processus d'absorption et de diffusion entraînant une perte d'énergie (Figure 4). Environ 170 $W.m^{-2}$ du rayonnement reçu est directement renvoyé vers l'espace par les nuages, les aérosols et d'autres constituant atmosphériques (Figure 4). Le rayonnement solaire atteignant la surface terrestre (océan+surfaces continentales) est plus ou moins réfléchi selon l'albédo. L'albédo moyen de la terre est de 0.3 ce qui veut dire que la terre reflète en moyenne 30% du rayonnement solaire (courtes longueurs d'ondes). Les 71% d'énergie provenant du soleil (et dans une moindre mesure du rayonnement atmosphérique infra-rouge, Ra) disponibles en surface vont être utilisés pour produire de la chaleur sensible, de la chaleur latente (énergie nécessaire à l'évaporation de l'eau et à l'évapotranspiration des plantes). Le reste de l'énergie disponible en surface est absorbé par les différents corps du système (sol, végétation) puis réémis vers l'espace sous forme de rayonnement infrarouge (longues longueurs d'ondes comprises entre 3 et 60 µm). Le bilan radiatif de la terre peut être traduit par l'équation suivante :

$$Rn = (1 - \alpha s)Rg + R_a - \varepsilon(\sigma TS^4) \quad (1)$$

Où Rn est le rayonnement net, αs est l'albédo de surface, Rg est le rayonnement solaire (ou rayonnement global) incident à la surface, le terme $(1 - \alpha s)Rg$ correspond à la partie du rayonnement global absorbée par la surface terrestre (donc non réfléchi), Ra représente le rayonnement atmosphérique, le terme $\varepsilon(\sigma TS^4)$ correspond à l'émission du rayonnement infrarouge terrestre conditionné par l'émissivité de surface (ε), par la constante de Stefan-Boltzmann (σ) et par la température de surface (*TS*).

2.2 Le bilan d'énergie de la Terre

L'équation du bilan d'énergie à la surface représente la façon dont le rayonnement net à la surface terrestre (soit l'énergie disponible en surface) va se répartir en différents flux d'énergie (Figure 4). Cela se traduit par l'équation suivante :

$$Rn = LE + H + G + (\Delta S + P) \quad (2)$$

Rn, le rayonnement net, correspond à la quantité d'énergie disponible en surface en W m^{-2}. Le flux de chaleur latente est noté *LE* et il correspond à la quantité d'énergie nécessaire pour la vaporisation de l'eau en surface c'est à dire à l'énergie nécessaire pour l'évaporation et pour la transpiration des plantes en d'autres termes l'évapotranspiration (ETR). H correspond au flux de chaleur sensible, c'est un transfert de chaleur par convection depuis la surface vers les basses couches de l'atmosphère. Contrairement au flux de chaleur latente (LE), la chaleur sensible entraîne une modification de la température. G est le flux de conduction de chaleur dans le sol. Il résulte de la différence de température entre la surface et la température de sol de référence. Les termes *ΔS* et *P* correspondent respectivement à la variation de stockage de chaleur dans la végétation et P la quantité d'énergie utilisée par la photosynthèse ce qui représente au maximum 2 à 3% du Rn. *ΔS* et *P* sont souvent ignorés lors du calcul de *Rn* dans les systèmes relativement simple où la végétation n'est pas très dense (Moore and Fisch, 1986), ce qui est le cas dans cette étude. Ceci simplifie l'équation (2) et la traduit comme suit :

$$Rn = LE + H + G \quad (3)$$

2.3 L'albédo de surface (α)

L'albédo est la fraction du rayonnement solaire réfléchie par une surface. C'est une grandeur adimensionnelle renseignant la capacité réflective des surfaces. Il est généralement calculé dans les gammes de longueurs d'ondes allant du visible (0.4-0.7 µm) à l'infrarouge moyen (0.3 –4.0 µm) soit la fenêtre correspondant au rayonnement solaire (Figure 5). L'albédo varie entre 0 et 1 ce qui veut dire que plus la valeur est proche de 0. moins la surface reflète le rayonnement solaire (ex. l'asphalte) et plus la valeur est proche de 1 plus l'objet reflète le

rayonnement solaire (ex. la neige). La figure 5 montre les signatures spectrales de l'eau, du sol nu et de la végétation. L'albédo moyen du sol nu est plus élevé que celui de l'eau et de la végétation dans le visible (0.4-0.7µm) raison pour laquelle l'œil humain perçoit les sols plus clairs que la végétation. En revanche, dans l'infrarouge moyen (pouvant aller jusqu'à 20µm) la réflectance du sol nu reste plus élevée que celle de la végétation. La réflectance de la végétation est plus faible que celle de l'eau et du sol nu dans le visible mais reste plus élevée dans le proche-infrarouge. Par ailleurs, l'albédo à large bande étant calculé sur la fenêtre regroupant le visible, le proche-infrarouge et l'infrarouge moyen, les valeurs observées sur les sols nus sont généralement plus faibles que celles observées sur la végétation sauf pour certains types de sols très réfléchissants comme des sols sableux ou calciques.

Les changements d'albédo de surface dépendent généralement de l'occupation du sol (ex. forêt, prairie, zone urbaine), de l'état de surface (ex. humidité du sol, stade de végétation, rugosité) et de la composition biochimique initiale de la surface comme par exemple la teneur en matière organique du sol, la teneur en fer ou la quantité de pigments photosynthétiques dans la végétation (Cierniewski et al., 2018; Post et al., 2000).

Les pratiques agricoles, comme la réduction de labour et l'apport de paillis (Davin et al., 2014) ou l'introduction de couverts intermédiaire (Carrer et al., 2018), en fonction de leur intensité et de leur durée peuvent également affecter la dynamique interannuelle de l'albédo de surface. Selon Davin et al., (2014), la suppression du labour combiné avec le maintien du paillis en surface comparé au labour conventionnel entraîne une augmentation de l'albédo de surface d'environ 0.1. Carrer et al., (2018) ont montré que l'introduction des couverts intermédiaires durant les périodes d'intercultures en Europe pourrait augmenter l'albédo de surface d'environ 4%. L'application du biochar peut également avoir des effets sur l'albédo. (Genesio et al., 2012) ont mesuré une baisse de l'albédo de surface du sol nu d'environ 80% juste après l'application du biochar et d'environ 40% sur l'ensemble de la période culturale (du semis à la récolte). Des approches de "géo-ingérie" ont suggéré l'augmentation de l'albédo de surface comme levier d'atténuation en sélectionnant des espèces de plantes à fort pouvoir réfléchissant compte tenu de l'albédo du sol nu généralement plus faible que celui de la végétation (Ridgwell et al., 2009). Des changements d'occupation du sol comme

la déforestation et la reforestation peuvent aussi impacter l'albédo de surface et plusieurs études suggèrent que dans certaines zones du globe l'effet climatique net de l'afforestation pourrait être réchauffant à cause de la forte chute d'albédo engendrée (Betts, 2000; Hasler et al., 2024; Rohatyn et al., 2022; Rotenberg and Yakir, 2010).

L'albédo joue un rôle clef sur le bilan d'énergie de la terre principalement à deux niveaux : au sommet de l'atmosphère et en surface. Il gouverne la quantité de rayonnements courtes longueurs d'ondes absorbée ou émise par la surface terrestre. L'évaluation complète de la réponse climatique liée aux changements d'albédo est très complexe et fait appel à des modèles couplés globaux sol-atmosphère-océan. Des approches plus simples ont été proposées par les scientifiques comme la calcul du forçage radiatif instantané au sommet de l'atmosphère induit par le changement d'albédo (Betts, 2000; Forster et al., 2007; Lenton and Vaughan, 2009)**.**

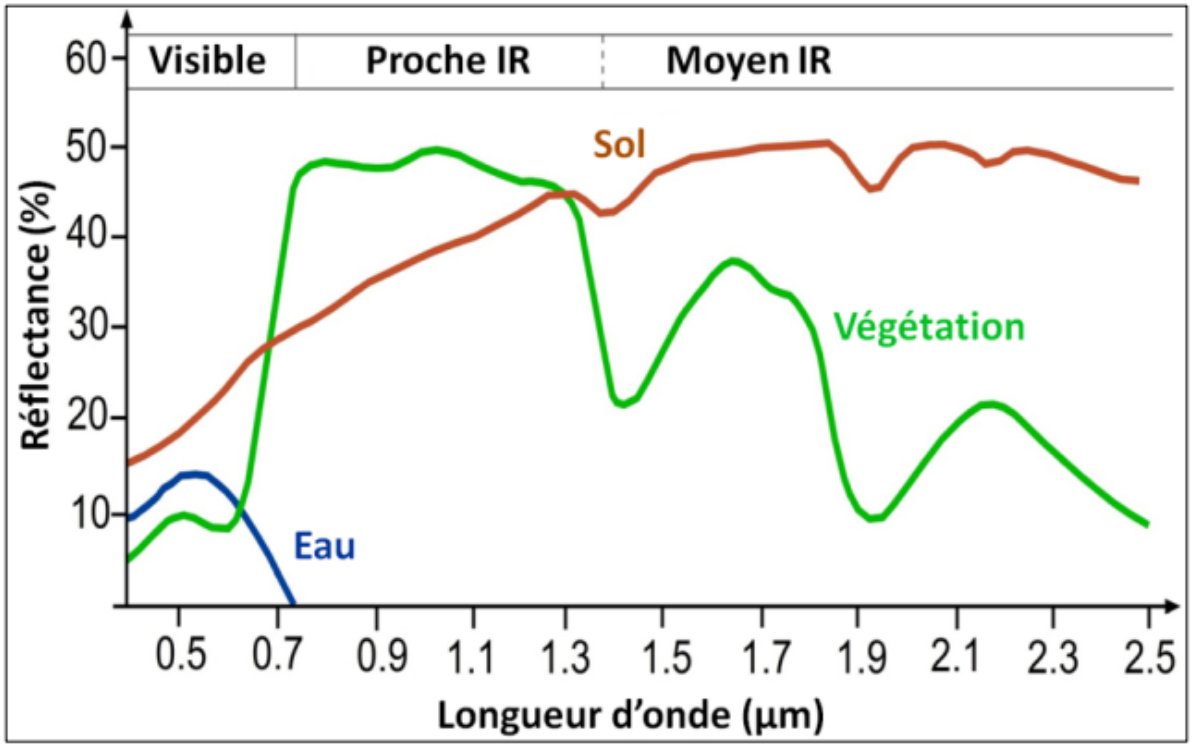

Figure 5. Signatures spectrales de différentes composantes dans le visible, proche infrarouge et dans infrarouge moyen **(Begue et al., 2016)**.

2.4 La notion de forçage radiatif

Le forçage radiatif (RF) est une métrique utilisée pour évaluer toute perturbation d'équilibre entre la quantité d'énergie entrant et sortant dans le système Terre/Atmosphère (IPCC, 2014). En d'autres termes, c'est une modification du bilan radiatif (changement sur les rayonnements courtes et grandes longueurs d'onde) à la tropopause ou au sommet de l'atmosphère. Le RF peut être dit instantané (iRF) quand son évaluation ne tient pas compte des modifications de la température stratosphérique. Il est dit effectif (effective radiative forcing, ERF en anglais) quand toutes les perturbations comme celle de la troposphère sont prises en compte (O'Connor et al., 2020). Le RF est largement utilisé dans la littérature scientifique pour quantifier/évaluer les changements d'état de surface impactant son albédo (Bright and Lund, 2021; Sieber et al., 2019) et/ou les changements des composantes atmosphériques (Forster et al., 2007; Lenton and Vaughan, 2009)**.**

2.4.1 Forçage radiatif dû à la modification d'albédo de surface

Les changements de pratiques peuvent affecter l'albédo de surface. Ce dernier peut entraîner une perturbation de l'équilibre du bilan radiatif et donc du bilan d'énergie. En effet, le système climatique terrestre se réajuste pour trouver un nouvel équilibre quand un forçage radiatif survient par la modification de sa température (Forster et al., 2007). Diverses méthodologies ont été proposées pour calculer le RF entraîné par un changement d'albédo de surface. Elles ont des degrés de complexité différents allant des modèles de transfert radiatif avancé (Betts, 2000; Cai et al., 2016) aux méthodes empiriques simples (Muñoz et al., 2010). Dans notre étude, le RF induit par le changement d'albédo est évalué au sommet de l'atmosphère instantanément (*iRF*$\triangle\alpha$) et donc avant l'établissement de d'un nouvel équilibre du système et il est traduit de manière suivante en se basant sur l'étude de Muñoz et al., (2010) :

$$iRF \triangle \alpha(i) = -SW_{in(i)} \times Ta(i) \times \triangle \alpha(i) \quad (4)$$

Ou *iRF*$\triangle\alpha(i)$ représente le forçage radiatif instantané induit par le changement d'albédo de surface (exprimé en W m^{-2}) d'un jour *i*, SW_{in} (W m^{-2}) est le rayonnement incident de courtes longueurs d'ondes (0.3 - 2,8 µm), *Ta* correspond à la capacité de l'atmosphère à transmettre

le rayonnement et elle résulte du rapport entre le rayonnement incident ondes courtes (*SWin*) et le rayonnement au sommet de l'atmosphère (R_{TOA}). R_{TOA} est obtenu par une équation du temps se basant sur le modèle de Fu-Liou (Fu and Liou, 1993).

$$Ta = \frac{SW_{in(i)}}{R_{TOA}} \quad (5)$$

△α représente le changement d'albédo de surface.

L'augmentation de l'albédo due à un changement de pratique entraîne une augmentation de la fraction de rayonnement courte longueur d'ondes réfléchie par la surface ce qui va induire un RF négatif (refroidissement). En effet dans ce cas il reste moins d'énergie en surface pour réchauffer l'atmosphère et ce refroidissement induit peut-être comparé à un effet de refroidissement induit par une séquestration équivalente de CO_2 atmosphérique. L'effet refroidissant est en grande partie contrôlé par l'énergie disponible en surface et il est accentué si l'énergie qui reste en surface est utilisée pour faire de la chaleur latente (*i.e.* évapotranspiration) durant les périodes de croissance des plantes (Ceschia et al., 2017). Si l'énergie restante est utilisée pour faire de la chaleur sensible et du rayonnement infrarouge, l'effet refroidissement causé par l'augmentation d'albédo serait réduit voire compensé. Ces effets de l'albédo ayant un impact sur la partition d'énergie (H et LE) s'opèrent au niveau local et donc sur le climat environnant comme la modification temporaire de l'humidité de l'air et ou de la température de surface (Luyssaert et al., 2014). Une baisse d'albédo induite par une modification d'utilisation de la terre entraîne un RF positif (effet réchauffant) qui peut être assimilé à une augmentation de CO_2 équivalente atmosphérique se traduisant par un changement de température à l'échelle globale.

Les RF liés aux variations d'albédo de surface dans cette étude sont calculés à l'échelle locale. Pour évaluer le forçage radiatif induit par les changements d'albédo à l'échelle globale, il serait nécessaire d'utiliser des modèles couplés surface-atmosphère.

Les effets biogéophysiques de l'albédo de surface peuvent être aussi comparés aux effets biogéochimiques des émissions de gaz à effets de serre et de la séquestration de carbone. De récentes études ont montré la possibilité de convertir les forçages radiatifs causés par l'albédo en équivalent CO_2 ce qui facilite la comparaison des deux effets. La comparaison de ces effets a mené à une prise de conscience sur les potentiels effets significatifs que pourraient avoir certaines pratiques culturales sur l'atténuation du changement climatique

(Bright and Lund, 2021; Carrer et al., 2018; Davin et al., 2020; Hirsch et al., 2018a; Pique et al., 2023). En conséquence, des études récentes ont montré que pour certains changements de gestion, les *iRF⊿α* avaient des impacts du même ordre de grandeur que les effets biogéochimiques à court terme. Dans le cadre de cette étude nous nous focaliserons sur deux types de gestions qui sont deux principes clefs de la CA que sont le non-travail du sol (no-tillage en anglais) et la couverture du sol par des résidus de cultures ou *mulching* comparé à la pratique du labour conventionnel ou "*conventional tillage"* en anglais (voir chapitre I).

2.4.2 Conversion RFα en équivalent CO_2

Le terme équivalent CO_2 représente la quantité de dioxyde de carbone qui produirait le même potentiel de réchauffement que la quantité spécifiée de ce gaz ou d'un mélange de gaz à effet de serre émis intégré sur une période donnée. Toutefois, il faut noter que la concentration en équivalent CO_2 permet de faire la comparaison des forçages radiatifs de différents GES à un moment donné mais n'évalue cependant pas les réponses correspondantes du changement climatique ou un forçage futur. En général, aucune relation n'est établie entre les émissions en équivalent CO_2 et les concentrations. La conversion en équivalent CO_2 a longtemps concerné les gaz à effet de serre en s'appuyant sur le leur pouvoir de réchauffement global (PRG) ou *global warming potential (GWP*) en anglais. Le PRG des GES étant connu *i.e.* 1 pour CO_2, 28 pour CH_4 et 273 pour N_2O sur un horizon de 100 ans (IPCC, 2023). La prise en compte du PRG de ces GES mélangé de la même manière dans l'atmosphère permet facilement de comparer leurs effets sur le climat entre eux. Néanmoins, la conversion d'un RF local d'ordre biogéophysiques, comme les changements d'albédo de surface, pour comparer son effet climatique aux effets biogéochimiques est une tâche plus complexe.

Plusieurs méthodes ont été développées pour convertir les RFs engendrés par les variations d'albédo de surface (Betts, 2000; Bright et al., 2016; Bright and Lund, 2021; Forster et al., 2007; Schimel, 1995). Les méthodes les plus utilisées sont : la méthode de EESF pour *"emissions equivalent of shortwave forcing"* qui se base sur le *"airborn fraction"* **AF**, la

méthode **GWP** et la méthode **TDEE** (Time dependency emission equivalent) selon Bright et Lund (2021). La méthode EESF est développée pour la première fois par Betts 2000. Elle est exprimé en Kg CO_2-eq.m^{-2}

$$ESSF = \frac{RF\triangle\alpha}{k_{CO_2}AeAF} \quad (6)$$

où $RF\triangle\alpha$ correspond au forçage radiatif instantané lié à une variation d'albédo exprimé en W.m^{-2}, kCO_2 représente l'efficience radiative moyenne globale du CO_2 en W m^{-2} Kg^{-1} à une concentration de 389 ppm (Joos et al., 2013), *Ae* est la superficie de la surface terrestre (5.1×10^{14} m^2) et *AF* correspond à la quantité de CO_2 d'origine anthropique qui reste dans l'atmosphère après un certain temps de séjour. Cette méthode, qui se base sur *AF*, ne tient pas compte de la dépendance temporelle de l'élimination du CO_2 atmosphérique. Mais elle s'avère très efficace si la variation d'albédo liée aux changements d'utilisations des terres n'a pas de dépendance temporelle (Bright et Lund 2021).

Bright et al. 2016 ont proposé une méthode alternative pour pallier à la non-prise en compte de la dépendance temporelle des variations de $RF\triangle\alpha$ dans la méthode EESF (equation 6). Les auteurs argumentent que si un scénario transitoire ou interannuel avait été modélisé l'application de la méthode EESF aurait largement surestimé les émissions équivalentes de CO_2. A cet effet, ils proposent la prise en compte explicite de la dépendance temporelle des processus de décroissance de CO_2 atmosphérique. Dès lors, une méthode alternative a été proposée par Bright et al. (2016) qui se traduit par l'équation suivante :

$$TDEE = Ae^{-1}K_{CO_2}^{-1}Y_{CO_2}^{-1}RF\Delta\alpha \quad (7)$$

où TDEE (Time dependency emission equivalent) est exprimé en Kg CO_2-eq m^{-2}, yCO_2 correspond aux séries de réponses d'impulsion de CO_2 intégrée sur un horizon de temps.

L'équation 8 traduit la méthode GWP utilisée par l'IPCC (IPCC, 2014). Cette méthode prend en compte la durée de vie du CO_2 dans l'atmosphère.

$$GWP\Delta\alpha = \frac{\sum_0^{t=TH} RF\Delta\alpha(t)}{A_E kCO_2 \sum_0^{t=TH} yCO_2(t)} \quad (8)$$

où GWP est exprimé en Kg CO_2-eq m^{-2}, *TH* correspond à l'horizon temporel (ex. 20. 100. 500 ans). *yCO_2* représente une fonction de réponse impulsionnelle du CO_2 dérivé dans Joos et al. (2013).

Le changement de température moyenne globale (ΔT) est aussi une métriquepour analyser l'impact climatique des changements de pratiques (Sieber et al., 2020). Cette métrique à l'avantage d'inclure l'effet temporel pour mieux mettre en avant la contribution relative des différents polluants. ΔT est exprimé de manière suivante.

$$\Delta T_i(TH) = \sum_{t=0}^{TH} G_i(t) \times AGTP_i(TH - t) \quad (9)$$

Où G correspond à un vecteur annuel d'un polluant i exprimé en kg à un temps t, $AGTP_i$ correspondant au changement de la température globale potentielle absolue après une perturbation d'un polluant i à t0 exprimé en K/kg. Pour les GES, l'AGTP est exprimé par l'équation suivante : $AGTP_i(TH) = e_i \int_{t=0}^{TH} IRF_{i(t)} \times IRF_T(TH - t)dt$ (10)

Où e_i correspond à l'efficience radiative, c'est-à-dire le forçage radiatif additionnel par unité d'augmentation de la masse du gaz i dans l'atmosphère (1.37 x 10^{-5} W m^{-2} ppb^{-1} pour le CO_2, 3.00 x 10^{-3} W m^{-2} ppb^{-1} pour N_2O), IRF_i représente la fraction d'un gaz restant dans l'atmosphère après une émission impulsionnelle. IRF_i est dérivé du modèle Bern Carbon Cycle pour le CO_2 (Joos et al., 2013), tandis que IRF_T décrit la réponse en température du système climatique à un forçage radiatif unitaire et est dérivé du modèle de climat HadCM3 (Boucher & Reddy, 2008) représentant les sensibilités climatiques de courtes et de longue durée avec un équilibre d'environ 1.06 K W m^{-2}.

L'étude de Sieber et al. (2020) ont adapté cette approche pour les forçages radiatifs induits par les modifications d'albédo de surface. Cette approche formule l'AGTP comme une intégrale de convolution de deux IRF_T de manière analogue à l'équation 10 et a donc été supposée identique à celle des gaz à effet de serre est exprimée suivant cette équation.

$$AGTP_\alpha(TH) = \sum_{j=1}^{2} C_j \times \left(\left(1 - e^{\frac{-TH}{dj}}\right) - \left(1 - e^{\frac{-(TH-a)}{dj}}\right) u(TH - a) \right) \quad (11)$$

Le premier terme exponentiel représente la réponse à un forçage soutenu, le second terme de l'équation élimine la réponse de la perturbation pour TH ≥ a. La fonction échelon de Heaviside u(t) a été définie ici pour renvoyer 1 pour t ≥ 0 et 0 sinon. L'élimination commence

à *a*, qui peut être interprété comme la durée de vie de la perturbation en années. c_j et d_j sont des grandeurs adimensionnelles dérivées du modèle HadCM3 (Boucher et Reddy, 2008) représentant respectivement les sensibilités climatiques de courtes (c1 = 0.631) et de longues durées (c2 = 0.429) et aux réponses climatiques de courtes (d1 = 8.4) et de longues durées (d2 = 409.5).

Ces métriques peuvent être utilisées dans le cadre d'évaluer l'impact climatique à différentes échelles temporelles. GWP est une métrique souvent utilisée pour convertir le RF de l'albédo en équivalent CO_2 pour le comparer avec les GES (Betts, 2000; Muñoz et al., 2010; Sieber et al., 2020). Sieber et al., (2020) ont utilisé cette métrique dans le cadre d'une analyse de cycle de vie (ACV) d'un système de bioénergie. Elle peut être aussi utilisée dans le cadre d'évaluer l'impact climatique des changements de pratiques (Liu et al., 2022a). Dans le cadre de ces travaux, le GWP est utilisé pour analyser l'effet climatique des changements de pratique en AC du fait de sa facilité de mise en œuvre et ΔT est utilisé également pour étudier la durée de vie des différents polluants et leurs contributions relatives.

2.5 Modélisation de l'albédo de surface

L'albédo est un paramètre clef du bilan d'énergie de la terre. Depuis l'ère industrielle, les changements d'occupation et d'utilisation des terres se sont accentués entraînant une modification de l'albédo de surfaces. Il gouverne l'énergie solaire restant à la surface du globe et a le pouvoir d'induire des forçages radiatifs positifs (réchauffement) ou négatifs (refroidissement). Toutefois l'albédo est peu, mal ou pas pris en compte dans nombre de modèles de systèmes de cultures. Il manque également dans les modèles de systèmes de cultures et dans nombre de schémas de surface des modèles de climat une prise en compte des effets des pratiques sur la modification de l'albédo de surface et de leurs conséquences sur la partition de l'énergie. Outre les pratiques, ces modèles ne prennent pas en compte certains déterminants de la variation d'albédo de surface comme l'humidité de la couche superficielle du sol, la couleur, l'effet de la sénescence des feuilles et des organes des plantes. **DSSAT** par exemple, qui est un modèle agrométéorologique très utilisé, calcule l'albédo de manière très simple en ne tenant pas compte de possibles variations selon les contextes

pédoclimatiques. Dans ce modèle l'albédo de surface varie entre l'albédo du sol (0.1) et de la végétation (0.2) dépendant du LAI durant la période de croissance (Équation I-9).

Le modèle **APSIM** calcul aussi l'albédo à peu près comme le modèle DSSAT avec un albédo du sol et un albédo de la canopée qui varie avec la croissance des plantes et donc avec le LAI (Équation 12).

$$\alpha_{DSSAT} = 0.1 \times e^{-0.7 \times LAI} + 0.2 \times (1 - e^{-0.7 \times LAI}) \quad (12)$$

$$\alpha_{APSIM} = \alpha sol + 0.25 \times (0.23 - \alpha sol) \times LAI \quad (13)$$

avec αsol représentant l'albédo du sol nu

Le modèle **STICS** (**S**imulateur Mul**TI**disciplinaire pour les **C**ultures **S**tandards) a une approche plus détaillée du calcul de l'albédo de surface (Équation 14). Dans ce dernier, l'albédo de surface varie entre l'albédo du sol nu et l'albédo de la végétation. L'albédo du sol nu est fonction de l'humidité de surface et de la présence ou non d'un couvert de paillis (Equation 13). L'albédo varie de la croissance des plantes, il est donc fonction du LAI.

$$\alpha_{STICS} = \alpha_{veg} - (\alpha_{veg} - \alpha_{sol}) \times e^{-0.75 \times LAI} \quad (14)$$

$$\alpha_{sol} = Pa_{sol} \times (1 - 0.517 \times \frac{HUR(i,1) - HUMIN(1)}{HUCC(1) - HUMIN(1)}) \times (1 - couvermulch(i)) + Pa_{mulch} \times couvermulch(i) \quad (15)$$

avec Pa_{sol} la valeur de paramètre d'albédo du sol sec, *HUR* correspond au contenu en eau de la couche superficielle, *HUMIN* est l'humidité au point de flétrissement de la couche superficielle, *HUCC* est l'humidité à la capacité au champ de la première couche, *couvermulch* est le taux de couverture du mulch et Pa_{mulch} correspond à la valeur de paramètre représentant l'albédo du mulch.

Le modèle de système de culture STICS peut simuler l'effet des pratiques (ex. mulch, no-tillage). Néanmoins, la prise en compte de l'effet albédo de la végétation est simpliste. En effet, STICS ne prend pas en compte l'effet de la phénologie sur la dynamiques d'albédo.

3. Justifications scientifiques et questions de recherches

Cette thèse vise 1) à évaluer l'impact climatique de deux pratiques d'agriculture de conservation des sols (*i.e.* no-tillage et mulching) en comparaison à une pratique conventionnelle, 2) à en quantifier les composantes biogéophysiques et biogéochimiques afin de comprendre et d'identifier ses potentiels leviers d'atténuation et d'adaptation selon

les contextes locaux.

Les questionnements scientifiques qui se sont posées durant cette thèse sont :

- Quels sont les impacts biogéophysiques, en particulier des effets albédo, du non travail du sol (no-tillage) et de la gestion des résidus de cultures (mulching) sur le climat ?
- Quels sont les déterminants de ces effets ?
- Sont-ils différents en fonction du type et/ou couleur du sol ?
- Sont-ils compensateurs ou amplificateur du potentiel d'atténuation de l'AC (Agriculture de Conservation) via les effets biogéochimiques ?

Pour ce faire deux approches ont été développées : 1) une approche terrain basée sur de l'instrumentation installée sur deux sites au Zimbabwe et des mesures faites de manière répétée durant la saison de culture et la période d'interculture, et 2) une approche par modélisation basée sur le modèle agronomique STICS pour permettre de mieux comprendre les processus étudiés et pour évaluer les capacités du modèle à reproduire les phénomènes observés.

Pour répondre aux questions posées, le travail a été divisé en trois grandes parties. La première partie de cette thèse est dédiée à la collecte et à l'analyse des données de terrain sur deux sites expérimentaux au Zimbabwe (voir chapitre I). Les dynamiques d'albédo de surface liés aux changements des pratiques agricoles ont été analysés pour des sols contrastés typiques de la région : un Lixisol abruptique sableux, de couleur claire, et un Ferralsol xanthique argileux, de couleur sombre. Ces sols sont très représentatifs de la région étudiée et en Afrique subsaharienne en générale (Figure 6).

Les interactions entre le type de sol et les systèmes de culture sur l'albédo de surface, la température du sol et le rayonnement infrarouge ont également été étudiées. De plus, la relation entre les dynamiques de l'albédo de surface et l'humidité du sol, ainsi qu'entre l'albédo de surface et l'indice de surface foliaire (LAI), a été examinée.

La seconde partie est consacrée à la comparaison des effets biogéochimiques et biogéophysiques de l'agriculture de conservation (AC) (voir chapitre II). La magnitude des effets biogéophysiques induits par les changements d'albédo de surface a été comparée aux

effets biogéochimiques, tels que le stockage du carbone (C) et les émissions de N_2O à court, moyen et long terme.

La troisième partie est exclusivement axée sur la modélisation des processus biogéophysiques à l'aide du modèle STICS (voir chapitre III). Ce chapitre est consacré à l'évaluation de la capacité du modèle STICS à prédire l'albédo de surface de différentes pratiques culturales sur deux types de sols contrastés.

Trois étapes principales ont été suivies :

- Une première étape de calibration de la culture du maïs en Afrique subsaharienne,
- Une évaluation du formalisme actuel de l'albédo à partir des données observées,
- Une amélioration du formalisme de l'albédo, suivie de l'analyse de son impact sur les autres variables produites par le modèle,
- Une évaluation et une validation du nouveau formalisme.

Ces modifications du formalisme permettraient de mieux analyser les effets biogéophysiques et biogéochimiques associés aux changements de pratiques agricoles, en utilisant le modèle STICS, dans l'optique d'identifier les leviers potentiels d'atténuation selon les contextes locaux.

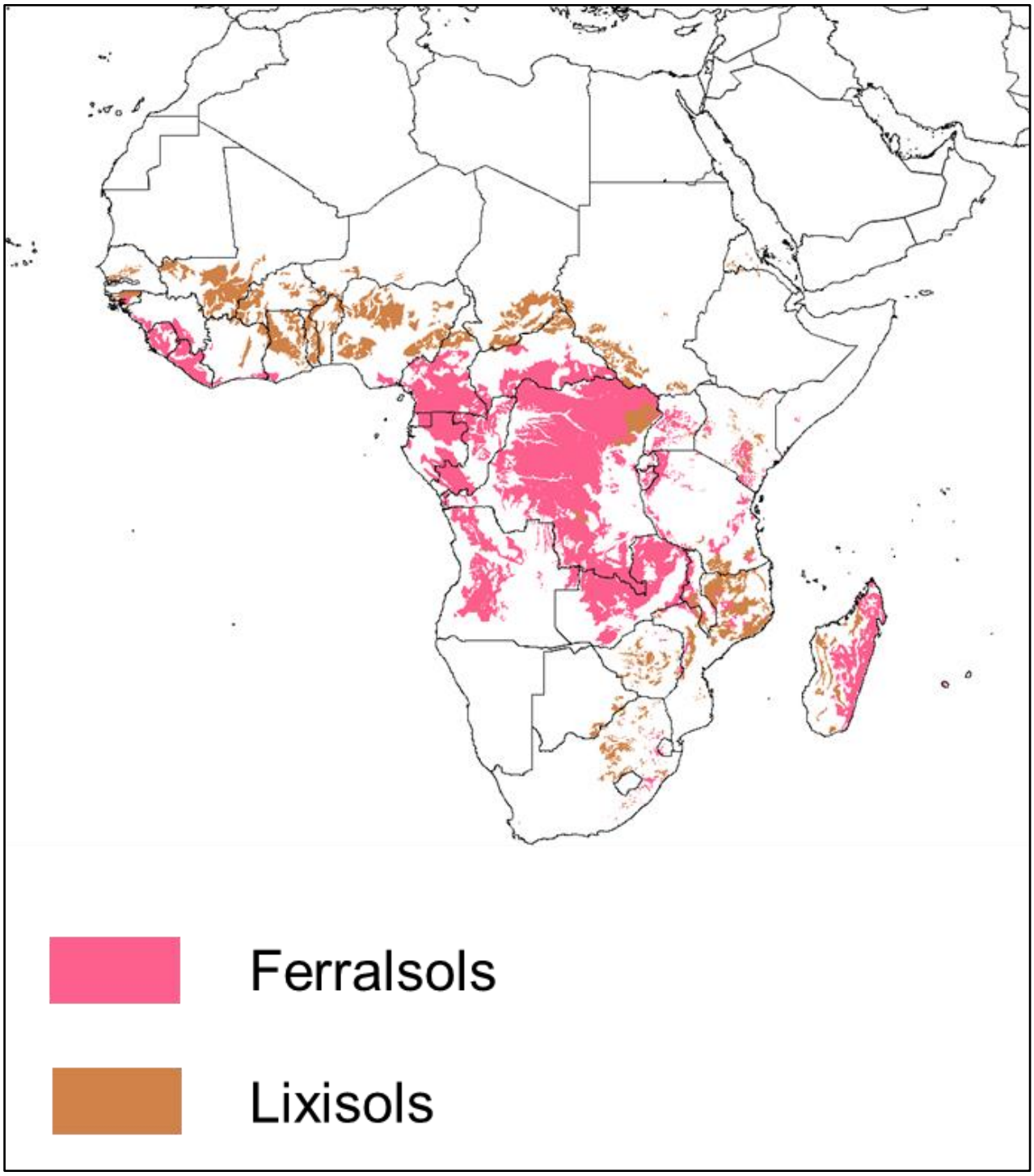

Figure 6. Représentativité des sols étudiés en Afrique. Les Lixisols et les Ferralsols sont très représentatifs en Afrique subsaharienne en se référant (Fisher et al., 2008)

Matériels et méthodes

1. Description des sites

Cette étude est réalisée sur deux expérimentations de longue durée du CIMMYT au Zimbabwe (Figure 7). Ces essais ont été établis depuis 2013 sur deux types de sol différents : un Ferralsol xanthique et un Lixisol abruptique. Le premier site se situe à dans le district de Mazowe (17°43'15.1"S 31°01'15.8"E) à X km d'Harare, la capitale du Zimbabwe, et il sera nommé dans cette étude UZF (University of Zimbabwe Farm). Le deuxième site se localise dans le district de Goromonzi à 20 km environ au nord d'Harare, dans le village de Domboshawa (17°36'23.3"S 31°08'26.8"E) appelé dans le cadre de cette étude DTC (Domboshawa Training Center). Les deux sites sont composés de 8 traitements répétés 4 fois mais dans le cadre de cette étude nous nous focalisons sur 3 d'entre eux qui sont : le Conventional Tillage[2] (CT), No Tillage[3] et No Tillage and Mulch[4] avec une monoculture de maïs (*Zea mays* L.).

[2] Labour traditionnel, agriculture avec travail du sol
[3] Semis direct sans travail préalable du sol
[4] semis direct avec sol couvert par des résidus de culture

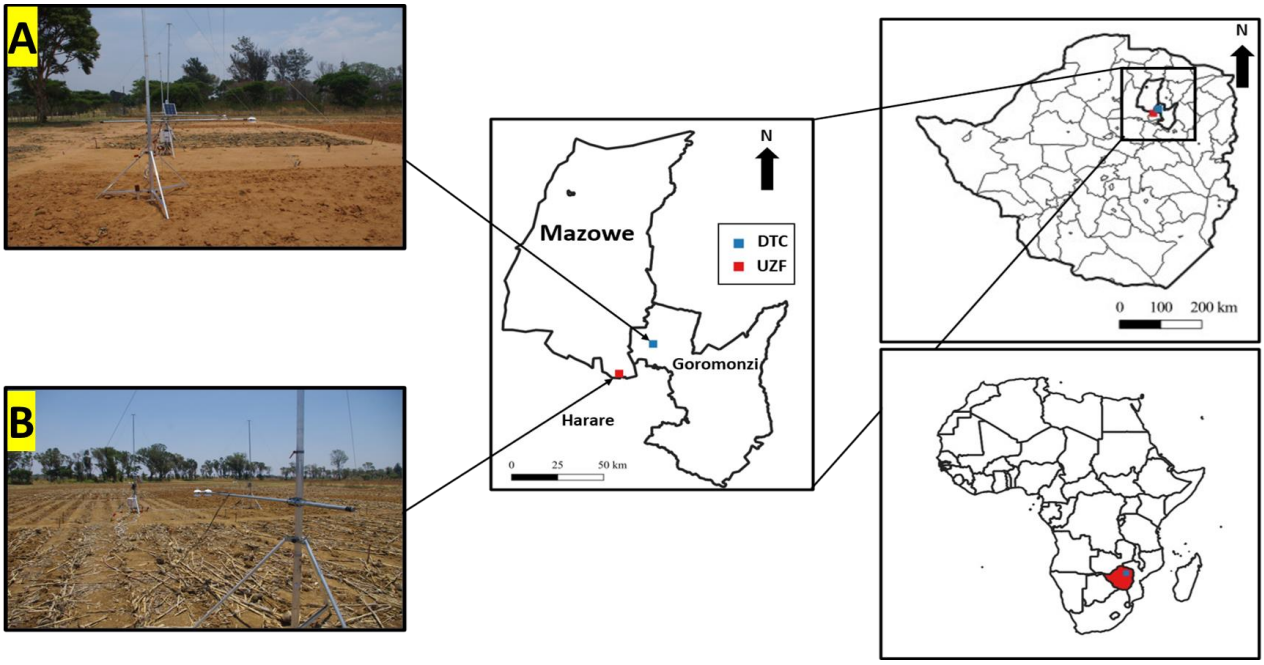

Figure 7. La figure (A) correspond au site situé à Domboshawa (DTC) et installé sur un sol sableux de type Lixisol, et la figure (B) correspond au site du CIMMYT (UZF) installé sur un sol plus argileux de type xanthic Ferralsol.

Table 1 : Description générale des deux sites ; coordonnées, traitements, types et propriétés de sols, moyennes annuelles mesurées sur chaque site. Les abréviations des traitements sont respectivement CT : Conventional tillage, NT : no-tillage, NTM : no-tillage with mulch.

			DTC	UZF
Caractéristiques	Coordonnées		17°36'23.3"S,31°08'26.8"E	17°43'15.1"S,31°01'15.8"E
	Traitements		CT, NT, NTM	CT, NT, NTM
	Dimension des placettes		12x6 m	12x6 m
	Type de culture		Maïs (*Zea mays* L.)	Maïs (*Zea mays* L.)
Sol	Type de sol		***Lixisol abruptique***	***Ferralsol xanthique***
	Texture 0-20 cm		Sable (80%), argile (10%), Limon (20%)	Sable (50%), argile (30%), Limon (20%)
Météo	Précipitations (mm)	2021/22	1219	907
		2022/23	1322	941
	Température Moyenne	2021/22	19.7	20.6
		2022/23	21.5	21.6
	Température minimale	2021/22	18.5	18.5
		2022/23	19.2	20.5
	Température maximale	2021/22	21.7	19.3
		2022/23	23.9	22.8

2. Mesure de la dynamique de la végétation

2.1 Dynamique d'indice foliaire (LAI)

L'indice foliaire leaf Area Index en anglais (LAI) est une grandeur physique exprimée en mètre carré de feuille par mètre carré de sol. Il est l'une des caractéristiques mesurées pour connaître l'état de la végétation et aussi quantifier la vitesse de croissance des plantes (N.J.J. Bréda, 2008).

Dans cette étude, le LAI2200c plant Canopy Analyzer de Li-COR a été utilisé pour mesurer le PAI (Plant Area, Index, i.e. la surface des feuilles + tiges + autres organes aériens) qui prend en compte l'ensemble des surfaces assimilatrices de la plante. Cet instrument permet de prendre des mesures sans attendre que la position du soleil change et enregistre aussi la

lumière à partir de 5 angles de zénith différents avec une seule lecture. Le capteur du LAI2200c reçoit juste les rayonnements inférieurs à 490 nm gamme de longueur d'onde où la réflectance et la transmittance des feuilles sont minimales. Le LAI220c calcul le PAI en faisant le ratio entre les mesures prises au-dessus de la canopée et en dessous. Ces données collectées sont utilisées pour la détermination du rayonnement intercepté par la canopée sur 5 angles.

Des mesures ont été prises pour chaque traitement sur chaque site en utilisant le même protocole avec une mesure au-dessus de la canopée et 4 mesures en dessous. Les mesures en dessous de la canopée sont réparties sur le transect entre deux rangs. La première mesure en dessous de la canopée est prise d'abord sous la canopée à 10 cm sous les feuilles les plus basses, à 25% du rang, au milieu du rang (50%) et à 75% du rang de départ et de manière diagonale (Figure 8). Les données sont directement enregistrées sur la console et à l'aide du logiciel FV2200C le PAI moyen par parcelle peut être calculé ainsi que les écart-types. Ces mesures ont été prises 3 semaines après le semis jusqu'à la sénescence du maïs.

2.2 Taux de couverture (GFCC)

Appelé dans cette étude GFCC comme Green Fractional Canopy Cover, le taux de couvert est aussi une variable qui nous renseigne sur le développement du couvert et la densité des feuilles. La fréquence de mesure est similaire à celle du LAI. Le GFCC est exprimé en pourcentage (%) de couverture du sol. L'application Canopeo (Patrignani and Ochsner, 2015) est utilisée pour mesurer le taux de couverture. Les mesures s'effectuent en prenant des photos à 50 cm au-dessus du couvert, l'application effectue une classification en séparant les pixels verts du reste en utilisant le **Excess Green Index** mettant en contraste les parties vertes du spectre avec le rouge et le bleu pour distinguer la végétation du sol (Patrignani and Ochsner, 2015). Pour chaque placette, 4 images sont prises et ces dernières sont moyennées pour avoir le taux de couverture de la parcelle (Figure 9).

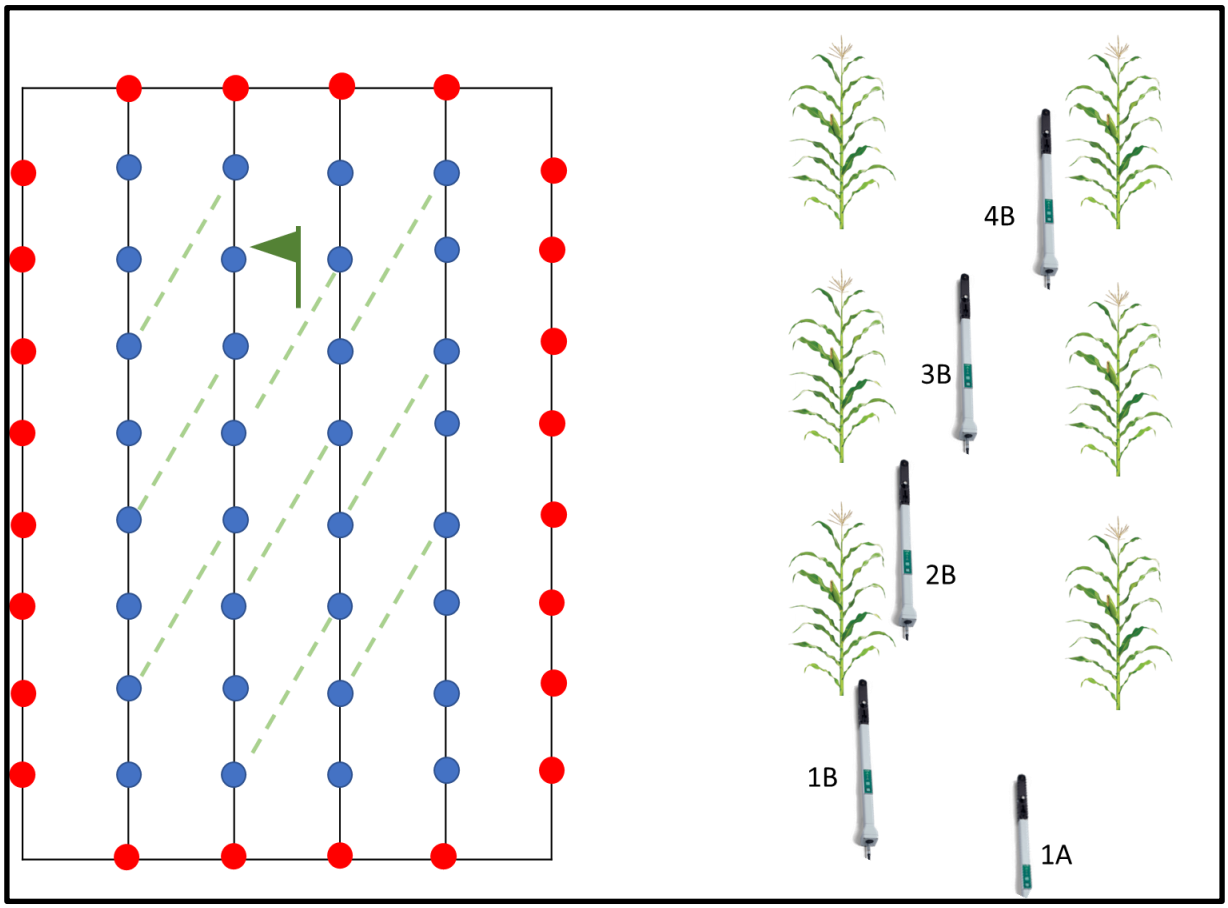

Figure 8. Protocole de mesure du PAI. 1A est la mesure prise au-dessus du couvert avec A comme "above", 1,2,3,4B avec B comme "below" sont les mesures prises en dessous du couvert. Les lignes discontinues vertes en diagonales représentent les transectes sur lesquelles les mesures ont été prises.

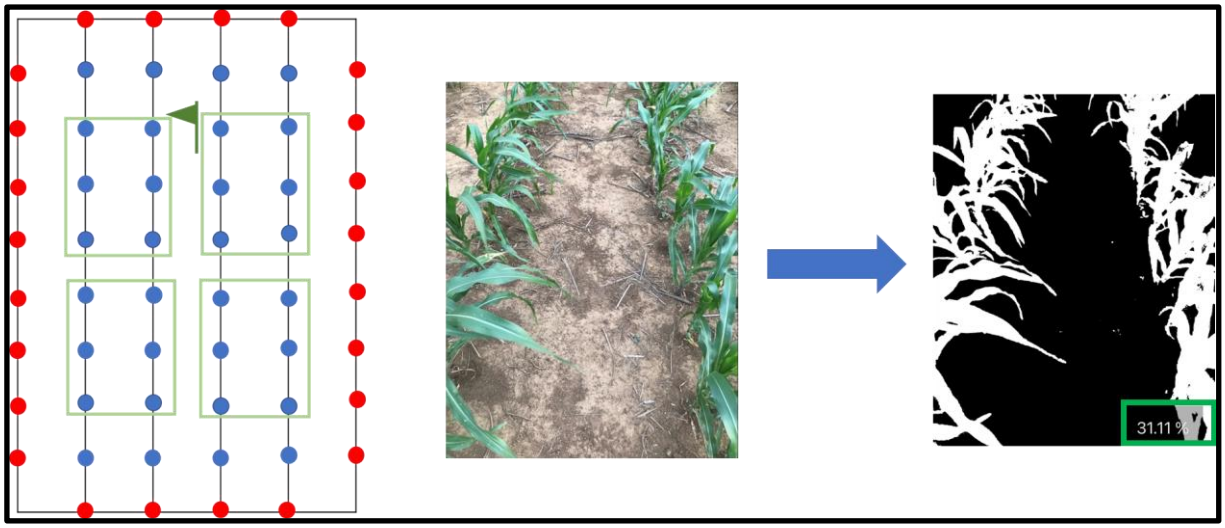

Figure 9. Protocole de mesure du taux de couverture. Les carrés verts représentent les photos prises sur les zones cibles pour mesurer le taux de couverture du sol par de la végétation verte avec l'application mobile Canopeo.

3. Mesure des variables météorologiques

3.1 Mesure du rayonnement courtes et longues longueurs d'ondes

Pour chaque site, trois (3) traitements ont été sélectionnés (CT, NT, NTM) (Figure 6). Des capteurs NR01 sont installés au centre de chaque parcelle pour mesurer le rayonnement solaire incident et réfléchi (SW_{in}, SW_{out}) et le rayonnement atmosphérique et terrestre de longue longueur d'onde (LW_{in}, LW_{out}). Le NR01 est un radiomètre à 4 composantes dont deux sont orientées vers le ciel et deux vers le sol (Diop, 2023) Nature Earth and Environment Reviews et présenté en Annexe 1 (Diop, 2023). L'instrument est équipé d'un pyranomètre à onde courte mesurant le rayonnement solaire incident et réfléchi entre 305 et 2800 nm et d'un pyrgéomètre mesurant le rayonnement à ondes longues couvrant entre 4500 et 50 000 nm (Figure 10). Les mâts sur lesquels les capteurs sont fixés ont été installés au centre des placettes pour que les mesures soient, au mieux, représentatives du traitement tout en évitant les effets de bords. L'albédo est mesuré par le pyranomètre en faisant le rapport entre le rayonnement onde courte réfléchi et incident (Équation 16). Les rayonnements ondes longues et ondes courtes mesurés par les pyranomètres et les pyrgéomètres permettent de calculer le rayonnement net (Équation 17). Les capteurs sont placés à 150 cm au-dessus du sol en période d'interculture, où le sol est nu ou couvert par des résidus, et 150 cm au-dessus de la canopée en période de végétation.

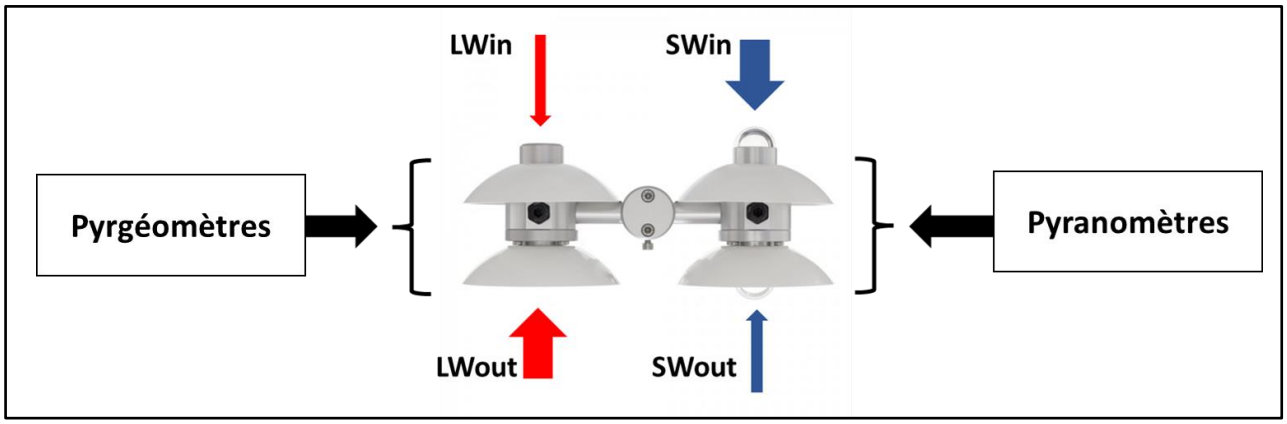

Figure 10. Radiomètre à 4 composantes. LWin représente le rayonnement grande longueur d'ondes entrant et LWout le rayonnement grande longueur d'onde sortant. SWin correspond au rayonnement courte longueur d'onde incident et SWout le rayonnement courte longueur d'onde réfléchi. Les capteurs mesurant les rayonnements courtes longueurs d'ondes sont les pyranomètres et ceux qui mesurent les rayonnement grandes longueurs d'ondes sont les pyrgéomètres.

Le dispositif expérimental est doté également d'une centrale d'acquisition avec des cartes de mémoire pouvant stocker les données selon la fréquence indiquée dans le programme. Dans le cadre de cette étude, les mesures sont stockées en suivant des moyennes semi-horaires (30 minutes).

L'expérimentation est aussi équipée d'une station météo ATMOS-41 (METERgroup, inc) qui mesure la température et l'humidité de l'air à 2 mètres, les précipitations, la direction et la vitesse du vent (Figure 10). Chaque parcelle est également équipée de sondes de température et d'humidité du sol (5TM et TEROS 11) à 1, 10 et 20 cm de profondeur (Figure 11).

$$\alpha = \frac{SWout}{SWin} \quad (16)$$

$$Rn = Swin - SWout + LWin - LWout \quad (17)$$

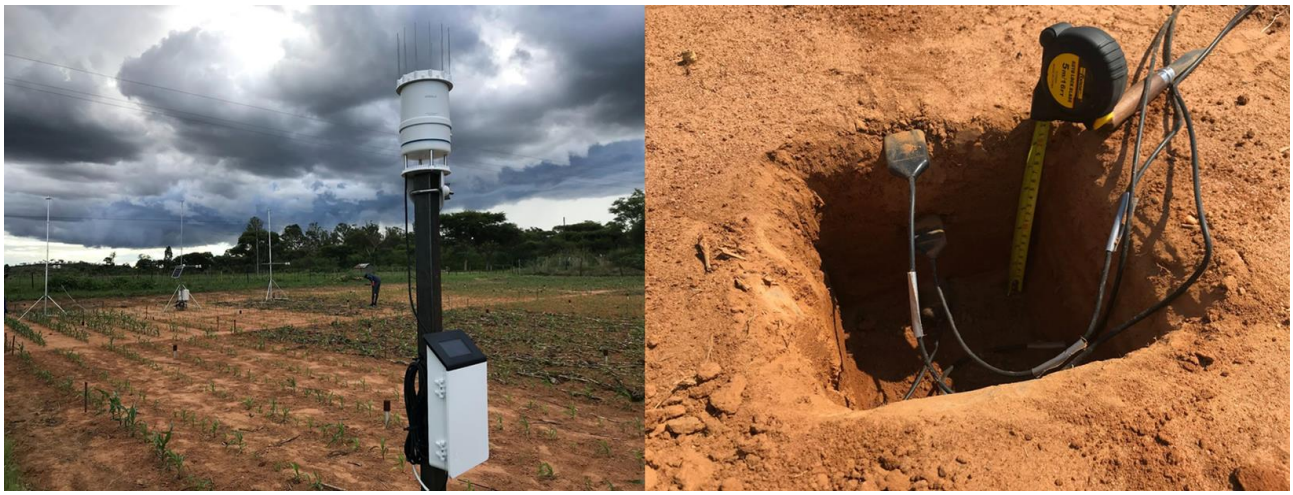

Figure 11. A gauche la station météo (METER group) pour mesurer la température de l'air, l'humidité de l'air, la vitesse du vent à 2 m de hauteur et la précipitation. A droite, les sondes pour mesurer en continu la température et l'humidité du sol à 1, 10 et 20 cm de profondeur.

4. Approche de modélisation

Une approche par modélisation a aussi été employée au cours de ces travaux de thèse dans l'optique de tester la capacité du modèle de système de culture STICS (**S**imulateur mul**TI**disciplinaire pour les **C**ultures **S**tandard) à simuler l'albédo, les composantes du bilan d'énergie et du bilan d'eau. STICS est de base un modèle de fonctionnement des cultures développé par l'INRA en 1996 (Brisson et al., 2003) pour le blé et le maïs. Avec le temps, le modèle a été enrichi et de nombreux processus y ont été ajoutés et il est adapté à une vingtaine d'espèces cultivées de types pérennes, annuelles, herbacées ou ligneuses. STICS est un modèle dynamique à pas de temps journalier simulant le fonctionnement d'un système se composant d'un couvert végétal, le sol et l'atmosphère qui est représenté par des variables climatiques d'entrée, et donc de forçage. Du point de vue informatique, le modèle a un fonctionnement modulaire et chaque module représente un ensemble de processus comme la phénologie, la croissance des feuilles, le bilan d'eau, la photosynthèse, le microclimat… Le modèle requiert des données climatiques en entrée décrivant quotidiennement l'état de l'atmosphère au voisinage du système tels que le rayonnement solaire incident, la température (maximum et minimum), et les précipitations, la vitesse du vent, l'humidité relative et l'évapotranspiration de référence (ET0). De plus, il simule l'impact des pratiques agricoles en intégrant des informations d'itinéraire technique comme la date de semis, les quantités et types d'engrais utilisés ou encore le calendrier d'irrigation.

4.1 Pourquoi STICS et quelles attentes ?

Le modèle STICS à une bonne représentation de la gestion des pratiques et notamment de celles qui concernent l'AC (labour, apport de paillis, absence de labour). De plus, il a été déjà calibré et validé sur beaucoup d'espèces de cultures dans différents contextes pédoclimatiques, et notamment le maïs qui la culture que j'étudie dans cette thèse. Aujourd'hui, le modèle se tropicalise de plus en plus avec des travaux menés par exemple en Afrique subsaharienne (Sow et al. 2024 ; Traoré et al. 2022) ou au Brésil (Affholder et al., 2003).

STICS est un modèle qui simule des processus biogéochimiques (ex. carbone du sol, émissions GES…) mais également des processus biogéophysiques tels que les changements d'albédo due aux effets de pratiques culturales, l'évapotranspiration…. Nonobstant, la représentation de certains processus demeure simpliste d'autant plus que le modèle n'était pas destiné à l'évaluation de fonctionnement de surface.

Dans cette étude, mon premier objectif était d'analyser la capacité de STICS à simuler les dynamiques d'albédo de surface et ses effets sur les composantes du bilan d'énergie (ex. Rn,G, H, LE) à partir des formalismes actuels (Équation 12 et 13, Figure 11) et aussi, si nécessaire de proposer des pistes d'amélioration de certains modules et/ou formalismes (voir Chapitre III). Les améliorations, si nécessaires, devaient se baser sur les observations faites durant deux saisons culturales sur les 2 sites au Zimbabwe, ce qui pourrait aussi me permettre d'avoir une meilleure compréhension des processus.

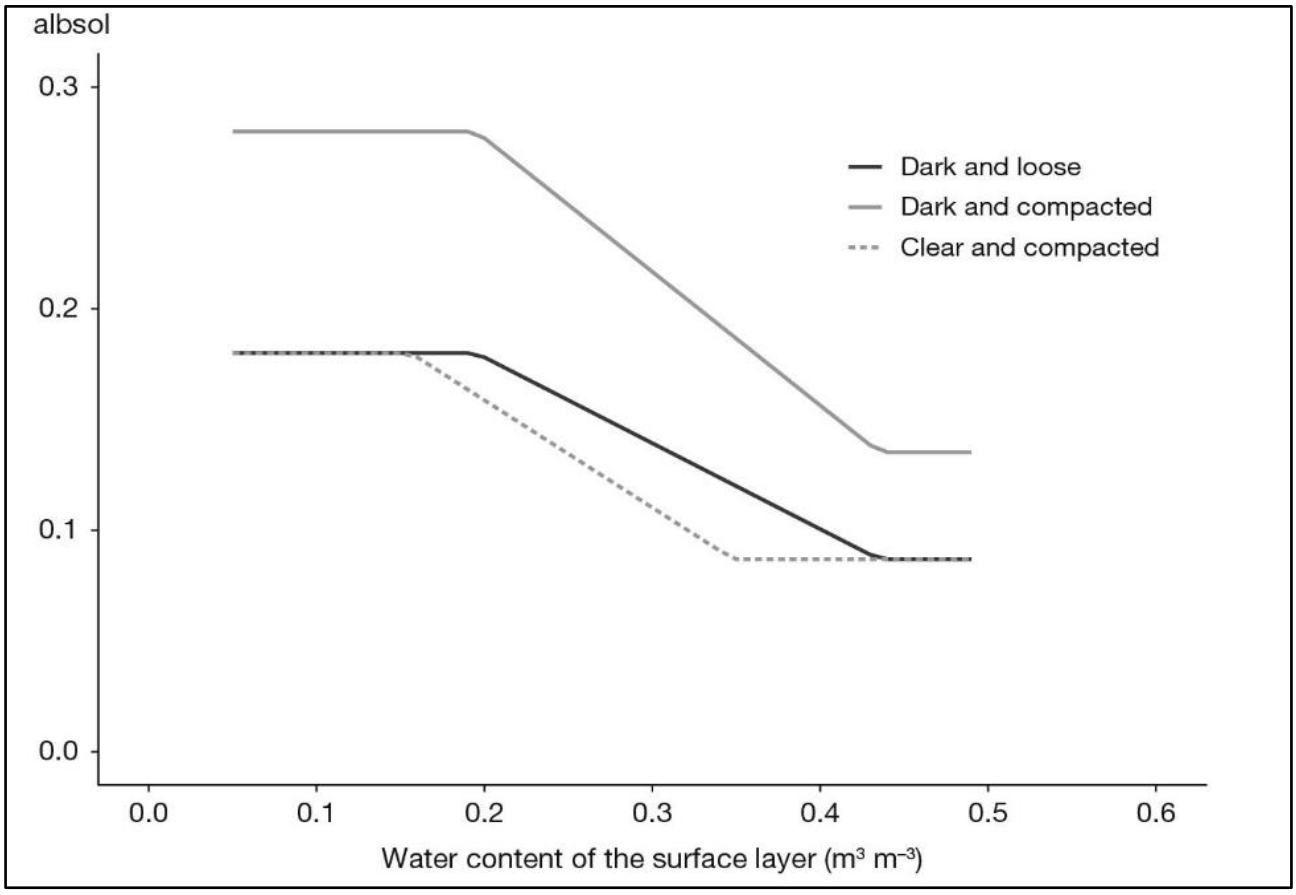

Figure 12. Représentation de la relation entre l'albédo de surface et le contenu en sol de la couche superficielle (Beaudoin et al., 2023)

Chapitre I : Albédo de surface et rayonnement thermique en agriculture de conservation

Ce chapitre est adapté d'un article soumis au journal Agricultural and Forest Meteorology.

Résumé en français :

Le potentiel de l'agriculture de conservation (CA) pour l'atténuation du changement climatique a été le plus souvent évalué en mettant l'accent sur les effets biogéochimiques tels que le stockage carbone et/ou les émissions de gaz à effet de serre. Cependant, des études récentes ont montré que les pratiques de gestion peuvent également influencer le climat local et global via des processus biogéophysiques, tels que les changements dans l'albédo de la surface. Actuellement, les études sur les effets biogéophysiques de la CA sont rares, en particulier en Afrique. Cette étude évalue les effets biogéophysiques des systèmes de culture en CA avec du maïs (*Zea mays* L.) en Afrique australe. Des mesures ont été effectuées de manière continue pendant deux années de culture sur deux sites expérimentaux à long terme au Zimbabwe, présentant des caractéristiques de sol contrastées : un site avec un Lixisol abruptic, sable rouge clair, et un site avec un Ferralsol xanthique, brun-jaune foncé et argileux. La dynamique de l'albédo de surface, du rayonnement à ondes longues, de l'indice de surface foliaire du maïs, de l'humidité et de la température du sol a été surveillée sous trois traitements différents : labour conventionnel (CT), non-labour (NT) et non-labour avec paillis (NTM). Au cours de la saison 2021/22, le paillis dans le NTM a été appliqué à la semence, tandis qu'il a été appliqué à la semence et après la récolte au cours de la saison 2022/23. Nos résultats ont montré que l'albédo de

surface moyen annuel sur deux ans sous NT (0.17) et NTM (0.17) a légèrement augmenté par rapport à CT (0.16) sur le sol argileux brun-jaune foncé, entraînant un forçage radiatif instantané négatif (iRF), c'est-à-dire un effet de refroidissement sur le climat. Les valeurs moyennes d'iRF étaient plus élevées au cours de la saison 2021/22 qu'au cours de la saison 2022/23, avec respectivement -0.83 W.m-2 vs. -0.43 W.m-2 pour NT et -1,43 W.m-2 vs. -1,03 W.m-2 pour NTM. Sur le sol sableux rouge clair, l'albédo de surface était plus élevé sous NT (0.27) que sous CT (0.24), mais beaucoup plus bas avec paillis (0.23). La rétention des résidus de culture a donc entraîné un forçage radiatif instantané positif, c'est-à-dire un effet de réchauffement sur le climat, de 1,14 W.m-2 et 2,77 W.m-2 au cours de la première et de la deuxième année de culture, respectivement.

En résumé, nos résultats démontrent l'importance de prendre en compte les effets biogéophysiques lors de l'étude des pratiques telles que l'agriculture de conservation pour l'atténuation du changement climatique. Ils suggèrent également que l'albédo du sol est une caractéristique du site importante qui doit être prise en compte lors de la promotion de l'agriculture de conservation pour l'atténuation du changement climatique.

Surface albedo and thermal radiation dynamics under conservation and conventional agriculture in subhumid Zimbabwe

Souleymane Diop[1,2,3*], Rémi Cardinael[3,4,5], Ronny Lauerwald[1], Morgan Ferlicoq[2], Christian Thierfelder[6], Regis Chikowo[5,6], Marc Corbeels[4,7], François Affholder[4,8,9], Frédéric Baudron[4], Eric Ceschia[2]

[1]Université Paris-Saclay, INRAE, AgroParisTech, UMR EcoSys, 91120 Palaiseau, France

[2]CESBIO–Univ. Toulouse III/CNRS/CNES/IRD/INRA, 18 avenue Edouard Belin, 31401 Toulouse Cedex 9, France

[3]CIRAD, UPR AIDA, Harare, Zimbabwe

[4]AIDA, Univ. Montpellier, CIRAD, Montpellier, France

[5]Department of Plant Production Sciences and Technologies, University of Zimbabwe, Harare, Zimbabwe

[6]International Maize and Wheat Improvement Center (CIMMYT), P.O. Box MP 163, Mount Pleasant, Harare, Zimbabwe

[7]IITA, International Institute of Tropical Agriculture, PO Box 30772, Nairobi 00100, Kenya

[8]CIRAD, UPR AIDA, Maputo, Mozambique

[9]Universidade Eduardo Mondlane, Faculdade de Agronomia e Engenharia

*Corresponding author. E-mail address: souleymanediop@myyahoo.com

Keywords: Sub-Saharan Africa, climate change mitigation, biogeophysical effects, no-tillage, mulch

Abstract

The potential of conservation agriculture (CA) for climate change mitigation has most often been assessed with a focus on biogeochemical effects such as soil organic carbon sequestration and greenhouse gas emissions. However, recent studies have shown that management practices may also impact local and global climates through biogeophysical processes, such as changes in the surface albedo. This study assessed the biogeophysical effects of CA cropping systems with maize (*Zea mays* L.) in Zimbabwe. Measurements were conducted continuously over two crop years at two long-term experimental sites with contrasting soil characteristics: an abruptic Lixisol and a xanthic Ferralsol. The dynamics of surface albedo, longwave radiation, the maize leaf area index, soil moisture and temperature were monitored under three different treatments: conventional tillage (CT), no-tillage (NT) and no-tillage with mulch (NTM). Our results revealed that the average annual surface albedo across two years under NT (0.17) and NTM (0.17) slightly increased relative to that under CT (0.16) on Ferralsol, resulting in negative instantaneous radiative forcing (iRF), i.e., a cooling effect on the climate. The average values of iRF were greater during the 2021/22 season than during the 2022/23 season, with values of -0.83 W m^{-2} vs. -0.43 W m^{-2} for NT and -1.43 W m^{-2} vs. -1.03 W m^{-2} for NTM, respectively. For Lixisol, the surface albedo was greater under NT (0.27) than under CT (0.24) but was much lower under mulch (0.23). The retention of crop residues therefore led to positive instantaneous radiative forcing, i.e., a warming effect on the climate. This warming effect was 1.14 W m^{-2} and 2.77 W m^{-2} during the first and second crop years, respectively. Overall, our results suggest that the soil background albedo is an important site characteristic that needs to be considered and

demonstrates the importance of considering biogeophysical effects when promoting practices such as CA for climate change mitigation.

1. Introduction

The climate impact of cropland management is usually assessed in terms of biogeochemical effects such as soil organic carbon (SOC) sequestration (Beillouin et al., 2023) or greenhouse gas emissions (Fuentes-Ponce et al., 2022). However, cropland management also affects local heat budgets through changes in surface albedo and thus the fraction of solar radiation that is absorbed and transformed into heat energy and further through changes in the partitioning of the generated heat energy between soil heat fluxes, latent and sensible heat fluxes, and infrared radiation (Lobell et al., 2006; Davin and de Noblet-Ducoudré, 2010; Hirsch et al., 2017). Recent studies have shown that these biogeophysical effects play non negligible roles in the overall climate impact of land use and land management practices (Luyssaert et al., 2014), as they can substantially add to or offset positive biogeochemical effects (Betts, 2000; Kaye and Quemada, 2017; Pique et al., 2023). In croplands, the surface albedo may vary due to various factors, such as crop species, sowing density, crop phenological stage, soil type, topsoil organic matter content, surface roughness, soil moisture and soil coverage by mulch (Matthias et al., 2000; Oguntunde et al., 2006; Cai et al., 2016; Cierniewski et al., 2018). Changes in the surface albedo of croplands may lead to cooling or warming effects at local and global scales (Betts, 2000; Akbari et al., 2009; Sieber et al., 2022).

Conservation agriculture (CA), which covers a range of cropping practices based on minimum soil disturbance, permanent soil cover with crop residues or cover crops, and crop diversification, has been widely promoted for its positive impact on SOC sequestration, although this effect is often limited in magnitude (Franzluebbers, 2010; Powlson et al., 2016; Corbeels et al., 2020). CA practices can, however, also have strong biogeophysical effects.

For example, (Horton et al., 1996) reported that retaining crop residues in no-tillage systems increases the surface albedo on dark soils during bare fallow periods. (Davin et al., 2014) proposed that no-tillage practices lead to local cooling of European croplands in summer due to increased albedo, outweighing reduced evaporation. (Hirsch et al., 2018b) modelled the biogeophysical effects of conservation agriculture, which indicated local cooling in midlatitude regions but potential warming in tropical areas. Finally, (Lobell et al., 2006) reported that, globally, no-tillage systems adopted for croplands cause cooling by approximately 0.2°C, which is comparable to their biogeochemical cooling effect.

The climatic effects of CA were evaluated mostly through the "radiative forcing" (RF) concept. RF is a metric that is used to quantify the changes in the Earth's energy balance (radiation received and emitted by the Earth) that are induced by natural and anthropogenic drivers. Changes in RF may be a result of increasing atmospheric CO_2 concentrations that absorb and re-emit downwards more of the longwave radiation that is emitted by the surface of Earth (Betts, 2000). These changes can also result from a change in the albedo of the atmosphere (cloud cover) or of the surface (Forster et al., 2007). The effects of changes in surface albedo on climate can be quantified via RF metrics (Betts, 2000; Schwaiger and Bird, 2010; Carrer et al., 2018; Bright and Lund, 2021). However, most changes in surface albedo result in changes in energy partitioning (e.g., latent and sensible heat fluxes) and therefore in atmospheric "adjustments" that moderate the instantaneous shortwave radiative forcing (iRF) from albedo changes (Bright and Lund, 2021). Longwave radiation is also an important component of the surface energy budget (Bright et al., 2017; Liao et al., 2020; Breil et al., 2023). The net effects of changes in energy partitioning and iRF are the so-called "effective radiative forcing" (ERF), which is a better indicator of the effective impact of climate change.

Recent model simulations have shown that atmospheric adjustments can either offset albedo change-driven iRF or reinforce it further (Forster et al., 2016; Andrews et al., 2017; Bellouin et al., 2020; Smith et al., 2020). Therefore, assessing the effects of cropland management on both the surface albedo and the infrared radiation emitted by the surface not only helps researchers understand the interactions between the energy flux exchanges between soil, plants and the atmosphere but also their potential interactions with greenhouse gases in the atmosphere (Aydinalp and Cresser, 2008).

To date, no studies have addressed the impact of no-tillage and crop residue retention practices on the surface albedo and longwave radiation for different soil types in Sub-Saharan Africa. In this context, how these agricultural practices modify soil moisture, soil temperature, and crop growth dynamics and their subsequent consequences for the energy budget of these systems are currently not known.

In this study, we examined the effects of no-tillage and crop residue retention (two of the principles of CA) versus conventional tillage at two experimental sites with contrasting soil properties in subhumid Zimbabwe, both with maize monocultures. We evaluated the impacts of these two land management practices on the surface albedo and outgoing longwave radiation and surface temperature dynamics on a daily basis, as well as their interactions with soil type, topsoil moisture and temperature, and crop growth. The changes in surface albedo that resulted from no-tillage and residue mulching, compared with conventional tillage (CT) without mulching, were used to compute the instantaneous radiative forcing (iRF) of both CA practices. Our main hypotheses are that CA has distinct effects on surface albedo dynamics and instantaneous radiative forcing (iRF) as well as on longwave radiation, depending upon 1) the presence or absence of soil tillage and crop

residues on the soil surface, 2) the soil type, and 3) the controlling effects of crop growth and soil moisture dynamics.

2. Materials and methods

2.1 Experimental sites

The study was carried out at two experimental sites in Zimbabwe, established in 2013 by the International Maize and Wheat Improvement Center (CIMMYT): the Domboshawa Training Center (DTC) site in the district of Goromonzi (17°36'23.3"S; 31°08'26.8''E), located approximately 30 km north of Harare, and the University of Zimbabwe Farm (UZF) site in the district of Mazowe (17°43'15.1"S; 31°01'15.8"E), located approximately 10 km north of Harare and approximately 20 km from the DTC site. The experimental sites are characterized by two different soil classes: an abruptic Lixisol (light-coloured red sandy soil, FAO classification, 1997) at DTC and a xanthic Ferralsol (dark-coloured yellowish-brown clayey, FAO classification, 1997) at UZF. The soil at the DTC has a light texture in the top 0–20 cm layer (sandy loam with 15% clay), with an abrupt textural change to sandy clay loam with 30% clay in the 20-40 cm layer (Shumba et al., 2023). The soil texture at UZF is sandy-clay-loam with 34% clay in the first 20 cm (Shumba et al., 2023). The sites both have a subtropical climate with annual minimum and maximum mean temperatures of 12°C and 25°C, respectively, and a rainy season from November to April (Mapanda et al., 2010; Shumba et al., 2023) (Figure I-1). In our study, we conducted field measurements during two cropping years from October 2021 to October 2023. At the DTC, the cumulative rainfall amounts during the first (2021/22) and second (2022/23) cropping years were 1219 mm and 1132 mm, respectively. At UZF, the

total rainfall amounts were 907 mm and 941 mm during the first and second cropping years, respectively.

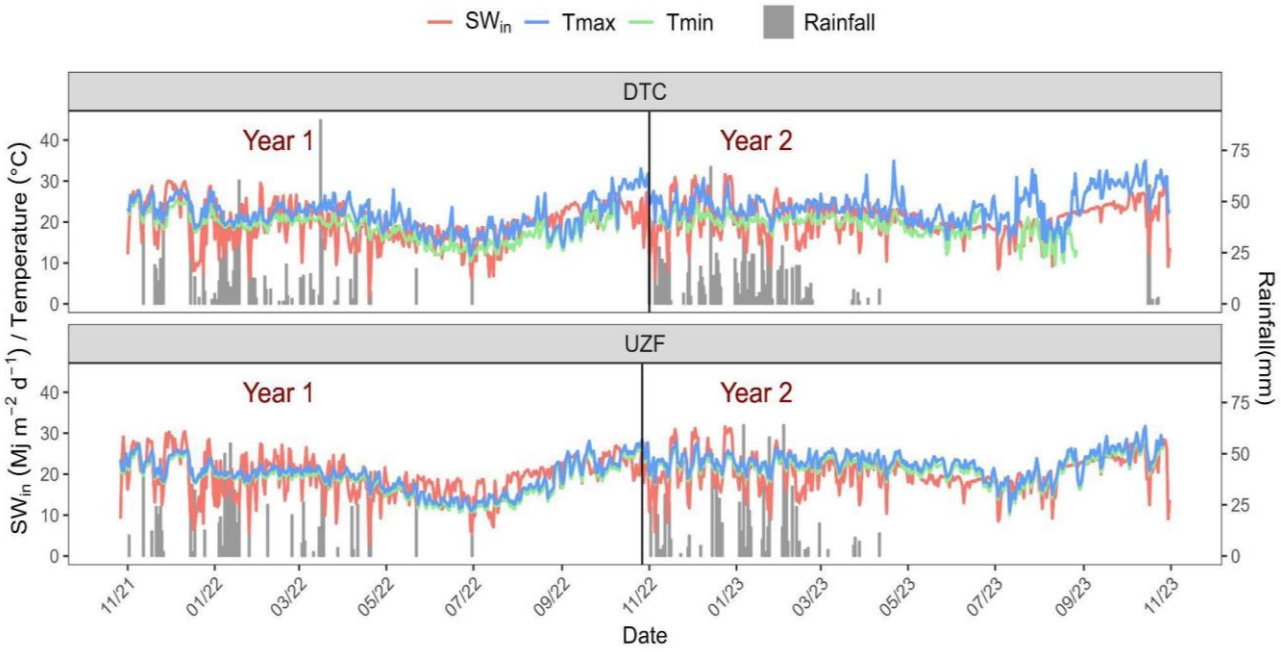

Figure I-1. Daily temperatures, shortwave incoming solar radiation and rainfall over two cropping years at the DTC and UZF sites.

2.2 Experimental treatments

An identical experimental design was set up at both sites, and the treatments were the same in every season since the beginning of the experiment. The dimensions of the experimental plots were 12 × 6 m, and the main crop was maize (*Zea mays* L.). For our study, we considered three of the eight treatments that were established at the sites (Mhlanga et al., 2022): conventional tillage (CT), no-tillage (NT) and no-tillage with mulch (NTM) with continuous maize cropping. The maize crop was sown with a spacing of 25 cm within rows and 90 cm between rows to achieve a plant density of 44,444 plants ha^{-1}. Two or three seeds were sown

per planting hole, and the crop was thinned to one plant per pit after emergence. In the CT treatment, tillage was performed with a hand hoe at both sites, and all the maize residues were removed after harvest. In the NT and NTM treatments, the soil was not tilled, and the maize was sown in planting basins dug with a hand hoe at approximately 15 cm depth at UZF, whereas at DTC, the seeds were placed in riplines made with an animal-drawn ripper (Magoye ripper). Compound fertilizers (nitrogen (N), phosphorus (P) and potassium (K)) were applied to the maize rows at sowing at application rates of 11.6 kg N ha^{-1}, 10.6 kg P ha^{-1} and 9.6 kg K ha^{-1}, respectively. The first and second top dressings were applied four and eight weeks after sowing, respectively, with 23 kg N ha^{-1} each in the form of ammonium nitrate (Shumba et al., 2023).

In the NTM treatment, 2.5 t DM ha^{-1} of maize residue from the previous cropping season was placed on the soil surface approximately two weeks before sowing the maize. After the maize harvest, farmers practising CA in Zimbabwe frequently store their crop residues during the dry season to avoid their consumption by cattle that freely graze in fields during that period. Mulch is thus applied shortly before sowing in the following season, when the cattle are moved to grazing areas away from cultivated land. In that case, the soil is bare during the dry season, even under CA. However, some farmers in Zimbabwe have fences around their fields to prevent cattle grazing and prefer to leave the residues on the soil after harvest, as do most CA practitioners globally, and the soil is never bare. To investigate the impacts of these two management options on the albedo, outgoing longwave radiation and surface temperature dynamics, we varied the setup of the NTM between the first and second cropping years. In the first cropping year, the soil was not covered in the dry season, whereas in the second cropping year, crop residues were directly applied to the soil after harvest and

remained there during both the dry and growing seasons. Based on the image processing of pictures taken approximately 1.5 m above the plots four weeks after mulch application, we estimated that the mulch covered 45% of the soil. Additionally, the kinetic decomposition of the mulch was assessed within 0.25-m^2 quadrats that were sampled on six different dates. The results revealed that 70% and 36% of the mulch at UZF and DTC, respectively, decomposed within three months after application (Figure S1).

2.3 Field measurements

2.3.1 Shortwave and longwave radiation sensors

The sites were equipped with three 4-component net radiometers (NR01, Hukseflux Thermal Sensors, Delft, Netherlands) to monitor incoming (in) and outgoing (out) shortwave (SW) and longwave (LW) radiation (SW_{in}, SW_{out}, LW_{in}, LW_{out}, respectively) for each treatment. This type of radiometer is commonly used for surface albedo monitoring (Sieber et al., 2019). It consists of a pair of pyranometers and a pair of pyrgeometers, with one pair facing upwards and the other facing downwards (Diop, 2023).

The pyranometers measure SW solar radiation in the wavelength spectrum from 0.3 to 2.8 µm, which encompasses the visible and near-infrared spectra. The surface albedo (α) is derived from the two opposite directions of the pyranometer measurements and is calculated with the following equation:

$$\alpha = \frac{SW_{out}}{SW_{in}} \quad \text{(I-1)}$$

where α is the surface albedo, SW_{out} (W m^{-2}) is the amount of solar radiation that is reflected by the Earth's surface and SW_{in} (W m^{-2}) is the global incoming solar radiation.

In our study, the surface albedo was measured continuously at both experimental sites during the growing season from November to April and during the dry season corresponding to the bare fallow period from May to October.

The pyrgeometers are thermal sensors that measure the incoming and outgoing longwave radiation (LW_{in}, LW_{out}, respectively) expressed in W m^{-2} in the wavelength spectrum between 4.5 and 50 µm.

The four-component net radiometers were mounted horizontally on a mast and placed 1.5 m above the ground during the bare fallow period, with a field of view (FOV) of 180° for the pyranometers and 150° for the pyrgeometers. During the growing season, the height of the instruments was adjusted each week to maintain a distance of 1.5 m above the plant canopy. The masts were placed in the middle of the plots to avoid edge effects due to the surrounding land surfaces. The energy balance studies should follow the ISO/TR 9901 guidelines. This norm recommends the height at which the sensors should be mounted to minimize the errors from shadowing effects and to maximize the signal that comes from the targeted area. For small plots, the recommended height is between 1.5 and 2 metres. The challenge in this case is to ensure that the FOV of the downfacing sensors targets the area of interest (sample) as much as possible and avoids mixing with signals from the surrounding areas. A downfacing pyranometer positioned at a height *h* above the area of interest with a radius of *X sample* metres subtends an angle from the nadir expressed as follows:

$$\theta_{sample} = tan^{-1}(\frac{Xsample}{h}) \quad \text{(I-2)}$$

The contribution of the area of interest to be sampled relative to the total signal measured corresponds to the sine of Θ_{sample}. In our study, the sensors were mounted 1.5 m above the target 3 m from the nearest border of the plot, meaning that the total contribution of the plot to be sampled was 89% of the total signal. The remaining 11% of the signal originates from the surrounding areas outside the plot, which were also cropped with maize and therefore have very similar albedo values. We thus conclude that the degree of pollution of our observed signal with contributions from outside the plot of interest is acceptable. Moreover, in our study, we are more interested in the relative changes in surface albedo between treatments (to calculate radiative forcings), specifically no-tillage vs. tillage and mulch vs. no mulch, than in absolute albedo values. As the protocols used to measure shortwave and longwave radiation are similar across treatments as well as the surrounding cover around the plots, our measurements can be considered robust.

The radiometers were connected to a CR1000 datalogger (Campbell Scientific Inc., Logan, UT, USA), which recorded data every minute. The data were then averaged at half-hourly intervals.

During the measurement campaign, we encountered technical issues with the pyranometers for a few days during the dry season between September and October, leading to a loss of albedo data. These data gaps were filled using the albedo-soil moisture relationship developed for the sites (see Table S1 in the Supplemental Materials). We also encountered a technical problem when monitoring the longwave radiation at the UZF site during an extended period of the first year, which caused considerable data gaps at this site that could not be filled.

2.3.2 Weather station and soil sensors

A weather station, ATMOS 41 (Meter Group, Inc., Pullman, WA, USA), was used to monitor the air temperature, relative humidity, wind speed and direction, rainfall and vapour pressure. These data were recorded on a second datalogger (METER ZL6, Meter Group, Inc., Pullman, WA, USA)**.** The high-frequency measurements (every minute) were averaged at half-hourly time intervals to be consistent with the radiometer measurements.

The soil temperature and soil moisture were monitored at 1, 10, and 20 cm soil depths and at 5-minute intervals with ECH2O sensors (Meter Group, Inc., Pullman, WA, USA) in each of the plots equipped with NR01 sensors. The ECH2O sensors were connected to the METER ZL6 datalogger. These sensors were installed in the middle of the plots between two maize rows.

2.3.3 Crop measurements

The plant area index (PAI) is the ratio of the total plant area (e.g., leaves, stems, and organs) per soil surface area expressed in square metres of the plant surface per square metre of the soil surface. It is a key indicator used to evaluate vegetation structure (Yan et al., 2019) and is closely related to the CO_2, water and energy fluxes at the plant stand level (Béziat, 2009; Béziat et al., 2013). In our study, we used an LAI 2200C plant canopy analyser (LI-COR Biosciences, Lincoln, NE, USA) to obtain indirect measurements of the PAI. We monitored the PAI every two weeks during the two cropping years. A measurement consisted of one acquisition above the crop canopy and four acquisitions on the diagonal, one on the maize row, one at 25% from the row, one in the middle of two rows and one at 75% distance

between two rows from the starting point. The measurements were repeated six times per plot at each site to better integrate the field variability in crop growth. The FV2200 software of the LAI-2200 plant canopy analyser was used to process the data and to compute the means and standard deviations of the PAI for each treatment and measurement date.

The green fractional canopy cover (GFCC) is closely related to crop growth, light interception and evapotranspiration (Irmak and Kukal, 2022). The GFCC was obtained via the Canopeo® mobile application developed at Oklahoma State University (Patrignani and Ochsner, 2015). Canopeo® is a tool that uses a simple classification of the pixels in a photograph based on the excess green ratio. The output of Canopeo® is a binary image that is composed of white pixels representing high green ratios and black pixels representing the nongreen parts of plants. It has been used in several studies to monitor the GFCC (Jàuregui et al., 2019; Liang et al., 2012), including in Zimbabwe (Namatsheve et al., 2024).

2.4 Instantaneous radiative forcing

We calculated the instantaneous radiative forcing (iRF) (i.e. radiative forcing without accounting for possible changes in the temperature of the troposphere; see the IPCC 2018 glossary) values at the top of the atmosphere (TOA) for the NT and NTM treatments compared with the CT treatment during two years at the two experimental sites by using the method of (Muñoz et al., 2010)as follows:

$$iRF \triangle \alpha(i) = -SW_{in(i)} \times Ta(i) \times \triangle \alpha(i) \quad \text{(I-3)}$$

with $Ta(i) = \frac{SW_{in}}{R_{TOA}}$, (I-4)

where $SW_{in(i)}$ represents the daily incoming shortwave solar radiation of day i in W m^{-2}, $Ta(i)$ represents the atmospheric transmittance of day i, and R_{TOA} represents the radiation at the

top of the atmosphere. *Ta* is calculated at the daily time step in contrast to using a mean annual constant *Ta* of approximately 0.85, as applied in (Lenton and Vaughan, 2009). The R_{TOA} is calculated as a function of latitude by using a sophisticated equation involving time according to the Fu–Liou radiative transfer model (Fu and Liou, 1993), as in (Carrer et al., 2018). $\Delta\alpha$ is the daily mean surface albedo difference between a given treatment, namely, NT or NTM and a reference, which is the CT treatment in this study. The result is expressed in W m^{-2}. Positive iRF values represent a warming effect on climate, whereas negative values represent a cooling effect on climate.

2.5 Statistical analyses

The statistical analyses were conducted using R software (R Core Team 2023). First, we checked whether the data had a normal distribution by using the Shapiro-Wilk test and visualized it with quantile–quantile plots. Differences in the seasonal variations in the surface albedo were analysed via one-way ANOVA via the *ggpubr* package (Kassambara A, 2023). The fitted model was chosen based on the lowest Bayesian information criterion (BIC). The statistical significance of the differences between treatments (CT, NT, NTM), sites (DTC, UZF) and seasons (2021/22, 2022/23) was tested via Tukey's HSD test at a p value < 0.05.

3. Results

3.1 Effects of treatments and soil type on the surface albedo

The daily surface albedo dynamics across the different treatments, namely, conventional tillage (CT), no-tillage (NT), and no-tillage with mulch (NTM), varied at the two experimental

sites, UZF and DTC, during the two cropping years (Figure I-2 A, C). Globally, the surface albedo is greater at DTC than at UZF. Before sowing, high albedo values were observed at both sites. During the period from soil preparation to maize emergence, the CT treatment had a lower albedo than did the NT and NTM treatments at both sites. This difference was attributed to tillage in the CT treatment, which increased the surface roughness of the soil. After mulch application, the surface albedo increased in the dark-coloured yellowish-brown clayey xanthic Ferralsol at UZF and, conversely, decreased in the light-coloured red sandy soil at DTC. Throughout the two cropping years, the xanthic Ferralsol at UZF presented a lower average surface albedo than did the abruptic Lixisol at DTC (Table I-1). At both sites, the surface albedo was generally greater during the dry season, when the soil was bare and dry, than during the growing season.

3.1.1 The surface albedo values during the growing season

At UZF, during the growing season of the first cropping year (2021/22), the highest surface albedo values were recorded at the peak of plant growth (measured by the plant area index, or PAI) for all the treatments. Although there was no significant difference in albedo between NT and CT during this season due to similar crop development, the NTM treatment displayed higher albedo values as a result of more developed crops. During the growing season of the second cropping year (2022/23), the albedo reached its peak value during the maize senescence phase (Figure I-2C). Across all three treatments, the surface albedo remained similar during this season due to the uniform crop growth (Figure I-2D).

At DTC, the average surface albedo during the growing seasons of the two consecutive copping years was significantly greater in the NT treatment than in the NTM and CT treatments (Table I-1). For NT, the albedo values ranged from 0.15-0.30, whereas the albedo values of the NTM and CT treatments ranged from 0.14-0.23 and 0.16-0.28, respectively. Despite these differences in albedo, the NT and NTM treatments were associated with lower crop development (Figure I-2 B, C) than the CT treatment was, particularly at maximum development for both growing seasons.

3.1.2 Surface albedo values during fallow periods

During the dry fallow periods, the surface albedo was generally greater than that during the growing season at both UZF and DTC (Figure I-2). This was particularly obvious at DTC, where the albedo of the bare sandy soil exceeded that of the maize stands. At UZF, the presence of mulch in the NTM treatment slightly increased the surface albedo, whereas at DTC, the mulch had the opposite effect, reducing the albedo of the sandy soil. The overall difference in albedo between treatments during the fallow periods was more pronounced at DTC, where the NT treatment consistently presented a higher albedo than both the CT and NTM treatments did.

After the maize harvest, the surface albedo increased for all the treatments at both sites in both cropping years (Table I-S2). At DTC, this postharvest increase in albedo was most noticeable in the CT treatment. When mulch was reintroduced in the NTM treatment after harvest in the second cropping year, the effect on albedo differed among the sites. At DTC, mulch significantly reduced the albedo, whereas at UZF, it led to a slight increase.

Table I-1. Mean surface albedo values during the growing seasons (i.e. from maize emergence to harvest); the fallow periods (i.e. the dry seasons, when the soil is bare or covered by only crop residues) and the cropping years (i.e. the whole period from October to the following October, including both the growing and bare fallow periods).

		UZF			DTC		
Season	Treatment						
		Growing season	Fallow period	Cropping year	Growing season	Fallow period	Cropping year
2021/22	CT	0.15 (±0.02)b	0.18 (±0.02)b	0.17 (±0.02)b	0.19 (±0.03)b	0.26 (±0.03)b	0.23 (±0.05)b
	NT	0.15 (±0.02)b	0.19 (±0.02)a	0.17 (±0.03)a	0.21 (±0.04)a	0.29 (±0.03)a	0.25 (±0.05)a
	NTM	0.16 (±0.02)a	0.18 (±0.02)b	0.17 (±0.02)ab	0.19 (±0.02)b	0.25 (±0.04)c	0.22 (±0.04)b
2022/23	CT	0.15 (±0.02)b	0.17 (±0.01)c	0.16 (±0.02)b	0.20 (±0.03)b	0.29 (±0.04)b	0.24 (±0.05)b
	NT	0.15 (±0.01)ab	0.19 (±0.02)a	0.17 (±0.02)a	0.22 (±0.03)a	0.32 (±0.04)a	0.27 (±0.05)a
	NTM	0.15 (±0.01)a	0.18 (±0.02)b	0.17 (±0.02)a	0.19 (±0.02)c	0.26 (±0.03)c	0.22 (±0.04)c

CT: Conventional tillage, NT: No-tillage, NT: No-tillage and mulch. In 2022/23, mulch was also applied after harvest and was present during the fallow period. The errors in brackets represent standard deviations: N=157 for the growing season 2021/22 at DTC, N=154 for the growing season 2021/22 at UZF, N=141 for the growing season 2022/23 at DTC, N=138 for the growing season 2022/23 at UZF, N=210 for the fallow period 2021/22 at DTC, N=215 for the fallow period 2021/22 at UZF, N=226 for the fallow period 2022/23 at DTC, N=232 for the fallow period 2022/23 at UZF, N= 365 for the cropping years 2021/22 and 2022/23 at DTC, and N= 365 for the cropping years 2021/22 and 2022/23 at UZF.

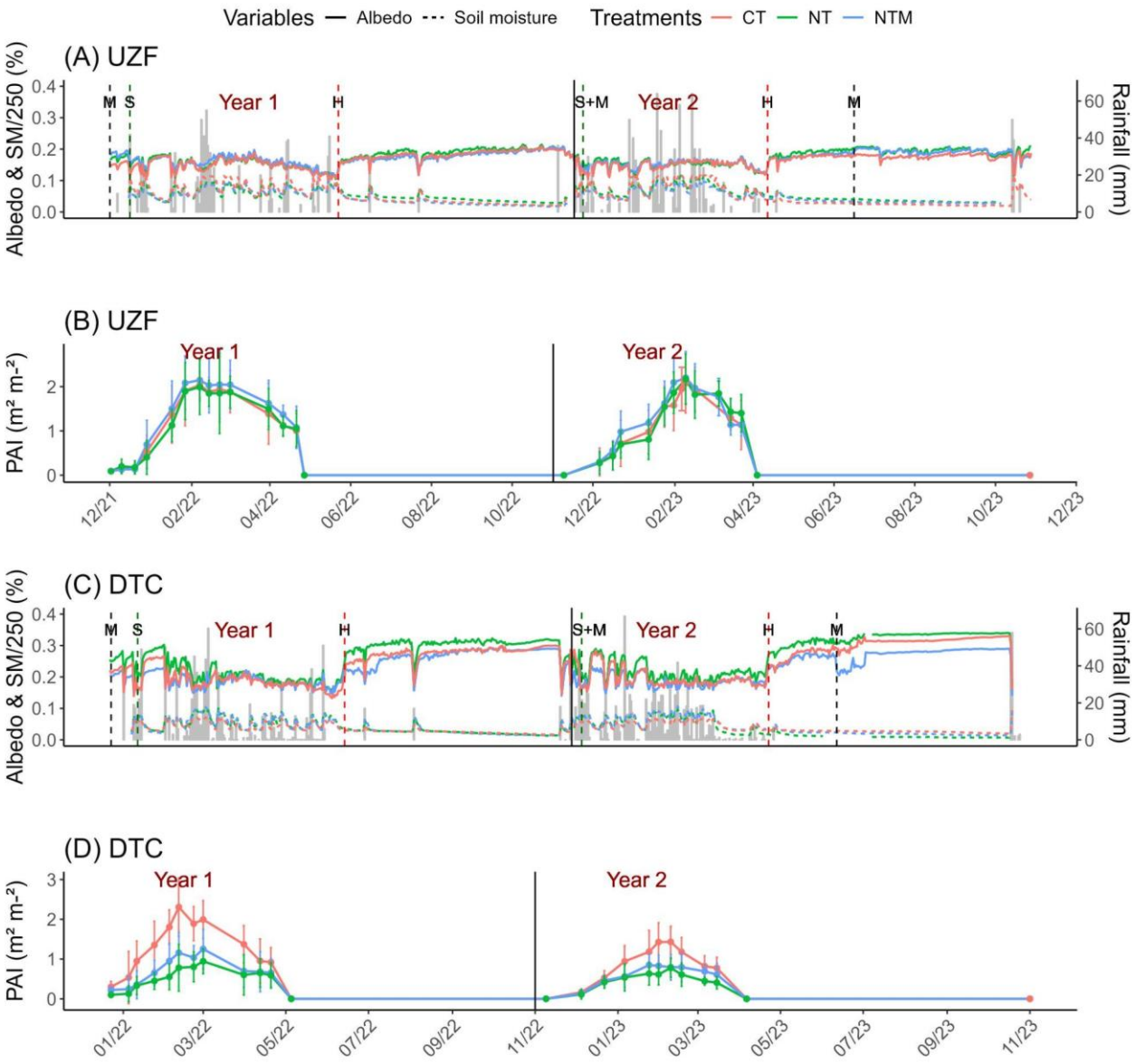

Figure I-2. (A, C) The dynamics of the top (1 cm depth) soil moisture (SM) divided by 250 to fit at the same y-Axis as the surface albedo (dashed lines) and the surface albedo (solid lines) at UZF (Ferralsol, dark-coloured) and DTC (Lixisol, light-coloured),) for three treatments: conventional tillage (CT, salmon); no-tillage (NT, green); and no-tillage with mulch (NTM, blue) during the 1st (2021/22) and 2nd (2022/23) cropping years in Zimbabwe. (B, D) Plant area index (PAI) dynamics at UZF and DTC, respectively. The error bars represent the standard deviations (N=6). The light blue bars represent daily rainfall. The vertical green dashed lines represent the maize sowing dates, the red dashed lines represent the harvest dates, and the black dashed lines represent the application of mulch after harvest. S: Sowing, H: Harvest, and M: Mulching. The solid vertical dark lines represent the end of the first cropping year and the beginning of the second cropping year. Tillage and mulching in the first cropping year were performed before the start of the measurements. Tillage and the 1st mulch application during the second cropping year were performed at maize sowing. In year 2, mulch was also applied after harvest.

3.2 Crop growth effect on surface albedo

Figures I-2B and I-2D show the PAI dynamics during both cropping years at both sites. The PAI dynamics indicate that crop growth was greater at UZF than at DTC. At UZF, the PAI dynamics were similar between the treatments during the growing seasons of both cropping years. Slightly higher maximum PAI values were observed for the NTM treatment than for the CT and NT treatments (Table I-2). In contrast, at DTC, significant differences in the PAI dynamics between treatments were observed. During both growing seasons, the average PAIs were significantly greater under CT than under NT and NTM. These findings indicate that, compared with the CT treatment, the latter two treatments resulted in less crop growth. Furthermore, crop growth was lower in the second cropping year (2022/23) than in the first cropping year (2021/22) (Table I-2). The GFCC experienced the same dynamics as the PAI for each site and treatment (Figure I-S2).

Table I-2. Maximum PAI (± standard deviation, N=6) and green fractional canopy cover (± standard deviation, N = 4) during 2 successive cropping years at the Domboshawa training center (DTC) and University of Zimbabwe farm (UZF). CT: Conventional tillage, NT: No-tillage, NTM: No-tillage and mulch.

		DTC		UZF	
Cropping year	Treatment	PAI max ($m^2 m^{-2}$)	GFCC max (%)	PAI max ($m^2 m^{-2}$)	GFCC max (%)
2021/22	CT	2.30 (±0.7)	75 (±4.35)	2.04 (±0.3)	73 (± 2.57)
	NT	0.94 (±0.3)	37 (±3.54)	1.99 (±0.6)	72 (±3.12)
	NTM	1.25 (±0.5)	46 (±2.03)	2.14 (±0.5)	78 (±4.22)
2022/23	CT	1.43 (±0.4)	44 (±3.62)	2.08 (±0.7)	65 (±2.52)
	NT	0.78 (±0.2)	21 (±1.4)	2.16 (±0.6)	64 (±7.08)
	NTM	0.84 (±0.3)	29 (±2.63)	2.20 (±0.6)	66 (±8.7)

Figure I-3 shows the changes in surface albedo during the growing seasons in relation to the PAI dynamics across sites and treatments. In the first cropping year, an increase in surface albedo was observed with crop growth, levelling off upon reaching the maximum PAI. With the beginning of senescence, the surface albedo presumably decreased due to changes in leaf properties (e.g., angle and colour). The nature of this relationship can be described as a "hysteresis" effect. (See Figure I-3).

The results for the second cropping year were slightly different, and the hysteresis effect was not observed. Overall, less crop growth with less soil cover was observed than in the first cropping year (Table I-2). As a consequence, the GFCC was lower at both sites, particularly for the NT and NTM treatments. The lower canopy cover in the second cropping year

explains why the surface albedo dynamics were driven mostly by the soil albedo rather than by crop vegetation.

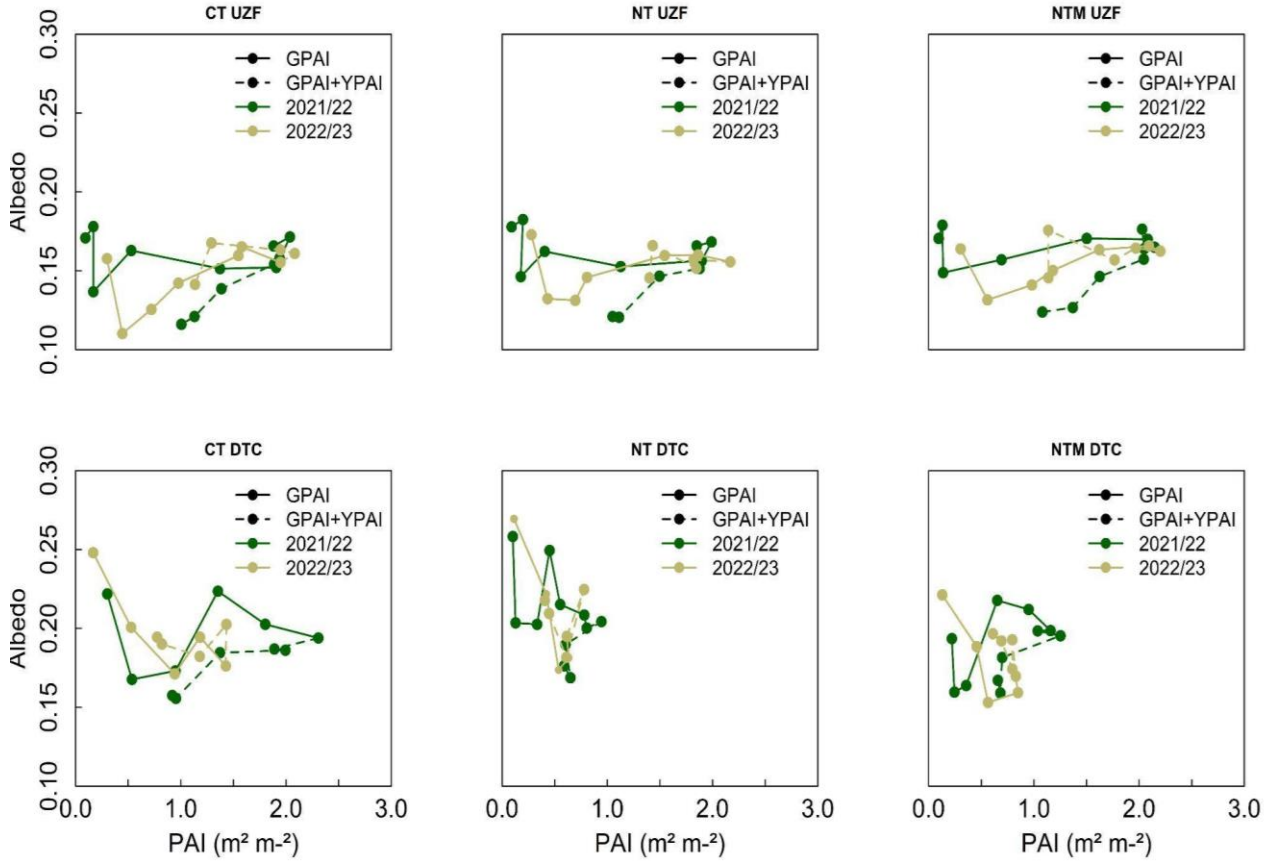

Figure I-3. Dynamics of the surface albedo as a function of the plant area index (PAI). The solid lines correspond to the maize growing phase with only the green PAI (labelled "GPAI"), and the dashed lines correspond to the senescence phase, during which the leaves have both green and yellow tissues (labelled "GPAI + YPAI" with YPAI standing for yellow PAI). The green colour represents the 2021/22 season, and the light khaki colour represents the 2022/23 season.

3.3 Effect of topsoil moisture on daily surface albedo

Figures I-2A and I-2C (dashed lines) illustrate the dynamics of the topsoil (0–1 cm) water content during both seasons at both sites. At UZF, the topsoil moisture in the CT treatment was greater than for the NT and NTM treatments during the growing season (Figure 2A).

After harvest at the end of the rainy season, a decrease in topsoil moisture was observed. During this period, the soil moisture in NT was slightly greater than that in the CT and NTM treatments. However, at DTC, the topsoil moisture was higher in the NTM treatment during both growing seasons (Figure I-2C). After harvest, there was no significant difference between the treatments in the first cropping year. In the second cropping year, the soil moisture after harvest was significantly greater in the CT and NTM treatments than in the NT treatment.

The topsoil moisture and surface albedo were negatively correlated at both sites, especially during the bare fallow periods (Figure I-4). During the bare fallow periods, rainfall events increased the topsoil moisture, which decreased the soil albedo until the topsoil dried out again, causing the albedo to return to a value close to that before the rain. With respect to crop growth, the effects of rainfall events on the soil albedo were less pronounced, particularly when the PAI was above 1 $m^2 m^{-2}$. Strong and significant relationships ($p < 2.2e^{-16}$) were found for the three treatments at each site. At DTC, the strongest correlation was observed in the CT treatment, with R^2 values of 0.80 and 0.84 in the first and second cropping years, respectively. For the NT and NTM treatments, the correlations were lower but significant, with R^2 values of 0.67 and 0.51 in the first cropping year and 0.72 and 0.71 in the second cropping year, respectively. At UZF, the highest correlation was observed for the CT treatment in the first cropping year, with an R^2 of 0.79, whereas the R^2 values were 0.73 and 0.71 for the NT and NTM treatments, respectively. The correlation between albedo and topsoil moisture was highest during the bare fallow periods and weakened with increasing crop growth.

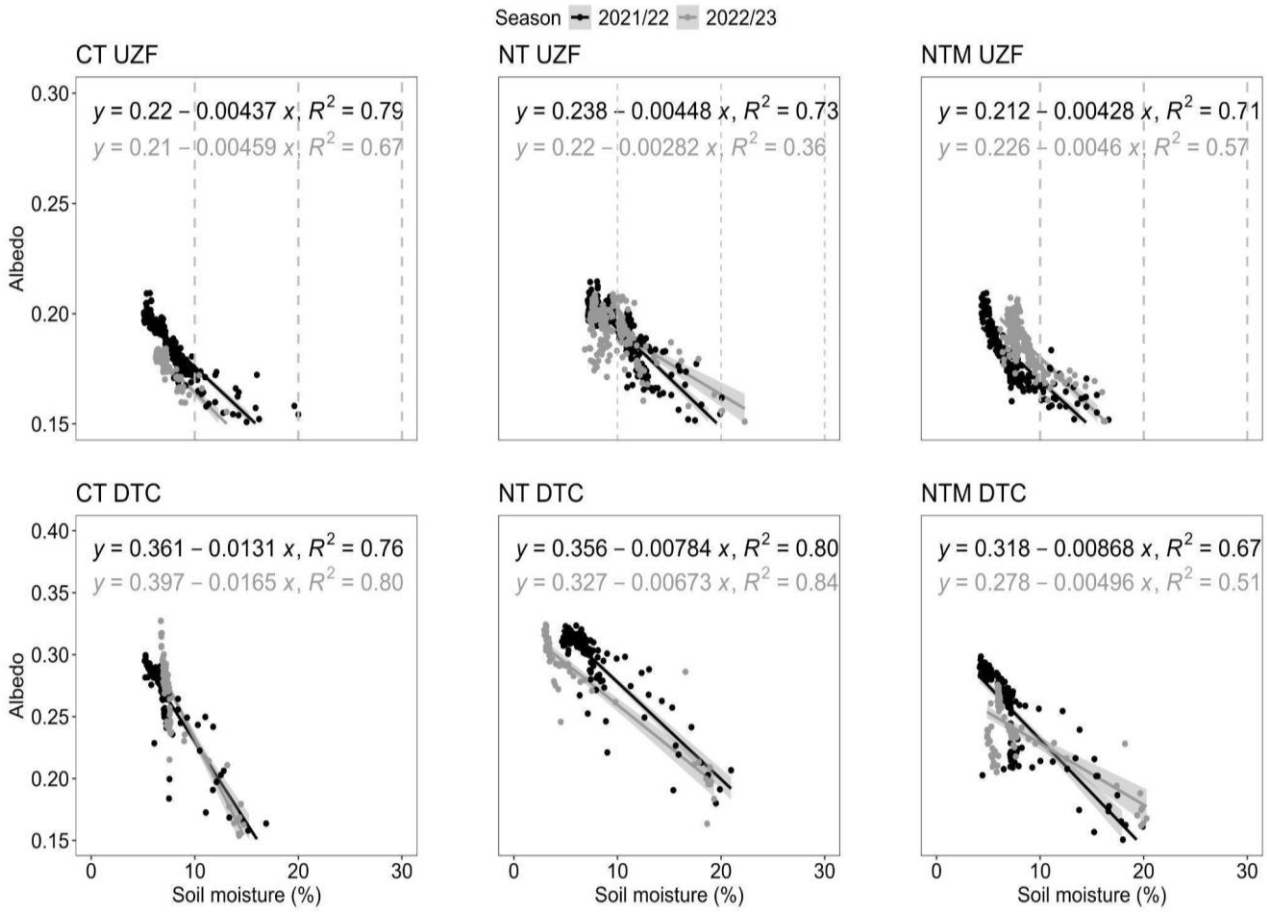

Figure I-4. Correlations between topsoil moisture (1 cm soil depth) and surface albedo on a xanthic Ferralsol (top, University of Zimbabwe farm (UZF)) and on an abruptic Lixisol (top, Domboshawa training center (DTC)) and for CT: conventional tillage, NT: no-tillage, NT: no-tillage and mulch. The data are shown for the periods between soil preparation for sowing and emergence and after harvest until the next soil preparation of the following cropping season.

3.4 Radiative forcing, thermal radiation and topsoil temperature

3.4.1 Daily instantaneous radiative forcing (iRF)

At UZF, the daily iRFs for NT compared to those for CT corresponded to cooling effects during most of the growing season as well as during the entire bare fallow period (Figure I-5), corresponding to mean iRFs of -0.83 W m^{-2} during the first (2021/22) cropping year and -1.43 W m^{-2} during the second (2022/23) cropping year. The NTM treatment led to a cooling

effect during the two successive growing seasons and to a warming effect during the first fallow period. On an annual basis, the mean iRFs of the NTM treatment were -0.43 W m^{-2} during the first cropping year and -1.03 W m^{-2} during the second cropping year. The mulch was applied after harvest in the cropping year, increasing the surface albedo and subsequently increasing the cooling effect during the bare fallow period by -0.60 W m^{-2}.

At DTC, negative daily iRF values were observed under NT relative to those under CT in both cropping years. This cooling effect was greater during the bare fallow period than during the growing season, with mean annual iRF values of -3.34 W m^{-2} and -2.78 W m^{-2} in the first (2021/22) and second (2022/23) cropping years, respectively. Under the NTM treatment, a positive iRF relative to the CT treatment was observed during the bare fallow periods and at the early crop development stage. During the later stages of crop growth, negative iRF values were observed. The resulting mean iRF values were 1.14 W m^{-2} for the first cropping year and 2.77 W m^{-2} for the second cropping year. The application of mulch after harvest in the second cropping year increased the iRF by 1.64 W m^{-2}.

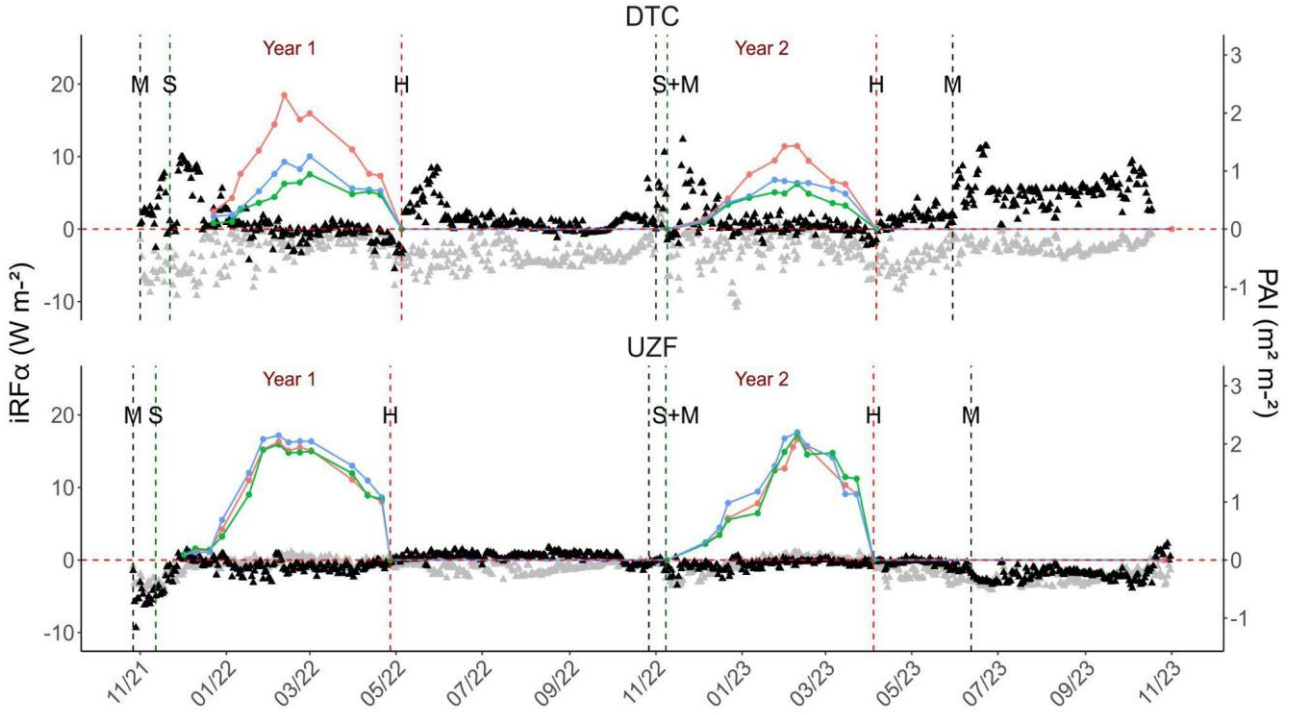

Figure I-5. Daily instantaneous radiative forcing (iRF) of no-tillage (NT, grey triangles) and no-tillage with mulch (NTM, black triangles) systems compared with conventional tillage (CT) systems. Interpolated dots represent the dynamics of the plant area index (PAI) in the three treatments: CT in salmon, NT in green, and NTM in blue. The green and red vertical dashed lines represent the sowing (S) and harvest (H) dates, respectively. The black dashed line represents the mulch (M) application date. The solid vertical dark line represents the end of the first cropping year and the beginning of the second cropping year. Tillage and mulching in the first cropping year were completed before the beginning of the measurements. Tillage and the 1st mulch application during the second cropping year were completed at maize sowing. In the 2nd cropping year, mulch was also applied after maize harvest.

3.4.2 Daily outgoing longwave (LW_{out}) radiation and topsoil temperature

Figure 6A shows the LW_{out} dynamics during the two successive cropping years at UZF. At this site, the daily LW_{out} values for the NT and NTM treatments were very similar to those for the CT treatment before and during the growing season. However, after mulch application following maize harvest in 2023 (see Figure I-6A), a decrease in LW_{out} was observed for the NTM treatment, whereas the LW_{out} dynamics under the NT treatment remained similar to

those under the CT treatment. The mean LW_{out} values during the bare fallow period under the NT and CT treatments were 485 and 486 W m^{-2}, respectively. Compared with the CT and NT treatments, the NTM treatment had a lower LW_{out} value because of the buffering effect of the mulch layer, with an average LW_{out} value of 480 W m^{-2} during the whole fallow period. With similar crop growth between treatments (see Figure I-2B), no significant differences in LW_{out} were observed between treatments during the growing season in 2022/23. During this period, the mean LW_{out} values were 461 W m^{-2} for NT and CT and 460 W m^{-2} for NTM.

At UZF, no significant differences were detected in the topsoil (0–1 cm) temperature dynamics between the NT and CT treatments during the first (2021/22) and second (2022/23) cropping years (Figure I-6B). In the second cropping year, a rapid decrease in temperature was observed under the NT treatment compared with the CT treatment immediately after maize harvest. The surface temperature was lower under the NTM treatment than under the CT treatment because the mulch covered the soil before sowing, during crop growth and after maize harvest during the second cropping year. Similar observations were made in the second cropping year, with a 5°C difference between the NTM and CT treatments just after the maize harvest. The cooling observed in the NTM treatments can partially explain the differences in LW_{out} between the NTM treatment and the CT and NT treatments.

At DTC, the daily LW_{out} values were very similar between the treatments during the bare fallow periods in both cropping years (Figure I-6C), with values of 458 W m^{-2} and 475 for NT and 464 W m^{-2} and 481 W m^{-2} for CT in the first and second cropping years, respectively. In contrast, during the growing season, the differences in LW_{out} were significant between the CT and NT treatments and between the CT and NTM treatments due to greater crop growth under the CT treatment. During the growing season, the mean LW_{out} values under NT

compared with those under CT were 464 vs. 455 W m^{-2} and 468 vs. 460 W m^{-2} during the first and second cropping years, respectively. The small difference in LW_{out} between the NT and CT treatments during crop growth was due to the lower PAI resulting from poorer crop growth. During the bare fallow period, the mean LW_{out} values for the NTM treatment were 461 and 437 W m^{-2} in the first and second cropping years, respectively. Compared with the CT treatment, the NTM treatment resulted in poorer crop growth, resulting in average LW_{out} values of 462 W m^{-2} and 470 W m^{-2}, whereas the LW_{out} values of the first and second growing seasons were 455 W m^{-2} and 460 W m^{-2}, respectively.

In both cropping years, the topsoil temperatures were generally similar between the NT and CT treatments during crop growth periods, except during the early stages of crop growth in the first cropping year (Figure I-6D). However, lower daily topsoil temperatures were observed after maize harvest in the NT treatment than in the CT treatment during both cropping years. The daily topsoil temperatures were significantly lower in the NTM treatment than in the CT treatment during the early stages of crop growth and throughout the cropping year, probably because of the buffering effect of the mulch layer on the soil temperature.

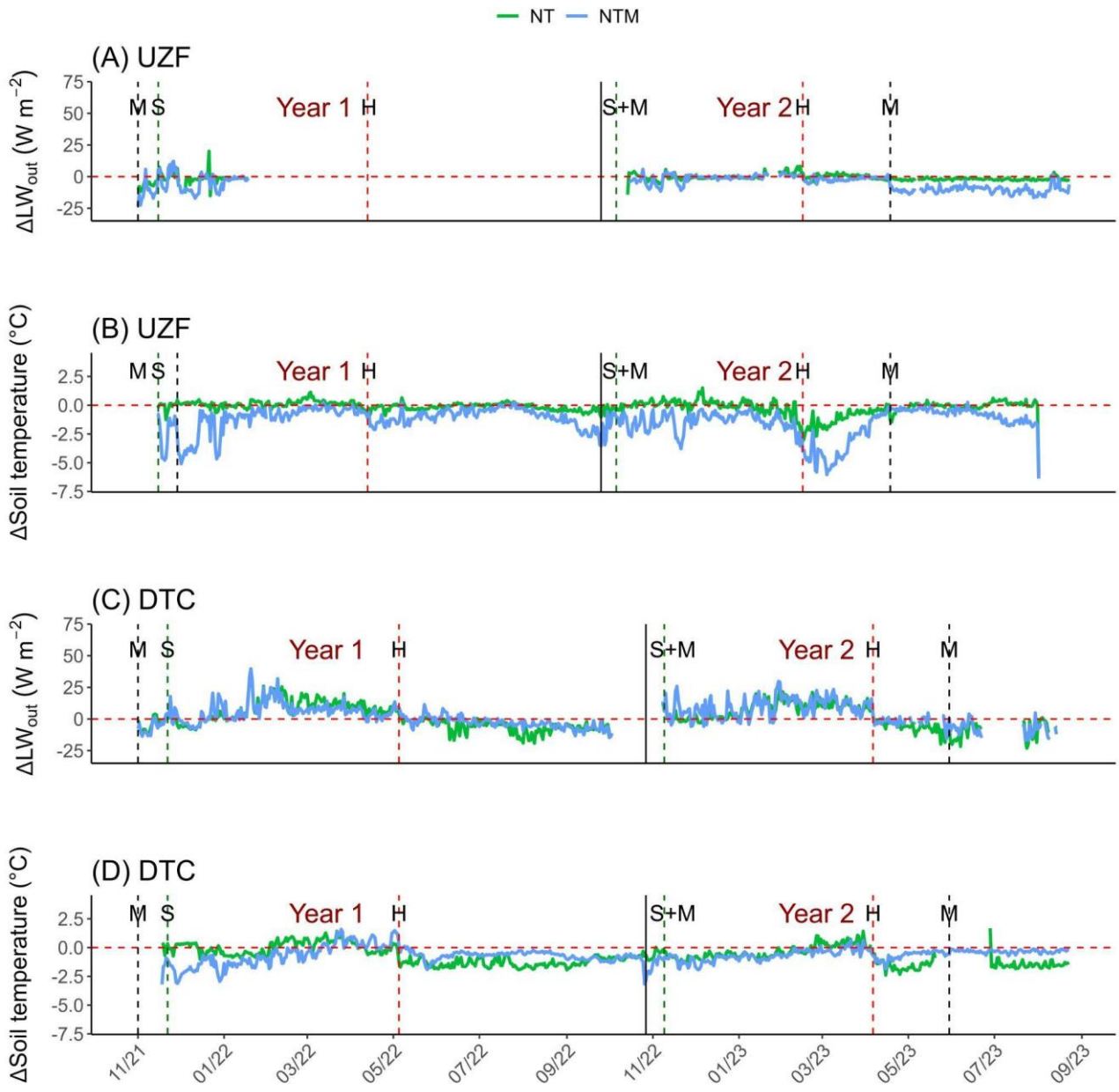

Figure I-6. Dynamics of outgoing longwave radiation dynamics (LW_{out}) (A and C) between no-tillage (NT) and conventional tillage (CT) (green lines) and between no-tillage with mulch (NTM) and CT (blue lines) at the UZF and DTC sites. Topsoil temperatures (1 cm) during two cropping years (2021/22 and 2022/23) between NT and CT (green lines) and between NTM and CT (blue lines). The green and red dashed lines represent the sowing (S) and harvest (H) dates, respectively. The black dashed line represents the mulch (M) application date. The solid vertical dark line represents the end of the first cropping year and the beginning of the second cropping year. Tillage and mulching in the first cropping year were performed before the beginning of the measurement. Tillage and 1st mulch application during the second cropping year were performed at sowing. Mulch was also applied after harvest.

4. Discussion

4.1 Interactive effects of soil type and cropping system on the dynamics of the surface albedo

In this study, we showed that no-tillage and maize residue mulching can have significant effects on the surface albedo dynamics and on the longwave radiation from the soil surface. While no-tillage generally increases the soil albedo due to the lower soil surface roughness, mulch either increases or decreases the surface albedo depending on the soil surface properties.

We observed that the brightness of the soil surface modulates the effects of mulching and no-tillage on the surface albedo and iRF. In a previous work, (Post et al., 2000) reported that soil surface colour is an important driver of the surface albedo. (Horton et al., 1996) also reported that the albedo of light-coloured crop residues may be greater than that of dark-coloured yellow-brown soil; therefore, a layer of crop residues can reduce the soil surface reflectance.

Soil colour is determined by several factors, such as the organic carbon content. At our experimental sites, the soil organic carbon contents were measured as described by (Shumba et al., 2024). In the topsoil layer (0–5 cm) of the abruptic Lixisol (DTC), the soil organic carbon contents were 0.6 g C kg^{-1} for the CT and NT treatments, whereas for the NTM treatments, the contents was 0.8 g C kg^{-1}. In xanthic Ferralsol (UZF), the soil organic carbon contents was higher, at 1.80 g C kg^{-1} for CT, 1.85 g C kg^{-1} for NT and 2.1 g C kg^{-1} for NTM ((Shumba et al., 2024). Mineral components such as iron oxides also determine soil colour (Cierniewski et al., 2018). For example, a field study by (Rosenberg et al., 1983) demonstrated the contrast

between a dry sandy soil with albedo values ranging between 0.25 and 0.45 and a dark soil with albedo values ranging between 0.16 and 0.17, which aligns with the observations in the soils of our study. At DTC, the mulch on a clear sandy soil therefore reduced the surface albedo, whereas at UZF, the maize residues increased the surface albedo. In southeastern France, (Davin et al., 2014) also reported that the mulch of crop residues on no-tilled loamy soil increased the surface albedo (by approximately 0.1) compared with tilled soils without mulch.

At DTC, we observed that the surface albedo in the NTM treatment was lower than in the other treatments, even before mulch application at sowing and after harvest (the mulch decomposed at that time), when the soil rugosity was comparable among the treatments. The reason is likely that the annual mulch application at this site slightly increased the soil organic carbon content by 0.25 g C kg^{-1} and 0.30 g C kg^{-1} compared with the NT and CT treatments, respectively (Shumba et al., 2024). The climate benefit associated with soil organic carbon sequestration was therefore partly or totally counterbalanced by the positive iRF effect induced by the soil darkening effect (Post et al., 2000). In another study, Pique et al. (2023) reported a significant risk of losing part of the climate benefit of soil organic carbon sequestration through soil albedo darkening effects if soils are not permanently covered once carbon farming practices are implemented.

Soil roughness also affects the surface albedo and its dynamics between treatments (e.g., CT vs. NT), especially under dry conditions, which corroborates previous findings under similar pedo-climatic conditions in West Africa (Oguntunde et al., 2006). At our sites, we observed differences in the surface albedo between the CT and NT treatments after soil preparation for maize sowing at UZF and between the CT and NT treatments at DTC during the bare

fallow period. At UZF, the difference in surface albedo between the NT and CT treatments before sowing could be caused by tillage, which increases the surface roughness, causing more incident solar radiation to be trapped and reducing the surface albedo, as shown in previous studies (Matthias et al., 2000; Oguntunde et al., 2006; Cierniewski et al., 2015). At DTC, the difference between the NT and CT treatments during the bare fallow period could be explained by the presence of surface soil crusts in the NT treatment, which were absent in the CT treatment. In addition, before sowing, the surface soil layer in the NT treatment was smooth and very bright compared with that in the CT treatment. In contrast, the difference in soil roughness between the CT and NT treatments was very small after the maize harvest and during the following fallow period.

4.2 Effects of maize growth on surface albedo dynamics

According to (Hatfield and Carlson, 1979) and (Breuer et al., 2003), the albedo of maize varies between 0.16 and 0.25 across varieties. However, due to the light-coloured red sandy soil at the DTC, the high surface albedo value of 0.21 in the NT treatment during the maize growing season was due to weak maize growth and vegetation cover (Table I-2). In contrast, low surface albedo values of 0.19 during the growing season were observed in the CT treatment, which was characterized by better development of the maize stand than the NT treatment; this means that at this site, the surface albedo of the maize stand was lower than that of the bare soil. Several studies in temperate regions have, however, shown the opposite: soil coverage by cover crops leads to increases in surface albedo compared with bare fallow soil

(Carrer et al., 2018; Lugato et al., 2020; Pique et al., 2023). Exceptions were observed for light-coloured soils by (Kaye and Quemada, 2017) and Carrer et al. (2018).

During the two cropping years, the surface albedo values during the growing season were almost always lower than those of the bare soil surface during fallow periods in all the treatments and at both sites (Figure I-2A and I-2C). The surface albedo of bare soil was strongly driven by topsoil moisture. During the growing season, the different treatments affected the surface albedo because of incomplete vegetation coverage; this suggests that the surface albedo was driven during the growing season by both crop phenology and soil moisture. The GFCC did not reach 100% at either site (Table 2), which may explain the influence of management-induced changes in topsoil organic matter and moisture content on the surface albedo dynamics. These effects are especially pronounced at DTC, where there is low crop and foliage growth. The surface albedo values reach saturation with high PAI values and may even decline subsequently as internal reflections become more pronounced (Bsaibes et al., 2009). During the maize senescence phase, leaves wilt, which modifies both leaf colour and canopy structure. Due to the wilted leaves, the vegetation cover decreased, but the soil was shadowed more by the vegetated parts when the sun stood lower. The soil shadowing effect of plants works as a radiation trap and reduces the amount of reflected shortwave radiation (He et al., 2021; Wang et al., 2007). Another important driver of the decreased albedo during senescence is the lower reflectance and therefore lower albedo of yellow leaves than of green leaves. For example, an increase in surface albedo during the development stage and a decrease in surface albedo with senescence were observed for maize in the study of (Jacobs and van Pul, 1990). (Oguntunde and van de Giesen, 2004)

reported a significant increase in albedo from emergence to maturity in maize, followed by a slight decrease during maturity due to the occurrence of yellow tissues in the plants.

4.3 Changes in iRF and LW_{out} caused by tillage and crop residue management

Changes in the surface albedo impact the amount of solar radiation that is absorbed by the Earth's surface. A reduction in surface albedo, indicating lower reflectivity, results in increased absorption of solar energy, causing local warming (Liu et al., 2022a). Conversely, an increase in albedo, signifying higher reflectivity, results in diminished absorption and induces cooling (Carrer et al., 2018). In both the light-coloured red sandy soil at DTC and the dark-coloured yellow-brown clayey soil at UZF, the systematic cooling effect of NT compared with that of CT is explained by a greater albedo during both the growing season and the bare fallow periods. According to Davin et al. (2014), no-tillage without mulch in European croplands caused a global cooling effect and, locally, decreased surface temperatures during heatwave events. This local attenuation of heatwaves makes no-tillage practices an interesting climate adaptation strategy (Seneviratne et al., 2018a). A modelling study by Lobell et al. (2006) further demonstrated the potential impact that no-tillage could have on the climate if applied globally; they estimated a reduction in the global mean temperature of approximately 0.2°C (Lobell et al., 2006), which is quite substantial.

At the DTC, the application of mulch led to a decrease in the surface albedo. Compared with bare sandy soil, mulch has a lower albedo at this site, leading to a decrease in the surface albedo and a positive iRF in the NTM treatment. In contrast, at UZF, the soil surface has a darker colour than mulch does, which results in a cooling effect through mulching. However,

the benefit of mulching on the local temperature regime could be significantly offset by other effects, namely, a reduction in the evaporation flux, an increase in surface temperature, and an increase in the sensible heat flux (Davin et al., 2014).

The other important biophysical effect that is induced by no-tillage and crop residue management involves the modification of topsoil temperatures and, consequently, the longwave radiation emitted (Breil et al., 2023; Bright et al., 2017; Donohoe et al., 2014). The DTC site experienced a significant difference in longwave radiation emitted from NT during the growing season. This difference can be explained by the better crop growth in the CT treatment than in the other two treatments. As a result, evaporation was likely greater in the CT treatment than in the CT and NT treatments, and this process can reduce the soil temperature and longwave radiation emitted by the surface during the growing season. For example, (Ceschia et al., 2017) demonstrated that the albedo-induced cooling effect of cover crops could be magnified when their effects on longwave radiation and the Bowen ratio (i.e., the ratio of sensible heat flux to latent heat flux near the surface) are accounted for. Furthermore, the authors highlighted that cover crops caused, on average, a 2.5°C decrease in local topsoil temperature compared with the bare soil treatment, which could have slowed organic matter mineralization.

4.4 Limitations and perspectives

Continuous monitoring of the albedo, surface temperature and LW_{out} helped us to better understand the biophysical effects of CA practices and their consequences for climate change mitigation. The detailed information collected in this study contributes to a better

assessment of the climatic impact of land management and can be fed into soil–crop models or Earth system models for better simulations of the impacts beyond the field scale. However, changes in management practices affect the local climate not only through albedo effects on iRF or through changes in LW_{out} but also through other biogeophysical processes, such as changes in evapotranspiration, sensible vs. latent heat fluxes and soil water content (Idso et al., 1975; Rost and Mayer, 2006; O'Brien and Daigh, 2019) and through biogeochemical effects (changes in soil organic carbon and greenhouse gas emissions) (Powlson et al., 2016). In our study, we did not conduct an analysis of the changes in latent or sensible heat fluxes to investigate the effect of management on energy partitioning at the surface (Davin et al., 2014; Ceschia et al., 2017). However, complementary studies have been conducted on soil organic carbon storage and greenhouse gas emissions (Shumba et al., 2023, 2024) at our sites. The results of these studies provide the opportunity to compare the biogeophysical and biogeochemical effects of CA practices to estimate their net climatic impact; this will be investigated in our next study, which will compare these effects both in the short term and in the long term. Modelling efforts would be valuable for exploring aspects that were not investigated in this study, such as management effects on the partitioning between sensible and latent heat fluxes. Coupled surface–atmosphere modelling, which incorporates feedback effects, is essential for assessing the net climatic impact of CA practices on regional and global climates.

5. Conclusion

Based on in situ measurements, we studied how the soil type, soil moisture, crop growth and management practices impact the surface albedo and longwave radiation dynamics, as well as subsequent instantaneous radiative forcing. Independent of the soil type, the no-tillage treatment increased the surface albedo compared with conventional tillage; this resulted in a systematic albedo cooling effect due to no-tillage practices during both the growing season and the bare fallow period. However, the retention of crop residues has different effects on the surface albedo depending on the soil type. In bright sandy soil (abruptic Lixisol), the surface albedo decreased, leading to positive instantaneous radiative forcing with a warming effect, whereas in darker soil (xanthic Ferralsol), the surface albedo increased, leading to a cooling effect. For a given practice, the biogeophysical effects and impacts on climate are therefore very context specific. These effects are not negligible and should be considered together with the biogeochemical effects of CA practices to establish more efficient climate mitigation strategies.

Supplementary materials

Table I-S1. Gap filling equations for albedo based on the relationship between bare soil surface albedo and soil moisture.

		UZF	DTC
Season			
2021/22	CT	y = 0.22-0.00437x	y = 0.344-0.0106x
	NT	y = 0.238-0.00448x	y = 0.398-0.0165x
	NTM	y = 0.212-0.00428x	y = 0.342-0.00592x
2022/23	CT	y = 0.21-0.00459x	y = 0.328-0.00678x
	NT	y = 0.22-0.00282x	y = 0.308-0.00726x
	NTM	y = 0.226-0046x	y = 0.278-0.00494x

Table I-S2. Mean (±standard deviation N = 5) surface albedo of dry soil 5 days before and after key land management activities on an abruptic lixisol and a xanthic Ferralsol. CT: Conventional tillage, NT: No-tillage, NT: No-tillage and mulch. In 2022/23, mulch was also applied after harvest and was present during the fallow period. *Corresponds to albedo values measured under wet conditions.

	Sites	**UZF**			**DTC**		
Cropping year	Treatments	CT	NT	NTM	CT	NT	NTM
2021/22	Before ploughing	N/A	N/A	N/A	N/A	N/A	N/A
	After ploughing	0.15 (±0.003)	-		0.22 (±0.004)	-	-
	Before mulching	N/A	N/A	N/A	N/A	N/A	N/A
	After mulching	-		0.18 (±0.006)	-	-	0.21 (±0.003)
	Before harvest	0.11 (±0.003)	0.11 (±0.01)	0.12 (±0.004)	0.16 (±0.01)	0.20 (±0.01)	0.19 (±0.01)
	After harvest	0.15 (±0.01)	0.16 (±0.006)	0.15 (±0.008)	0.23 (±0.02)	0.27 (±0.01)	0.22 (±0.005)
2022/23	Before ploughing	0.13 (±0.02)*	-	-	0.21 (±0.05)*	-	-
	After ploughing	0.12 (±0.01)*	-	-	0.16 (±0.01)*	-	-
	Before mulching	-	-	0.14 (±0.009)*	-	-	0.18 (±0.02)*
	After mulching	-	-	0.14 (±0.009)*	-	-	0.17 (±0.01)*
	Before harvest	0.12 (±0.02)	0.12 (±0.02)	0.12 (±0.02)	0.20 (±0.02)	0.23 (±0.02)	0.20 (±0.02)
	After harvest	0.16 (±0.01)	0.16 (±0.01)	0.16 (±0.01)	0.24 (±0.001)	0.28 (±0.002)	0.23 (±0.004)

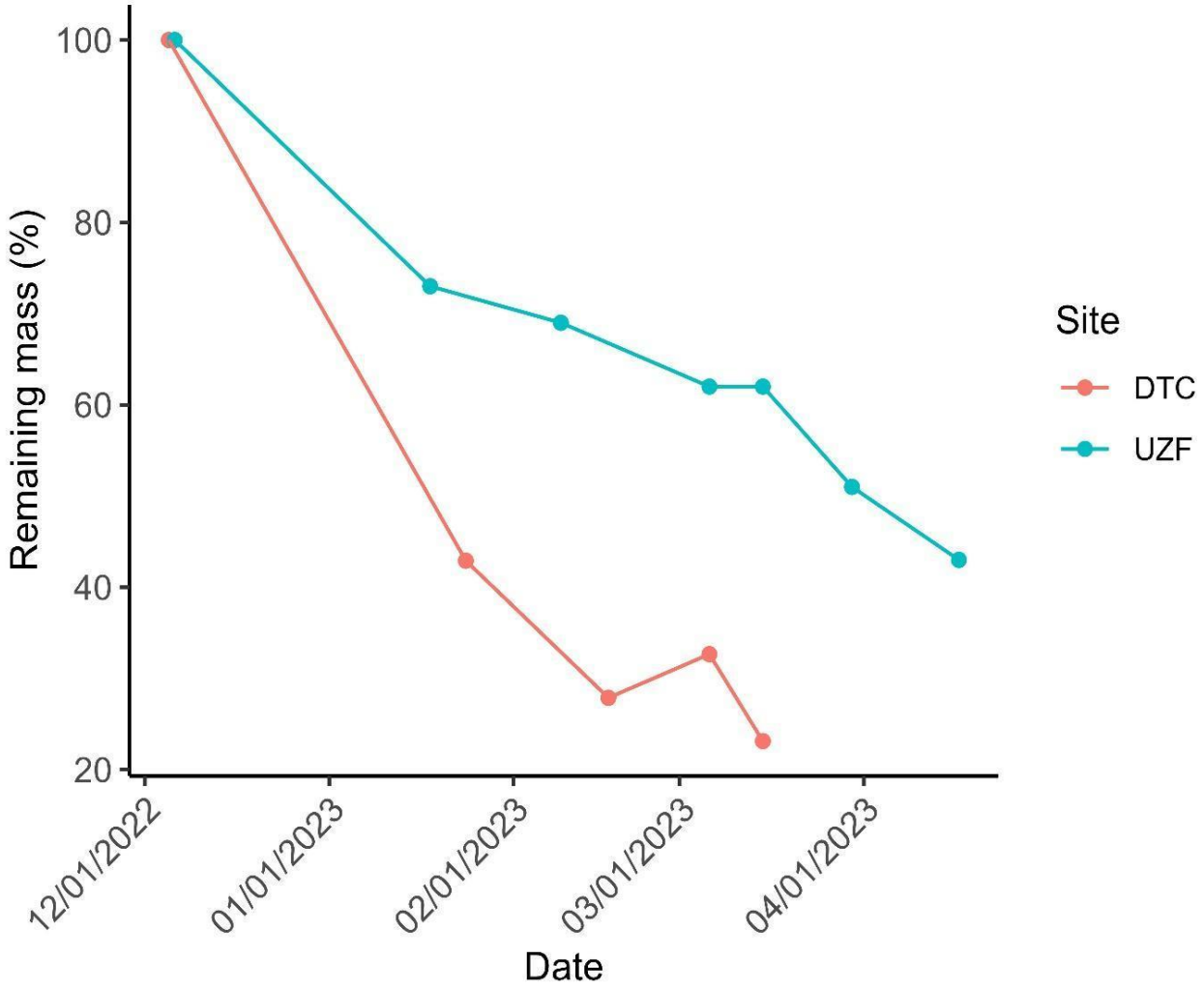

Figure I-S1. Kinetic decomposition of crop residues (mulch) on an abruptic Lixisol (DTC) and on a xanthic Ferralsol (UZF) during the growing season 2022/23.

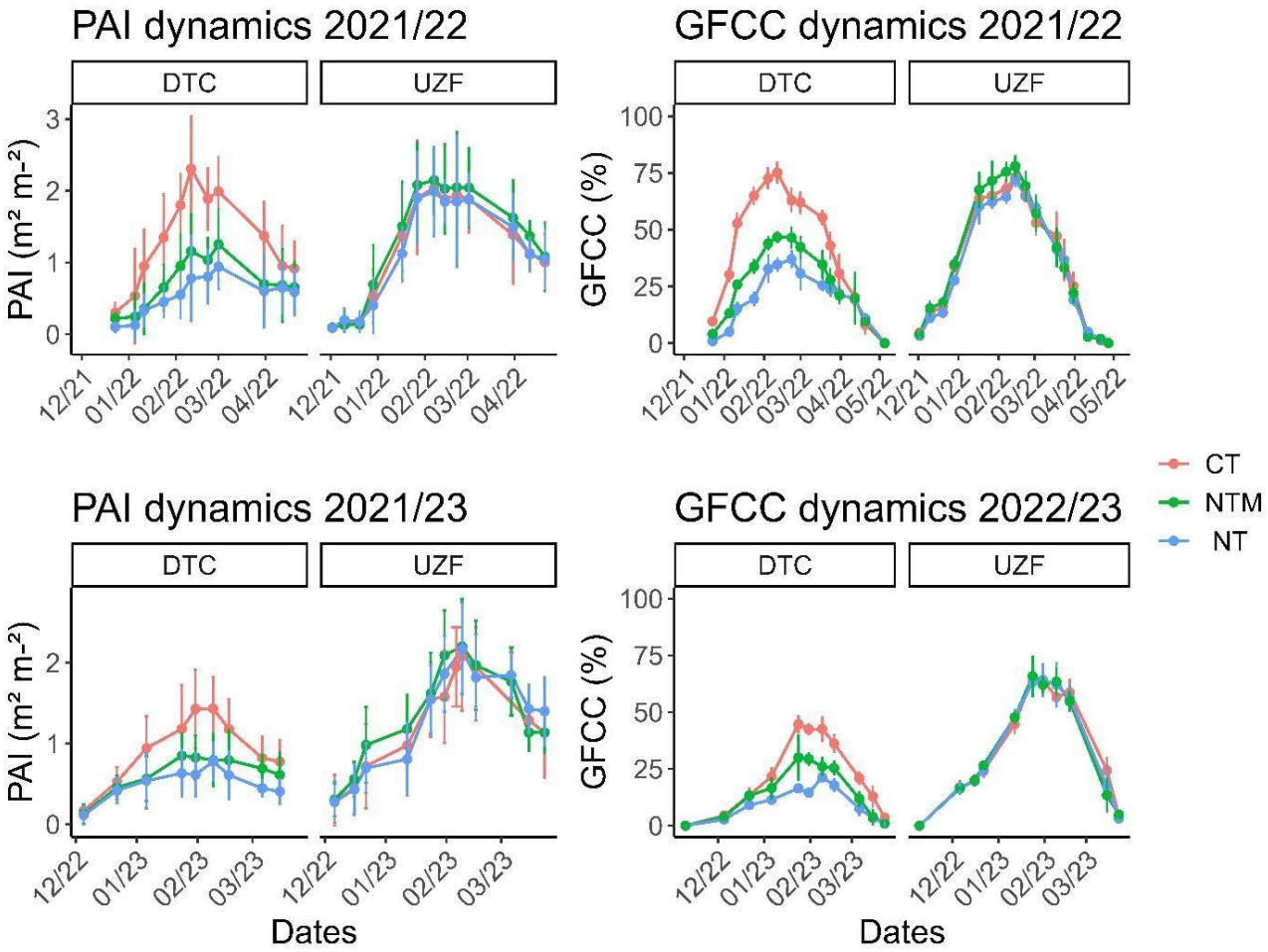

Figure I-S2. PAI and GFCC dynamics during 2021/22 and 2022/23 growing seasons at DTC and UZF sites for CT: Conventional tillage, NT: No-tillage, NTM: No-tillage and mulch.

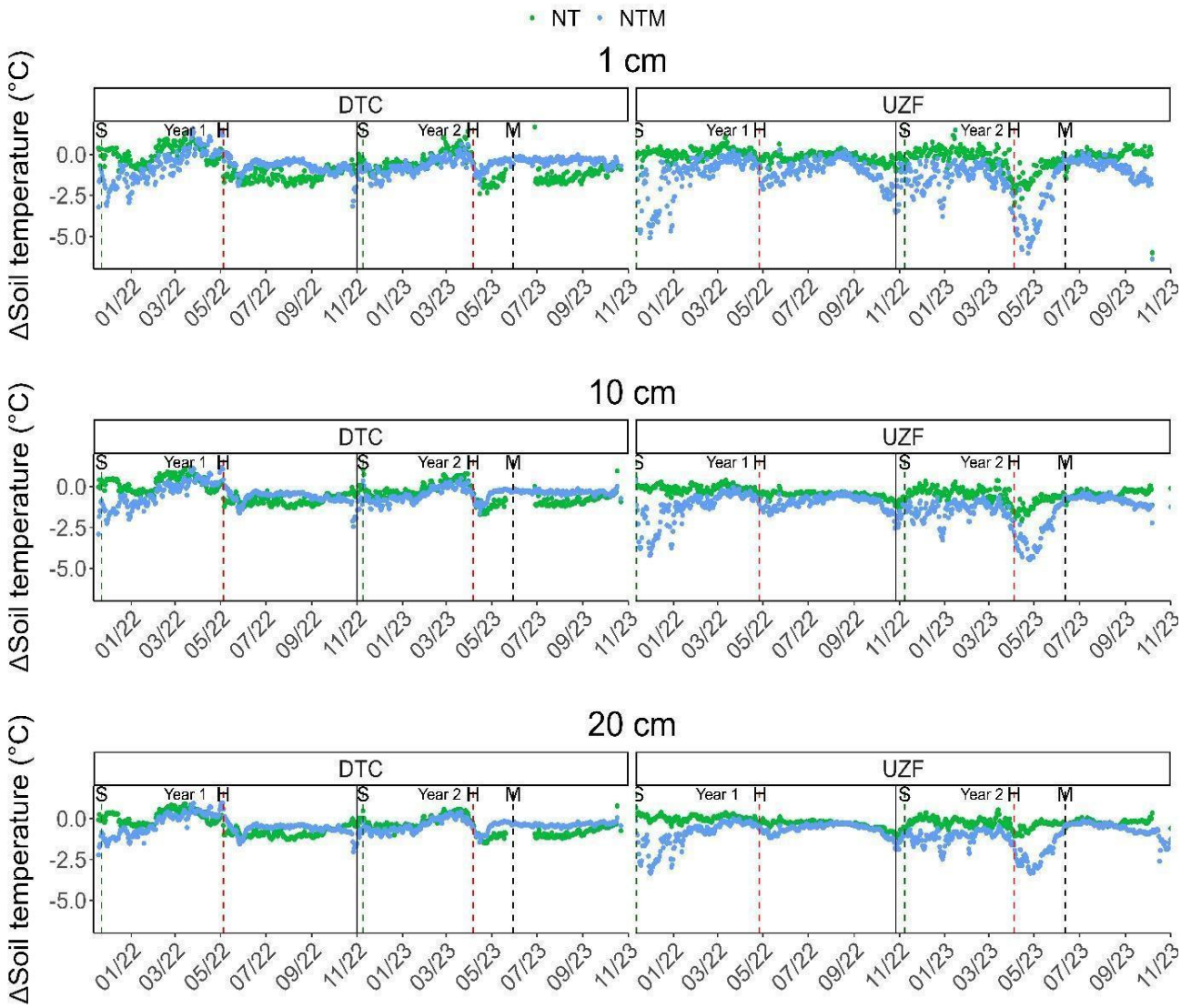

Figure I-S3. Soil temperature difference between NT and NTM compared to CT at 1, 10 and 20 cm depth during 2021/22 and 2022/23 on an abruptic Lixisol (DTC) and on a xanthic Ferralsol (UZF). CT: Conventional tillage, NT: No-tillage, NTM: No-tillage and mulch. The vertical green dashed line is the sowing date and the red dashed line is the harvest date and black dashed line represents the application of mulch after harvest for each cropping year and site. S: Sowing, H: Harvest, M: Mulching. The solid vertical dark line is the end of the first cropping year and the beginning of the second. Tillage and mulching in the first cropping year is done before the beginning of measurement. Tillage and 1st mulch application during the second cropping year is done at sowing. In 2022/23, mulch was also applied after harvest and was present during the fallow period.

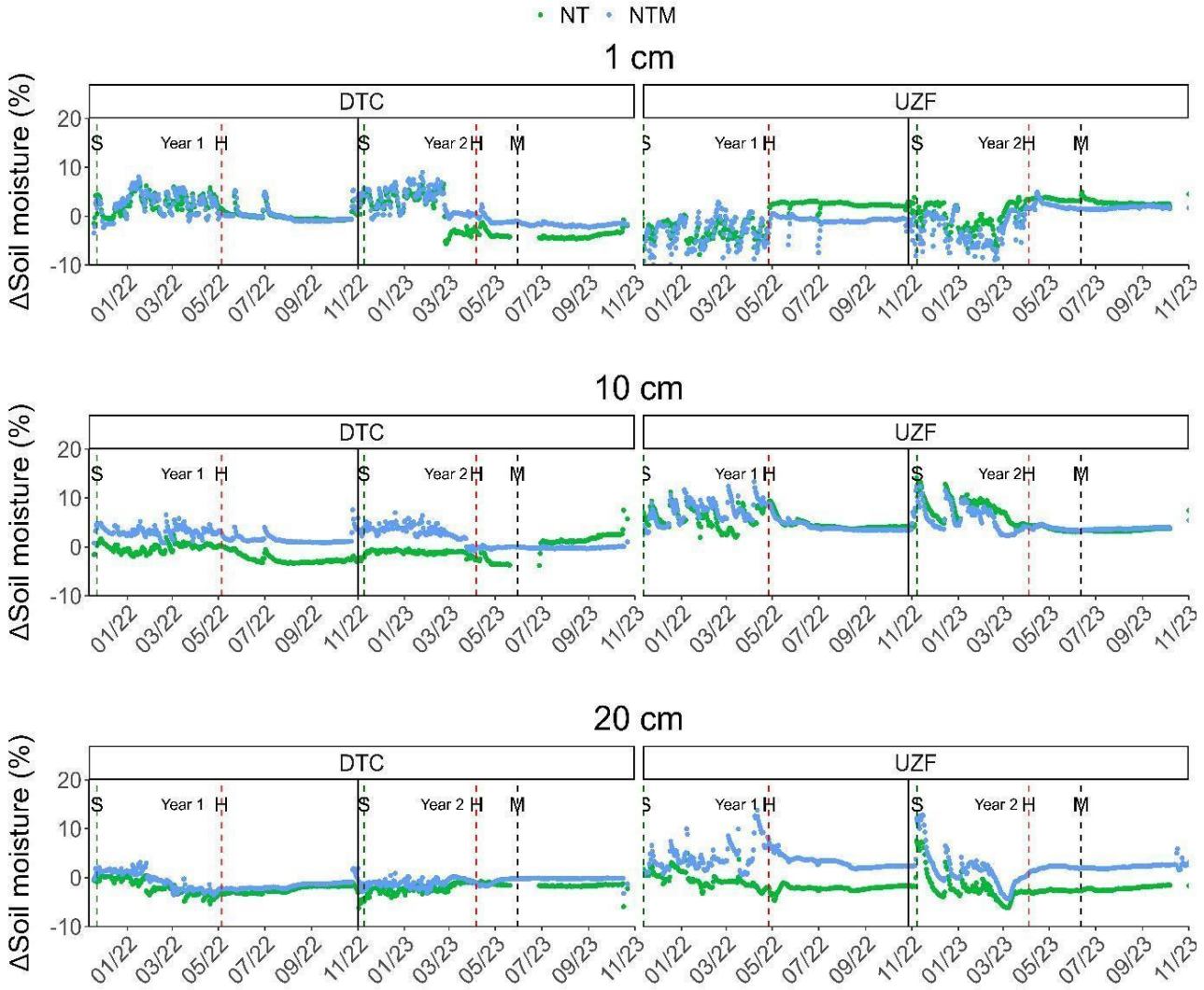

Figure I-S4. Daily soil moisture difference between NT and NTM compared to CT at 1, 10 and 20 cm depth during 2021/22 and 2022/23 on an abruptic Lixisol (DTC) and on a xanthic Ferralsol (UZF). CT: Conventional tillage, NT: No-tillage, NTM: No-tillage and mulch. The vertical green dashed line is the sowing date and the red dashed line is the harvest date and black dashed line represents the application of mulch after harvest for each cropping year and site. S: Sowing, H: Harvest, M: Mulching. The solid vertical dark line is the end of the first cropping year and the beginning of the second. Tillage and mulching in the first cropping year is done before the beginning of measurement. Tillage and 1st mulch application during the second cropping year is done at sowing. In year 2, mulch was also applied after harvest and was present during the fallow period.

Chapitre II : Analyse des effets biogéophysiques et biogéochimiques des pratiques de l'AC en Afrique Subsaharienne

Ce chapitre est adapté d'un article en cours de soumission.

Résumé en français :

Les pratiques de l'agriculture de conservation (AC) telles que la suppression du labour et la gestion des résidus de culture (*mulch*) sont essentielles pour l'adaptation et l'atténuation du changement climatique, en augmentant les stocks de carbone organique du sol (COS) et en modifiant les émissions de protoxyde d'azote (N_2O). Cependant, leur impact sur l'albédo de surface et sur le climat global est encore peu étudié, en particulier en Afrique subsaharienne. Cette étude examine l'impact climatique net de la suppression du labour et de la gestion des résidus de cultures en surface par rapport au labour conventionnel dans deux essais de longue durée au Zimbabwe, en se concentrant sur un abruptic Lixisol et xanthic Ferralsol. Les mesures sur deux ans incluent les stocks de COS jusqu'à 1 m de profondeur, les émissions de N_2O et l'albédo de surface. Le modèle de carbone du sol ICBM a été utilisé pour prédire les stocks de carbone sur 30 ans de pratiques d'agriculture de conservation (CA). Les résultats ont montré que le semis direct avec paillage augmentait significativement le carbone organique du sol (SOC) dans la couche superficielle (0-30 cm), avec des stocks prédits atteignant 12.42 Mg C ha^{-1} à DTC et 17 Mg C ha^{-1} à UZF après 30 ans de pratiques CA. En revanche, le semis direct sans paillage a observé de légères pertes de SOC à DTC, avec des pertes estimées à environ 1.11 Mg C ha^{-1} sur 30 ans. À UZF, le semis direct sans paillage a augmenté les stocks de SOC d'environ 3.26 Mg C ha^{-1}.Les résultats ont montré que la suppression du labour avec des résidus en surface augmentait significativement les stocks de COS, en particulier dans la couche superficielle. Sur le Ferralsol, les résidus de culture ont augmenté l'albédo de surface, renforçant l'atténuation climatique. À l'inverse, sur le Lixisol, les résidus de culture ont réduit l'albédo de surface, annulant les bénéfices du COS et entraînant un effet de réchauffement net. Les deux sites ont montré de faibles émissions de

N_2O, indiquant un impact climatique non significatif. L'étude souligne la nécessité de considérer à la fois les effets biogéophysiques et biogéochimiques dans l'évaluation du potentiel d'atténuation climatique de l'AC.

Balancing biogeochemical gains and surface albedo shifts: climate impacts of no-tillage and mulching in Southern Africa

Souleymane Diop[1,2,3], Rémi Cardinael[3,4,5], Ronny Lauerwald[1], Petra Sieber[6], Christian Thierfelder[7], Regis Chikowo[5,7], Marc Corbeels[4,8], Armwell Shumba[3,9], Eric Ceschia[2]

[1]Université Paris-Saclay, INRAE, AgroParisTech, UMR EcoSys, 91120 Palaiseau, France

[2]CESBIO–Univ. Toulouse III/CNRS/CNES/IRD/INRAE 18, avenue, Edouard Belin, bpi 2801, 31401 Toulouse Cedex 9, France

[3]CIRAD, UPR AIDA, Harare, Zimbabwe

[4]AIDA, Univ. Montpellier, CIRAD, Montpellier, France

[5]Department of Plant Production Sciences and Technologies, University of Zimbabwe, Harare, Zimbabwe

[6]Institute for Atmospheric and Climate Science, ETH Zürich, Zürich, Switzerland

[7]International Maize and Wheat Improvement Center (CIMMYT), P.O. Box MP 163, Mount Pleasant, Harare, Zimbabwe

[8]IITA, International Institute of Tropical Agriculture, PO Box 30772, Nairobi 00100. Kenya

[9]Fertilizer, Farm Feeds and Remedies Institute, Department of Research and Specialist Services, Ministry of Lands, Agriculture, Fisheries, Water and Rural Development, Harare, Zimbabwe

Keywords: Biogeophysical effects, biogeochemical effects, sub-saharan Africa, albedo, soil organic carbon, net climatic effect, climate change mitigation

Abstract

Conservation agriculture (CA) practices such as no-tillage and mulching are pivotal for climate change mitigation, enhancing soil organic carbon (SOC) stocks and altering nitrous oxide (N_2O) emissions. However, their impact on surface albedo and overall climate benefits including adaptation is under-researched, especially in Africa. This study examines the net climate impact of no-tillage and no-tillage with mulch versus conventional tillage in two long-term experiments in Zimbabwe, focusing on abruptic Lixisol and xanthic Ferralsol soils. Measurements over two years included SOC stocks down to 1m depth, N_2O emissions, and surface albedo. The ICBM soil carbon model were used to predicted carbon stocks over 30 years of CA pratices. Results showed that no-tillage with mulching significantly increased SOC in the topsoil with stocks predicted to reach 12.42 Mg C ha^{-1} at DTC and 17 Mg C ha^{-1} at UZF after 30 years of CA practice. Conversely, no-tillage without mulch observed slight SOC losses at DTC, predicted to result in approximately 1.11 Mg C ha^{-1} losses over 30 years. At UZF, no-tillage without mulch increased SOC stocks by about 3.26 Mg C ha^{-1}. On the Ferralsol, mulching enhanced surface albedo, contributing to cooler temperatures. Conversely, on the Lixisol, mulching decreased surface albedo, offsetting SOC benefits and causing a net warming effect. Both sites exhibited low N_2O emissions, indicating a non-significant climate impact. The study underscores the necessity of considering both biogeophysical and biogeochemical effects in evaluating CA's climate mitigation potential.

1. Introduction

The agricultural sector plays a crucial role in climate change mitigation strategies due to its current impact on greenhouse gas (GHG) emissions, but also due to its potential for carbon removal (Lal, 1997; Smith and Olesen, 2010; Kim et al., 2021; Zheng et al., 2023). Conservation agriculture (CA) practices, such as no-tillage and crop residue retention (mulching), have been widely promoted for their positive effects on soil conservation, water retention, and soil organic carbon (SOC) sequestration (Derpsch et al., 2010; Pittelkow et al., 2014; Powlson et al., 2016; Corbeels et al., 2020; Li et al., 2022). Recent studies have shown that no-tillage and mulching practices can impact the climate mitigation potential through both biogeophysical and biogeochemical effects.

Biogeophysical effects of CA are linked to changes in surface albedo, *i.e.* the fraction of solar radiation that is reflected and thus not absorbed by the Earth's surface, but also to changes in energy partitioning at the surface leading to changes in the global and local energy budgets (Davin et al., 2014; Hirsch et al., 2018a; Seneviratne et al., 2018b). Changes in surface albedo directly affect Earth's radiative balance at the top of the atmosphere (TOA), thereby inducing an instantaneous radiative forcing (RF) on the global climate system.

The RF concept is a useful and simple approach to compare the importance of biogeophysical effects, i.e., changes in surface albedo, and biogeochemical effects, such as SOC sequestration or GHGs emissions (Betts, 2000; Pielke et al., 2002). No-tillage and mulching practices may enhance SOC storage through increased inputs of plant residues and improvement of soil structure with a protective effect on SOC stocks (Blanco-Canqui and Lal, 2008). No-tillage and mulching can also affect microbial processes involved in nitrogen cycling, potentially altering emissions of nitrous oxide (N_2O) (Akhtar et al., 2020; Suleiman et al., 2018). Investigating the magnitude and dynamics of SOC and N_2O emissions in response to these practices is essential for evaluating their overall climate impact (Guenet et al., 2021).

Other practices like cover crops or biochar also impact biogeochemical and biogeophysical (e.g. albedo, energy partitioning) processes at different time horizons and scales and both categories of processes have comparable effects on climate in magnitude when using RF as proxy of the global mean temperature response (Bozzi et al., 2015; Genesio et al., 2016;

Ceschia et al., 2017; Carrer et al., 2018; Lugato et al., 2020; Pique et al., 2023). Therefore, it is crucial to account for both biogeochemical and biogeophysical processes to assess their net climatic effect (Cherubini et al., 2012; Sieber et al., 2020). However, the importance of surface albedo changes depends on context-specific factors such as soil type, land management practices, and local climate (Sieber et al., 2020).

A common method to compare biogeophysical and biogeochemical effects involves linking instantaneous radiative forcing of surface albedo change (iRFΔα) to the radiative forcing (RF) from equivalent emissions of CO_2 (Sieber et al., 2020). The relative climate impact of surface albedo change strongly depends on the evaluation time frame. Surface albedo changes result in a RF that lasts only as long as the new state in surface albedo persists, while GHG-induced RF lasts longer and decreases exponentially over decades to centuries (Sieber et al., 2020). Climate metrics like Global Warming Potential (GWP) and global mean temperature change (ΔT) involve subjective choices regarding the type of metric and time horizon (Manne and Richels, 2001; Tanaka et al., 2010). GWP is a commonly used metric that expresses climate impact over different time horizons, defined as the time-integrated RF from a pulse emission relative to that of a pulse emission of CO_2 (Sarofim and Giordano, 2018). It is typically calculated for a time horizon, leading to unequal weighting of surface albedo effects and long-lived climate forcers (Peters et al., 2011). ΔT captures the timing of GHG fluxes and iRFΔα throughout the period of interest, making it useful for comparing short-term and long-term climate forcers. Comparing effects of surface albedo changes and GHG emissions, depending on the study goal requires a time-dependent climate metric. Several methods have been developed to express climate impacts over time using GHG emissions data or iRFΔα in bioenergy LCA (Bright et al., 2012).

In this study, we measured SOC stock changes, N_2O emissions and surface albedo dynamics in two long-term experiments in sub-humid Zimbabwe. Moreover, we include two common, but contrasting soil types in our study, and investigate their impact on the mitigation potential of CA. For the treatment with mulch, we assess two mulch cover scenarios 1) temporary mulch cover (scenario 1, 6 months from sowing to harvest) and 2) permanent mulch cover (scenario 2, 1 year mulch cover from sowing to the sowing of following year) To our knowledge, this is the first study that quantifies the effects of CA practices on SOC

stocks, N_2O emissions and surface albedo, and estimates the related net climate impact. Moreover, it is in general one of the rare studies quantifying climate effects of CA in Sub-Saharan Africa. Our results have important implications for a re-evaluation of these management strategies and related agricultural and environmental policies in this region of the world.

2. Materials and methods

2.1 Experimental sites and treatments

Fieldwork was conducted during two cropping years (2021/2022 and 2022/2023) at two CA experimental sites in Zimbabwe, both established in 2013 and managed by the International Maize and Wheat Improvement Center (CIMMYT). The trials were implemented on distinct soil types: a light-coloured sandy abruptic Lixisol (FAO classification, 1997) at the Domboshawa Training Center (DTC) in the Goromonzi district (17°36'23.3"S; 31°08'26.8''E), situated 30 km from Harare, and a dark-coloured clayey xanthic Ferralsol (FAO classification, 1997) in the Mazowe district (17°43'15.1"S; 31°01'15.8"E) at the University of Zimbabwe Farm (UZF), which is located approximately 10 km from Harare and about 20 km from the first site. DTC soils have a sandy loam texture in the first 30 cm with 18% of clay, 11% of silt and 71%. At UZF, soils have a sandy-clay-loam texture in the first 30 cm, with 31% of clay, 8% of silt and 61% of sand. Cumulative rainfall at DTC was 1219 mm in the 2021/22 cropping year and 1132 mm in that of 2022/23. At UZF, total rainfall was 907 mm in and 941 mm in these two cropping years, respectively.

The experimental design was identical at both sites, and the treatments remained consistent across all seasons since the inception of the experiment. The plots for the study were of 12 m x 6 m dimensions, with a mono-culture of maize (*Zea Mays* L.). Our investigation focused on three treatments: conventional tillage (CT), no tillage (NT), and no tillage with mulch (NTM). Soil N_2O emissions were monitored during the cropping years of 2019/20 and 2020/21 (Shumba et al., 2023) and SOC stocks were quantified in 2021 down to 1 m depth (Shumba et al., 2024). Surface albedo was measured continuously from October 2021 to October 2023 (Diop et al., under review).

2.2 Surface albedo measurements

Four-component net radiometers were used to monitor surface albedo (α) for each treatment. They comprised two pyranometers and two pyrgeometers, with one from each pair oriented upward and the other facing downward. α is measured by the pyranometers within the spectrum ranging from 0.3 to 2.8 µm wavelength, covering the visible spectrum and near-infrared (Diop, 2023). α is derived from the ratio of reflected (downward sensor) to incoming radiation (upward sensor) of the pyranometers using the following equation (Equation III-1):

$$\alpha = \frac{SW_{out}}{SW_{in}} \quad \text{(II.1)}$$

The 4-component net radiometers were horizontally affixed to a mast and positioned 1.5 m above the ground during the fallow period. Throughout the growing season, the height was adjusted to be consistently 1.5 m above the maize canopy. To minimize the impact of surrounding land surfaces, the masts were placed in the center of the plot. The NR01 devices were linked to a datalogger type CR1000 (Campbell Scientific Inc, Logan, UT, USA) for the continuous recording of data at one-minute intervals. Subsequently, the recorded values were averaged at a half-hourly timestep. For more details concerning the measurements and data processing refer to Diop et al., (under review).

Two scenarios of mulch application were investigated. The first scenario (scenario 1), applied in 2021/22, corresponds to a mulch application at sowing. This is the common CA practice for farmers in mixed crop-livestock systems in Zimbabwe. Maize residues are stored after harvest and during the dry season to avoid grazing by cattle, and only applied at sowing when cattle are in the communal grazing areas. The mulch will entirely be decomposed during the rainy season, and the mulch soil cover period is therefore six months. The second scenario (scenario 2), applied in 2022/23, corresponds to a mulch application directly after maize harvest. This practice is found in some homefields that are fenced, therefore avoiding cattle grazing of the residues. During the dry season, mulch is not decomposed and can therefore have a long-lasting effect on surface albedo. The mulch will then decompose during the rainy season. The mulch soil cover period is therefore one year.

2.3 Soil nitrous oxide emissions

N_2O emissions were measured using static chambers, a common methodology to measure GHG emissions from croplands. N_2O emissions were measured from 24 experimental plots at DTC and UZF sites during 2019/20 and 2020/21 cropping seasons (Shumba et al., 2023). During 2020/21 N_2O sampling was also extended during the dry fallow period (May-September 2021). Measurements were taken between two maize plants within the same row as well as between two rows of maize. Gas sampling was conducted between 10 am and 12 pm. N_2O was measured through gas chromatography employing electron capture detectors. N_2O fluxes were determined by computing the change in concentration between the 0 and 48-minute sampling intervals (see more details in (Shumba et al., 2023).

2.4 Soil organic carbon stocks

Soil sampling was conducted in May 2021 8 years after initialization of the trials at both sites and on each of the three treatments. SOC stocks were measured down to a depth of 100 cm and calculated using the equivalent soil mass (ESM) method to account for any change in soil bulk density (Ellert and Bettany, 1995; Gál et al., 2007; Lee et al., 2011; Wendt and Hauser, 2013; von Haden et al., 2020). Nevertheless, significant treatment effects were limited to the top 30 cm at DTC and the top 20 cm at UZF (see Table 2 of Shumba et al 2024), and we therefore focus on the top-soil defined as 0-30 cm profile depth. Annual SOC stock change (ΔSOC) rates were calculated by dividing the stock change by the number of years between the implementation of the trials and the SOC measurements, i.e., 8 years. (Shumba et al., 2024). Here the reference is conventional tillage (CT) for which SOC stocks were assumed to be in steady state.

2.5 Climate impact assessment

2.5.1 Instantaneous radiative forcing induced by albedo change

In this study, we computed the instantaneous radiative forcing (*iRF*) at the top of the atmosphere (TOA) under NT and NTM practices relative to CT as reference for both sites and over both cropping years employing the method of (Muñoz et al., 2010):

$$iRF \triangle \alpha(i) = -SW_{in(i)} \times Ta(i) \times \triangle \alpha(i) \quad \text{(II-2)}$$

where, SW_{in} is the daily global radiation of the day i, Ta represents the daily atmospheric transmittance of the day i and $\Delta\alpha$ is the daily mean surface albedo difference between a given treatment (NT or NTM) and a reference (CT treatment) of the day i. The result is expressed in W.m^{-2}. Annual mean $iRF\Delta\alpha$ values were assessed based on daily outcomes, with positive values indicating a warming effect and negative values a cooling effect.

2.5.2 Metrics

Surface albedo change climate impact is expressed as GWP using 20 and 100 years THs as representative of the short-term objectives of regional mitigation and adaptation strategies and the long-term goals of the Paris Agreement, respectively, and ΔT as an indicator of impacts over time. Therefore, we used the GWP approach with a TH of 20 and 100 years (GWP_{20}. GWP_{100}) to assess albedo climate impact expressed in kg CO_2 ha^{-1} described in equation II-3. Incorporating the timing of these impacts, can more accurately depict the relative influence of climate forcers with varying perturbation durations (Boucher and Reddy, 2008; Sieber et al., 2020).

$$GWP\Delta\alpha = \frac{\sum_{y=1}^{t=TH} RF\Delta\alpha(y)}{AGWP_{CO2}^{TH}} \quad \text{(II-3)}$$

where TH represents the metric time horizon in years, $RF\Delta\alpha$ is a vector of the annual mean instantaneous radiative forcing induced by a local change in albedo expressed in W.m^{-2}. AGWP corresponds to the Absolute Global Warming Potential of CO_2 ($AGWP_{CO2}$) with a

characterization factor of 40.1×10^{12} kg CO_2e for GWP_{20} and 10.9×10^{12} kg CO_2e for GWP_{100} for an annual mean RF induced by albedo change (Myhre et al., 2013).

The global warming potential (GWP) metric was used to convert N_2O emissions and SOC sequestration to CO_2 equivalents (CO_2-eq.) as suggested by the IPCC (Ipcc, 2023). While changes in SOC stocks can directly be translated into CO_2 release or sequestration, each kg of emitted N_2O has to be converted into 273 kg CO_2-eq. Note that the same conversion factor is valid for 20 and 100 years TH. The GWP of N_2O and SOC were computed following equations 6 and 7, respectively. Note that here further conversions from mass of N to mass of N_2O (44/28, eq. II-4) and from mass of C to mass of CO_2 (44/12, eq. II-5) are included.

$$GWP_{\Delta N_2O} = \left(N_2O_{treatment} - N_2O_{reference(CT)}\right) \times (44/28) \times 273 \quad \text{(II-4)}$$

$$GWP_{\Delta SOC} = \left(\Delta SOC_{treatment} - \Delta SOC_{reference(CT)}\right) \times (44/12) \quad \text{(II-5)}$$

Also, to evaluate time dependent climate impact of NT or NTM relative to CT, we used global mean temperature change (ΔT), a characterization model developed by (Ericsson et al., 2013) for GHGs adapted for albedo (see Sieber et al., 2020). The climate response of N_2O and SOC in terms of global mean temperature response was evaluated using the impulse response function (IRF) expressed as follows:

$$\Delta T_i(TH) = \sum_{t=0}^{TH} G_i(t) \times AGTP_i(TH - t) \quad \text{(II-6)}$$

where $G_i(t)$ in kg represents a vector of an annual forcing agent i, SOC and N_2O in this study. $AGTP_i$ corresponds to the absolute global temperature potential of a forcing agent expressed in K kg^{-1}. $\Delta T_i(TH)$ provides the response to emissions and forcings across various years up to the time horizon (TH) by performing the convolution in eq. II-6.

AGTP of SOC and N_2O is obtained by performing the convolution integral of IRFs (see Sieber et al., (2020) for more details).

The same magnitude of N_2O emissions was considered over 30 years of practices of CA. For albedo under both mulch scenarios, a constant value was used as long as the practice is maintained. Long term climate impact assessed with ΔT of SOC is based on the outputs of the ICBM model.

2.5.3 Simulation of changes in soil organic carbon storage

We used the ICBM (Introductory Carbon Balance Model) model to simulate the evolution of SOC stocks at an annual time step (Andrén and Kätterer, 1997). The model was firstly developed in Sweden and has been applied with good performances in other pedoclimatic contexts in Sub-Saharan Africa, including Kenya (Andrén et al., 2012) and Ivory Coast (Cardinael et al., 2022). ICBM is a simple model and consists of a young (*Y*) and an old (*O*) carbon pool. The *Y* pool represents the fresh organic carbon, while the *O* pool corresponds to the stabilised organic carbon (eq. II-7 and II-8). SOC stocks at equilibrium were defined by assuming that the CT treatment is at equilibrium. The model requires few inputs and model parameters, making it quite simple to calibrate with observation data (see Table III-S1). To run the model, the organic carbon inputs to the soil were defined as the cumulative carbon inputs of a given treatment from 2013-2021 based on (Shumba et al., 2024), shaping a sole *Y* pool with a specific decomposition (k_Y) and humification (h) constants depending on organic carbon inputs and clay content as described in equation 3. External factors, such as climate and soil cultivation, are encapsulated within the "r_e" parameter, which is specific for each site and treatment (Kätterer and Andrén, 1999). r_e determines the climate interaction with decomposition coefficients. Its calculation requires climatic data at daily time step, soil data and crop properties (Menichetti et al., 2024). Adjustments of the *h* coefficient (*e.g.*, in light-coloured sandy or dark-coloured clayey soil) were made to minimise errors between observations and simulations. We started the calibration procedure for the NT and NTM treatments using default parameters applied by earlier studies in Sub-Saharan Africa (Andrén et al., 2007; Cardinael et al., 2022). We then calculated r_e parameter following the method developed by (Menichetti et al., 2024) based on meteorological data recorded at our two sites. The evolution in SOC dynamics in response to the different treatments simulated by ICBM allow us to assess short-term and long-term impacts of no-tillage and mulching practices on SOC sequestration.

$$Y_{t+1} = (Y_t + I_t).\, e^{-ky.re} \quad \text{(II-7)}$$

$$O_{t+1} = \left(O_t - h\frac{Ky\cdot(Y_t+I_t)}{k_o-k_y} \right) \cdot e^{-ko.re} + h\frac{Ky.(Y_t+I_t)}{k_o-k_y} \cdot e^{-ky.re} \quad \text{(II-8)}$$

3. Results

3.1 Effects of CA practices on SOC

Figure II-1 shows the effect of CA practices on SOC simulated using Introductory Carbon Balance Model (ICBM) at Domboshawa Training Center (DTC) site with a light-coloured sandy soil and University of Zimbabwe Farm (UZF) site with a dark-coloured clayey soil under 30 years of continued management of conventional tillage (CT), no-tillage (NT) and no-tillage with mulch (NTM). At DTC, a slight loss of SOC stock was observed after 8 years in NT (Shumba et al.,2024), and it is predicted to reach approximately 1.11 Mg C ha^{-1} losses over 30 years of CA practices with the ICBM model (Figure III-1). SOC stock increased under NTM (+2.9 Mg C ha^{-1} in 0-30 cm after 8 years) and it is expected to reach +12.42 Mg C ha^{-1} compared to CT with ICBM, corresponding to an average accumulation rate of 0.41 Mg C ha^{-1} y^{-1} by the end of the assumed 30 years of continued management.

At UZF, NT showed a slight increase in SOC stocks of about 3.26 Mg C ha^{-1} relative to CT, and NTM significantly increased SOC stocks up to 17 Mg C ha^{-1} compared to CT (Figure II-1) with the model ICBM, representing an average SOC accumulation rate of 0.56 Mg C ha^{-1} y^{-1} at the end of the assumed 30 years of CA practices. This indicates a relatively low impact of NT on SOC stocks at the two sites, whereas NTM results in significant increases in SOC stocks over 30 years compared to CT.

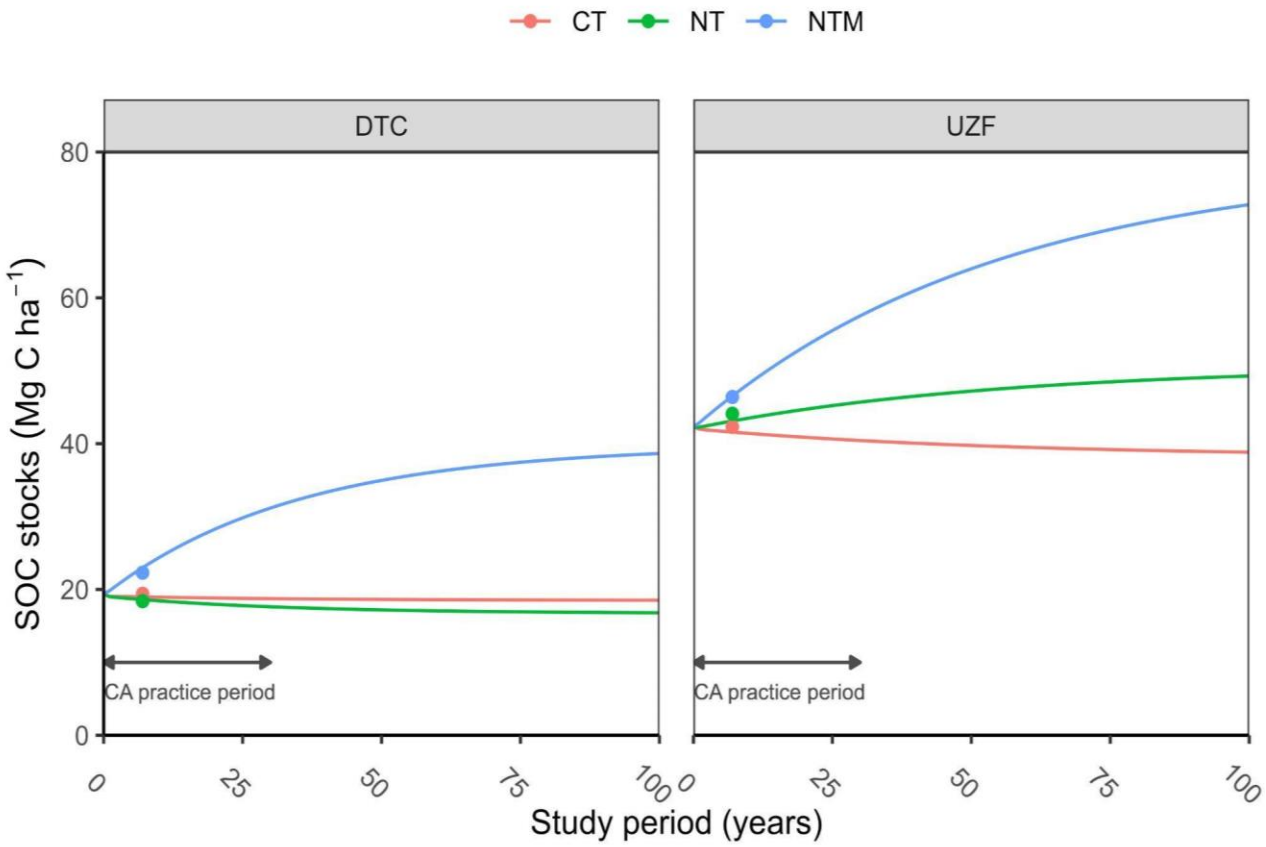

Figure II-1. Soil organic carbon stocks (0-30 cm) simulated by the ICBM model for no-tillage (NT, green) and no-tillage with mulch (NTM with mulch, blue) relative to the reference conventional tillage (CT, red). Dots represents SOC measured 8 years after the start of the trials.

3.2 Climate impact of CA practice

In the light-coloured sandy Lixisol at DTC, 30 years of NT practices led to a SOC loss (Figure II-1), representing a warming effect on global mean temperature with a maximum of $+0.9\times10^{-11}$K ha^{-1} in year 42 (Figure II-2) before decreasing by 23% by the year 100. This warming effect was dampened by the increase in surface albedo over 50 years resulting in a net cooling effect with a maximum of -3.48×10^{-11} K ha^{-1}, before it turned then into a net warming effect after 50 years, reaching $+0.6\times10^{-11}$ K ha^{-1} at year 100 (Figure II-2). Reduced N_2O emissions led to a slight cooling effect of around -0.5×10^{-11} K ha^{-1}. It resulted in a net cooling effect on global mean temperature of -2.17 and -0.59×10^{-11} K ha^{-1} over 20 and 100 years, respectively (Table II-S3).

For NTM at DTC, SOC sequestration initially led to a strong cooling effect with a peak of cooling of -2.65×10^{-11} K ha^{-1} in year 42. However, a strong decrease in surface albedo was observed at this site following crop residues retention. This induced a warming effect on global mean temperature of +0.88 and +2.15×10^{-11} K ha^{-1} in scenario 1 and 2 respectively (with a maximum at year 30. Figure II-2). In a 100-year TH, the warming effects on global mean temperature caused by crop residue retention are 0.47 and 1.15×10^{-11} K ha^{-1} in scenario 1 and 2 respectively. A small warming from additional N_2O emissions of around +0.15×10^{-11} K ha^{-1} was also observed. It resulted in a net warming effect on global mean temperature of +0.3 and 1.57×10^{-11} K ha^{-1} for scenario 1 and 2 respectively within 30 years of crop residue management over 20 years TH. Over 100 TH, the net climatic effects of mulching are reduced by 50% under both scenarios of crop residue management.

In the dark-coloured clayey Ferralsol at UZF, additional SOC storage under NT compared to CT resulted in cooling effects of -1.52×10^{-11} K ha^{-1} over 100 years TH. NT practices over 30 years induce an additional cooling effect on global mean temperature of -0.65 and -0.34×10^{-11} K ha^{-1} over 20 and 100 THs respectively. This cooling effect was large during the 30 years where the practice was maintained and significant up to year 50 before reaching a near-neutral effect in year 100. Concerning N_2O emissions, a non-significant warming effect was observed. Overall, it resulted in a net cooling effect of -1 ×10^{-11} K ha^{-1} for scenario 1 and -1.57×10^{-11} K ha^{-1} for scenario 2.

Additional SOC storage at NTM compared to CT had a cooling effect on global mean temperature of -2.85×10^{-11} K ha^{-1} over 100 years. Increases of surface albedo following crop residues retention induced a moderate cooling effect that was more pronounced in scenario 2 than in scenario 1. In scenario 1, the strongest net cooling effect was observed in year 30 were -3.94×10^{-11} K ha^{-1} while a peak of cooling effect in scenario 2 was -4.62×10^{-11} K ha^{-1} at year 30 which was then slightly reduced due to the decrease at the end of CA practices. Changes in N_2O emissions were very low over 100 years, resulting in a small and no-significant effect. It resulted in a net cooling effect of -1.19 and 1.68×10^{-11} K ha^{-1} at TH 20 2 times less than TH 100 where net cooling effect on global mean temperature were 3.01 and 3.26×10^{-11} K ha^{-1} for scenario 1 and scenario 2 respectively.

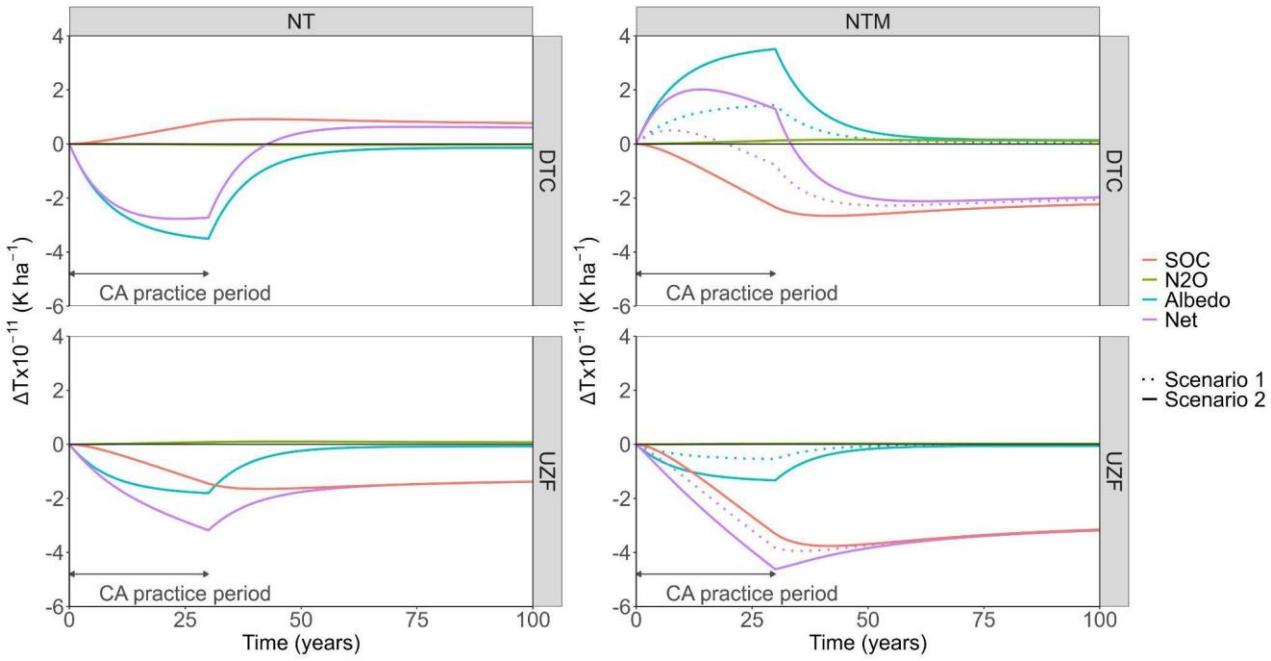

Figure II-2. Change in global mean temperature due to change in SOC stock (red line), N_2O emissions (green line) and surface albedo (blue line) under no-tillage (NT on the left) and no-tillage and mulch (NTM, on the right) compared to conventional tillage (CT) on a light-coloured sandy Lixisol (DTC, up) and on a dark-coloured clayey Ferralsol (UZF, bottom). The net climate effect (purple line) includes effects of changes in surface albedo, N_2O emissions and SOC sequestration. Dashed lines represent the scenario with temporary mulch cover (scenario 1) and solid lines represent the scenario with permanent mulch cover (scenario 2).

Climate impacts of 30 years of CA practices assessed with GWP (Figure II-3) show the same relative magnitude as global mean temperature change. At DTC, in the NT treatment, net cooling effects of -2.56 Mg CO_2-eq ha^{-1} yr^{-1} over a 20 years TH and of -0.65 Mg CO_2-eq ha^{-1} yr^{-1} at a 100 years TH were observed with a contribution from surface albedo changes of 97% at TH 20 and 91% at TH 100. A slight warming effect due to SOC loss was observed but totally offset by surface albedo change effects. Also, slight reductions in N_2O emissions led to a very small cooling effect of about -0.01 Mg CO_2-eq ha^{-1} yr^{-1} in the NT treatment compared to CT over 100 years (Table II-S4).

At DTC, the NTM treatment had a net warming effect at TH 20 years, more pronounced under the permanent mulch cover scenario (Table II-S4), but a net cooling effect at TH 100 years. Increase in SOC stock provided a significant cooling effect in NTM compared to CT with -0.87 Mg CO_2-eq ha^{-1} yr^{-1} at TH 100 years (Figure II-3). N_2O emissions resulted in a minor additional warming effect in the NTM of +0.07 Mg CO_2-eq ha^{-1} yr^{-1} at TH 100 years.

Increased surface albedo in the NTM treatment resulted in a warming effect of +0.89 Mg CO_2-eq ha^{-1} yr^{-1}, dampening the benefit of SOC leading to near-neutral net climate effect in the scenario 1. In scenario 2 the warming effect caused by mulching is about 2 times higher, causing a net warming effect of +1.38 Mg CO_2-eq ha^{-1} yr^{-11} at TH 20 years. At TH 100 years, the 30 years of CA practices show a cooling effect under the scenario with temporary mulch cover which is reduced by 63% under the scenario with permanent mulch cover.

In the light-coloured sandy Lixisol at DTC, the increase in surface albedo offsets the warming effect of the SOC loss in NT compared to CT whatever the TH considered. However, the benefit of SOC is dampened by warming caused by decrease of surface albedo change at TH 20. while at TH 100 a cooling effect is observed after 30 years of CA crop residues management.

At UZF, the NT treatment had a net climate cooling impact compared to CT of -1.25 Mg CO_2-eq ha^{-1} yr^{-1} at TH 20 years and of -0.77 Mg CO_2-eq ha^{-1} yr^{-1} at TH 100 years with a contribution of 50% over 20 years and 20% over 100 years from surface albedo changes. SOC sequestration contributed around 49% to the net cooling effect at TH 20 years and 79% at TH 100 years. A small and no significant warming effect of about -0.04 Mg CO_2-eq ha^{-1} yr^{-1} was caused by N_2O emissions in the NT treatment compared to CT over 100 years. NTM treatment had a net cooling effect compared to CT especially under the permanent mulch cover scenario. SOC sequestration led to a significant cooling effect in NTM compared to CT with -1.49 Mg CO_2-eq ha^{-1} yr^{-1} at TH 100 years (Figure II-3). N_2O emissions resulted in a minor additional warming effect in NTM of +0.01 Mg CO_2 eq ha^{-1} yr^{-1} at TH 100 years. In scenario 1, the increase in surface albedo in the NTM treatment resulted in a cooling effect of -1.82 Mg CO_2-eq ha^{-1} yr^{-1}, reinforcing the net climate cooling effect. In scenario 2, the albedo cooling effect caused by mulching is about two times higher than in scenario 1, causing a net cooling effect of -2.31 Mg CO_2-eq ha^{-1} yr^{-1} at TH 20 years. On a 100 years TH, 30 years of CA practices show a reduction of surface albedo contribution to the cooling effect by 70% for both mulch scenarios

For both treatments at UZF, the increase in surface albedo strengthened the benefit of SOC sequestration, resulting in a pronounced net cooling effect in NTM. In this dark-coloured clayey soil both biogeophysical and biogeochemical effects have the same direction.

Overall, when considering both biogeochemical and biogeophysical effects, mulching had a contrasting effect depending on the soil type (soil colour), especially with permanent mulch cover. The cooling effect due to SOC sequestration in the dark-coloured clayey Ferralsol at UZF was strengthened by the increase in surface albedo, but was reduced and even offset in the light-coloured sandy Lixisol at DTC.

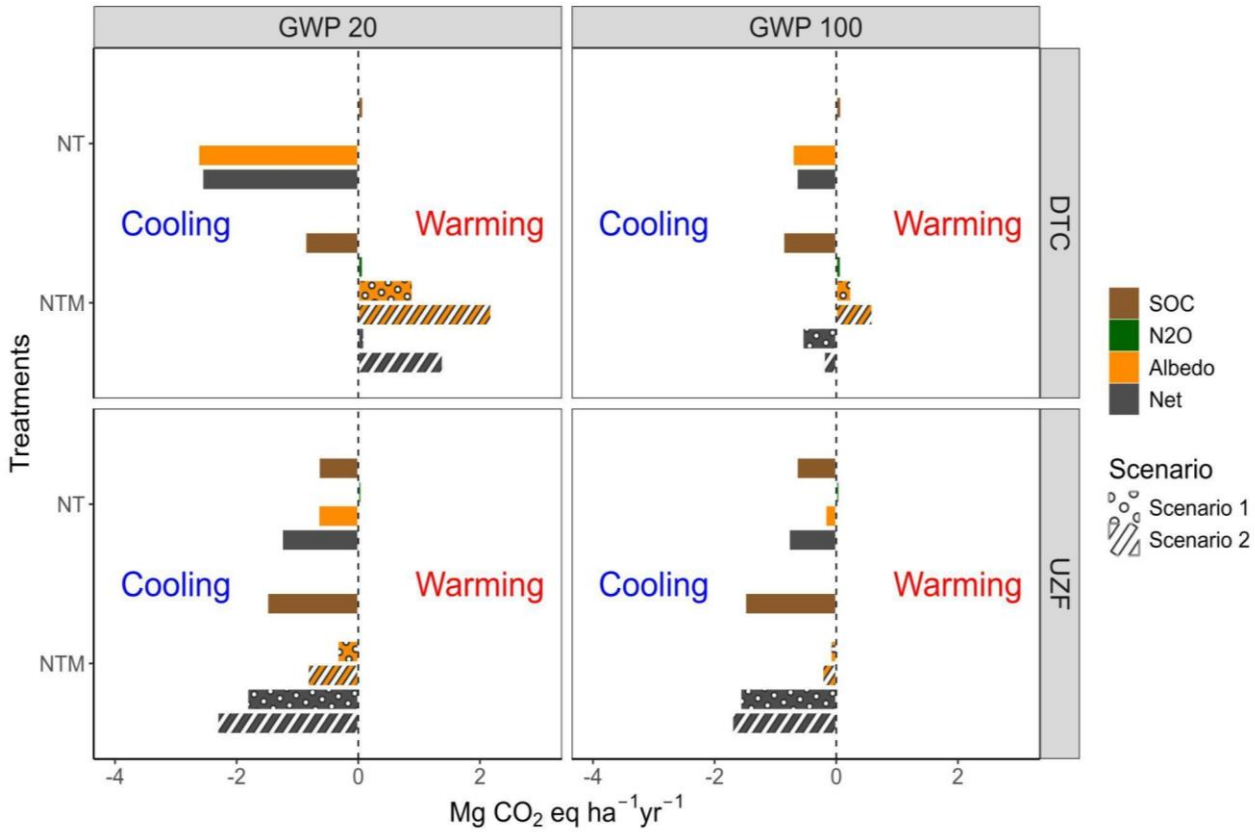

Figure II-3. Climate impact due to SOC sequestration, N_2O emissions and surface albedo changes expressed as GWP (Mg CO_2 eq ha^{-1} yr^{-1}) considering 20 and 100 years time horizons under no-tillage (NT) and no-tillage with mulch (NT) compared to conventional tillage (CT) on a light-coloured sandy soil Lixisol (DTC) and on a dark-coloured clayey Ferralsol (UZF). Scenario 1 represents temporary mulch cover and scenario 2 represents permanent mulch cover.

4. Discussion

4.1 Biogeochemical effect of CA

Our results showed that at the UZF site increased SOC sequestration in NT and NTM treatments resulted in a significant cooling effect, with a more pronounced cooling effect under the NTM treatment because of higher SOC storage increase, due to minimum soil

disturbance and high organic carbon inputs (Nyamadzawo et al., 2008; Wang et al., 2020). The study further revealed contrasting effects on SOC stocks between NT and NTM treatments at the DTC site, where the NT treatment led to a slight SOC loss and induced a warming effect, whereas the NTM treatment increased the SOC stock and induced a cooling effect. NT and NTM practices had a small effect on N_2O emissions, with a resulting climatic impact that is negligible compared to that of SOC sequestration. This is in contradiction with Guenet et al., (2021)who suggested that increased N_2O emissions in no-till systems could offset the climate benefit from SOC storage. Low N_2O emissions in this context could be explained by the low mineral nitrogen inputs (60 kg N ha^{-1} yr^{-1}) applied within three times and on the maize row only, probably increasing nitrogen use efficiency. Fertiliser use in Sub-Saharan Africa is particularly low (about 13-20 kg N ha^{-1} yr^{-1}) compared to the Global North (Dimkpa et al., 2023; Falconnier et al., 2023; Shumba et al., 2023), and N_2O emissions are therefore lower. Moreover, the long dry fallow period is also an important aspect explaining low N_2O emissions (Cardinael et al., 2024).

4.2 Soil type and management practices impacts on biogeophysical effect

Our findings highlight the different impacts of soil management practices on surface albedo change and net climate effects across various soil types and agricultural practices. The results outline the importance of considering the environmental context when evaluating tillage and crop residues management practises for climate change mitigation strategies. NT practice increases surface albedo because of the decrease of surface roughness which is an important driver of surface albedo (Post et al., 2000; Sieber et al., 2022). The application of maize residues on dark-coloured clayey soil at UZF increases surface albedo, leading to a cooling effect with a more pronounced effect for permanent mulch cover compared to temporary one. However, in the light-coloured sandy soil at DTC mulching has an opposite effect, reducing surface albedo, leading to a warming effect, again with a more important climate impact for permanent mulch cover. These findings are in line with (Horton et al., 1996), who demonstrated that retaining crop residues in no-till systems enhances surface albedo on dark soils during bare fallow periods. In addition, Horton et al., (1996) showed

that crop residues colour may decrease or increase surface reflectance depending on soil type.

Our study did not take into account the possible soil darkening effect due to an increase in top-soil SOC concentrations with time, and the subsequent decrease in surface albedo as in Pique et al., (2023). Therefore, the climatic impact of soil darkening effect has not been quantified here but the direction of this effect could be estimated. When the soil is covered by mulch for 6 months, the benefit of SOC increase would be dampened by the soil darkening effect leading to a decrease in surface albedo, particularly when the mulch has been decomposed and the crops harvested. This effect would be probably stronger in the light-coloured sandy soil because of initial lower SOC stocks. When mulch covers the soil during the whole year, the negative effect due to soil darkening would be less, but still of potential importance as crop residues only cover approximately 45% of the soil (Diop et al., under review). Pique et al., (2023) warned of a substantial risk of losing some climate benefits from SOC storage due to decrease in soil albedo following soil darkening if soils are not kept permanently covered after carbon farming practices are adopted.

4.3 Global and local climate effects

Our results address the effects of CA management practices on global mean temperature. No-tillage practices have a net cooling effect on global mean temperature on both sites compared to CT. Surface albedo makes a major contribution to this cooling effect. Similarly, Lobell et al., (2006) showed that reduced-tillage under global no-tillage scenario has a global cooling effect about 0.2 °C due to surface albedo increases, of the same magnitude as the cooling effects of the simultaneous SOC sequestration using a coupling of Community Atmosphere model (CAM, (Collins et al., 2004)) and Community Land Model (CLM, (Oleson et al., 2004)). CA management practices have not only an effect on the global climate, but also on the local air and surface temperature. Hirsch et al., (2018b) modelled the biogeophysical impacts of CA at global scale, revealing a local cooling effect in mid-latitude regions and potential warming in tropical areas. No-tillage with crop residues management practices in European croplands can decrease surface temperatures locally during extreme

heat waves, which is thus considered as an adaptation strategy to the increase in this phenomenon (Davin et al., 2014; Seneviratne et al., 2018a). Nevertheless, in Davin et al. (2014) the cooling effect due to albedo change is dampened by surface energy partitioning effects with a reduction in the evaporation flux, an increase in surface temperature, and an increase of the sensible heat flux. In our study, we did not consider the change in sensible and latent heat flux which is an important part of energy partitioning at the surface in order to quantify the overall biogeophysical effect (Ceschia et al., 2017)

4.4 Climate metrics

Global mean surface temperature is a time-dependent climate metric reflecting the timing of emissions and forcing (Ericsson et al., 2013; Sieber et al., 2020). This time-dependent effect is shown in the result of climate impact assessed with ΔT but not in the case for GWP. GWP is a simple method to convert RFs to CO_2 equivalent allowing the comparison of the magnitude of biogeophysical and biogeochemical climate impacts (Betts, 2000). We used in this study IPCC GWP conversion factors for CO_2 and N_2O over 20- and 100-years TH. It's very simple to assess climate impact of different CA practices at different timescales. For surface albedo, a characterization factor was used to convert annual mean iRF derived from (Sieber et al., 2020). The limit of using GWP metric conversion factors is in the assessment of climate impact dynamics using different time duration of management practices resulting in unequal weight of short-term and long-term climate forcers (Sieber et al., 2020). A similar finding, relative to our study was observed in (Sieber et al., 2020), where the potential of climate change mitigation of temporary SOC was overestimated and the climate impact of surface albedo change was underestimated on longer timescales. These metrics serve to measure the impact of emissions of different GHGs on climate change. They function as 'exchange rates' facilitating the comparison of emissions across different policies, regions, countries, sources, and sectors (Myhre et al., 2013).

4.5 Limits of our study

There is uncertainty whether a unit RF from albedo change causes the same global mean temperature change as one unit RF from changes in CO_2 concentration, which is typically expressed as climate sensitivity. Climate sensitivity for albedo RF relative to CO_2 RF ranges 0.5-1.02 for global land use change scenarios simulated with different climate models (Davin et al., 2007; Davin and de Noblet-Ducoudré, 2010). The calculation method of iRF albedo is a simple analytical approach based on a single layer radiative transfer model. There are also uncertainties in the instantaneous radiative forcing calculation. The uncertainties of this method are mostly from atmospheric transmittance, which need more sophisticated climate models including local cloud cover data (Muñoz et al., 2010). In addition, this method is quite old and newer methods that account for spatial-temporal variations in atmospheric conditions including cloud cover have existed recently(Bright and Lund, 2021; Sieber et al., 2020) and these methods do not require sophisticated climate models. Concerning the inventory data, we provide one year of SOC measurement to calibrate the ICBM model. More observational samples could enhance the quality of model outputs to reduce uncertainties from the model. Interannual variability of N_2O emissions were not considered in this study, the same magnitude was applied for each year to assess N_2O climate impact.

5. Conclusion

Our study highlighted the need to consider both biogeophysical and biogeochemical effects to fully assess the climate mitigation potential of conservation agriculture practices. On both light-coloured sandy Lixisol and dark-coloured clayey Ferralsol, mulching increased SOC stock compared to conventional tillage. Differences as well as the total magnitude of N_2O emissions were small, reflecting low rates of fertiliser application that are typical for Sub-Saharan Africa. The retention of crop residues affected surface albedo differently depending on soil type. On the light-coloured sandy Lixisol, it reduced the surface albedo, contributing around 70% to the net warming effect. Conversely, on the dark-coloured clayey Ferralsol, it increased surface albedo, resulting in a contribution of 63% to net cooling effect. Therefore, the same land management practice could either mitigate or exacerbate climate change

depending on soil type, and more precisely soil colour. These results call for caution when promoting conservation agriculture as a climate smart agriculture practice or as a nature base solution. Similar approaches considering both biogeochemical and biogeophysical effects should be promoted when evaluating the climatic impact of nature-based solutions in order to develop more efficient climate mitigation strategies.

Supplementary materials

Table II-S1. Parametrization of ICBM carbon model

		DTC	UZF	
Parameter	Descriptions	Value	Value	References
Y0	Young C pool, initial	0.97	1.27	5% of O0
O0	Old C pool, initial	18.43	41.031	Shumba et al., 2024
kY	Decomposition constant for Y	0.8	0.8	Andrén and Kätterer, 1997
kO	Decomposition constant for O	0.0065	0.0065	Andrén and Kätterer, 1997
re CT	External factors CT	1.2	2.1	Calibration
re NT	External factors NT	2.2	2.1	Calibration
re NTM	External factor NTM	0.8	2.1	Calibration
h	Humification coefficient	0.14	0.5	Calculated according to Andrén et al. (2004)

Table II-S2. Surface albedo difference of No-tillage (NT) and No-tillage with mulch (NTM) relative to Conventional-tillage (CT).

		DTC	UZF
Seasons	Treatments	Value	Value
2021/22	NT	0.025 (±0.013)	0.006 (±0.006)
	NTM	-0.008 (±0.016)	0.011 (±0.009)
2022/23	NT	0.021 (±0.013)	0.004 (±0.011)
	NTM	-0.023 (±0.022)	0.008 (±0.008)

Table II-S3. Climate impact including albedo change using ΔT (K ha^{-1}).

		DTC		UZF	
		NT	NTM	NT	NTM
ΔT(20)	N2O	-0.005	+0.03	+0.01	+0.005
	SOC	+0.21	-0.6	-0.38	-0.86
	Albedo	-2.37	-	-0.65	-
	Albedo Scenario 1	-	+0.88	-	-0.33
	Albedo Scenario 2	-	+2.15	-	-0.82
	Net	-2.17	-	-1	-
	Net Scenario 1	-	+0.3	-	-1.19
	Net Scenario 2	-	+1.57	-	-1.68
ΔT(100)	N2O	-0.02	+0.1	+0.07	+0.02
	SOC	+0.69	+2.01	-1.25	-2.85
	Albedo	-1.27		-0.34	-
	Albedo Scenario 1	-	+0.47	-	-0.18
	Albedo Scenario 2	-	+1.15	-	-0.43
	Net	-0.59	-	-1.52	-
	Net Scenario 1	-	-1.43	-	-3.01
	Net Scenario 2	-	-0.75	-	-3.26

Table II-S4. Climate impact including albedo change using GWP express in Mg CO_2 ha^{-1} yr^{-1}.

		DTC		UZF	
		NT	NTM	NT	NTM
GWP (20)	N2O	-0.013	+0.073	+0.047	+0.014
	SOC	+0.079	-0.87	-0.64	-1.49
	Albedo	-2.63	-	-0.65	-
	Albedo Scenario 1	-	+0.89	-	-0.34
	Albedo Scenario 2	-	+2.18	-	-0.83
	Net	-2.56	-	-1.25	-
	Net Scenario 1	-	+0.09	-	-1.82
	Net Scenario 2	-	+1.38	-	-2.31
GWP (100)	N2O	-0.013	+0.073	+0.047	+0.01
	SOC	+0.079	-0.87	-0.64	-1.49
	Albedo	-0.71		-0.17	-
	Albedo Scenario 1	-	+0.24	-	-0.09
	Albedo Scenario 2	-	+0.59	-	-0.22
	Net	-0.65	-	-0.77	-
	Net Scenario 1	-	+0.55	-	-1.57
	Net Scenario 2	-	+0.20	-	-1.71

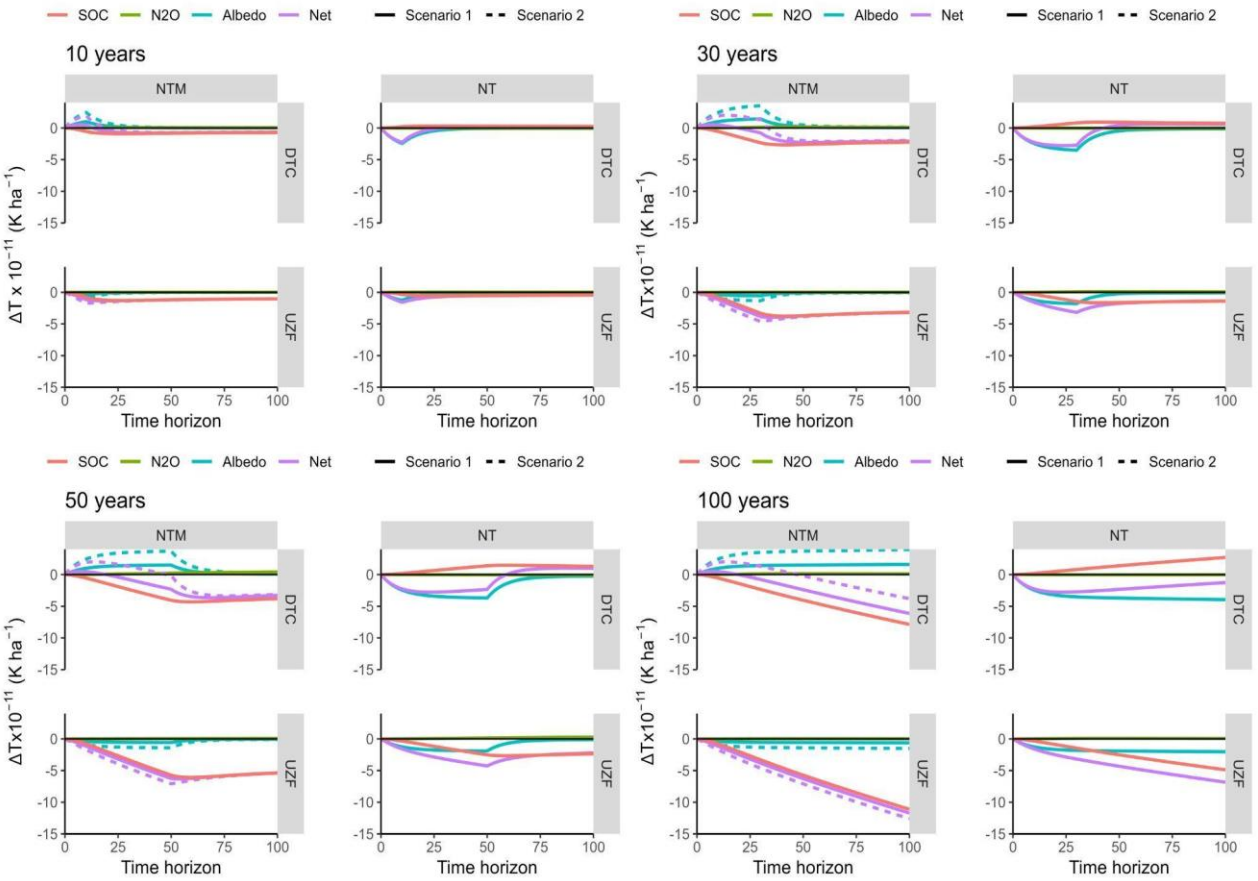

Figure II-S1. Change in global mean temperature due to change in SOC stock (red line), N_2O emissions (green line) and surface albedo (blue line) under no-tillage (NT on the left) and no-tillage and mulch (NTM, on the right) compared to conventional tillage (CT) on a light-coloured sandy Lixisol (DTC, up) and on a dark-coloured clayey Ferralsol (UZF, bottom) over 10. 30. 50 and 100 years of practice of no-tillage (NT) and no-tillage with mulch (NTM). The net climate effect (purple line) includes effects of changes in surface albedo, N_2O emissions and SOC sequestration. Dashed lines represent the scenario with temporary mulch cover (scenario 1) and solid lines represent the scenario with permanent mulch cover (scenario 2).

Chapitre III : Modélisation de l'albédo de surface avec le modèle de système de cultures STICS

Ce chapitre est adapté d'un article en cours de préparation.

Résumé en français :

L'agriculture de conservation (AC) est largement promue pour ses effets biogéochimiques bénéfiques sur le climat, tels que la séquestration du carbone organique dans les sols et la réduction des émissions de gaz à effet de serre. Cependant, les pratiques de l'AC influencent également les effets biogéophysiques, notamment par des changements d'albédo de surface. Les pratiques peuvent modifier de manière significative la dynamique de l'albédo de surface dans les parcelles agricoles. Malgré cela, l'impact de ces pratiques sur les changements d'albédo de surface est souvent omis dans de nombreux modèles de système de culture. Le modèle de système de culture STICS est reconnu pour sa compréhension détaillée des processus par lesquels la gestion des pratiques affecte diverses variables agro-environnementales dans des contextes pédoclimatiques divers. Cette étude visait à évaluer la capacité du modèle STICS à simuler les variations de l'albédo de surface au cours d'une année de culture de maïs (*Zea mays* L.) dans deux sites expérimentaux de longue durée avec des types de sols contrastés en Afrique subsaharienne. Les données collectées sur deux ans, incluant l'indice foliaire (LAI), la teneur en eau du sol, la biomasse sèche aérienne, le rendement en grains, et l'albédo de surface, ont été utilisées dans cette étude. Pour mieux refléter les processus observés, nous avons introduit un nouveau formalisme pour l'albédo de surface intégrant les effets des feuilles sénescentes, ainsi qu'une amélioration du calcul de l'évaporation du sol. Les résultats ont indiqué que le modèle simulait efficacement la phénologie des cultures (rRMSE de 1,2% pour l'anthèse et 1,3% pour la maturité), la teneur en eau du sol (rRMSE de 14%), et le LAI (rRMSE de 14%). Cependant, il surestimait la biomasse aérienne (rRMSE de 42%) et le rendement en grains (rRMSE de 74%). En ce qui concerne l'albédo de surface, le formalisme existant menait à une surestimation pendant la phase de sénescence. L'inclusion des feuilles sénescentes dans le calcul a amélioré la

précision des simulations. De plus, le nouveau formalisme pour l'évaporation du sol a joué un rôle crucial dans l'amélioration de la simulation de l'albédo de surface. Cette étude met en évidence le potentiel du modèle STICS à simuler l'impact des pratiques de gestion des terres sur l'albédo de surface. Cette approche est prometteuse pour évaluer les impacts climatiques à la fois sur les effets biogéophysiques et biogéochimiques dans divers contextes pédoclimatiques.

Simulating surface albedo dynamics under conservation agriculture using the STICS soil-crop model – Application to two Sub-Saharan sites

Souleymane Diop[1,2,3], Rémi Cardinael[3,4,5], Gatien Falconnier[3,4,5,6], Ronny Lauerwald[1], Christian Thierfelder[6], François Affholder[3,4,7], Regis Chikowo[5,8], Patrice Lecharpentier[9], Eric Ceschia[2]

[1]Université Paris-Saclay, INRAE, AgroParisTech, UMR EcoSys, 91120 Palaiseau, France

[2]CESBIO–Univ. Toulouse III/CNRS/CNES/IRD/INRAE 18, avenue, Edouard Belin, bpi 2801, 31401 Toulouse Cedex 9, France

[3]CIRAD, UPR AIDA, Harare, Zimbabwe

[4]AIDA, Univ. Montpellier, CIRAD, Montpellier, France

[5]Department of Plant Production Sciences and Technologies, University of Zimbabwe, Harare, Zimbabwe

[6]International Maize and Wheat Improvement Center (CIMMYT), P.O. Box MP 163, Mount Pleasant, Harare, Zimbabwe

[7]Univ. Eduardo Mondlane, Faculdade de Agronomia e Engenharia Florestal (FAEF), Maputo, Mozambique

[8]Plant, Soil and Microbial Sciences Department, Michigan State University, East Lansing, MI 48824, USA

[9]INRAE, US1116 AgroClim, Avignon cedex 9 France

Keywords: Biophysical effect, Energy partitioning, Albedo, land management, conservation agriculture, Modelling, STICS, energy budget

Abstract

Conservation agriculture (CA) has been widely promoted for its beneficial biogeochemical effects on climate, such as soil organic carbon sequestration and the reduction of greenhouse gas emissions. However, CA practices also influence biogeophysical effects, particularly through changes in surface albedo. Land management practices can significantly alter surface albedo dynamics in croplands. Despite this, the impact of these practices on surface albedo changes is often not accounted for in many soil-crop models. The STICS soil-crop model is known for its comprehensive process-based understanding of how land management practices affect various agro-environmental variables across diverse pedoclimatic contexts. This study aimed to evaluate the capacity of the STICS model to simulate surface albedo variations during a cropping year under maize (Zea mays L.) cultivation at two long-term experimental sites with contrasting soil types in Sub-Saharan Africa. Data collected over two years, including Leaf Area Index (LAI), soil water content, dry aboveground biomass, grain yield, and surface albedo, were used in this study. To better reflect processes observed, we introduced a new formalism for surface albedo that incorporates the effects of senescent leaves, along with an improved soil evaporation calculation. The results indicated that the model effectively simulated crop phenology (rRMSE of 1.2% for anthesis and 1.3% for maturity), soil water content (rRMSE of 14%), and LAI (rRMSE of 14%). However, it overestimated aboveground biomass (rRMSE of 42%) and grain yield (rRMSE of 74%). Regarding surface albedo, the existing formalism led to an overestimation during the senescence phase. The inclusion of senescent leaves in the calculation improved the accuracy of the simulations. Additionally, the new soil evaporation formalism played a crucial role in enhancing the simulation of surface albedo. This study highlights the potential of the STICS soil-crop model to simulate the impact of land management practices on surface albedo. This approach is promising for assessing the climate impacts on both biogeophysical and biogeochemical effects in various pedoclimatic contexts.

1. Introduction

Understanding the interactions between agricultural management practices and climate is critical for sustainable development, especially in regions vulnerable to climate change, such as Sub-Saharan Africa. Conservation agriculture (CA) is a sustainable farming practice that integrates minimal soil disturbance, permanent soil cover (crop residues mulch, cover crops…), and crop diversification (rotations, intercropping…) to enhance agricultural productivity while mitigating environmental impacts (Derpsch et al., 2010; Hobbs et al., 2008). The climate mitigation potential of CA has been mostly assessed on biogeochemical effects (soc organic carbon sequestration (SOC) and greenhouse gas (GHG) emissions) while biogeophysical effects such surface albedo change and evapotranspiration are often ignored. Recently, studies demonstrated that biogeophysical effects can achieve climate mitigation by altering local energy budgets through change in surface albedo (Davin et al., 2014; Hirsch et al., 2017). Surface albedo is the fraction of incoming solar radiation reflected back to space by the Earth's surface. It's a key component driving the energy partitioning that involves the balance between sensible and latent heat flux (Stephens et al., 2015). Genesio et al., (2012) showed that agriculture management such as biochar application may decrease surface albedo and modify surface energy balance. In addition, (Liu et al., 2022a) assessed the surface albedo climate impact due to the conversion of conventional tillage to no-tillage management practices in the Canadian prairies. Dynamic process-based soil-crop models can be a useful tool to assess climate impact variability (Yin and Leng, 2020). Currently, there are no studies focusing on the Modelling of the impact of land management practices on surface albedo and energy partitioning using soil-crop models. Then, STICS soil-crop model can be a simple alternative to assess the impact of agricultural practices on surface albedo dynamics.

STICS (**S**imulateur mul**TI**disciplinaire pour les **C**ultures **S**tandard) is a dynamic process-based soil-crop model that has been used for assessing agronomic and environmental performances under contrasted pedo-climatic conditions (Falconnier et al., 2019). STICS model has demonstrated its robustness and capability in simulating a wide range of pedoclimatic context, maintaining a well-balanced approach to complexity, coherence, and input requirements (Coucheney et al., 2015). For example, (Saadi et al., 2022) assessed

evapotranspiration and soil water content using resistive and crop coefficient approaches which are available in STICS mode in Eastern Canada. Constantin et al., (2015) compared STICS and AqYield which is a simpler model to predict yield and soil water content for irrigated crops. In the same vein, Scopel et al., (2004) explored the impact of direct seeding and crop residue retention on water use and maize production under contrasted tropical sites in southern America.

Actual soil evaporation formalism of STICS leads to an underestimation in semi-arid conditions with a long dry season (Sow et al., 2024). This formalism assumes that the topsoil reaches field capacity after every rainfall event. This approach can be used in temperate regions where initial soil conditions between two rainfall events are not too variable and depend mostly on the potential evaporation (Affholder, 2001).

In our study, the model was calibrated in two contrasted soil types in subhumid Zimbabwe in maize crop under conventional tillage (CT), no-tillage (NT) and no-tillage with mulch (NTM) treatments during 3 years. Based on in-situ measurements of surface albedo and surface soil water content (SWC), our objectives are to assess the ability of STICS, with its current formalisms, to simulate surface albedo and SWC, which influence albedo, for contrasting land management practices (Conventional tillage (CT), No-tillage (NT), and No-tillage with mulch (NTM)). The aim is to evaluate the impact of these practices on albedo and radiative forcing (RF). To achieve this, we are testing 1) a new formalism for albedo that accounts for the albedo of senescent tissues, and 2) a new formalism for simulating surface evaporation, which indirectly affects surface albedo through topsoil water content.

2. Materials and methods

2.1 Experiments description and location

Field data were collected at two long-term experimental sites established in 2013 by the International Maize and Wheat Improvement Center (CIMMYT) in Zimbabwe: Domboshawa Training Center (DTC) in the district of Goromonzi (17°36'23.3"S; 31°08'26.8''E) and the University of Zimbabwe Farm (UZF) in the district of Mazowe (17°43'15.1"S; 31°01'15.8"E). The trials were conducted on two different soil classes, an abruptic Lixisol (FAO classification,

1997) at in DTC and xanthic Ferralsol (FAO classification, 1997) at UZF. Soils at DTC have a light texture on the top layer 0-20 cm (sandy-loam with 15% clay content), changing into sandy-clay-loam with 30% clay content in 20-40 cm (Shumba et al. 2023a, b) (Figure IV-1). The soil texture at UZF is sandy-clay-loam with 34% of clay content in the first 20 cm (Shumba et al. 2023a, b). The sites are both under sub-tropical climate with annual minimum and maximum mean temperature of respectively 12°C and 25°C and a cropping season from November to April (Mapanda et al. 2010; Shumba et al. 2023). The rainfall cumulated during the first and the second measurements period were 1210mm and 1012mm at DTC respectively, 907mm and 805mm at UZF.

The experimental setup remained consistent at both locations, and the treatments have been unchanged throughout all cropping years since the start of the experiment. The study utilised plots measuring 12 x 6 meters, with Maize (*Zea Mays* L.) as the main crop. Our research concentrated on three treatments: Conventional Tillage (CT), No Tillage (NT), and No Tillage with Mulch (NTM).

2.2 In situ data

2.2.1 SW_{in}, Albedo and heat flux monitoring

Four-component net radiometers were utilised to observe shortwave incoming and outgoing and longwave incoming and outgoing radiation. This device consists of two pyranometers and two pyrgeometers, each pair featuring one facing upward and the other downward (more details in Diop 2023). surface albedo (α) for each treatment is derived from shortwave radiation following eq.1 covering the visible and near infrared spectrum (0.3 to 2.8 µm).

$$\alpha = \frac{SW_{out}}{SW_{in}} \quad \text{(III-1)}$$

Here, α represents surface albedo, SW_{out} (W.m^{-2}) signifies the amount of solar radiation reflected by the surface, and SW_{in} (W.m^{-2}) denotes the global incoming radiation. Pyrgeometers, which are thermal sensors, quantify incoming and outgoing longwave radiation (LWin, LWout) within the wavelength range of 4.5 to 50 µm, expressed in W.m^{-2}.

The 4-component net radiometers were horizontally mounted on a mast and positioned at a height of 1.5 meters above the ground during the fallow period. Throughout the growing season, the sensor's height was dynamically adjusted to always remain 1.5 meters above the crop canopy. To reduce the influence of the surrounding terrain, the masts were centrally located within the plot. The NR01 devices were connected to a CR1000 datalogger (Campbell Scientific Inc, Logan, UT, USA) for continuous data recording at one-minute intervals. The recorded values were subsequently averaged over half-hour time intervals.

2.2.2 Soil moisture monitoring

Soil moisture was measured during using a neutron probe up to a depth of 1 meter. The neutron probe was site-calibrated using gravimetric soil moisture samples collected from the field. To ensure the accuracy of the measurements, soil samples were extracted at various depths, dried, and weighed to determine their gravimetric water content. This data was then used to develop a calibration curve for the neutron probe, ensuring precise readings across different soil types and conditions.

In addition to the neutron probe measurements, soil moisture sensors were installed at depths of 1 cm, 10 cm, and 20 cm, with ECH2O sensors (Meter group, Inc., USA), at 5-minute intervals within each plot containing NR01 sensors. To further improve the reliability of the data, an intercalibration process was performed between the neutron probe data and the readings obtained from the soil moisture sensors. This intercalibration allowed for cross-verification of moisture levels, ensuring the consistency and precision of the soil moisture measurements throughout the study period. The ECH2O sensors were linked to the METER ZL6 datalogger and strategically positioned in the central region of the plot for each treatment, between two rows of maize during 2 successive cropping years from October 2021 to October 2023.

2.2.3 Leaf area index data

Leaf Area Index (LAI) represents the ratio of the total leaf area per unit of soil surface, expressed as square meters of plant surface per square meter of soil surface. In our investigation, indirect measurements of LAI were obtained using the LAI 2200C plant canopy analyzer (LI-COR Biosciences GmbH, USA). LAI was monitored every two weeks throughout 2 cropping years (2021/22-2022/23). Measurements were taken once between two maize rows above the canopy and four times diagonally at 25% from the row, in the middle of two rows, and at 75% from the starting point, at a depth of 10 cm below the leaves (see Diop et al in (under review) for more details).

2.2.4 Weather data

Campbell stations were installed near plots of each site to monitor maximum temperature (Tmax), minimum temperature (Tmin) and mean temperature (Tmean) and relative humidity (RH) at 2 m from the ground on a half-hour time interval from October 2021 to October 2023. Furthermore, at the experimental site, there are continuous recordings of air temperature and relative humidity at a height of 2 meters above the ground, obtained from a nearby meteorological station. For this purpose, an ATMOS 41 weather station from Meter Group, Inc., USA, was employed to monitor various meteorological parameters, including air temperature, relative humidity, wind speed and direction, rainfall, and vapor pressure.

2.3 Modelling methodology

2.3.1 STICS model

STICS model (Simulateur mulTIdisciplinaire pour les Cultures Standard) is a crop growth simulation model used in agriculture (Brisson et al., 2008, 2003). It is a daily time-step cropping system model that simulates agronomic variables such as leaf area index, yield, biomass, and biophysical variables like longwave radiation, evapotranspiration, crop temperature, soil albedo, and crop albedo. It's a powerful tool to evaluate water balance and Nitrogen balance of croplands. It was primarily designed to simulate the growth of a variety

of crops i.e., wheat, maize, barley, perennial crops. The model takes into account various biophysical and environmental factors that influence crop growth, such as weather, soil properties, and crop management practices. STICS is often used for agronomic and environmental assessment, as well as for evaluating the effects of scenarios like climate change or different management practices (Debaeke, 2004; Schnebelen et al., 2004; Constantin et al., 2015; Tribouillois et al., 2018). Nevertheless, there is poor relevant representation of the energy partitioning and albedo in sub-Saharan Africa. This study will focus on the capacity of STICS to simulate plant development and production and soil water content after it has been calibrated but also albedo using the current and a new formalism using continuous measurements on two contrasted soil classes in subhumid Zimbabwe.

2.3.2 Calibration steps

Before any evaluation of STICS capacity to simulate albedo, the model was calibrated on maize (*Zea Mays* L.) in southern Africa in Harare. The model was calibrated using in-situ data of phenology, soil water content, leaf area index, biomass and grain yield 18 simulation units (usm) across 3 years of measurement. This calibration step is adopted by other authors in the same order and described in detail in (Falconnier et al., 2019; Sow et al., 2024; Traoré et al., 2022).

2.3.3 Soil parametrization

The model was parametrised for the soil properties of a light-coloured red sandy soil (Abruptic Lixisol) and of a brown-yellowish clayey soil (Xanthic Ferralsol) splitted into five layers: 0-1 cm, 1-10cm, 10-20 cm, 20-40 cm, 40-105 cm. Soil water properties were parameterized first by defining for each layer water at field capacity (HUCC) and wilting point (HUMIN) based on soil water content measured after filtering outliers that can represent soil water saturation. For each layer soil bulk density is defined as input based on field measurements realised by (Shumba et al., 2024). Soil texture (clay, sand and silt), total soil nitrogen and total soil carbon were measured by soil sampling at 0–5, 5–10. 10–15 and 15–20 cm (Shumba et al., 2024, 2023).

2.3.4 Current soil evaporation formalism

Currently, soil evaporation is calculated at soil level and then distributed over the soil profile (Beaudoin et al., 2023). The actual formalism (Evap1) of soil evaporation in STICS is based on two steps of calculation. The first step is the estimation of potential soil evaporation related to available energy in the soil profile and the second step is the estimation of actual soil evaporation related to water availability (Brisson and Perrier, 1991). Actual soil evaporation is a semi-empirical method following two phases after a rain event. The first phase assumes a potential evaporation after a rain event until the cumulative daily evaporation reaches a threshold q0 (table 1). The second phase consists of a decrease in evaporation depending on the weather and soil type. Soil evaporation calculation is also related to the presence of any mulch as described in equation 11.2 using radiative transfer option and 11.3 if energy balance option is used (Beaudoin et al., 2023). The actual evaporation formalism statement is characterised by a little variation of soil conditions from a rainfall event to another and the time required to reach a given soil moisture level depends mainly on potential evaporation. This hypothesis is valid in temperate regions where soil water before establishment of crop is near to field capacity.

2.3.5 New soil evaporation formalism

The current formalism did not reflect the condition of tropical regions which is characterised by a long dry season. The new soil evaporation formalism (Evap2) derived from Affholder, (2001) tried to take into account explicitly soil water state before long months without rainfall by 1) integrating a function of the repartition of evaporation in the soil 2) looking the impact of low water content rate affected the soil evaporation and 3) defined a layer affected by evaporation. Conversely to the previous formalism, this formalism calculates total evaporation before splitted within layers and expressed following this equation.

$$E0s(z) = E0s \times rh^{betevap} \quad \text{(III-2)}$$

$$E0s(z) = condsol \times eos \times e^{-(6.91\times z-1)/(zmlchmax-1)} \quad \text{(III-3)}$$

$$rh = \frac{HUR(z)-(10\times HA)}{HUCC(z)-(10\times HA)} \quad \text{(III-4)}$$

Where *E0s(z)* represents potential evaporation of the layer *z*, *condsol* plays on how the available soil water is distributed in the soil, *eos* represents potential soil evaporation of the profil, *zmlchmax* corresponds to the soil thickness affected by evaporation, *rh* is a function of the reduction of *E0s* based on the soil water content, *HUR(z)* corresponds to the water content of layer z and *HUCC* is the soil water content of field capacity of layer *z*. *HA* is the residual moisture estimated using clay content and soil bulk density.

2.3.6 Surface albedo α

Surface albedo in STICS is varying between soil albedo ($P\alpha_{sol}$) and vegetation ($P\alpha_{veg}$) (Brisson et al. 2007). Albedo of maize varies between 0.16 and 0.23 across species (Hatfield and Carlson, 1979). $Albedo_{sol}$ is subject to changes based on factors such as the soil type, the moisture level in the top layer, and the presence of mulch (i.e., plastics mulch, crop residues…) or vegetation cover (eq.2). It exhibits a linear decline with the moisture content of the surface layer. According to Brisson et al. 2007, this relationship is derived from experimental data collected across various soil types and water at field capacity (HUCC) and wilting point. Albedo of soil is represented in the model following eq. III-5.

$$Albedo_{sol} = Pa_{sol} \times (1 - 0.517 \times \frac{HUR(i,1)-HUMIN(1)}{HUCC(1)-HUMIN(1)}) \times (1 - couvermulch(i) + Pa_{mulch} \times couvermulch(i) \quad \text{(III-5)}$$

Pa_{sol} is parameter to define albedo of bare dry soil, HUR is a water content in the layer, HUCC represents the water content at field capacity, HUMIN corresponds to humidity at wilting point, couvermulch corresponds to the mulch coverage rate, and Pa_{mulch} is the albedo of mulch.

Surface albedo is calculated based on equation (3):

$$Surface\ albedo = Pa_{greenveg} - (Pa_{greenveg} - Albedo_{sol(i)}) \times e^{-0.75\times LAI(i)} \quad \text{(III-6)}$$

2.3.7 Including yellow leaves into α calculation

Referring to Diop et al., (under review), surface albedo has experienced a decrease during senescence at both sites and all treatments. However, this decrease with the apparition of yellow leaves has not been taken into account in STICS. We hypothesise that including yellow leaves into albedo calculation could be able to improve albedo simulations and could have effects on the component of energy budget simulated by the model. Then, surface albedo including yellow leaves is calculated using the following equation:

$$Surface\ albedo\ = albveg\ \ - (albveg - Albedo_{sol(i)}) \times e^{-0.75 \times LAI(i)} \quad \text{(III-7)}$$

Where,

$$albveg\ =\ (1/LAItot) * (Albyellow * LAIyellow + Albegreen * LAIgreen) \quad \text{(III-8)}$$

LAItot corresponding to the total LAI (green+yellow leaf area index), Albyellow is the parameter defining the albedo for yellow leaves and Albgreen represents the albedo green leaves.

2.3.8 Model performance evaluation

The performance of the model is evaluated graphically and quantitatively by calculating the rRMSE (Normalised Root Mean Square Error), R^2 (determination coefficient), EF (Efficiency) by using the following equations:

$$rRMSE\ =\ \frac{RMSE}{\bar{O}bs} \quad \text{(III-9)}$$

$$\text{with } RMSE\ =\ \sqrt{\frac{1}{n}\sum_{i=1}^{n}\ \ (Obs_i - Sim_i)} \quad \text{(III-10)}$$

$$EF\ = 1 - \frac{\sum_{i=1}^{n}\ \ (Obs_i - Sim_i)}{\sum_{i=1}^{n}\ \ (Obs_i - \bar{O}bs_i)} \quad \text{(III-11)}$$

Where Obs_i and Sim_i represent observations and simulations for i^{th} measurement, $\bar{O}bs$ is the mean of observed data and n corresponds to the total number of observations. rRMSE depicted the relative model prediction errors. EF is the model efficiency based on the comparison between the model simulation with a constant model such as the average of

measurements. EFs ranged between -∞ and 1, which negative value indicates that the constant has better performance than the model and a value of 1 corresponds to the perfect model.

3. Results

3.1 Crop development: Leaf Area index dynamics

The model reproduced fairly phenological stages across all sites, years and treatments with an underestimation at flowering and the physiological maturity particularly in the NT and NTM treatments at DTC (Figure III-1A, B) during the first cropping year (2021/22). During the second cropping year the model did not reproduce fairly the phenological stage of all treatments at DTC because of the lower crop development experienced in this site.

At UZF, the model reproduced with good agreement phenological stages from emergence to harvest for all treatments. For both sites and cropping years, the model simulated fairly the temporal dynamics of LAI for all treatments (Figure III-1A, B).

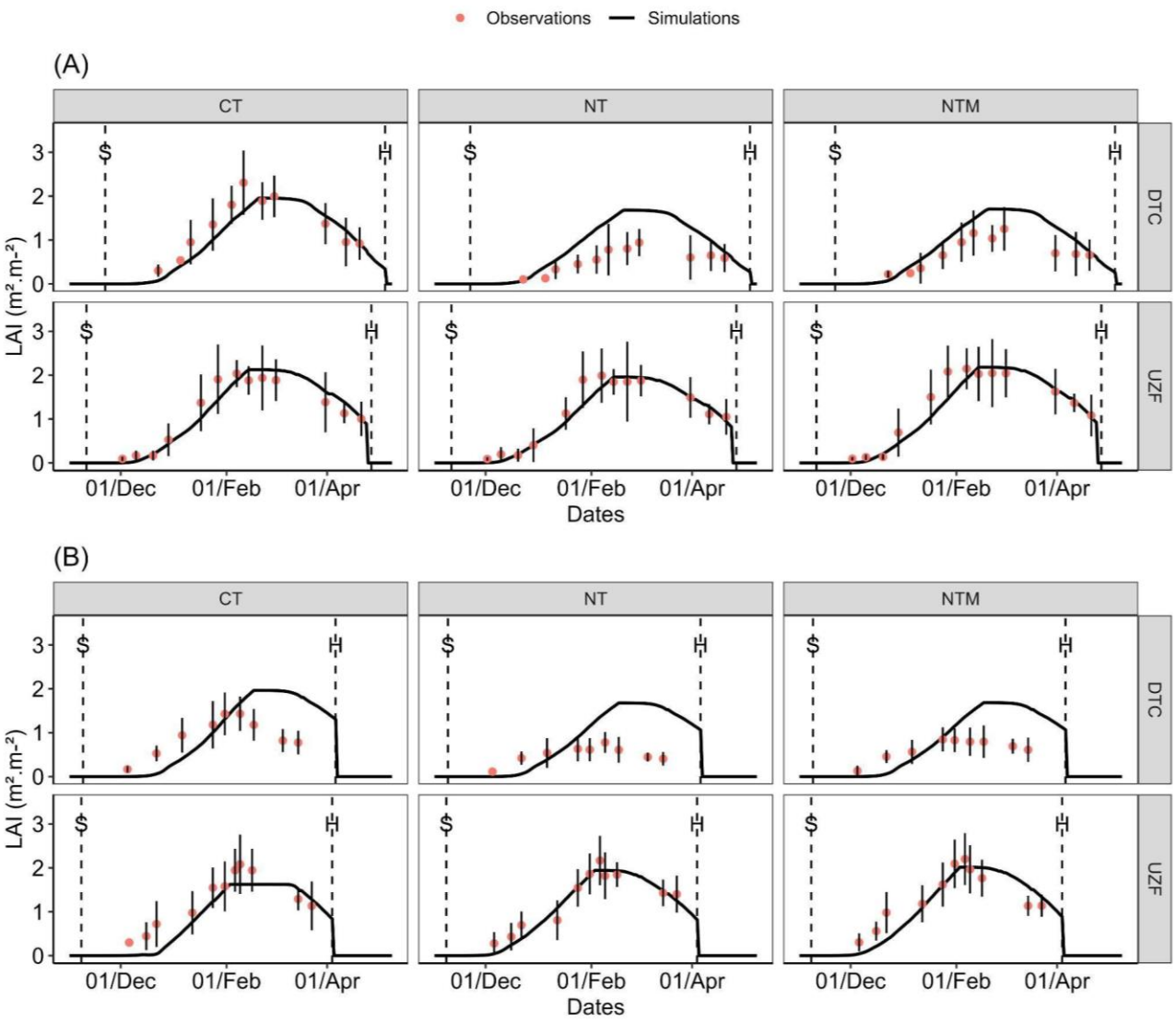

Figure III-1. Leaf Area Index (LAI) dynamics observed (red dots) and simulations (black lines) during (A) 2021/22 (B) and 2022/23 cropping years for Conventional tillage (CT), No-tillage (NT) and No-tillage with mulch (NTM) at DTC and UZF sites.

3.2 Observations and simulations agreement of Leaf Area Index, biomass and yield

Figure III-2 compared the agreement between observed and simulated values for Leaf Area Index (LAI) (A), total aboveground biomass (AGB) (B), and grain yield (C), showing varying levels of model performance. For LAI, the model performed well, with a relatively good R^2 of 0.66, indicating that 66% of the variance in the observed data is explained by the model, though the rRMSE of 39.57% suggests significant errors, and an acceptable efficiency factor (EF) of 0.578.

In the case of AGB, the model performed poorly with a negative EF (-0.038), despite an R^2 of 0.64, showing that while it captures the general trend, its predictions deviate substantially from the observed data. The rRMSE of 41.65% further highlights this error.

Grain yield showed the worst performance, with a high rRMSE of 76.20% and a strongly negative EF (-1.406), indicating a significant mismatch between simulated and observed values. Although the R^2 of 0.558 shows that some variance is captured, the model's predictive accuracy for yield is very limited. Overall, while the model captures trends to a certain extent (moderate R^2 values), its accuracy is compromised by high error rates and poor performance, particularly in predicting AGB and yield. Grain yield measured varied within site year and management practices from 0.3-5.8 t ha^{-1}). The model agreement with observation of grain yield is not sufficient enough. Nevertheless, the model is able to reproduce the variability of maize grain yield between treatment depending on years, soil type.

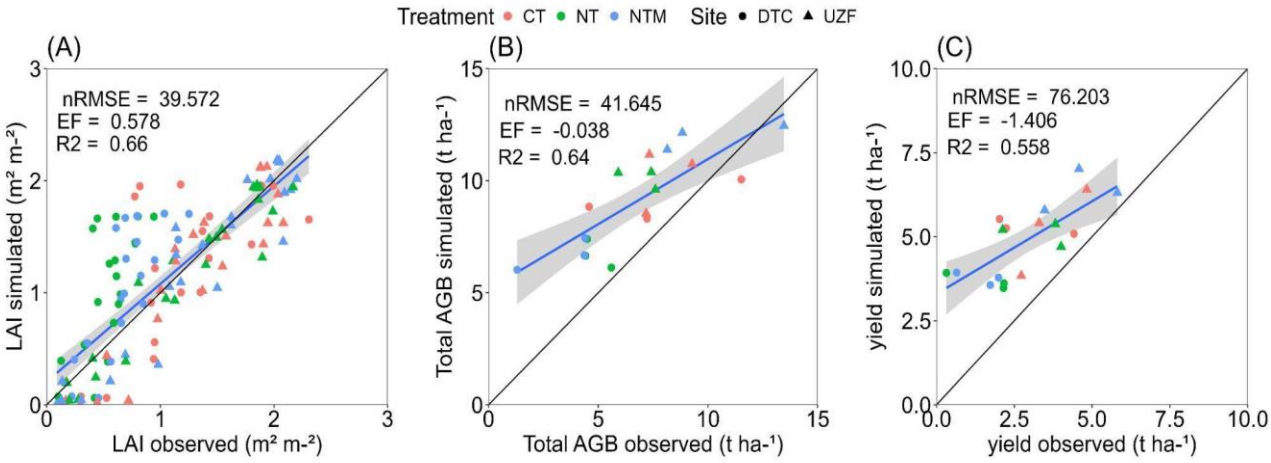

Figure III-2. Observations vs STICS simulations of (A) Leaf Area Index (LAI), (B) Total Aboveground Biomass (AGB), and (C) grain yield of maize. at DTC and UZF sites under Conventional-tillage CT (red dots), NT (green dots) and NTM (blue dots) treatments during 2021/22 and 2022/23 cropping years.

3.3 Soil water content dynamics

3.3.1 Soil water content over the soil profile

Figure 2 allows us to evaluate the capacity of STICS to simulate the soil water content integrated along the whole soil profile using the actual formalism of soil evaporation and

the new one supposed to better take into account Sub-Saharan Africa pedoclimatic conditions. Currently, simulations are quite close with both formalisms. Before and during crop development soil water content dynamics are well simulated over the whole profile at both site and all treatments using both versions with a 0.5 EF for Evap1 and Evap2 and low error rRMSE of 14% for all usms pooled together. Yet the simulations diverge from the measurements during the senescence phase leading to lower soil water content after harvest in both versions.

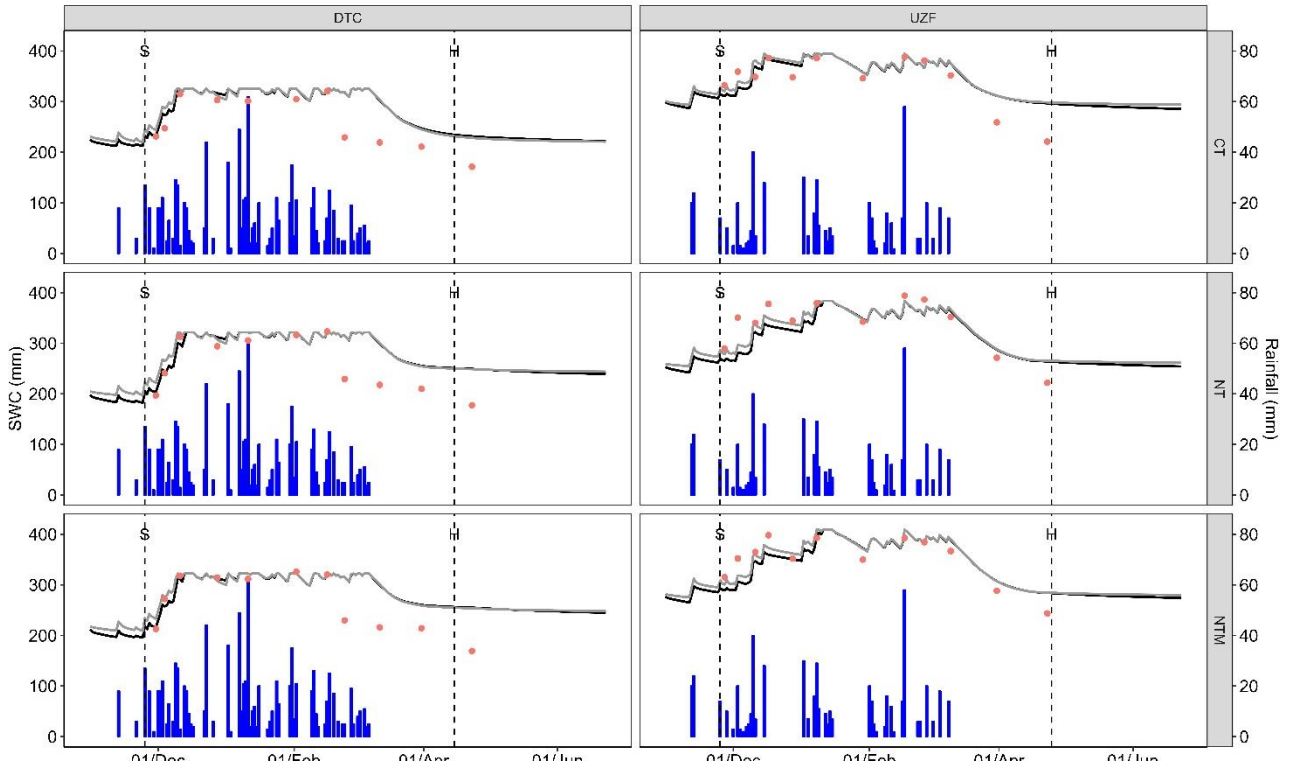

Figure III-3. Soil water content (SWC) 0-105 cm observation (red dots) and simulations with the current soil evaporation formalism (black lines, Evap1) and with the new soil evaporation formalism (grey lines, Evap2) at DTC (left) and UZF (right) sites. Measurements were done during the 2020/21 cropping year by using neutron probe.

3.3.2 Topsoil moisture

Figure III-3 shows that the topsoil water content (0-1 cm) is overall better simulated by the model using the Evap2 than with the Evap1 with EF of 0.39 and 0.5, respectively, for the Evap1 and the Evap2 and high errors for the Evap1 compared to the Evap2 (41% against 37% Figure S2). Nevertheless, soil water content reaches field capacity for each rainfall event

for both formalisms of soil evaporation. This pattern is observed at both sites, treatments and cropping years leading to an overstation of soil moisture during small rain events (Figure III-3).

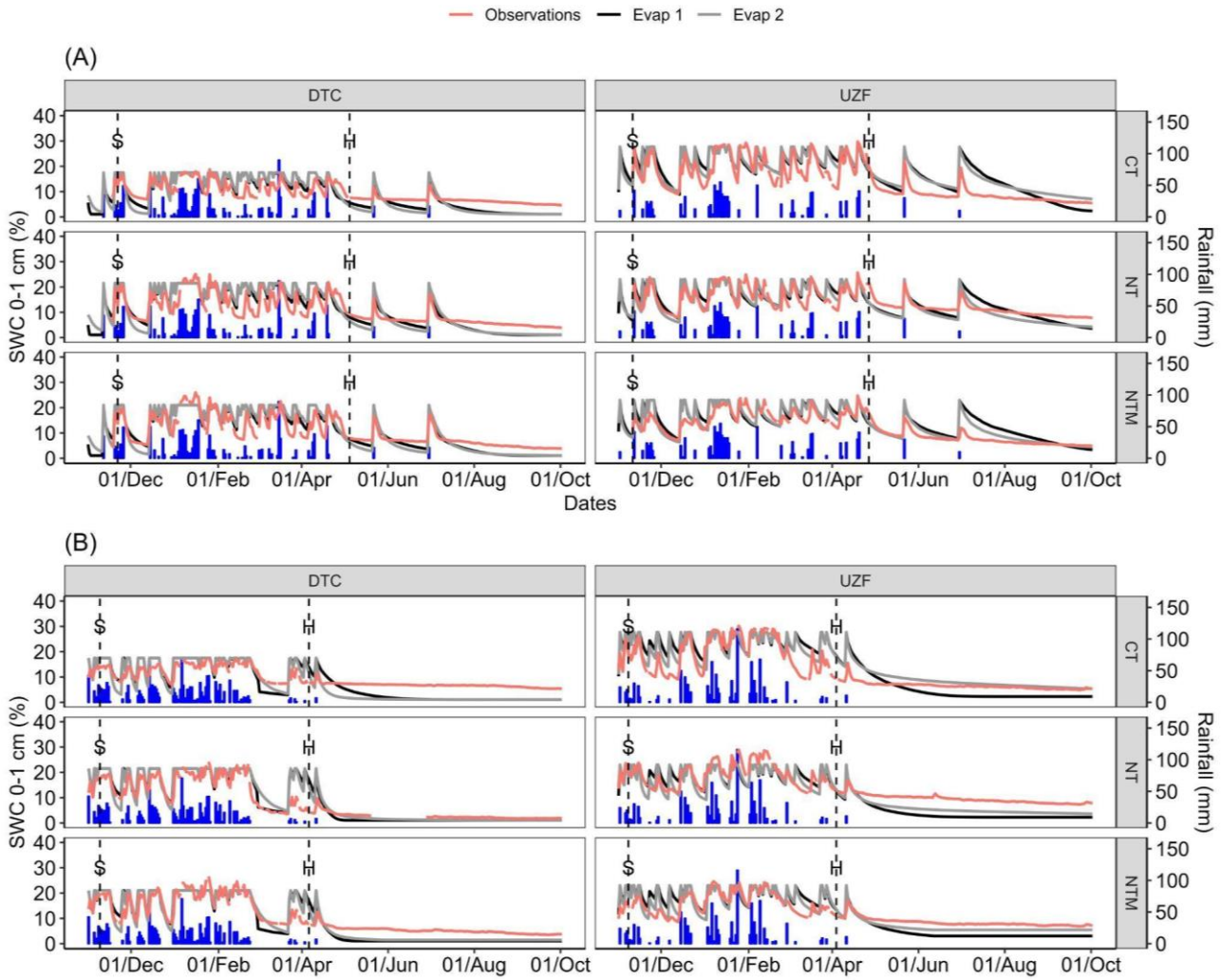

Figure III-4. Topsoil moisture (0-1 cm) observation (red lines) and simulations with the current soil evaporation formalism (black lines, Evap1) and with the new soil evaporation formalism (grey lines, Evap2) at DTC (left) and UZF (right) sites. Measurements were conducted during the (A) 2021/22 and 2022/23 (B) cropping years.

3.4 Albedo dynamics

3.4.1 Simulating surface albedo considering the current surface albedo formalism

The current formalism (Albedo 1) of surface albedo in the standard version of STICS allowed the simulations to closely match the observations during the fallow period (i.e., bare soil or

mulch covering the soil) as well as during crop growth (Figure III-4). Overall, the model's performance was acceptable for each treatment at the both sites, though the low model efficiencies (EFs) suggested a need for enhancement. The relatively low rRMSEs indicated low prediction errors during the 2021/22 and 2022/23 cropping years (Table III-1). However, the model struggled to accurately reproduce temporal surface albedo dynamics, particularly during the senescence period (from the appearance of yellow leaves to harvest) at both sites.

At DTC, from sowing to the beginning of senescence (the vegetative period), the model fairly reproduced surface albedo dynamics, with slight underestimations, especially in the CT and NT treatments during the 2021/22 cropping year. The model underestimated surface albedo in the NTM treatment during the early crop growth phase of the 2021/22 cropping year. In the second season, the model underestimated surface albedo across all treatments in the early vegetative phase, though it captured surface albedo dynamics well from maximum LAI to harvest, with some underestimation just before harvest. During the fallow periods, the model accurately reproduced surface albedo for all treatments in 2021/22. However, in the second cropping year (2022/23), the application of mulch after harvest was not well simulated by the model. The decrease in surface albedo at the beginning of senescence was moderately captured, but the decline just before harvest was poorly simulated across all treatments at DTC (Figure III-5).

At the UZF site, the model showed lower performance, with efficiencies ranging from -1.90 to 0.28. While the rRMSEs were in the same range as at DTC, they were lower during the second cropping year (2022/23) compared to the first (2021/22) (Table III-1). The model aligned well with observations during the vegetative phase, though it slightly underestimated surface albedo just after sowing in all treatments during both cropping years. This underestimation was more pronounced in the second cropping year, particularly in the CT and NT treatments. The model did not capture the decrease in surface albedo during senescence well in any treatment at UZF. During the fallow period, the model tended to slightly underestimate surface albedo across all treatments in the first season. However,

the agreement between observations and simulations was more accurate in the second cropping year compared to the first.

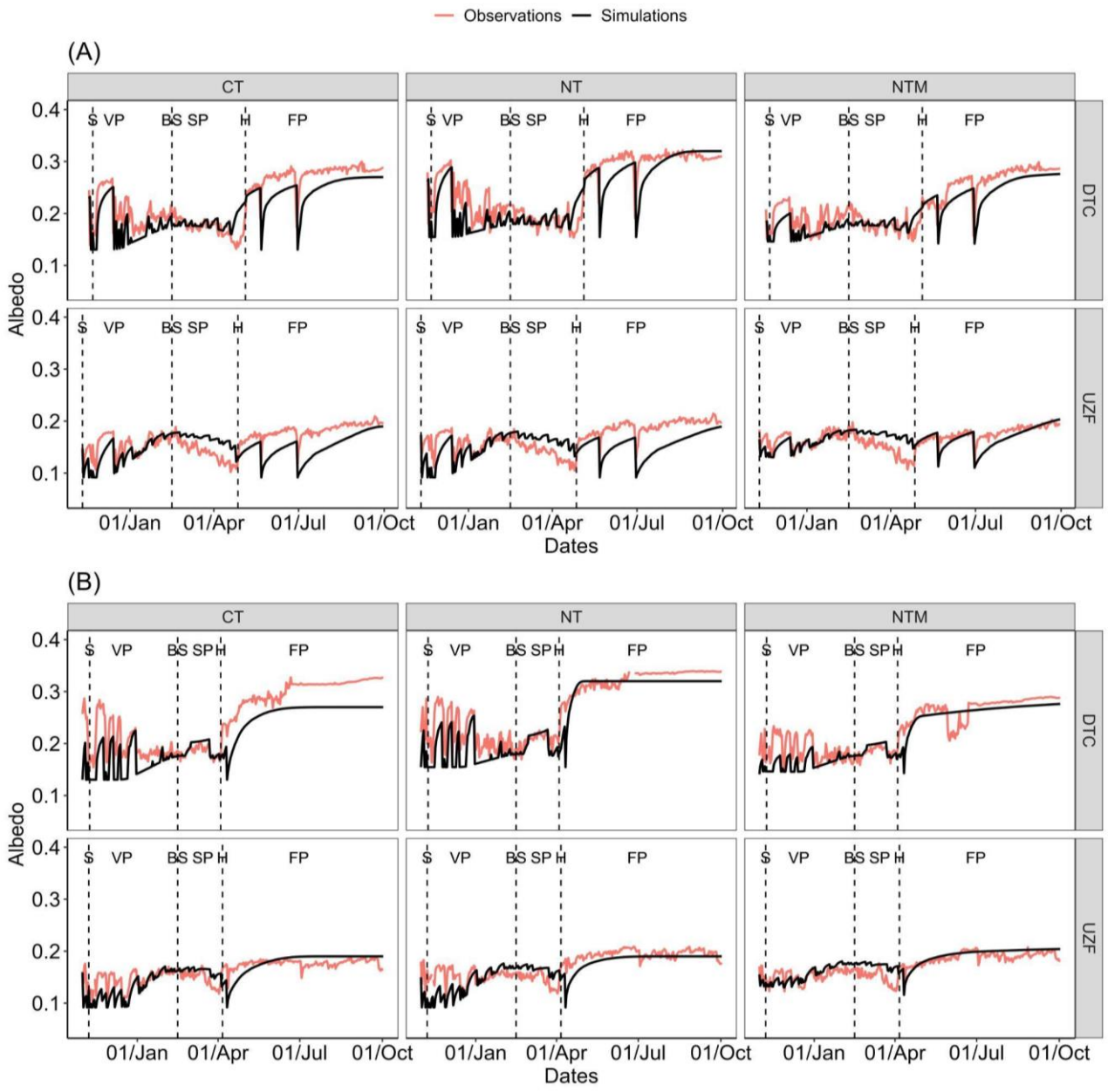

Figure III-5. Surface albedo observed (red line) and simulated (dark line) using the current formalism of surface albedo (Albedo 1) by the STICS soil-crop model during the (A, top) 2021/22 and (B, bottom) 2022/23 cropping years at DTC and UZF. CT = conventional tillage, NT = no-tillage and NTM = no-tillage with mulch. S: Sowing, VP: Vegetative period, BS: Beginning of senescence, SP: Senescence period, FP: Fallow period

3.4.2 Simulating surface albedo considering senescent tissues

Including the surface albedo of senescent leaves (Albedo 2) resulted in a good agreement

between observations and simulations during the senescence period at both sites, across cropping years, and in all treatments (Figure III-6). At DTC, the simulation of surface albedo improved significantly in terms of performance (Table III-1). The prediction errors, as demonstrated by the rRMSEs, were generally lower across both cropping years when using the new formalism compared to the current one.

At UZF, the decrease in surface albedo due to plant senescence was well captured by the model, as indicated by the EF and rRMSE performance metrics (Table III-1). Overall, the EFs were better with the new formalism (-0.96 to 0.6 in Albedo 1 and -2.29 to -0.6 in Albedo 2). The rRMSEs were also lower with the new formalism of surface albedo than with the current formalism across all treatments during both cropping years (Table III-1).

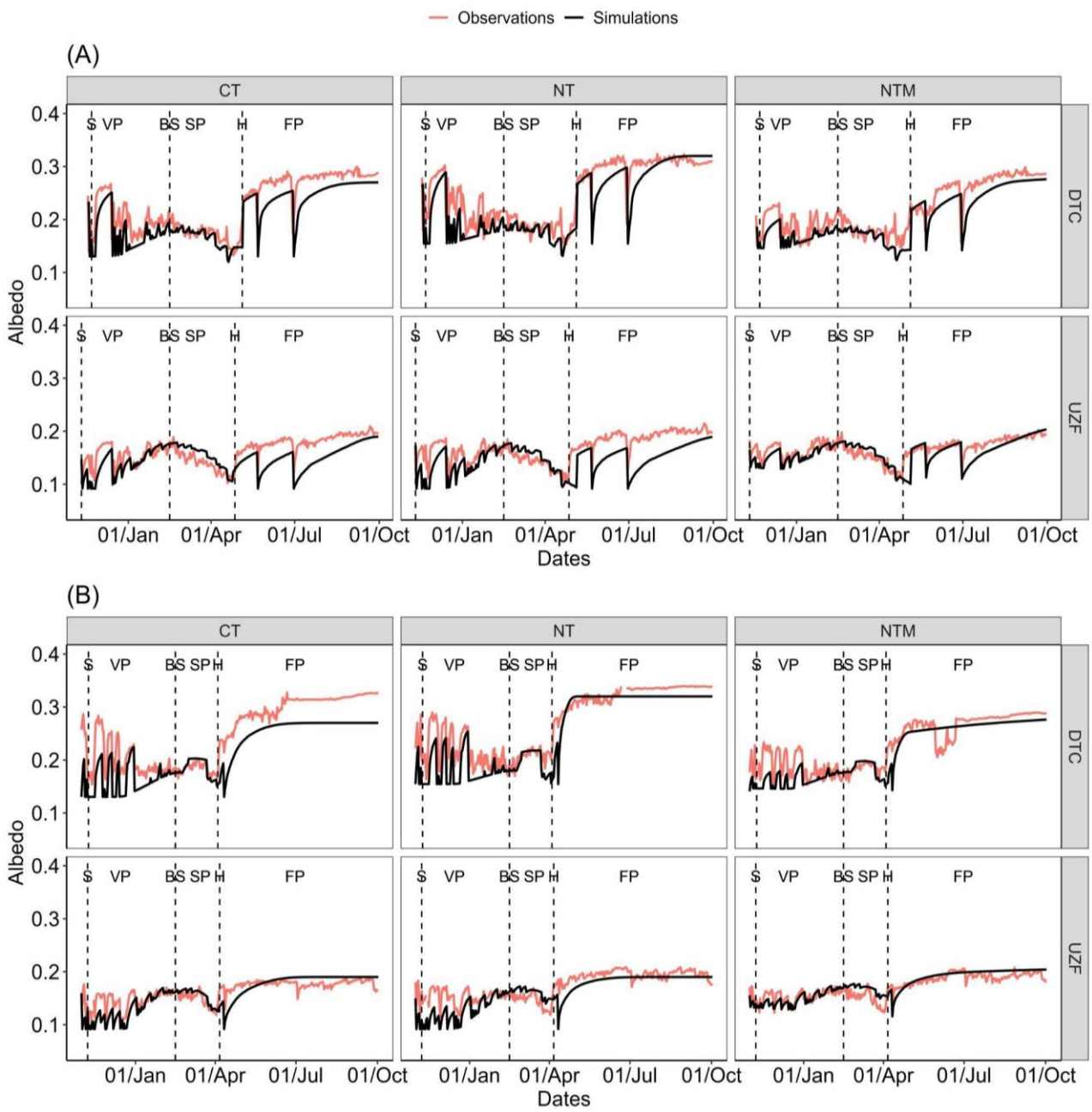

Figure III-6. Surface albedo observed (red line) and simulated (dark line) using the new formalism of surface albedo (Albedo 2) by the STICS soil-crop model during the (A, top) 2021/22 and (B, bottom) 2022/23 cropping years at DTC and UZF. CT = conventional tillage, NT = no-tillage and NTM = no-tillage with mulch. S: Sowing, VP: Vegetative period, BS: Beginning of senescence, SP: Senescence period, FP: Fallow period

Table III-1. Model performances of surface albedo simulated during senescence phase using the current (Evap 1) and the new (Evap 2) formalism of soil evaporation combined to the actual (Albedo 1) and the new (Albedo 2) formalism of surface albedo under Conventional tillage (CT), No-tillage (NT) and No-tillage with mulch (NTM) at DTC and UZF sites.

		Versions	Albedo 1			Albedo 2		
Cropping years	**Sites**	**Treatments**	**EF**	**rRMSE**	**R2**	**EF**	**rRMSE**	**R2**
2021/22	**DTC**	**CT**	-1,27	14,61	0,05	0,28	8,21	0,57
		NT	-1,15	12,30	0,01	-0,55	10,42	0,27
		NTM	-0,15	9,50	0,04	-1,16	13,06	0,20
	UZF	**CT**	-1,03	19,98	0,67	0,43	10,56	0,76
		NT	-1,24	18,44	0,74	0,51	8,95	0,70
		NTM	-1,03	19,39	0,69	0,68	7,73	0,75
2022/23	**DTC**	**CT**	-0,05	6,00	0,49	-0,57	7,32	0,41
		NT	-0,56	8,29	0,33	-2,09	11,66	0,16
		NTM	-0,04	5,58	0,33	-1,30	8,28	0,12
	UZF	**CT**	-0,60	11,99	0,53	0,46	6,94	0,74
		NT	-1,71	15,02	0,44	-0,69	11,87	0,63
		NTM	-2,29	16,93	0,41	-0,96	13,05	0,62

3.4.3 Simulating surface albedo considering senescent tissues and new soil evaporation formalism

At the DTC site, the current formalism of soil evaporation, combined with the new surface albedo calculation, outperformed the new formalism in terms of model efficiency, determination coefficient (R2), and normalized root mean squared errors (rRMSEs) across all treatments during both cropping years (Table III-2).

At the UZF site, the new soil evaporation model, coupled with the new surface albedo formalism, significantly improved simulations when considering the entire cropping year (Figure III-7) for both years and across all treatments. The new formalism improved the accuracy of surface albedo predictions, especially during the fallow period, with overall EFs ranging between 0.2 and 0.6 and rRMSEs between 6-14%, compared to EFs ranging from -0.12 to 0.5 and rRMSEs of 13-18% (Table III-2).

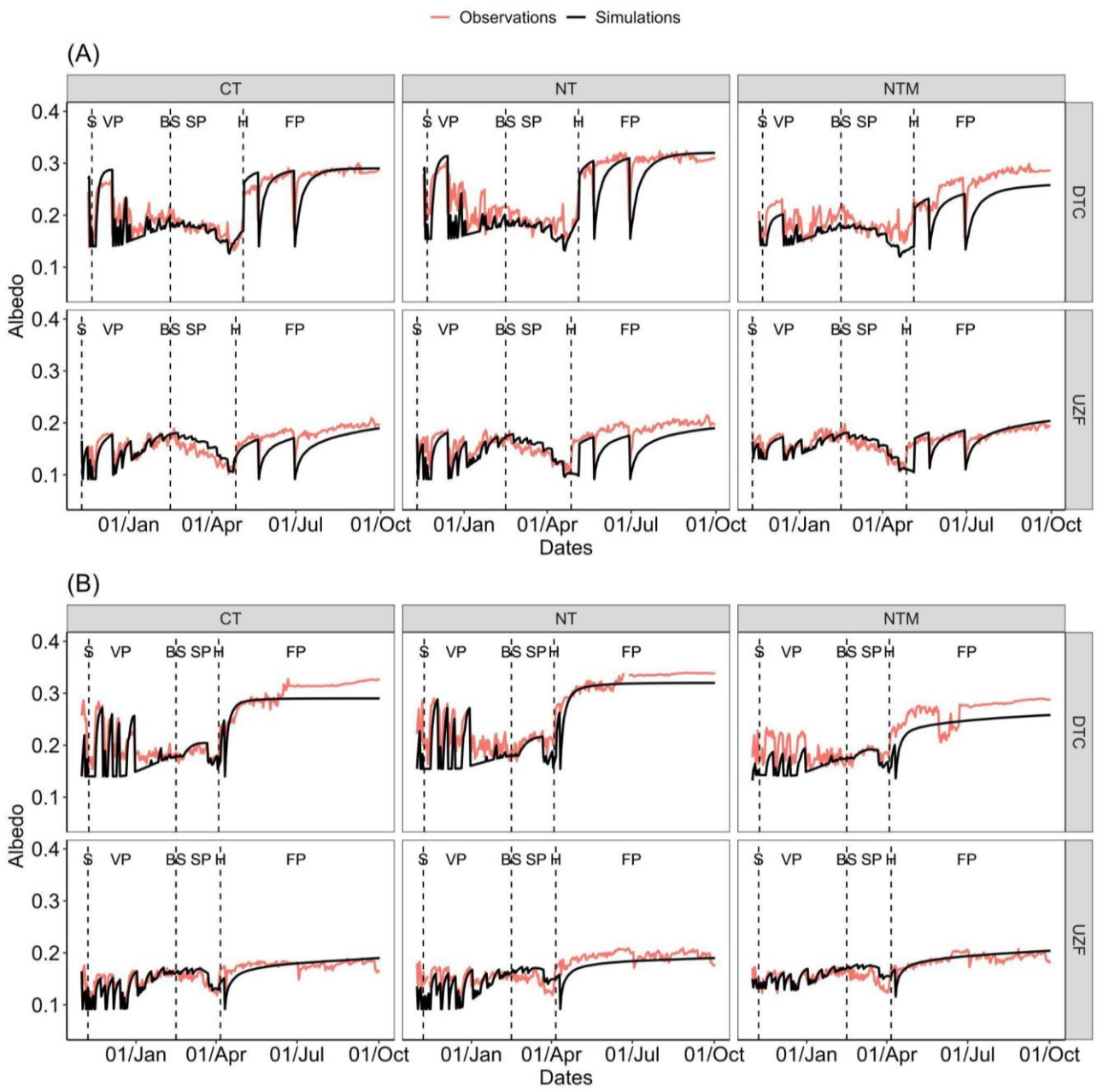

Figure III-7. Surface albedo observed (red line) and simulated (dark line) combining the current formalism of surface albedo (Albedo 1) and new formalism of soil evaporation (Evap 2) by the STICS soil-crop model during the (A, top) 2021/22 and (B, bottom) 2022/23 cropping years at DTC and UZF. CT = conventional tillage, NT = no-tillage and NTM = no-tillage with mulch. S: Sowing, VP: Vegetative period, BS: Beginning of senescence, SP: Senescence period, FP: Fallow period

Table III-2. Model performances of surface albedo simulated over the two cropping years (2021/22 and 2022/23) using the current (Evap 1) and the new (Evap 2) formalism of soil evaporation combined to the actual (Albedo 1) and the new (Albedo 2) formalism of surface albedo under Conventional tillage (CT), No-tillage (NT) and No-tillage with mulch (NTM) at DTC and UZF sites.

		Versions	Evap1 + Albedo 1			Evap2 + Albedo 1			Evap1+ Albedo 2			Evap2 + Albedo 2		
Cropping years	Sites	Treatments	EF	rRMSE	R2	EF	rRMSE	R2	EF	rRMSE	R2	EF	rRMSE	R2
2021/22	DTC	CT	0.54	14.77	0.67	0.64	13.14	0.69	0.58	14.10	0.79	0.70	11.85	0.78
		NT	0.57	14.15	0.69	0.55	14.49	0.68	0.58	14.01	0.76	0.56	14,40	0.75
		NTM	0.70	11.32	0.79	0.51	14.34	0.76	0.66	12.09	0.83	0.45	15.32	0.79
	UZF	CT	-0.42	17.65	0.17	0.15	13.66	0.31	-0.23	16.42	0.34	0.35	11.91	0.51
		NT	-0.55	18.67	0.11	0.03	14.74	0.27	-0.60	18.95	0.33	0.01	14.93	0.50
		NTM	0.02	11.04	0.23	0.21	9.96	0.39	0.23	9.81	0.55	0.45	8.32	0.65
2022/23	DTC	CT	0.43	17.61	0.80	0.76	11.39	0.84	0.43	17.69	0.81	0.76	11.43	0.85
		NT	0.73	11.34	0.88	0.76	10.68	0.90	0.71	11.67	0.88	0.74	10.99	0.90
		NTM	0.71	10.63	0.81	0.55	13.19	0.80	0.70	10.87	0.81	0.54	13.39	0.81
	UZF	CT	-0.12	12.43	0.57	0.28	9.92	0.58	-0.04	11.99	0.64	0.38	9.23	0.66
		NT	0.12	13.24	0.45	0.27	12.10	0.45	0.09	13.44	0.56	0.28	12.02	0.56
		NTM	0.52	8.57	0.66	0.56	8.16	0.66	0.65	7.34	0.75	0.70	6.79	0.75

4. Discussion

4.1 Crop development calibration in Zimbabwe

STICS crop model was initially developed for temperate regions. To date, several studies have tried to adapt it in different pedoclimatic conditions. For example, Sow et al. (2024) have calibrated STICS for pearl millet (*Pennisetum glaucum*) to assess water and nitrogen limitations on millet growth in open fields and in a park of *Faidherbia albida* in Senegal. Scopel et al. (2004) assessed the impact of mulching effect on water use efficiency and production risk associated with rainfall variability in semi-arid and humid tropical sites in southern America. Maize crop (*Zea mays* L.) has already been calibrated for STICS in various contexts mostly in temperate conditions (Brisson et al., 2002; Jégo et al., 2011) and in tropical ones (Affholder et al., 2003).

In our study, we calibrated the model on maize in two contrasted soil types in subhumid Zimbabwe under conventional and CA management practices. We focused on a medium maturity maize variety with a length of 110-120 days after sowing from emergence to

physiological maturity (Hlatywayo et al., 2016). In addition, the model gave fair performances on LAI and biomass simulations with a rRMSEs ranging from 39 to 42% for all sites and treatments pooled together corresponding to the range of performances for first calibrations in Sub-Saharan Africa e.g., for sorghum 21 to 41% (Traoré et al., 2022) and for pearl millet 21 to 39% (Sow et al., 2024). For grain yield the model was not able to t properly reproduce the low values, probably because of the errors of predictions on LAI and biomass. The larger prediction errors were for the NT and NTM treatments at DTC. In these two treatments, soil compaction and high runoff were observed and the model was not able to reproduce these processes leading probably to an underestimation of water stress and roots growth. In addition, we use the empirical function of growth rate for aboveground biomass during grain filling to calibrate grain yield without any observation. More detailed information such as number of grains, biomass at flowering would provide better results of grain yield prediction.

4.2 Drivers of surface albedo and their accounting in the STICS model

Soil moisture is a key determinant for surface albedo variations (Oguntunde et al., 2006; Li and Hu, 2009; Yang et al., 2020) and an increase in soil moisture induces a decrease of surface albedo. Yet, the current version of STICS soil-crop model did not take into account the effect of topsoil moisture temporal variations on surface albedo calculations (Beaudoin et al., 2023). Also, the dynamic of topsoil moisture is highly dependent on the soil evaporation simulation. To date, the soil evaporation module of STICS properly simulates soil evaporation in Sub-Saharan Africa contexts during bare soil periods (Sow et al., 2024). The change in soil coverage by the vegetation also affected surface albedo. In cropland, the crop development can increase surface albedo or decrease it (e.g., at DTC because of light coloured soil). (Carrer et al., 2018) showed that cover crops increase surface albedo in most European cropland. Phenology also has impacts on surface albedo dynamics. At UZF, our measurements showed an increase in surface albedo from sowing to maximum LAI and then a decrease with the apparition of senescence leaves (Diop et al. under review). Song (1999) observed the same behaviour in maize and winter wheat crops. The current version of STICS simulated senescent

leaves but did not take into account their specific albedo on the calculation of surface albedo. In this study, we included the effect of senescent leaves on the calculation of surface albedo and the results show an improvement compared to the current formalism (Figure S3). However, there are still some differences between observations and simulation during the senescence phase particularly at the UZF site, probably because of overestimations and dynamics of the senescent leaves for all treatments.

The STICS model takes into account crop residues' effect on soil evaporation and drainage (Constantin et al., 2015). However, it has some issues in predicting surface albedo in the treatment with mulch as the model was not able to reproduce with accuracy the mulch decay over time. Solving this problem would probably improve the simulations of surface albedo dynamics with mulch.

The STICS model also accounts for the effect of soil work and other practices related to CA on agronomic and environmental variables. Alletto et al., (2022) investigated the effect conservation tillage and different cover crops species on the maize production, on soil nitrogen and soil water dynamics vs. conventional tillage using STICS. The effects of these management practices are implicitly taken into account in the surface albedo calculation (Beaudoin et al., 2023) through the dry soil surface albedo parameter (*albedo*). The implementation of ploughing effect explicitly on surface albedo calculation would probably improve the accuracy of simulations because of change of soil surface roughness after multiple rainfall events.

The effects of other determinants of surface albedo such as soil colour (Cierniewski et al., 2015), soil texture (Cierniewski and Kuśnierek, 2010), iron content and soil organic carbon content are not explicitly implemented in the model either. Doing so would probably allow better accounting for surface albedo dynamics following changes in management practices such as the soil darkening effect following biochar (Genesio et al., 2012) or increase in organic carbon content with carbon farming practices (Pique et al., 2023).

4.3 Limits and perspectives

Surface albedo is a key component of the Earth's energy budget. Understanding the change of surface albedo may help to better assess their effect on the climate and identify potential levers for climate mitigation throughout change in land management practices. Modelling is a good approach to explore land management effect on surface albedo change under CA and The STICS soil-crop proves to be well adapted to analyse the effects of management practices in Sub-Saharan Africa such as, conventional tillage, no-tillage and crop residue retention. Nevertheless, the model had some difficulties in accurately simulating surface albedo. In our study, we did not conduct analysis on the instantaneous radiative forcing (iRF) induced by albedo changes following land management change as it was done in Diop et al. (under review) based on our field measurement. However, STICS has often been used to simulate SOC in Sub-Saharan Africa (Couëdel et al., 2024) and N_2O emissions (Da Silva et al., 2024) in Brazilia. Therefore, it could be a powerful tool to compare biogeophysical effects (surface albedo, energy partitioning) and biogeochemical effects (SOC sequestration and greenhouse gas emissions) on climate by editing virtual experiments to assess net climate impact of CA in Sub-Saharan Africa. In addition, it could be coupled to a land surface model such as ORCHIDEE as in Chen et al. (2016) to assess the climate effect of CA on regional and global scales.

5. Conclusion

In this study, we calibrated the STICS soil-crop model on maize crop to match observations of phenology, water dynamics, LAI, biomass and grain yield at two sites having contrasted soil types in subhumid Zimbabwe. Then, we tested the capacity of STICS model to simulate surface albedo using the standard version of soil evaporation that we compare to a new soil evaporation formalism from Affholder (2001). Also, we calculated surface albedo using the current formalism and a new one for the albedo of senescent tissues. The results show that the standard version of soil evaporation combined with the current formalism of surface albedo gives satisfactory results. However, considering the albedo of senescent leaves in the surface albedo calculation enhanced the accuracy of simulation during crop senescence. The

new soil evaporation formalism also improved the simulation of surface albedo. Nevertheless, the new soil evaporation module did not have a significant effect on crop development simulations and needed some adjustments.

Supplementary materials

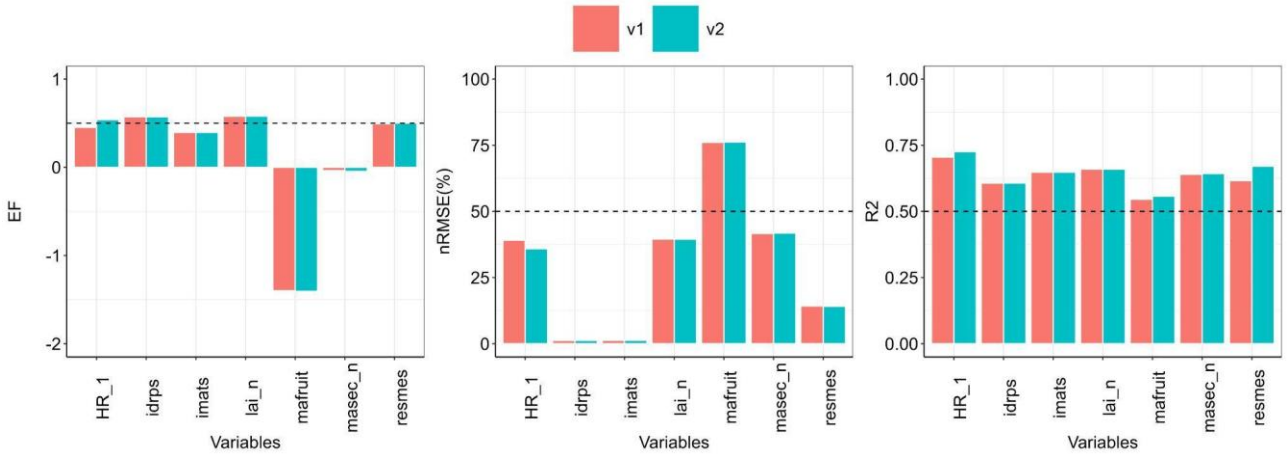

Figure III-S1. STICS-soil crop model performances on calibrated variables pooled together : HR_1 = Soil water content (0-1 cm depth), idrps = anthesis, imats = physiological maturity, lai_n = Leaf Area Index (LAI), mafruit = grain yield, masec_n = dry aboveground biomass, resmes = soil water content in the profile (0-105 cm depth). Evap1 is the calibration using the actual formalism of soil evaporation and Evap2 is the calibration using the new soil evaporation formalism. During 2021/22 and 2022/23 cropping years

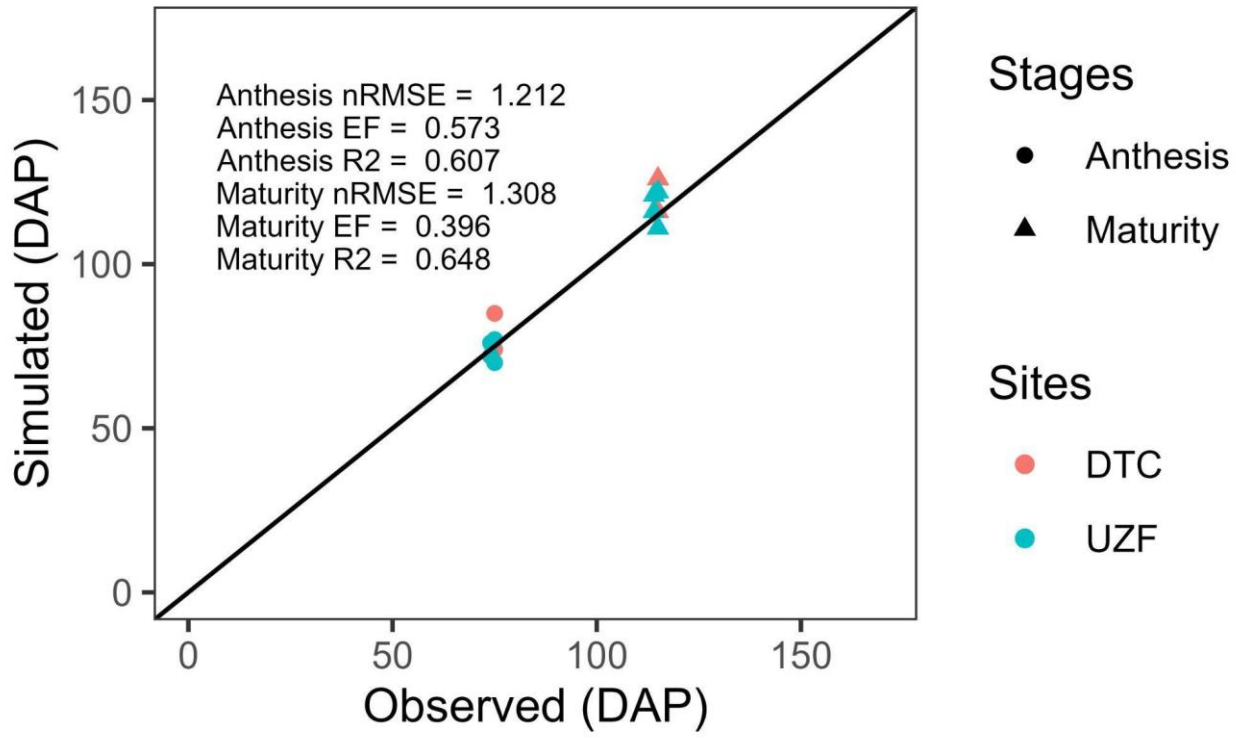

Figure III-S2. Crop phenology calibration. Here two stages were calibrated anthesis (circles) and physiological maturity (cones) at DTC (red dots) and UZF (blue dots) expressed as days after planting (DAP).

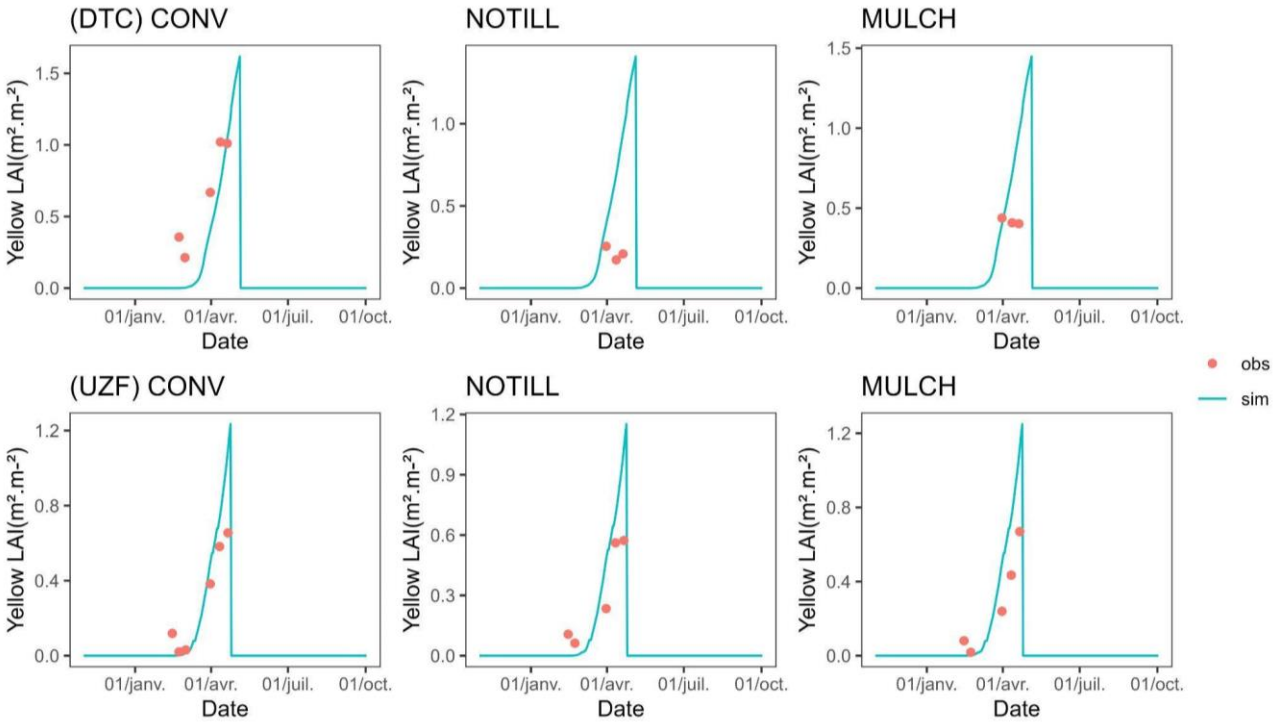

Figure III-S3. Senescence LAI observed (red dots) and simulated (blue lines) dynamics at DTC (top) and UZF (bottom) sites under conventional tillage (CT) no-tillage (NT) and no-tillage with mulch (NTM).

Table III-S1. Soil parameters defined in the STICS crop model for experiments on an Abruptic Lixisol (DTC) and on a Xanthic Ferralsol (UZF) in Zimbabwe subhumid. (*) represents new parameters of the new soil evaporation module

	Sites	DTC			UZF				
Parameters	Description	CT	NT	NTM	CT	NT	NTM	units	Source
albedo	Albedo of bare dry soil	0.27	0.3	0.23	0.19	0.19	0.21	-	Diop, 2023
albveg	Albedo of green vegetation	0.23	0.23	0.23	0.23	0.23	0.23	-	Breuer et al., (2003)
q0	cumulative soil evaporation above which evaporation rate is decreased	10	10	10	5	5	5	mm	STICS
cfes	parameter defining the soil contribution to evaporation versus depth	2.5	2.5	2.5				-	STICS
condsol*	plays on how the available soil water is distributed in the soil	0.2	0.2	0.2	0.3	0.3	0.3	-	Optimisation
betevap*	Parameter defining how low water content reduces evaporation	1.5	1.5	1.5	3.5	3.5	3.5	-	Optimisation
zmlchmax*	the soil thickness affected by evaporation	30	30	30	20	20	20	cm	Optimisation

Chapitre IV : Discussion générale et conclusion

1. Préambule

L'agriculture de conservation (AC) qui associe la réduction du travail du sol, la couverture permanente du sol par des résidus de cultures ou par des cultures intermédiaires et la diversification des espèces cultivées, est l'une des solutions fondées sur la nature (*nature-based solutions* en anglais) pour atténuer le réchauffement climatique (Maia et al., 2022; Miralles-Wilhelm, 2023). Cette approche permet non seulement de stocker du C dans les sols agricoles mais également de réduire les émissions de GES. Les pratiques culturales suggérées par l'AC modifient également les états de surface comme l'albédo ainsi que la répartition des flux d'énergie à la surface (ex. le rapport de Bowen ou la température de surface). Cependant, ces rétroactions biogéophysiques ne sont actuellement pas intégrées dans les scénarios à faibles émissions du GIEC. Comprendre les processus biogéochimiques (stockage C dans les sols, émissions GES) et les processus biogéophysiques (albédo de surface, évapotranspiration, rayonnement infrarouge…) de l'AC est un préalable pour quantifier l'effet climatique net et identifier les potentiels leviers d'atténuation des changements climatiques. Différentes méthodologies existent à ce jour pour étudier l'impact des changements de pratiques sur le climat, comme les mesures *in-situ* et la modélisation. Les mesures *in-situ* permettent de comprendre les processus et leurs interactions, de paramétrer et d'améliorer certains formalismes dans les modèles. Ces travaux de thèse se sont intéressés à la combinaison de ces approches afin de permettre l'amélioration de nos connaissances sur le fonctionnement des systèmes de culture en AC en Afrique subsaharienne et ainsi pouvoir mieux cibler et quantifier les leviers d'action pour lutter contre les changements climatiques.

De nos jours, peu d'études s'intéressent à la comparaison des effets biogéochimiques et biogéophysiques de l'agriculture de conservation et en Afrique subsaharienne aucune étude n'est répertoriée dans la littérature. Le peu d'études scientifiques abordant ce sujet ont été menées dans des systèmes de culture en climat tempéré et peu se sont baseés sur des mesures terrains (Davin et al., 2014; Kaye and Quemada, 2017; Ceschia et al., 2017). Beaucoup d'entre elles s'appuient sur des données d'inventaires avec son lot d'incertitudes,

et sur de la télédétection spatiale à moyenne ou basse résolution (Lugato et al., 2020). D'autres études ne s'intéressent qu'aux effets biogéochimiques comme la séquestration de carbone (Corbeels et al., 2020; Powlson et al., 2016), les émissions de GES (Fuentes-Ponce et al., 2022), ou uniquement aux effets biogéophysiques en se basant sur la modélisation (Hirsch et al., 2018b).

Le but de ces travaux est de combler le gap de connaissance en Afrique subsaharienne où ces études sont absentes. Un des volets de cette thèse s'intéresse au suivi et à l'analyse des données d'albédo de surface, de rayonnement infrarouge, d'indice foliaire (LAI) et d'humidité du sol ainsi que des données météorologiques sur trois systèmes de culture en agriculture de conservation *i.e.* le labour conventionnel (*conventional tillage*, (CT) en anglais), la suppression du labour (*no-tillage* (NT), en anglais) et la suppression du labour combiné avec la couverture du sol par des résidus de culture (*mulch*) (*no-tillage with mulch*, (NTM) en anglais) dans deux sites avec des types de sol contrastés : un abruptic Lixisol à Domboshawa (DTC) et un xanthic Ferralsol à *University of Zimbabwe Farm* (UZF). Le deuxième volet de ces travaux s'inscrit dans une perspective de comparaison des effets biogéochimiques, ici la séquestration C et les émissions de N_2O, et des effets biogéophysiques, ici l'albédo de surface sur un scénario de 30 ans de pratique du no-tillage et du mulching (versus le CT) avec des horizons temporels de 20 et 100 ans. Le dernier volet concerne la modélisation de l'albédo de surface en utilisant le modèle de système de cultures STICS (Brisson et al., 2003). Le but recherché dans cette partie était d'évaluer les capacités du modèle à reproduire les dynamiques d'albédo de surface et l'identification de potentiels points d'amélioration du point de vue des formalismes ou de la paramétrisation. Les améliorations proposées vont permettre de réaliser dans des travaux ultérieurs une analyse des effets couplées (biogéochimiques+biogéophysiques) des pratiques de AC, de réaliser des scénarios climatiques exploratoires et d'effectuer une extrapolation à l'échelle continentale.

2. L'analyse des effets couplés : l'importance de considérer l'albédo

De nombreuses études explorant les potentiels leviers d'atténuation du changement climatique liés aux pratiques ne s'intéressent qu'aux effets biogéochimiques, et plusieurs ont

déjà démontré l'importance d'inclure les effets biogéophysiques, comme l'albédo de surface (Betts, 2000; Kaye and Quemada, 2017; Lugato et al., 2020; Pique et al., 2023). Des études ont montré que les effets biogéophysiques associés aux changements d'occupation des sols peuvent avoir des magnitudes et des directions similaires à ceux des effets liés aux changements de pratiques (Luyssaert et al., 2014). Dans cette étude, les changements d'albédo de surface entraînent des bénéfices climatiques allant de -1,27 à +1,15 t CO_2-éq ha^{-1} an^{-1} pour les pratiques du NT et du NTM, en se basant sur un PRG avec un temps d'intégration de 100 ans. Ces chiffres se situent dans les mêmes ordres de grandeur que le potentiel d'atténuation du stockage de carbone dans les sols en Afrique subsaharienne, estimé à 0.28-0.96 t C ha^{-1} an^{-1} (Powlson et al., 2016), soit -1 à -3,34 t CO_2-éq ha^{-1} an^{-1}. Les résultats obtenus ont montré un antagonisme des effets sur les sols sableux clairs associé à la mise en place des pratiques de l'AC, et un effet de synergie sur les sols argileux sombres. Avec un scénario de 6 mois de maintien des résidus de culture, l'effet de refroidissement sur les sols argileux foncés est renforcé, quel que soit l'horizon temporel considéré. L'effet opposé est observé sur les sols sableux clairs, avec un fort réchauffement sur une échelle de 20 ans et un effet neutre sur 100 ans, annihilant ainsi le bénéfice climatique du stockage de carbone. Ainsi, ces pratiques culturales pourraient être des solutions fondées sur la nature pour contribuer à l'atténuation des changements climatiques, avec d'autres pratiques comme les couverts intermédiaires (Ceschia et al., 2017; Kaye and Quemada, 2017; Carrer et al., 2018; Pique et al., 2023) et d'autres techniques de géo-ingénierie. Les pratiques telles que la suppression du labour et la gestion des résidus en surface ne sont pas les seuls systèmes de cultures permettant de contribuer à l'atténuation du changement climatique via l'augmentation de l'albédo de surface. Kaye and Quemada (2017) ont démontré que les couverts intermédiaires en Espagne et aux États-Unis pourraient aussi augmenter l'albédo de surface et contribuer à l'atténuation du changement climatique d'environ -0.25 t CO_2-éq ha^{-1} an^{-1}, ce qui se situe dans les ordres de grandeur des pratiques de suppression du labour et de gestion des résidus en surface. Néanmoins, les auteurs ont souligné une large variabilité du potentiel d'atténuation via les effets d'albédo de surface (-0.39 à +1,11 t CO_2-éq ha^{-1} an^{-1}), qui dépend fortement de la variabilité de l'albédo du sol, du couvert et de la présence ou non d'une couverture neigeuse. Dans la même veine, Liu et al. (2022b)

considèrent que sur un horizon temporel de 50 ans, la conversion du labour conventionnel à la suppression du labour pourrait réaliser une atténuation de 10 à 15 t CO_2 ha^{-1}. (Ridgwell et al., 2009) ont proposé une méthode de géo-ingénierie consistant à augmenter l'albédo des parcelles agricoles en sélectionnant des cultivars avec un fort pouvoir réfléchissant. Ils ont montré qu'une augmentation de l'albédo de la canopée de 0.04 pourrait contribuer à un effet de refroidissement global de 0.11 °C.

Les limites de cette étude sont entre autres l'absence de quantification des incertitudes. Très peu de données temporelles concernant les effets biogéochimiques notamment pour calibrer la projection du stockage de C avec les modèles de sol ici ICBM (ex. Le Noë et al., 2023). Aussi, ni les effets d'assombrissement du sol sur les traitements avec des résidus en surface ni les rétroactions du climat ne sont pas prises en compte et ceci peut être une des limites de cette étude.

Au vu des résultats obtenus dans ces travaux de thèse, plusieurs perspectives s'ouvrent pour améliorer cette étude. L'utilisation de modèles climatiques prenant en compte toutes les rétroactions pourrait être un point d'amélioration futur. Plusieurs modèles, à l'image du modèle de surface ORCHIDEE ou des modèles du GIEC comme IPSL-CM6A-LR, ne prennent toujours pas en compte les effets des changements de pratiques culturales et les effets d'albédo, considérés jusqu'à aujourd'hui comme négligeables (Pique, 2021). Ces exercices de modélisation permettraient de quantifier les effets biogéophysiques locaux et globaux et d'évaluer les extrêmes climatiques en Afrique subsaharienne. Les résultats de cette étude montrent l'importance de considérer ensemble les effets biogéophysiques et biogéochimiques pour quantifier les effets climatiques nets associés aux pratiques culturales, et ainsi proposer des pistes d'atténuation et améliorer les stratégies d'adaptation aux changements climatiques selon le contexte local.

3. Qu'en est-il pour l'adaptation ?

Les effets d'albédo de surface sont souvent étudiés pour leur potentiel d'atténuation. Néanmoins, les changements d'albédo de surface peuvent être une solution basée sur la nature pertinente pour l'adaptation aux changements climatiques, notamment dans les

surfaces agricoles qui sont parmi les plus vulnérables aux extrêmes de températures et à la sécheresse (Seneviratne et al., 2018a). Les auteurs ont également souligné, via des exercices de modélisation, que l'augmentation de l'albédo de surface de 0.1 pourrait réduire l'effet de réchauffement régional, allant de 2 à 3 °C sur la température diurne maximale annuelle, et jusqu'à 1 °C sur la température moyenne annuelle. Ce refroidissement local peut engendrer, durant les étés très chauds, un ralentissement de la décomposition de la matière organique (MO) du sol, ce qui pourrait contribuer à une augmentation potentielle du stockage de carbone (C). Davin et al., (2014) affirment que l'augmentation de l'albédo est particulièrement efficace lors des journées d'été très chaudes avec un fort rayonnement. Cet effet permet ainsi la conservation de l'humidité du sol grâce au maintien des résidus en surface tout au long de l'année, ce qui favorise un refroidissement évaporatif en période de chaleur, et peut réduire la récurrence des stress hydriques durant les chaleurs extrêmes. Singarayer and Davies-Barnard (2012) montrent que certaines techniques de géo-ingénierie, comme l'augmentation de l'albédo de surface des cultures, peuvent être une approche à moindre coût pour contrebalancer la hausse des températures au niveau local. Ils ajoutent que cette approche pourrait aussi être déterminante pour la sécurité alimentaire et pourrait avoir des retombées positives sur la productivité. L'adaptation via ces effets biogéophysiques n'est évaluée qu'à une échelle locale, sans tenir compte des possibles téléconnexions climatiques et de leurs conséquences dans d'autres régions et/ou contextes pédoclimatiques (Singarayer and Davies-Barnard, 2012). De plus, ce sont des pratiques qui ne sont pas facilement applicables à l'échelle nationale, voire globale. En Afrique subsaharienne, par exemple, la suppression du labour conjuguée au maintien des résidus de paillis est largement promue, mais peu adoptée en raison des compromis entre la nourriture du bétail et l'agriculture (Baudron et al., 2014). D'autres pratiques ont des effets antagonistes à d'autres bénéfices climatiques, comme l'assombrissement du sol par les résidus de cultures ou même par les couverts intermédiaires, entraînant un potentiel stockage additionnel de carbone dans le sol, mais accentuant l'effet de réchauffement de l'albédo.

4. L'albédo de surface dans les modèles

Beaucoup de modèles de système de culture ou de surface considèrent l'albédo de surface comme une constante. Or, l'albédo de surface peut être influencé par beaucoup de facteurs comme la teneur en eau, le couvert végétal (Oguntunde and van de Giesen, 2004), la couleur (Post et al., 2000), la rugosité (Cierniewski et al., 2013), la teneur en fer et en matière organique du sol. A ce jour, il existe peu de modèles de système de cultures ou de modèle climatique prenant en compte les effets de pratiques culturales sur l'albédo de surface et potentiellement sur les composantes du bilan d'énergie. Généralement, l'albédo de végétation est pris en compte de manière simpliste dans les modèles ne tenant pas en compte par exemple l'effet de la sénescence des feuilles à la différence de Béziat et al. (2013) avec le modèle iCARE. Le modèle de système de culture STICS (Brisson et al., 2003) est l'un des rares modèles qui simule la dynamique d'albédo en fonction de la teneur en eau de la couche surfacique, de la couleur du sol (pris en compte implicitement), et de la présence des résidus de cultures ou mulch en plastique en surface (Beaudoin et al., 2023).

Durant ces travaux de thèse, la modélisation de l'albédo de surface occupait une partie importante du travail. Partant des observations qui sont faites, une amélioration du formalisme d'albédo de surface a été proposée en y intégrant en plus de l'albédo de végétation verte, l'albédo des tissus sénescents. Le nouveau formalisme d'albédo montre une amélioration des simulations de l'albédo de surface avec des résultats nettement plus précis que le formalisme actuel (voir chapitre III). L'intégration d'un formalisme pour améliorer l'évaporation de l'eau dans le sol dans le contexte pédoclimatique d'Afrique subsaharienne qui connaissent de longues périodes de saison sèche a eu un apport considérable aux simulations d'albédo. Ce nouveau calcul d'évaporation du sol combiné au nouveau formalisme d'albédo a amélioré la simulation d'albédo de surface en période de sol nu comme en période de culture (voir Tableau III-2).

La non prise en compte de certains processus peut être source d'incertitudes sur les simulations dans les modèles, dans notre cas une surestimation de certaines variables de sorties clés comme la biomasse et le rendement. Par exemple, le ruissellement est pris en compte dans les paramètres généraux du modèle STICS alors que dans certaines conditions, il pourrait être spécifique au site ou traitement pour éviter d'appliquer les mêmes facteurs

pour toutes les unités de simulations. De plus, il reste d'autres limites à ce modèle concernant la gestion des résidus de culture sur la simulation d'albédo. Il se trouve que le modèle dans ces paramètres ne tient en compte que de l'albédo du mulch plastique (*albedomulchplastique*), l'intégration des mulch de résidus de culture pourrait être un avantage pour améliorer la précision de la simulation d'albédo.

A ce stade, STICS prend en compte de manière implicite la couleur du sol dans le paramètre *albsol* représentant la valeur d'albédo du sol nu et sec. D'autres facteurs peuvent être pris en compte pour intégrer de manière explicite la couleur du sol comme le teneur en fer (Fe) et la teneur de MO du sol. Cette dernière serait aussi utile pour quantifier l'effet d'assombrissement du sol due à une augmentation de la MO associé à certaines pratiques comme les couverts intermédiaires (Pique et al., 2023), les résidus de cultures (Gaur and Mukherjee, 1980), ou le biochar (Bozzi et al., 2015). Dans une étude, Post et al. (2000) montre la relation qui existe entre les couleurs de Munsell et l'albédo. Cette approche pourrait aussi être intégrée dans le calcul d'albédo dans le modèle STICS. Dans de prochaines études, explorer l'impact de l'albédo de surface simulé sur les autres composantes comme le rayonnement net, le rayonnement thermique et la température de surface ajouterait de la matière sur la compréhension des processus biogéophysiques. Le couplage des modules de pratiques avec le modèle de sol-végétation-atmosphère ORCHIDEE comme dans les travaux de (De Noblet-Ducoudré et al., 2004) pour mieux représenter certains processus dans les parcelles agricoles pourrait être un puissant outil de spatialisation des effets couplés.

Dans le cadre cette thèse, l'utilisation du modèle ORCHIDEE-CROP était prévu. D'ailleurs j'ai suivi des formations allant dans ce sens et j'ai réalisé des simulations avec ce modèle en Afrique subsaharienne (les résultats ne sont pas présentés dans ce manuscrit). Faute de temps je n'ai pu développer cette partie dans la thèse, et de ce fait, ouvre une belle perspective de ce travail pour la spatialisation des effets couplés.

Au-delà de la modélisation spatialisée, la télédétection est aussi une approche pertinente pour comprendre l'effet des processus biogéophysiques et biogéochimiques sur de vastes espaces à moindre coût.

5. Approches spatialisées des effets couplés

5.1 ORCHIDEE-CROP : une potentielle perspective à l'analyse spatialisée des effets couplés

Le modèle ORCHIDEE (**OR**ganising **C**arbon and **H**ydrology **I**n **D**ynamic **E**cosyst**E**ms) est un modèle de surface terrestre (Krinner et al., 2005) qui peut être utilisé par exemple dans les études explorant le cycle carbone dans les différents réservoirs, et ou l'impact des activités anthropiques sur les changements d'occupation des terres et sur le climat. Ce modèle peut fonctionner en tandem avec un modèle de circulation globale atmosphère-océan IPSL (Institut Pierre Simon Laplace), permettant ainsi une interaction bidirectionnelle entre les conditions atmosphériques et la surface terrestre. Ce modèle permet de quantifier les effets des changements de la surface terrestre sur le climat et inversement et ainsi prendre en compte les rétroactions. Cependant, si l'étude se concentre uniquement sur les changements de la surface terrestre, ORCHIDEE peut être utilisé de manière autonome. Dans cette configuration, le modèle reçoit les conditions atmosphériques à partir des fichiers de forçage et peut être appliqué à n'importe quelle résolution allant d'une grille à une échelle globale. Le modèle ORCHIDEE est composé de schémas groupant des modules qui intègrent un ensemble de processus 1) le schéma "SECHIBA" regroupant toutes les modules simulant, le bilan d'eau, le bilan d'énergie et les processus biogéochimiques et anthropiques 2) les codes des processus biogéochimiques et anthropiques sont groupés dans un schéma nommé "STOMATE". Dans ce modèle, plusieurs modules peuvent être activés ou désactivés en fonction des buts de l'étude et de plus l'exécution ne nécessite pas toujours l'activation de "STOMATE". Dans le modèle ORCHIDEE, la végétation est divisée en 13 types fonctionnels de plantes (PFTs, comme *plant functional types* en anglais) incluant le sol nu, 8 classes de forêts, deux classes de végétation naturelles (C3 et C4) et deux classes de cultures (C3 et C4) ayant la même phénologie que la végétation naturelle. Un couplage du modèle de surface et un modèle agronomique basé sur des processus comme STICS est un moyen efficace pour la prise en compte des dynamiques de changement d'occupation et d'utilisation des espaces agricoles et aide à mieux comprendre ses interactions avec l'environnement et le climat.

5.2 Intégration d'un modèle de culture dans un modèle de surface

La version "CROP" du modèle ORCHIDEE est faite pour inclure les espaces agricoles et leurs interactions avec le climat et l'environnement. Ce modèle simule des processus clés tels que la photosynthèse, la respiration, la croissance des cultures, l'hydrologie, et le cycle des nutriments, en tenant compte des pratiques agricoles et des variations climatiques (Wu et al., 2016). Il est utilisé pour étudier l'impact du changement climatique sur les rendements agricoles, optimiser les pratiques agricoles, et soutenir la formulation de politiques d'adaptation et d'atténuation des changements climatiques. Dans l'étude de De Noblet-Ducoudré et al. (2004), les auteurs ont couplé le modèle ORCHIDEE et le modèle de système de culture STICS version 4.0 pour pouvoir simuler certaines variables agronomiques qui y sont déjà prises en compte de manière très détaillée. Gervois et al. (2004), ont intégré des modules du modèles STICS version 4.0 dans ORCHIDEE avec comme objectif d'investiguer les interactions entre la gestion des pratiques, la croissance des cultures et le climat et de démontrer pourquoi la végétation naturelle ne peut être utilisée pour reproduire la phénologie des cultures dans les modèles globaux. La naissance d'ORCHIDEE-CROP est le fruit d'intégration d'un module de phénologie des cultures, d'itinéraire techniques (ex. décision de récolte, fertilisation en azote…) dans le but de simuler les processus biogéophysiques et biogéochimiques et leurs interactions dans les surfaces agricoles. Pour ce faire, les auteurs se sont basés sur une paramétrisation de quelques cultures en régions tempérées, ex. blé d'hiver et le maïs déjà calibrés avec satisfaction avec une description détaillée des processus avec le modèle STICS (Brisson et al., 2002). Dans les travaux de (Wu et al., 2016) avec la version ORCHIDEE-CROP (v0) les auteurs ont montré la capacité de ORCHIDEE-CROP pour simuler la phénologie des cultures, les flux C et d'énergie du maïs et du blé d'hiver en Europe.

5.3 L'apport du couplage des deux modèles dans notre étude

STICS a une bonne représentation des pratiques et leur impact sur les cycles biogéochimiques et ORCHIDEE à une bonne capacité à simuler les flux d'énergie et peut se coupler à des modèles de circulation globale. Le couplage de ces deux modèles donne

l'opportunité de tenir en compte les effets couplés (biogéophysiques+biogéochimiques) des gestions des pratiques dans les espaces agricoles sur le climat. Il peut constituer un puissant outil d'identification des antagonismes et synergies des effets pour la promotion de certaines pratiques culturales pour atténuer le changement climatique et faciliter l'adaptation. Doté déjà des sorties spatialisées, le couplage pourrait être un outil intéressant pour comprendre les processus cités précédemment à l'échelle régionale (dans notre étude Afrique subsaharienne) et globale. L'utilisation de ce modèle couplé avec l'atmosphère permettrait de simuler l'impact global de l'adoption de l'agriculture de conservation au niveau régional (dans le cadre de cette étude en Afrique) en tenant en compte les téléconnexions sur climat avec d'autres contrées au niveau régional et global.

Le modèle ORCHIDEE prend déjà en compte l'albédo de surface, il est calculé en faisant une paramétrisation des différentes composantes de la surface terrestre (*i.e.* sol, végétation, couverture neigeuse). Nonobstant, ORCHIDEE n'intègre pas encore un module de gestion de pratiques comme la gestion des résidus de cultures, les cultures associées ou les couverts intermédiaires… pouvant impacter l'albédo de surface. Il serait aujourd'hui difficile d'utiliser le modèle pour faire des scénarios d'agriculture de conservation et d'en comprendre ses effets biogéophysiques associées aux changements de pratiques. Des études ultérieures pourraient se pencher sur la mise en place de cette approche afin d'en identifier ses potentialités et ses limites pour mieux comprendre l'enjeux des changements de pratiques sur le climat à différentes échelles.

5.4 L'apport de la télédétection spatiale

La télédétection spatiale pourrait aussi être un outil pertinent pour analyser les effets couplés à large échelle et à faible coût. Aujourd'hui, des mesures d'albédo de surface peuvent être réalisées à partir d'images satellite à moyenne résolution spatiale et temporelle ex. MODIS (Gao et al., 2014; Sieber et al., 2022) et à haute résolution spatiale et temporelle ex. Landsat (Liang et al., 2002; Tasumi et al., 2008), Sentinel-2 (Bonafoni and Sekertekin, 2020; Lin et al., 2022). Ces produits pourraient aider à comprendre les variations spatiales et temporelles d'albédo de surface corrélée à l'occupation et l'utilisation des terres. De nouvelles missions comme le satellite franco-indien TRISHNA prévu en 2026 serait aussi une perspective

nouvelle pour mesurer l'albédo et la température de surface à très haute résolution spatiale et temporelle sans passer par des estimations complexes et très sensibles aux conditions locales (Liang et al., 2002; Tasumi et al., 2008).

Concernant les effets biogéochimiques, des études sur la quantification du bilan carbone des parcelles agricoles via des produits satellitaires à haute résolution spatiale et temporelle sont en cours de réalisation au CESBIO avec la chaîne de traitement AgriCarbon-EO (Wijmer et al., 2024). AgriCarbon-EO permet de simuler la biomasse, les rendements, les flux de CO_2 et les bilans de carbone des cultures ainsi que la quantification de leurs incertitudes, avec une résolution de 10 mètres à partir des cartes de cultures, de sols, des données climatiques et des produits satellites assimilés dans un modèle agrométéorologique SAFYE-CO_2 (Pique et al., 2020). De plus, des études sur la cartographie du C des sols en utilisation la télédétection sont en cours de réalisation (Urbina-Salazar et al., 2023; Vaudour et al., 2019) et ceci constitue également une perspective majeure dans l'analyse des effets couplées et leur variations spatiales et temporelles.

Néanmoins ces travaux sont en train d'être réalisés majoritairement en milieu tempéré, leur application en Afrique subsaharienne reste encore minoritaire et demande plus de données terrains pour valider les modèles et les observations satellites.

Conclusion générale

Ces travaux de recherche ont permis d'améliorer notre compréhension de certains processus biogéophysiques associés à la mise en œuvre de pratiques d'agriculture de conservation, suppression du labour (NT, pour no-tillage) et au maintien des résidus en surface (NTM, pour no-tillage+mulch), par rapport aux pratiques d'agriculture conventionnelle (*i.e.* labour, enfouissement des résidus ; CT pour conventional tillage) en Afrique subsaharienne, en utilisant des mesures de terrain et la modélisation.

Durant 2 années culturales, des mesures de rayonnement à courtes et longues longueurs d'onde, de température et d'humidité du sol, d'indice foliaire et de taux de couverture ont été réalisées en continu sur deux expérimentations de longue durée au Zimbabwe subhumide. Ces mesures ont permis : 1) de quantifier l'effet de la suppression du labour et de la gestion des résidus sur la dynamique de l'albédo et la température du sol, 2) d'étudier les interactions entre types de sol et systèmes de culture sur la dynamique de l'albédo de surface, 3) d'explorer les variations de l'albédo de surface au cours de la saison de culture en lien avec le développement du couvert et la dynamique de la teneur en eau du sol. Les résultats obtenus ont montré une augmentation de l'albédo du NT comparé au CT, quel que soit le type de sol étudié, et un effet contrasté du NTM selon le type de sol. Pour les sols sableux clairs, les résidus de culture en surface diminuent l'albédo, ce qui entraîne par conséquent un effet de réchauffement, contrairement aux sols argileux sombres où les résidus de culture augmentent l'albédo de surface, causant ainsi un effet de refroidissement. Néanmoins, cette étude pourrait être améliorée en quantifiant le rapport de Bowen (H/LE) pour une meilleure prise en compte des effets biogéophysiques sur le climat local. Ces résultats ont été utilisés pour comparer les effets biogéophysiques liés aux changements d'albédo de surface induits par les changements de pratiques avec les effets biogéochimiques associés à la séquestration du C dans le sol et aux émissions de N_2O étudiés dans une thèse antérieure. Cela a permis que l'effet climatique net entraîné par ces changements de pratiques culturales soit quantifié.

L'étude de l'effet climatique entraîné par les changements de pratiques s'est principalement basée sur un scénario de 30 ans de mise en œuvre des nouvelles pratiques (suppression du

labour et maintien des résidus en surface), comparé au labour conventionnel, et d'analyse de leurs impacts climatiques. Deux métriques ont été utilisées pour comparer les effets albédo et les effets biogéochimiques : le pouvoir de réchauffement global (*global warming potential*, GWP en anglais) et le changement de la température globale, notamment pour leur pertinence, leur simplicité de mise en œuvre, et leur prise en compte des durées de séjour dans l'atmosphère des polluants à courte et longue durée. Les résultats obtenus montrent un effet bénéfique des pratiques d'agriculture de conservation sur les sols argileux sombres, avec un effet d'atténuation prononcé lié à la suppression du labour associée à la couverture permanente du sol par les résidus. Sur ce type de sol, les effets de stockage du C et les effets de changement de l'albédo de surface se renforcent mutuellement. À l'opposé, sur les sols sableux clairs, les résidus ont des effets antagonistes aux bénéfices acquis par la séquestration du C dans le sol. Sur les deux sites, les émissions de N_2O sont très faibles, et leur impact climatique, comparé aux autres effets, reste peu significatif. L'agriculture de conservation est largement promue en Afrique subsaharienne, mais l'adoption reste faible notamment en raison des compromis à trouver entre l'agriculture (apport des résidus au sol) et l'élevage (alimentation du bétail). Néanmoins, cette approche pourrait être améliorée en utilisant des modèles de systèmes de cultures permettant une analyse conjointe des processus biogéochimiques et biogéophysiques liés aux changements de pratiques.

Une autre partie de ce travail de thèse était donc axée sur la modélisation de l'albédo de surface avec le modèle de système de culture STICS en lien avec les changements de pratiques. Durant les exercices de simulation, les potentiels de STICS et ses lacunes pour simuler l'albédo de surface ont été identifiés en se basant sur les données de terrain collectées. Les formalismes du modèle ont été modifiés pour mieux prendre en compte les variations de l'albédo durant la phase de sénescence, ce qui a considérablement amélioré les simulations. Le modèle a été initialement développé pour un climat tempéré. Néanmoins, le modèle se "tropicalise" de plus en plus avec de nouvelles cultures. L'adaptation du modèle en zone tropicale reste inachevée, avec des processus qui ne reflètent pas encore les conditions climatiques, comme l'évaporation en zone subsaharienne avec de longues saisons sèches. Un nouveau formalisme d'évaporation du sol, reflétant mieux nos conditions d'étude, a également été essayé durant la thèse. Ce nouveau formalisme d'évaporation du

sol a un impact significatif sur les simulations d'albédo de surface. En guise de perspective pour ce travail de modélisation, il serait intéressant d'explorer l'impact du formalisme de l'albédo et de l'évaporation sur les composantes du bilan d'énergie, comme l'évapotranspiration et le rayonnement net déjà pris en compte dans le modèle. Un couplage du modèle avec des modèles de surface comme ORCHIDEE pourrait être une approche pertinente pour la spatialisation des effets couplés étudiés dans les deux premiers chapitres, à l'échelle régionale voire globale.

Ces travaux de thèse ont donc contribué à la compréhension de certains processus jusqu'ici absents dans les scénarios à faible émission du GIEC. Ils ont permis de comprendre que : 1) l'albédo des parcelles agricoles, souvent considéré comme constant dans les modèles de systèmes de cultures ou dans les modèles de surface, varie au cours de la saison, et ces variations dépendent de plusieurs facteurs (humidité de surface, rugosité, présence de couvert végétale ou de résidus en surface) ; 2) les effets biogéophysiques peuvent avoir des magnitudes et des directions similaires ou opposés à celles des effets biogéochimiques des pratiques agricoles sur le climat ; 3) les modèles de systèmes de cultures ne prennent pas encore suffisamment en compte les effets de l'albédo de surface en relation avec la gestion des pratiques, alors qu'ils pourraient constituer un atout pour comprendre les variations spatiales et temporelles des effets couplés à différentes échelles.

Références bibliographiques

Affholder, F., 2001. Modélisation de culture et diagnostic agronomique régional. Mise au point d'une méthode et application au cas du maïs chez les petits producteurs du Brésil Central (phdthesis). Institut national agronomique paris-grignon - INA P-G.

Affholder, F., Scopel, E., Neto, J.M., Capillon, A., 2003. Diagnosis of the productivity gap using a crop model. Methodology and case study of small-scale maize production in central Brazil. Agronomie 23, 305–325. https://doi.org/10.1051/agro:2003004

Akbari, H., Menon, S., Rosenfeld, A., 2009. Global cooling: increasing world-wide urban albedos to offset CO2. Climatic Change 94, 275–286. https://doi.org/10.1007/s10584-008-9515-9

Akhtar, K., Wang, W., Ren, G., Khan, Ahmad, Enguang, N., Khan, Aziz, Feng, Y., Yang, G., Wang, H., 2020. Straw mulching with inorganic nitrogen fertilizer reduces soil CO2 and N2O emissions and improves wheat yield. Science of The Total Environment 741, 140488. https://doi.org/10.1016/j.scitotenv.2020.140488

Alletto, L., Cassigneul, A., Duchalais, A., Giuliano, S., Brechemier, J., Justes, E., 2022. Cover crops maintain or improve agronomic performances of maize monoculture during the transition period from conventional to no-tillage. Field Crops Research 283, 108540. https://doi.org/10.1016/j.fcr.2022.108540

Andrén, O., Kätterer, T., 1997. ICBM: THE INTRODUCTORY CARBON BALANCE MODEL FOR EXPLORATION OF SOIL CARBON BALANCES. Ecological Applications 7, 1226–1236. https://doi.org/10.1890/1051-0761(1997)007[1226:ITICBM]2.0.CO;2

Andrén, O., Kihara, J., Bationo, A., Vanlauwe, B., Kätterer, T., 2007. Soil Climate and Decomposer Activity in Sub-Saharan Africa Estimated from Standard Weather Station Data: A Simple Climate Index for Soil Carbon Balance Calculations. ambi 36, 379–386. https://doi.org/10.1579/0044-7447(2007)36[379:SCADAI]2.0.CO;2

Andrén, Reacute N, T, K.T., J, J., B, W., Kristina, R.I.D.N., 2012. Soil carbon dynamics, climate, crops and soil type calculations using introductory carbon balance model (ICBM) and agricultural field trial data from sub-Saharan Africa. Afr. J. Agric. Res. 7, 5800–5809. https://doi.org/10.5897/AJAR12.205

Andrews, T., Betts, R.A., Booth, B.B.B., Jones, C.D., Jones, G.S., 2017. Effective radiative forcing from historical land use change. Clim Dyn 48, 3489–3505. https://doi.org/10.1007/s00382-016-3280-7

Aydinalp, C., Cresser, M.S., 2008. The effects of global Climate Change on agriculture. J. Agric.& Environ. Sci 672–676.

Batjes, N.H., 1996. Total carbon and nitrogen in the soils of the world. European J Soil Science 65, 10–21. https://doi.org/10.1111/ejss.12114_2

Baudron, F., Jaleta, M., Okitoi, O., Tegegn, A., 2014. Conservation agriculture in African mixed crop-livestock systems: Expanding the niche. Agriculture, Ecosystems & Environment, Evaluating conservation agriculture for small-scale farmers in Sub-Saharan Africa and South Asia 187, 171–182. https://doi.org/10.1016/j.agee.2013.08.020

Beaudoin, N., Lecharpentier, P., Ripoche-Wachter, D., Strullu, L., Mary, B., Léonard, J., Launay, M., Justes, É., 2023. Stics Soil Crop Model. éditions Quae. https://doi.org/10.35690/978-2-7592-3679-4

Begue, A., Louise, Leroux, Danny Lo, SEEN, Jean-Philippe, TONNEAU, Philippe, MORANT, 2016. Observation spatiale pour l'agriculture en Afrique : potentiels et défis.

Beillouin, D., Corbeels, M., Demenois, J., Berre, D., Boyer, A., Fallot, A., Feder, F., Cardinael, R., 2023. A global meta-analysis of soil organic carbon in the Anthropocene. Nat Commun 14, 3700. https://doi.org/10.1038/s41467-023-39338-z

Bellouin, N., Davies, W., Shine, K.P., Quaas, J., Mülmenstädt, J., Forster, P.M., Smith, C., Lee, L., Regayre, L., Brasseur, G., Sudarchikova, N., Bouarar, I., Boucher, O., Myhre, G., 2020. Radiative forcing of climate change from the Copernicus reanalysis of atmospheric composition. Earth System Science Data 12, 1649–1677. https://doi.org/10.5194/essd-12-1649-2020

Betts, R.A., 2000. Offset of the potential carbon sink from boreal forestation by decreases in surface albedo. Nature 408, 187–190. https://doi.org/10.1038/35041545

Béziat, P., 2009. Effets des conditions environnementales et des pratiques culturales sur les flux de carbone et d'eau dans les agrosystèmes (phd). Université de Toulouse, Université Toulouse III - Paul Sabatier.

Béziat, P., Rivalland, V., Tallec, T., Jarosz, N., Boulet, G., Gentine, P., Ceschia, E., 2013.

Evaluation of a simple approach for crop evapotranspiration partitioning and analysis of the water budget distribution for several crop species. Agricultural and Forest Meteorology 177, 46–56. https://doi.org/10.1016/j.agrformet.2013.03.013

Blanco-Canqui, H., Lal, R., 2008. No-Tillage and Soil-Profile Carbon Sequestration: An On-Farm Assessment. Soil Science Soc of Amer J 72, 693–701. https://doi.org/10.2136/sssaj2007.0233

Bonafoni, S., Sekertekin, A., 2020. Albedo Retrieval From Sentinel-2 by New Narrow-to-Broadband Conversion Coefficients. IEEE Geosci. Remote Sensing Lett. 17, 1618–1622. https://doi.org/10.1109/LGRS.2020.2967085

Boucher, O., Reddy, M.S., 2008. Climate trade-off between black carbon and carbon dioxide emissions. Energy Policy 36, 193–200. https://doi.org/10.1016/j.enpol.2007.08.039

Bozzi, E., Genesio, L., Toscano, P., Pieri, M., Miglietta, F., 2015. Mimicking biochar-albedo feedback in complex Mediterranean agricultural landscapes. Environ. Res. Lett. 10, 084014. https://doi.org/10.1088/1748-9326/10/8/084014

Breil, M., Krawczyk, F., Pinto, J.G., 2023. The response of the regional longwave radiation balance and climate system in Europe to an idealized afforestation experiment. Earth System Dynamics 14, 243–253. https://doi.org/10.5194/esd-14-243-2023

Breuer, L., Eckhardt, K., Frede, H.-G., 2003. Plant parameter values for models in temperate climates. Ecological Modelling 169, 237–293. https://doi.org/10.1016/S0304-3800(03)00274-6

Bright, R.M., Bogren, W., Bernier, P., Astrup, R., 2016. Carbon-equivalent metrics for albedo changes in land management contexts: relevance of the time dimension. Ecol Appl 26, 1868–1880. https://doi.org/10.1890/15-1597.1

Bright, R.M., Cherubini, F., Strømman, A.H., 2012. Climate impacts of bioenergy: Inclusion of carbon cycle and albedo dynamics in life cycle impact assessment. Environmental Impact Assessment Review 37, 2–11. https://doi.org/10.1016/j.eiar.2012.01.002

Bright, R.M., Davin, E., O'Halloran, T., Pongratz, J., Zhao, K., Cescatti, A., 2017. Local temperature response to land cover and management change driven by non-radiative processes. Nature Clim Change 7, 296–302. https://doi.org/10.1038/nclimate3250

Bright, R.M., Lund, M.T., 2021. CO₂-equivalence metrics for surface albedo change based on the radiative forcing concept: a critical review. Atmos. Chem. Phys. 21, 9887–9907. https://doi.org/10.5194/acp-21-9887-2021

Brisson, N., Gary, C., Justes, E., Roche, R., Mary, B., Ripoche, D., Zimmer, D., Sierra, J., BERTUZZI, P., Burger, P., Bussière, F., Cabidoche, Y.M., Cellier, P., Debaeke, P., Gaudillère, J.P., Hénault, C., Maraux, F., SEGUIN, B., Sinoquet, H., 2003. An overview of the crop model STICS. European Journal of Agronomy 18, 309–332. https://doi.org/10.1016/S1161-0301(02)00110-7

Brisson, N., Launay, M., Mary, B., Beaudoin, N., 2008. Conceptual basis, formalisations and parameterization of the STICS crop model 301.

Brisson, N., Perrier, A., 1991. A semiempirical model of bare soil evaporation for crop simulation models. Water Resources Research 27, 719–727. https://doi.org/10.1029/91WR00075

Brisson, N., Ruget, F., Gate, P., Lorgeou, J., Nicoullaud, B., Tayot, X., Plenet, D., Jeuffroy, M.-H., Bouthier, A., Ripoche, D., Mary, B., Justes, E., 2002. STICS: a generic model for simulating cropsand their water and nitrogen balances.II. Model validation for wheat and maize. Agronomie 22, 69–92. https://doi.org/10.1051/agro:2001005

Bsaibes, A., Courault, D., Baret, F., Weiss, M., Olioso, A., Jacob, F., Hagolle, O., Marloie, O., Bertrand, N., Desfond, V., Kzemipour, F., 2009. Albedo and LAI estimates from FORMOSAT-2 data for crop monitoring. Remote Sensing of Environment 14.

Cai, H., Wang, J., Feng, Y., Wang, M., Qin, Z., Dunn, J.B., 2016. Consideration of land use change-induced surface albedo effects in life-cycle analysis of biofuels. Energy Environ. Sci. 9, 2855–2867. https://doi.org/10.1039/C6EE01728B

Cardinael, R., Barton, L., Corbeels, M., Six, J., Rowlings, D., Shumba, A., Chikowo, R., Farrell, M., 2024. Soil NO emissions during dry fallow periods. Global Change Biology 30, e17403. https://doi.org/10.1111/gcb.17403

Cardinael, R., Guibert, H., Kouassi Brédoumy, S.T., Gigou, J., N'Goran, K.E., Corbeels, M., 2022. Sustaining maize yields and soil carbon following land clearing in the forest–savannah transition zone of West Africa: Results from a 20-year experiment. Field Crops Research 275, 108335. https://doi.org/10.1016/j.fcr.2021.108335

Carrer, D., Pique, G., Ferlicoq, M., Ceamanos, X., Ceschia, E., 2018. What is the potential of cropland albedo management in the fight against global warming? A case study based on the use of cover crops. Environ. Res. Lett. 13, 044030. https://doi.org/10.1088/1748-9326/aab650

Ceschia, E., Mary, B., Ferlicoq, M., Pique, G., Carrer, D., Dejoux, J.-F., dedieux, gérard, 2017. Potentiel d'atténuation des changements climatiques par les couverts intermédiaires. Innovations agronomiques.

Chen, Y.-Y., Ryder, J., Bastrikov, V., Mcgrath, M., Naudts, K., El Zohbi, J., Ottle, C., Peylin, P., Polcher, J., Valade, A., Black, A., Elbers, J., Moors, E., Foken, T., van Gorsel, E., Haverd, V., Heinesch, B., Tiedemann, F., Knohl, A., Luyssaert, S., 2016. Evaluating the performance of land surface model ORCHIDEE-CAN v1.0 on water and energy flux estimation with a single- and multi-layer energy budget scheme. Geoscientific Model Development 9, 2951–2972. https://doi.org/10.5194/gmd-9-2951-2016

Cherubini, F., Bright, R.M., Strømman, A.H., 2012. Site-specific global warming potentials of biogenic CO_2 for bioenergy: contributions from carbon fluxes and albedo dynamics. Environ. Res. Lett. 7, 045902. https://doi.org/10.1088/1748-9326/7/4/045902

Cierniewski, J., Ceglarek, J., Kaźmierowski, C., 2018. Estimating the diurnal blue-sky albedo of soils with given roughness using their laboratory reflectance spectra. Journal of Quantitative Spectroscopy and Radiative Transfer 217, 213–223. https://doi.org/10.1016/j.jqsrt.2018.06.003

Cierniewski, J., Karnieli, A., Kazmierowski, C., Królewicz, S., Piekarczyk, J., Lewińska, K., Goldberg, A., Wesolowski, R., Orzechowski, M., 2015. Effects of Soil Surface Irregularities on the Diurnal Variation of Soil Broadband Blue-Sky Albedo. IEEE Journal of Selected Topics in Applied Earth Observations and Remote Sensing 8. https://doi.org/10.1109/JSTARS.2014.2330691

Cierniewski, J., Karnieli, A., Kuśnierek, K., Goldberg, A., Herrmann, I., 2013. Approximating the average daily surface albedo with respect to soil roughness and latitude. International Journal of Remote Sensing 34, 3416–3424. https://doi.org/10.1080/01431161.2012.716530

Cierniewski, J., Kuśnierek, K., 2010. Influence of several size properties on soil surface

reflectance. Quaestiones Geographicae 29, 13–25. https://doi.org/10.2478/v10117-010-0002-9

Collins, W.D., Rasch, P.J., Boville, B.A., Hack, J.J., Mccaa, J.R., Williamson, D.L., Kiehl, J.T., Briegleb, B., Bitz, C., 2004. NCAR/TN-464+STR NCAR TECHNICAL NOTE.

Constantin, J., Willaume, M., Murgue, C., Lacroix, B., Therond, O., 2015. The soil-crop models STICS and AqYield predict yield and soil water content for irrigated crops equally well with limited data. Agricultural and Forest Meteorology 206, 55–68. https://doi.org/10.1016/j.agrformet.2015.02.011

Corbeels, M., Cardinael, R., Powlson, D., Chikowo, R., Gerard, B., 2020. Carbon sequestration potential through conservation agriculture in Africa has been largely overestimated Comment on: "Meta-analysis on carbon sequestration through conservation agriculture in Africa." Soil and Tillage Research 196, 1–3. https://doi.org/10.1016/j.still.2019.104300

Coucheney, E., Buis, S., Launay, M., Constantin, J., Mary, B., García de Cortázar-Atauri, I., Ripoche, D., Beaudoin, N., Ruget, F., Andrianarisoa, K.S., Le Bas, C., Justes, E., Léonard, J., 2015. Accuracy, robustness and behavior of the STICS soil–crop model for plant, water and nitrogen outputs: Evaluation over a wide range of agro-environmental conditions in France. Environmental Modelling & Software 64, 177–190. https://doi.org/10.1016/j.envsoft.2014.11.024

Couëdel, A., Falconnier, G.N., Adam, M., Cardinael, R., Boote, K., Justes, E., Smith, W.N., Whitbread, A.M., Affholder, F., Balkovic, J., Basso, B., Bhatia, A., Chakrabarti, B., Chikowo, R., Christina, M., Faye, B., Ferchaud, F., Folberth, C., Akinseye, F.M., Gaiser, T., Galdos, M.V., Gayler, S., Gorooei, A., Grant, B., Guibert, H., Hoogenboom, G., Kamali, B., Laub, M., Maureira, F., Mequanint, F., Nendel, C., Porter, C.H., Ripoche, D., Ruane, A.C., Rusinamhodzi, L., Sharma, S., Singh, U., Six, J., Srivastava, A., Vanlauwe, B., Versini, A., Vianna, M., Webber, H., Weber, T.K.D., Zhang, C., Corbeels, M., 2024. Long-term soil organic carbon and crop yield feedbacks differ between 16 soil-crop models in sub-Saharan Africa. European Journal of Agronomy 155, 127109. https://doi.org/10.1016/j.eja.2024.127109

Da Silva, F.A.M., De Oliveira, A.D., De Carvalho, A.M., Marchão, R.L., Luiz, A.J.B., Ribeiro, F.P.,

Müller, A.G., 2024. Effects of agricultural management and of climate change on N2O emissions in an area of the Brazilian Cerrado: Measurements and simulations using the STICS soil-crop model. Agriculture, Ecosystems & Environment 363, 108842. https://doi.org/10.1016/j.agee.2023.108842

Davin, E.L., de Noblet-Ducoudré, N., 2010. Climatic Impact of Global-Scale Deforestation: Radiative versus Nonradiative Processes. Journal of Climate 23, 97–112. https://doi.org/10.1175/2009JCLI3102.1

Davin, E.L., de Noblet-Ducoudré, N., Friedlingstein, P., 2007. Impact of land cover change on surface climate: Relevance of the radiative forcing concept. Geophysical Research Letters 34. https://doi.org/10.1029/2007GL029678

Davin, E.L., Rechid, D., Breil, M., Cardoso, R.M., Coppola, E., Hoffmann, P., Jach, L.L., Katragkou, E., de Noblet-Ducoudré, N., Radtke, K., Raffa, M., Soares, P.M.M., Sofiadis, G., Strada, S., Strandberg, G., Tölle, M.H., Warrach-Sagi, K., Wulfmeyer, V., 2020. Biogeophysical impacts of forestation in Europe: first results from the LUCAS (Land Use and Climate Across Scales) regional climate model intercomparison. Earth Syst. Dynam. 11, 183–200. https://doi.org/10.5194/esd-11-183-2020

Davin, E.L., Seneviratne, S.I., Ciais, P., Olioso, A., Wang, T., 2014. Preferential cooling of hot extremes from cropland albedo management. Proceedings of the National Academy of Sciences 111, 9757–9761. https://doi.org/10.1073/pnas.1317323111

De Noblet-Ducoudré, N., Gervois, S., Ciais, P., Viovy, N., Brisson, N., Seguin, B., Perrier, A., 2004. Coupling the Soil-Vegetation-Atmosphere-Transfer Scheme ORCHIDEE to the agronomy model STICS to study the influence of croplands on the European carbon and water budgets. Agronomie 24, 397–407. https://doi.org/10.1051/agro:2004038

Debaeke, P., 2004. Scenario analysis for cereal management in water-limited conditions by the means of a crop simulation model (STICS). Agronomie 24, 315–326. https://doi.org/10.1051/agro:2004035

Dellink, R., Lanzi, E., Chateau, J., 2019. The Sectoral and Regional Economic Consequences of Climate Change to 2060. Environmental and Resource Economics 72. https://doi.org/10.1007/s10640-017-0197-5

Derpsch, R., Benites, J.R., 2003. SITUATION OF CONSERVATION AGRICULTURE IN THE

WORLD.

Derpsch, R., Friedrich, T., Kassam, A., Li, H., 2010. Current Status of Adoption of No-till Farming in the World and Some of its Main Benefits. International Journal of Agricultural and Biological Engineering 3, 1–25. https://doi.org/10.25165/ijabe.v3i1.223

Dimkpa, C., Adzawla, W., Pandey, R., Atakora, W.K., Kouame, A.K., Jemo, M., Bindraban, P.S., 2023. Fertilizers for food and nutrition security in sub-Saharan Africa: An overview of soil health implications. Front. Soil Sci. 3. https://doi.org/10.3389/fsoil.2023.1123931

Diop, S., 2023. Four-component net radiometers to quantify albedo and heat fluxes in conservation agriculture. Nat Rev Earth Environ. https://doi.org/10.1038/s43017-023-00432-x

Donohoe, A., Armour, K.C., Pendergrass, A.G., Battisti, D.S., 2014. Shortwave and longwave radiative contributions to global warming under increasing CO2. Proceedings of the National Academy of Sciences 111, 16700–16705. https://doi.org/10.1073/pnas.1412190111

Ellert, B.H., Bettany, J.R., 1995. Calculation of organic matter and nutrients stored in soils under contrasting management regimes. Can. J. Soil. Sci. 75, 529–538. https://doi.org/10.4141/cjss95-075

Ericsson, N., Porsö, C., Ahlgren, S., Nordberg, Å., Sundberg, C., Hansson, P.-A., 2013. Time-dependent climate impact of a bioenergy system – methodology development and application to Swedish conditions. GCB Bioenergy 5, 580–590. https://doi.org/10.1111/gcbb.12031

Falconnier, G.N., Cardinael, R., Corbeels, M., Baudron, F., Chivenge, P., Couëdel, A., Ripoche, A., Affholder, F., Naudin, K., Benaillon, E., Rusinamhodzi, L., Leroux, L., Vanlauwe, B., Giller, K.E., 2023. The input reduction principle of agroecology is wrong when it comes to mineral fertilizer use in sub-Saharan Africa. Outlook Agric 52, 311–326. https://doi.org/10.1177/00307270231199795

Falconnier, G.N., Journet, E.-P., Bedoussac, L., Vermue, A., Chlébowski, F., Beaudoin, N., Justes, E., 2019. Calibration and evaluation of the STICS soil-crop model for faba bean to explain variability in yield and N2 fixation. European Journal of Agronomy 104, 63–77.

https://doi.org/10.1016/j.eja.2019.01.001

Forster, P., Ramaswamy, Venkatachalam, Artaxo, Paulo, Berntsen, Terje, Betts, Richard, Fahey, David W, Haywood, James, Lean, Judith, Lowe, David C, Raga, Graciela, Schulz, Michael, Dorland, Robert Van, Bodeker, G., Etheridge, D., Foukal, P., Fraser, P., Geller, M., Joos, F., Keeling, C.D., Keeling, R., Kinne, S., Lassey, K., Oram, D., O'Shaughnessy, K., Ramankutty, N., Reid, G., Rind, D., Rosenlof, K., Sausen, R., Schwarzkopf, D., Solanki, S.K., Stenchikov, G., Stuber, N., Takemura, T., Textor, C., Wang, R., Weiss, R., Whorf, T., Nakajima, T., Ramanathan, V., Ramaswamy, V, Artaxo, P, Berntsen, T, Betts, R, Fahey, D W, Haywood, J, Lean, J, Lowe, D C, Myhre, G., Nganga, J., Prinn, R., Raga, G, Schulz, M, Dorland, R Van, 2007. Changes in Atmospheric Constituents and in Radiative Forcing 106.

Forster, P.M., Richardson, T., Maycock, A.C., Smith, C.J., Samset, B.H., Myhre, G., Andrews, T., Pincus, R., Schulz, M., 2016. Recommendations for diagnosing effective radiative forcing from climate models for CMIP6. Journal of Geophysical Research: Atmospheres 121, 12,460-12,475. https://doi.org/10.1002/2016JD025320

Forster, P.M., Smith, C., Walsh, T., Lamb, W.F., Lamboll, R., Hall, B., Hauser, M., Ribes, A., Rosen, D., Gillett, N.P., Palmer, M.D., Rogelj, J., von Schuckmann, K., Trewin, B., Allen, M., Andrew, R., Betts, R.A., Borger, A., Boyer, T., Broersma, J.A., Buontempo, C., Burgess, S., Cagnazzo, C., Cheng, L., Friedlingstein, P., Gettelman, A., Gütschow, J., Ishii, M., Jenkins, S., Lan, X., Morice, C., Mühle, J., Kadow, C., Kennedy, J., Killick, R.E., Krummel, P.B., Minx, J.C., Myhre, G., Naik, V., Peters, G.P., Pirani, A., Pongratz, J., Schleussner, C.-F., Seneviratne, S.I., Szopa, S., Thorne, P., Kovilakam, M.V.M., Majamäki, E., Jalkanen, J.-P., van Marle, M., Hoesly, R.M., Rohde, R., Schumacher, D., van der Werf, G., Vose, R., Zickfeld, K., Zhang, X., Masson-Delmotte, V., Zhai, P., 2024. Indicators of Global Climate Change 2023: annual update of key indicators of the state of the climate system and human influence. Earth System Science Data 16, 2625–2658. https://doi.org/10.5194/essd-16-2625-2024

Franzluebbers, A.J., 2010. Achieving Soil Organic Carbon Sequestration with Conservation Agricultural Systems in the Southeastern United States. Soil Science Society of America Journal 74, 347–357. https://doi.org/10.2136/sssaj2009.0079

Fu, Q., Liou, K.N., 1993. Parameterization of the Radiative Properties of Cirrus Clouds.

Fuentes-Ponce, M.H., Gutiérrez-Díaz, J., Flores-Macías, A., González-Ortega, E., Mendoza, A.P., Sánchez, L.M.R., Novotny, I., Espíndola, I.P.M., 2022. Direct and indirect greenhouse gas emissions under conventional, organic, and conservation agriculture. Agriculture, Ecosystems & Environment 340, 108148. https://doi.org/10.1016/j.agee.2022.108148

Gál, A., Vyn, T.J., Michéli, E., Kladivko, E.J., McFee, W.W., 2007. Soil carbon and nitrogen accumulation with long-term no-till versus moldboard plowing overestimated with tilled-zone sampling depths. Soil and Tillage Research 96, 42–51. https://doi.org/10.1016/j.still.2007.02.007

Gao, F., He, T., Wang, Z., Ghimire, B., Shuai, Y., Masek, J., Schaaf, C., Williams, C., 2014. Multiscale climatological albedo look-up maps derived from moderate resolution imaging spectroradiometer BRDF/albedo products. J. Appl. Remote Sens 8, 083532. https://doi.org/10.1117/1.JRS.8.083532

Gaur, A.C., Mukherjee, D., 1980. Recycling of organic matter through mulch in relation to chemical and microbiological properties of soil and crop yields. Plant Soil 56, 273–281. https://doi.org/10.1007/BF02205856

Genesio, L., Miglietta, F., Lugato, E., Baronti, S., Pieri, M., Vaccari, F.P., 2012. Surface albedo following biochar application in durum wheat. Environ. Res. Lett. 7, 014025. https://doi.org/10.1088/1748-9326/7/1/014025

Genesio, L., Vaccari, F.P., Miglietta, F., 2016. Black carbon aerosol from biochar threats its negative emission potential. Glob Change Biol 22, 2313–2314. https://doi.org/10.1111/gcb.13254

Gervois, S., Noblet-Ducoudré, N. de, Viovy, N., Ciais, P., Brisson, N., Seguin, B., Perrier, A., 2004. Including Croplands in a Global Biosphere Model: Methodology and Evaluation at Specific Sites.

Gonzalez-Sanchez, E.J., Veroz-Gonzalez, O., Conway, G., Moreno-Garcia, M., Kassam, A., Mkomwa, S., Ordoñez-Fernandez, R., Triviño-Tarradas, P., Carbonell-Bojollo, R., 2019. Meta-analysis on carbon sequestration through Conservation Agriculture in Africa. Soil and Tillage Research 190, 22–30. https://doi.org/10.1016/j.still.2019.02.020

Guenet, B., Gabrielle, B., Chenu, C., Arrouays, D., Balesdent, J., Bernoux, M., Bruni, E., Caliman, J.-P., Cardinael, R., Chen, S., Ciais, P., Desbois, D., Fouche, J., Frank, S., Henault, C., Lugato, E., Naipal, V., Nesme, T., Obersteiner, M., Pellerin, S., Powlson, D.S., Rasse, D.P., Rees, F., Soussana, J.-F., Su, Y., Tian, H., Valin, H., Zhou, F., 2021. Can N2O emissions offset the benefits from soil organic carbon storage? Global Change Biology 27, 237–256. https://doi.org/10.1111/gcb.15342

Hasler, N., Williams, C.A., Denney, V.C., Ellis, P.W., Shrestha, S., Terasaki Hart, D.E., Wolff, N.H., Yeo, S., Crowther, T.W., Werden, L.K., Cook-Patton, S.C., 2024. Accounting for albedo change to identify climate-positive tree cover restoration. Nat Commun 15, 2275. https://doi.org/10.1038/s41467-024-46577-1

Hatfield, J.L., Carlson, R.E., 1979. Light quality distributions and spectral albedo of three maize canopies. Agricultural Meteorology 20, 215–226. https://doi.org/10.1016/0002-1571(79)90022-0

He, Y., Lin, E.S., Yu, Z., Tan, C.L., Tan, P.Y., Wong, N.H., 2021. The effect of dynamic albedos of plant canopy on thermal performance of rooftop greenery: A case study in Singapore. Building and Environment 205, 108247. https://doi.org/10.1016/j.buildenv.2021.108247

Hirsch, A.L., Guillod, B.P., Seneviratne, S.I., Beyerle, U., Boysen, L.R., Brovkin, V., Davin, E.L., Doelman, J.C., Kim, H., Mitchell, D.M., Nitta, T., Shiogama, H., Sparrow, S., Stehfest, E., van Vuuren, D.P., Wilson, S., 2018a. Biogeophysical Impacts of Land-Use Change on Climate Extremes in Low-Emission Scenarios: Results From HAPPI-Land. Earth's Future 6, 396–409. https://doi.org/10.1002/2017EF000744

Hirsch, A.L., Prestele, R., Davin, E.L., Seneviratne, S.I., Thiery, W., Verburg, P.H., 2018b. Modelled biophysical impacts of conservation agriculture on local climates. Glob Change Biol 24, 4758–4774. https://doi.org/10.1111/gcb.14362

Hirsch, A.L., Wilhelm, M., Davin, E.L., Thiery, W., Seneviratne, S.I., 2017. Can climate-effective land management reduce regional warming? J. Geophys. Res. Atmos. 122, 2269–2288. https://doi.org/10.1002/2016JD026125

Hlatywayo, R., Mhlanga, B., Mazarura, U., Mupangwa, W., Thierfelder, C., 2016. Response of Maize (Zea mays L.) Secondary Growth Parameters to Conservation Agriculture and

Conventional Tillage Systems in Zimbabwe. Journal of Agricultural Science 8. https://doi.org/10.5539/jas.v8n11p112

Hobbs, P.R., Sayre, K., Gupta, R., 2008. The role of conservation agriculture in sustainable agriculture. Phil. Trans. R. Soc. B 363, 543–555. https://doi.org/10.1098/rstb.2007.2169

Horton, R., Bristow, K.L., Kluitenberg, G.J., Sauer, T.J., 1996. Crop residue effects on surface radiation and energy balance? review. Theor Appl Climatol 54, 27–37. https://doi.org/10.1007/BF00863556

Idso, S.B., Jackson, R.D., Reginato, R.J., Kimball, B.A., Nakayama, F.S., 1975. The Dependence of Bare Soil Albedo on Soil Water Content. Journal of Applied Meteorology and Climatology 14, 109–113. https://doi.org/10.1175/1520-0450(1975)014<0109:TDOBSA>2.0.CO;2

IPCC, 2023. Climate Change 2021 – The Physical Science Basis: Working Group I Contribution to the Sixth Assessment Report of the Intergovernmental Panel on Climate Change, 1st ed. Cambridge University Press. https://doi.org/10.1017/9781009157896

Irmak, S., Kukal, M.S., 2022. Alteration in surface energy balance fluxes induced from long-term disk-tilled versus no-till management in maize production. Soil and Tillage Research 221, 105383. https://doi.org/10.1016/j.still.2022.105383

Jacobs, A.F.G., van Pul, W.A.J., 1990. Seasonal changes in the albedo of a maize crop during two seasons. Agricultural and Forest Meteorology 49, 351–360. https://doi.org/10.1016/0168-1923(90)90006-R

Jàuregui, J.M., Delbino, F.G., Brance Bonvini, M.I., Berhongaray, G., 2019. Determining yield of forage crops using the Canopeo mobile phone app. Journal of NZ Grasslands 41–46. https://doi.org/10.33584/jnzg.2019.81.385

Jégo, G., Pattey, E., Bourgeois, G., Drury, C.F., Tremblay, N., 2011. Evaluation of the STICS crop growth model with maize cultivar parameters calibrated for Eastern Canada. Agronomy Sust. Developm. 31, 557–570. https://doi.org/10.1007/s13593-011-0014-4

Joos, F., Roth, R., Fuglestvedt, J.S., Peters, G.P., Enting, I.G., von Bloh, W., Brovkin, V., Burke, E.J., Eby, M., Edwards, N.R., Friedrich, T., Frölicher, T.L., Halloran, P.R., Holden, P.B., Jones, C., Kleinen, T., Mackenzie, F.T., Matsumoto, K., Meinshausen, M., Plattner, G.-K.,

Reisinger, A., Segschneider, J., Shaffer, G., Steinacher, M., Strassmann, K., Tanaka, K., Timmermann, A., Weaver, A.J., 2013. Carbon dioxide and climate impulse response functions for the computation of greenhouse gas metrics: a multi-model analysis. Atmospheric Chemistry and Physics 13, 2793–2825. https://doi.org/10.5194/acp-13-2793-2013

Kätterer, T., Andrén, O., 1999. Long-term agricultural field experiments in Northern Europe: analysis of the influence of management on soil carbon stocks using the ICBM model. Agriculture, Ecosystems & Environment 72, 165–179. https://doi.org/10.1016/S0167-8809(98)00177-7

Kaye, J.P., Quemada, M., 2017. Using cover crops to mitigate and adapt to climate change. A review. Agron. Sustain. Dev. 37, 4. https://doi.org/10.1007/s13593-016-0410-x

Kim, D.-G., Grieco, E., Bombelli, A., Hickman, J.E., Sanz-Cobena, A., 2021. Challenges and opportunities for enhancing food security and greenhouse gas mitigation in smallholder farming in sub-Saharan Africa. A review. Food Sec. 13, 457–476. https://doi.org/10.1007/s12571-021-01149-9

Krinner, G., Viovy, N., de Noblet-Ducoudré, N., Ogée, J., Polcher, J., Friedlingstein, P., Ciais, P., Sitch, S., Prentice, I.C., 2005. A dynamic global vegetation model for studies of the coupled atmosphere-biosphere system. Global Biogeochemical Cycles 19. https://doi.org/10.1029/2003GB002199

Lal, R., 1997. Mulching Effects on Runoff, Soil Erosion, and Crop Response on Alfisols in Western Nigeria. Journal of Sustainable Agriculture 11, 135–154. https://doi.org/10.1300/J064v11n02_10

Laurent, F., 2015. L'Agriculture de Conservation et sa diffusion en France et dans le monde. Cybergeo: European Journal of Geography. https://doi.org/10.4000/cybergeo.27284

Le Noë, J., Manzoni, S., Abramoff, R., Bölscher, T., Bruni, E., Cardinael, R., Ciais, P., Chenu, C., Clivot, H., Derrien, D., Ferchaud, F., Garnier, P., Goll, D., Lashermes, G., Martin, M., Rasse, D., Rees, F., Sainte-Marie, J., Salmon, E., Schiedung, M., Schimel, J., Wieder, W., Abiven, S., Barré, P., Cécillon, L., Guenet, B., 2023. Soil organic carbon models need independent time-series validation for reliable prediction. Commun Earth Environ 4, 1–8. https://doi.org/10.1038/s43247-023-00830-5

Lee, X., Goulden, M.L., Hollinger, D.Y., Barr, A., Black, T.A., Bohrer, G., Bracho, R., Drake, B., Goldstein, A., Gu, L., Katul, G., Kolb, T., Law, B.E., Margolis, H., Meyers, T., Monson, R., Munger, W., Oren, R., Paw U, K.T., Richardson, A.D., Schmid, H.P., Staebler, R., Wofsy, S., Zhao, L., 2011. Observed increase in local cooling effect of deforestation at higher latitudes. Nature 479, 384–387. https://doi.org/10.1038/nature10588

Lenton, T.M., Vaughan, N.E., 2009. The radiative forcing potential of different climate geoengineering options. Atmos. Chem. Phys. 23.

Li, F., Zhang, G., Chen, J., Song, Y., Geng, Z., Li, K., Siddique, K.H.M., 2022. Straw mulching for enhanced water use efficiency and economic returns from soybean fields in the Loess Plateau China. Sci Rep 12, 17111. https://doi.org/10.1038/s41598-022-21141-3

Li, Y., Hu, Z., 2009. A study on parameterization of surface albedo over grassland surface in the northern Tibetan Plateau. Adv. Atmos. Sci. 26, 161–168. https://doi.org/10.1007/s00376-009-0161-6

Liang, L., Schwartz, M.D., Fei, S., 2012. Photographic assessment of temperate forest understory phenology in relation to springtime meteorological drivers. Int J Biometeorol 13.

Liang, S., Shuey, C.J., Russ, A.L., Fang, H., Chen, M., Walthall, C.L., Daughtry, C.S.T., Jr, R.H., 2002. Narrowband to broadband conversions of land surface albedo: II. Validation. Remote Sensing of Environment 17.

Liao, W., Liu, X., Burakowski, E., Wang, D., Wang, L., Li, D., 2020. Sensitivities and Responses of Land Surface Temperature to Deforestation-Induced Biophysical Changes in Two Global Earth System Models. Journal of Climate 33, 8381–8399. https://doi.org/10.1175/JCLI-D-19-0725.1

Lin, X., Wu, S., Chen, B., Lin, Z., Yan, Z., Chen, X., Yin, G., You, D., Wen, J., Liu, Qiang, Xiao, Q., Liu, Qinhuo, Lafortezza, R., 2022. Estimating 10-m land surface albedo from Sentinel-2 satellite observations using a direct estimation approach with Google Earth Engine. ISPRS Journal of Photogrammetry and Remote Sensing 194, 1–20. https://doi.org/10.1016/j.isprsjprs.2022.09.016

Liu, J., Desjardins, R.L., Wang, S., Worth, D.E., Qian, B., Shang, J., 2022a. Climate impact from agricultural management practices in the Canadian Prairies: Carbon equivalence due

to albedo change. Journal of Environmental Management 302, 113938. https://doi.org/10.1016/j.jenvman.2021.113938

Liu, J., Desjardins, R.L., Wang, S., Worth, D.E., Qian, B., Shang, J., 2022b. Climate impact from agricultural management practices in the Canadian Prairies: Carbon equivalence due to albedo change. Journal of Environmental Management 302, 113938. https://doi.org/10.1016/j.jenvman.2021.113938

Lobell, D.B., Bala, G., Duffy, P.B., 2006. Biogeophysical impacts of cropland management changes on climate. Geophys. Res. Lett. 33, L06708. https://doi.org/10.1029/2005GL025492

Lugato, E., Cescatti, A., Jones, A., Ceccherini, G., Duveiller, G., 2020. Maximising climate mitigation potential by carbon and radiative agricultural land management with cover crops. Environ. Res. Lett. 15, 094075. https://doi.org/10.1088/1748-9326/aba137

Luyssaert, S., Jammet, M., Stoy, P.C., Estel, S., Pongratz, J., Ceschia, E., Churkina, G., Don, A., Erb, K., Ferlicoq, M., Gielen, B., Grünwald, T., Houghton, R.A., Klumpp, K., Knohl, A., Kolb, T., Kuemmerle, T., Laurila, T., Lohila, A., Loustau, D., McGrath, M.J., Meyfroidt, P., Moors, E.J., Naudts, K., Novick, K., Otto, J., Pilegaard, K., Pio, C.A., Rambal, S., Rebmann, C., Ryder, J., Suyker, A.E., Varlagin, A., Wattenbach, M., Dolman, A.J., 2014. Land management and land-cover change have impacts of similar magnitude on surface temperature. Nature Clim Change 4, 389–393. https://doi.org/10.1038/nclimate2196

Maia, S.M.F., De Souza Medeiros, A., Dos Santos, T.C., Lyra, G.B., Lal, R., Assad, E.D., Cerri, C.E.P., 2022. Potential of no-till agriculture as a nature-based solution for climate-change mitigation in Brazil. Soil and Tillage Research 220, 105368. https://doi.org/10.1016/j.still.2022.105368

Manne, A.S., Richels, R.G., 2001. An alternative approach to establishing trade-offs among greenhouse gases. Nature 410, 675–677. https://doi.org/10.1038/35070541

Mapanda, F., Mupini, J., Wuta, M., Nyamangara, J., Rees, R.M., 2010. A cross-ecosystem assessment of the effects of land cover and land use on soil emission of selected greenhouse gases and related soil properties in Zimbabwe. European Journal of Soil Science 61, 721–733. https://doi.org/10.1111/j.1365-2389.2010.01266.x

Matthias, A.D., Fimbres, A., Sano, E.E., Post, D.F., Accioly, L., Batchily, A.K., Ferreira, L.G., 2000.

Surface Roughness Effects on Soil Albedo. Soil Sci. Soc. Am. J. 64, 1035–1041. https://doi.org/10.2136/sssaj2000.6431035x

Menichetti, L., Kätterer, T., Bolinder, M.A., 2024. Bayesian calibration of the ICBM/3 soil organic carbon model constrained by data from long-term experiments and uncertainties of C inputs. Carbon Management 15, 2304749. https://doi.org/10.1080/17583004.2024.2304749

Mhlanga, B., Pellegrino, E., Thierfelder, C., Ercoli, L., 2022. Conservation agriculture practices drive maize yield by regulating soil nutrient availability, arbuscular mycorrhizas, and plant nutrient uptake. Field Crops Research 277, 108403. https://doi.org/10.1016/j.fcr.2021.108403

Miralles-Wilhelm, F., 2023. Nature-based solutions in agricultural landscapes for reducing tradeoffs between food production, climate change, and conservation objectives. Front. Water 5. https://doi.org/10.3389/frwa.2023.1247322

Moore, C.J., Fisch, G., 1986. Estimating heat storage in Amazonian tropical forest. Agricultural and Forest Meteorology 38, 147–168. https://doi.org/10.1016/0168-1923(86)90055-9

Muñoz, I., Campra, P., Fernández-Alba, A.R., 2010. Including CO2-emission equivalence of changes in land surface albedo in life cycle assessment. Methodology and case study on greenhouse agriculture. Int J Life Cycle Assess 15, 672–681. https://doi.org/10.1007/s11367-010-0202-5

Myhre, G., Shindell, D., Bréon, F.-M., Collins, W., Fuglestvedt, J., Huang, J., Koch, D., Lamarque, J.-F., Lee, D., Mendoza, B., Nakajima, T., Robock, A., Stephens, G., Zhang, H., Aamaas, B., Boucher, O., Dalsøren, S.B., Daniel, J.S., Forster, P., Granier, C., Haigh, J., Hodnebrog, Ø., Kaplan, J.O., Marston, G., Nielsen, C.J., O'Neill, B.C., Peters, G.P., Pongratz, J., Ramaswamy, V., Roth, R., Rotstayn, L., Smith, S.J., Stevenson, D., Vernier, J.-P., Wild, O., Young, P., Jacob, D., Ravishankara, A.R., Shine, K., 2013. The Physical Science Basis. Contribution of Working Group I to the Fifth Assessment Report of the Intergovernmental Panel on Climate Change.

Namatsheve, T., Cardinael, R., Chikowo, R., Corbeels, M., Rugare, J.T., Mabasa, S., Ripoche, A., 2024. Do intercropping and mineral nitrogen fertilizer affect weed community

structures in low-input maize-based cropping systems? Crop Protection 176, 106486. https://doi.org/10.1016/j.cropro.2023.106486

Nyamadzawo, G., Chikowo, R., Nyamugafata, P., Nyamangara, J., Giller, K.E., 2008. Soil organic carbon dynamics of improved fallow-maize rotation systems under conventional and no-tillage in Central Zimbabwe. Nutr Cycl Agroecosyst 81, 85–93. https://doi.org/10.1007/s10705-007-9154-y

O'Brien, P.L., Daigh, A.L.M., 2019. Tillage practices alter the surface energy balance – A review. Soil and Tillage Research 195, 104354. https://doi.org/10.1016/j.still.2019.104354

Oguntunde, P., van de Giesen, N., 2004. Crop growth and development effects on surface albedo for maize and cowpea fields in Ghana, West Africa. International journal of biometeorology 49, 106–12. https://doi.org/10.1007/s00484-004-0216-4

Oguntunde, P.G., Ajayi, A.E., Giesen, N. van de, 2006. Tillage and surface moisture effects on bare-soil albedo of a tropical loamy sand. Soil and Tillage Research 85, 107–114. https://doi.org/10.1016/j.still.2004.12.009

Oleson, K., Dai, Y., Bonan, B., Bosilovichm, M., Dickinson, R., Dirmeyer, P., Hoffman, F., Houser, P., Levis, S., Niu, G.-Y., Thornton, P., Vertenstein, M., Yang, Z.-L., Zeng, X., 2004. Technical Description of the Community Land Model (CLM). https://doi.org/10.5065/D6N877R0

Patrignani, A., Ochsner, T.E., 2015. Canopeo: A Powerful New Tool for Measuring Fractional Green Canopy Cover. Agronomy Journal 107, 2312–2320. https://doi.org/10.2134/agronj15.0150

Peters, G.P., Aamaas, B., Berntsen, T., Fuglestvedt, J.S., 2011. The integrated global temperature change potential (iGTP) and relationships between emission metrics. Environ. Res. Lett. 6, 044021. https://doi.org/10.1088/1748-9326/6/4/044021

Pielke, R.A., Marland, G., Betts, R.A., Chase, T.N., Eastman, J.L., Niles, J.O., Niyogi, D. dutta S., Running, S.W., 2002. The influence of land-use change and landscape dynamics on the climate system: relevance to climate-change policy beyond the radiative effect of greenhouse gases. Philosophical Transactions of the Royal Society of London. Series A: Mathematical, Physical and Engineering Sciences 360, 1705–1719. https://doi.org/10.1098/rsta.2002.1027

Pique, G., 2021. Apport de la télédétection pour la simulation spatialisée des composantes du bilan carbone des cultures et des effets d'atténuation biogéochimiques et biogéophysiques des cultures intermédiaires (phd). Université de Toulouse, Université Toulouse III - Paul Sabatier.

Pique, G., Carrer, D., Lugato, E., Fieuzal, R., Garisoain, R., Ceschia, E., 2023. About the Assessment of Cover Crop Albedo Potential Cooling Effect: Risk of the Darkening Feedback Loop Effects. Remote Sensing 15, 3231. https://doi.org/10.3390/rs15133231

Pique, G., Fieuzal, R., Al Bitar, A., Veloso, A., Tallec, T., Brut, A., Ferlicoq, M., Zawilski, B., Dejoux, J.-F., Gibrin, H., Ceschia, E., 2020. Estimation of daily CO2 fluxes and of the components of the carbon budget for winter wheat by the assimilation of Sentinel 2-like remote sensing data into a crop model. Geoderma 376, 114428. https://doi.org/10.1016/j.geoderma.2020.114428

Pittelkow, C., Liang, X., Linquist, B., van Groenigen, K.J., Lee, J., Lundy, M., Van Gestel, N., Six, J., Venterea, R., Kessel, C., 2014. Productivity limits and potentials of the principles of conservation agriculture. Nature 517. https://doi.org/10.1038/nature13809

Post, D.F., Fimbres, A., Matthias, A.D., Sano, E.E., Accioly, L., Batchily, A.K., Ferreira, L.G., 2000. Predicting Soil Albedo from Soil Color and Spectral Reflectance Data. Soil Sci. Soc. Am. J. 64, 1027–1034. https://doi.org/10.2136/sssaj2000.6431027x

Powlson, D.S., Stirling, C.M., Thierfelder, C., White, R.P., Jat, M.L., 2016. Does conservation agriculture deliver climate change mitigation through soil carbon sequestration in tropical agro-ecosystems? Agriculture, Ecosystems & Environment 220, 164–174. https://doi.org/10.1016/j.agee.2016.01.005

Ridgwell, A., Singarayer, J.S., Hetherington, A.M., Valdes, P.J., 2009. Tackling Regional Climate Change By Leaf Albedo Bio-geoengineering. Current Biology 19, 146–150. https://doi.org/10.1016/j.cub.2008.12.025

Rohatyn, S., Yakir, D., Rotenberg, E., Carmel, Y., 2022. Limited climate change mitigation potential through forestation of the vast dryland regions. Science 377, 1436–1439. https://doi.org/10.1126/science.abm9684

Rosenberg, N.J., Blad, B.L., Verma, S.B., 1983. Microclimate: The Biological Environment. John

Wiley & Sons.

Rost, J., Mayer, H., 2006. Comparative analysis of albedo and surface energy balance of a grassland site and an adjacent Scots pine forest. Clim Res 12.

Rotenberg, E., Yakir, D., 2010. Contribution of Semi-Arid Forests to the Climate System. Science 327, 451–454. https://doi.org/10.1126/science.1179998

Rusinamhodzi, L., Corbeels, M., van Wijk, M.T., Rufino, M.C., Nyamangara, J., Giller, K.E., 2011. A meta-analysis of long-term effects of conservation agriculture on maize grain yield under rain-fed conditions. Agron. Sustain. Dev. 31, 657–673. https://doi.org/10.1007/s13593-011-0040-2

Saadi, S., Pattey, E., Jégo, G., Champagne, C., 2022. Prediction of rainfed corn evapotranspiration and soil moisture using the STICS crop model in eastern Canada. Field Crops Research 287, 108664. https://doi.org/10.1016/j.fcr.2022.108664

Sarofim, M.C., Giordano, M.R., 2018. A quantitative approach to evaluating the GWP timescale through implicit discount rates. Earth Syst Dyn 9, 1013–1024. https://doi.org/10.5194/esd-2018-6

Schimel, D.S., 1995. Terrestrial ecosystems and the carbon cycle. Global Change Biology 1, 77–91. https://doi.org/10.1111/j.1365-2486.1995.tb00008.x

Schnebelen, N., Nicoullaud, B., Bourennane, H., Couturier, A., Verbeque, B., Revalier, C., Bruand, A., Ledoux, E., 2004. The STICS model to predict nitrate leaching following agricultural practices. Agronomie 24, 423–435. https://doi.org/10.1051/agro:2004039

Schwaiger, H.P., Bird, D.N., 2010. Integration of albedo effects caused by land use change into the climate balance: Should we still account in greenhouse gas units? Forest Ecology and Management 260, 278–286. https://doi.org/10.1016/j.foreco.2009.12.002

Scopel, E., Fernando A.M. da Silva, Corbeels, M., Affholder, F., Maraux, F., 2004. Modelling crop residue mulching effects on water use and production of maize under semi-arid and humid tropical conditions. Agronomie 24, 383–395. https://doi.org/10.1051/agro:2004029

Séguy, L., Bouzinac, S., 1999. Cultiver durablement et proprement les 65.

Seneviratne, S.I., Phipps, S.J., Pitman, A.J., Hirsch, A.L., Davin, E.L., Donat, M.G., Hirschi, M.,

Lenton, A., Wilhelm, M., Kravitz, B., 2018a. Land radiative management as contributor to regional-scale climate adaptation and mitigation. Nature Geosci 11, 88–96. https://doi.org/10.1038/s41561-017-0057-5

Seneviratne, S.I., Wartenburger, R., Guillod, B.P., Hirsch, A.L., Vogel, M.M., Brovkin, V., van Vuuren, D.P., Schaller, N., Boysen, L., Calvin, K.V., Doelman, J., Greve, P., Havlik, P., Humpenöder, F., Krisztin, T., Mitchell, D., Popp, A., Riahi, K., Rogelj, J., Schleussner, C.-F., Sillmann, J., Stehfest, E., 2018b. Climate extremes, land–climate feedbacks and land-use forcing at 1.5°C. Phil. Trans. R. Soc. A. 376, 20160450. https://doi.org/10.1098/rsta.2016.0450

Shumba, A., Chikowo, R., Corbeels, M., Six, J., Thierfelder, C., Cardinael, R., 2023. Long-term tillage, residue management and crop rotation impacts on N2O and CH4 emissions from two contrasting soils in sub-humid Zimbabwe. Agriculture, Ecosystems & Environment 341, 108207. https://doi.org/10.1016/j.agee.2022.108207

Shumba, A., Chikowo, R., Thierfelder, C., Corbeels, M., Six, J., Cardinael, R., 2024. Mulch application as the overarching factor explaining increase in soil organic carbon stocks under conservation agriculture in two 8-year-old experiments in Zimbabwe. SOIL 10, 151–165. https://doi.org/10.5194/soil-10-151-2024

Sieber, P., Böhme, S., Ericsson, N., Hansson, P.-A., 2022. Albedo on cropland: Field-scale effects of current agricultural practices in Northern Europe. Agricultural and Forest Meteorology 321, 108978. https://doi.org/10.1016/j.agrformet.2022.108978

Sieber, P., Ericsson, N., Hammar, T., Hansson, P., 2020. Including albedo in time-dependent LCA of bioenergy. GCB Bioenergy 12, 410–425. https://doi.org/10.1111/gcbb.12682

Sieber, P., Ericsson, N., Hansson, P.-A., 2019. Climate impact of surface albedo change in Life Cycle Assessment: Implications of site and time dependence. Environmental Impact Assessment Review 77, 191–200. https://doi.org/10.1016/j.eiar.2019.04.003

Singarayer, J.S., Davies-Barnard, T., 2012. Regional climate change mitigation with crops: context and assessment. Phil. Trans. R. Soc. A. 370, 4301–4316. https://doi.org/10.1098/rsta.2012.0010

Smith, C.J., Kramer, R.J., Myhre, G., Alterskjær, K., Collins, W., Sima, A., Boucher, O., Dufresne, J.-L., Nabat, P., Michou, M., Yukimoto, S., Cole, J., Paynter, D., Shiogama, H., O'Connor,

F.M., Robertson, E., Wiltshire, A., Andrews, T., Hannay, C., Miller, R., Nazarenko, L., Kirkevåg, A., Olivié, D., Fiedler, S., Lewinschal, A., Mackallah, C., Dix, M., Pincus, R., Forster, P.M., 2020. Effective radiative forcing and adjustments in CMIP6 models. Atmos. Chem. Phys. 20, 9591–9618. https://doi.org/10.5194/acp-20-9591-2020

Smith, P., Olesen, J.E., 2010. Synergies between the mitigation of, and adaptation to, climate change in agriculture. The Journal of Agricultural Science 148, 543–552. https://doi.org/10.1017/S0021859610000341

Song, J., 1999. Phenological influences on the albedo of prairie grassland and crop fields. International Journal of Biometeorology 42, 153–157. https://doi.org/10.1007/s004840050099

Sow, S., Senghor, Y., Sadio, K., Vezy, R., Roupsard, O., Affholder, F., N'dienor, M., Clermont-Dauphin, C., Gaglo, E.K., Ba, S., Tounkara, A., Balde, A.B., Agbohessou, Y., Seghieri, J., Sall, S.N., Couedel, A., Leroux, L., Jourdan, C., Diaite, D.S., Falconnier, G.N., 2024. Calibrating the STICS soil-crop model to explore the impact of agroforestry parklands on millet growth. Field Crops Research 306, 109206. https://doi.org/10.1016/j.fcr.2023.109206

Stephens, G.L., O'Brien, D., Webster, P.J., Pilewski, P., Kato, S., Li, J., 2015. The albedo of Earth. Reviews of Geophysics 53, 141–163. https://doi.org/10.1002/2014RG000449

Suleiman, A.K.A., Lourenço, K.S., Pitombo, L.M., Mendes, L.W., Roesch, L.F.W., Pijl, A., Carmo, J.B., Cantarella, H., Kuramae, E.E., 2018. Recycling organic residues in agriculture impacts soil-borne microbial community structure, function and N2O emissions. Science of The Total Environment 631–632, 1089–1099. https://doi.org/10.1016/j.scitotenv.2018.03.116

Tanaka, K., Peters, G.P., Fuglestvedt, J.S., 2010. Policy Update: Multicomponent climate policy: why do emission metrics matter? Carbon Management 1, 191–197. https://doi.org/10.4155/cmt.10.28

Tasumi, M., Allen, R.G., Trezza, R., 2008. At-Surface Reflectance and Albedo from Satellite for Operational Calculation of Land Surface Energy Balance. J. Hydrol. Eng. 13, 51–63. https://doi.org/10.1061/(ASCE)1084-0699(2008)13:2(51)

Traoré, A., Falconnier, G.N., Ba, A., Sissoko, F., Sultan, B., Affholder, F., 2022. Modeling

sorghum-cowpea intercropping for a site in the savannah zone of Mali: Strengths and weaknesses of the Stics model. Field Crops Research 285, 108581. https://doi.org/10.1016/j.fcr.2022.108581

Tribouillois, H., Constantin, J., Justes, E., 2018. Cover crops mitigate direct greenhouse gases balance but reduce drainage under climate change scenarios in temperate climate with dry summers. Global Change Biology 24, 2513–2529. https://doi.org/10.1111/gcb.14091

Urbina-Salazar, D., Vaudour, E., Richer-de-Forges, A.C., Chen, S., Martelet, G., Baghdadi, N., Arrouays, D., 2023. Sentinel-2 and Sentinel-1 Bare Soil Temporal Mosaics of 6-Year Periods for Soil Organic Carbon Content Mapping in Central France. Remote Sensing 15, 2410. https://doi.org/10.3390/rs15092410

Valbuena, D., Erenstein, O., Homann-Kee Tui, S., Abdoulaye, T., Claessens, L., Duncan, A.J., Gérard, B., Rufino, M.C., Teufel, N., Van Rooyen, A., Van Wijk, M.T., 2012. Conservation Agriculture in mixed crop–livestock systems: Scoping crop residue trade-offs in Sub-Saharan Africa and South Asia. Field Crops Research 132, 175–184. https://doi.org/10.1016/j.fcr.2012.02.022

Vaudour, E., Gomez, C., Loiseau, T., Baghdadi, N., Loubet, B., Arrouays, D., Ali, L., Lagacherie, P., 2019. The Impact of Acquisition Date on the Prediction Performance of Topsoil Organic Carbon from Sentinel-2 for Croplands. Remote Sensing 11, 2143. https://doi.org/10.3390/rs11182143

von Haden, A.C., Yang, W.H., DeLucia, E.H., 2020. Soils' dirty little secret: Depth-based comparisons can be inadequate for quantifying changes in soil organic carbon and other mineral soil properties. Global Change Biology 26, 3759–3770. https://doi.org/10.1111/gcb.15124

Wang, H., Wang, S., Yu, Q., Zhang, Y., Wang, R., Li, J., Wang, X., 2020. No tillage increases soil organic carbon storage and decreases carbon dioxide emission in the crop residue-returned farming system. Journal of Environmental Management 261, 110261. https://doi.org/10.1016/j.jenvman.2020.110261

Wang, S., Trishchenko, A.P., Sun, X., 2007. Simulation of canopy radiation transfer and surface albedo in the EALCO model. Clim Dyn 29, 615–632. https://doi.org/10.1007/s00382-

007-0252-y

Wendt, J.W., Hauser, S., 2013. An equivalent soil mass procedure for monitoring soil organic carbon in multiple soil layers. European Journal of Soil Science 64, 58–65. https://doi.org/10.1111/ejss.12002

Wijmer, T., Al Bitar, A., Arnaud, L., Fieuzal, R., Ceschia, E., 2024. AgriCarbon-EO v1.0.1: large-scale and high-resolution simulation of carbon fluxes by assimilation of Sentinel-2 and Landsat-8 reflectances using a Bayesian approach. Geoscientific Model Development 17, 997–1021. https://doi.org/10.5194/gmd-17-997-2024

Wu, X., Vuichard, N., Ciais, P., Viovy, N., de Noblet-Ducoudré, N., Wang, X., Magliulo, V., Wattenbach, M., Vitale, L., Di Tommasi, P., Moors, E.J., Jans, W., Elbers, J., Ceschia, E., Tallec, T., Bernhofer, C., Grünwald, T., Moureaux, C., Manise, T., Ligne, A., Cellier, P., Loubet, B., Larmanou, E., Ripoche, D., 2016. ORCHIDEE-CROP (v0), a new process-based agro-land surface model: model description and evaluation over Europe. Geoscientific Model Development 9, 857–873. https://doi.org/10.5194/gmd-9-857-2016

Yan, G., Hu, R., Luo, J., Weiss, M., Jiang, H., Mu, X., Xie, D., Zhang, W., 2019. Review of indirect optical measurements of leaf area index: Recent advances, challenges, and perspectives. Agricultural and Forest Meteorology 265, 390–411. https://doi.org/10.1016/j.agrformet.2018.11.033

Yang, J., Li, Z., Zhai, P., Zhao, Y., Gao, X., 2020. The influence of soil moisture and solar altitude on surface spectral albedo in arid area. Environ. Res. Lett. 15, 035010. https://doi.org/10.1088/1748-9326/ab6ae2

Yin, X., Leng, G., 2020. Modelling global impacts of climate variability and trend on maize yield during 1980–2010. International Journal of Climatology 41. https://doi.org/10.1002/joc.6792

Zheng, J., Canarini, A., Fujii, K., Mmari, W.N., Kilasara, M.M., Funakawa, S., 2023. Cropland intensification mediates the radiative balance of greenhouse gas emissions and soil carbon sequestration in maize systems of sub-Saharan Africa. Global Change Biology 29, 1514–1529. https://doi.org/10.1111/gcb.16550

Annexes

Annexe 1 : Papier méthodologie

Article publié dans Nature Earth and Environment Reviews (2023) dans la section *trade of the tools*

DOI 10.1038/s43017-023-00432-x

Four-component net radiometers to quantify albedo and heat fluxes in conservation agriculture

To date, the potential of land management for climate change mitigation has primarily been evaluated with a focus on soil organic carbon sequestration or greenhouse gas emissions. However, land management practices can also achieve climate change mitigation through biogeophysical effects, such as changes in the local energy budget owing to modifications in surface albedo (that is, the fraction of incoming sunlight reflected back to space from the surface of the Earth and thus not absorbed and transformed into heat), or changes in evapotranspiration that represents an export of latent heat. To obtain a picture of the biophysical effects of conservation agriculture on climate change mitigation, surface albedo and heat fluxes must be quantified. Four-component net radiometers can be used to monitor incoming and outgoing shortwave (albedo) and longwave (heat flux) radiation. This instrument consists of a pair of pyranometers and a pair of pyrgeometers, with one of each pair facing upwards and the other one facing downwards. A pyranometer measures the ratio of reflected versus incoming shortwave solar radiation (0.3-2.8 µm) to enable the calculation of surface albedo. The pyrgeometer measures longwave radiation (4.5-50 µm), either emitted as infrared radiation or converted as sensible or latent heat flux, and allows the calculation of the amount of thermal energy stored or lost by the surface. Albedo and heat flux measurements can quantify the effect of various conservation agricultural practices on the local energy budget. Preliminary results show that mulching with crop residues on clayey soils can increase albedo, leading to a local cooling effect. However, on light-coloured sandy soils, this approach could have the opposite effect. This result shows that land management approaches can alter the local heat budget, which — depending on the soil type — can either offset or contribute to the climate change mitigation that mulching can achieve by

slightly increasing the carbon stored by the soil. Four-component net radiometers could therefore have an important role in determining the biophysical effects, such as the change in surface albedo, of various conservation agriculture practices for climate change mitigation in specific soil types.

Figure A1 : Dispositif expérimental des radiomètres 4 composantes pour mesurer l'albédo et le rayonnement thermique (CREDIT : Rémi Cardinael ©)

Annexe 2 : Liste des figures

Figure 1. La figure en haut représente la moyenne globale de la concentration atmosphérique des gaz à effets de serres (CO2, CH4, N2O) (https://www.eea.europa.eu/). La figure en bas représente les anomalies de températures moyennes globales depuis 1850 (https://www.ncei.noaa.gov/) 3

Figure 2. Contribution de 1750 à 2023 des principales composantes anthropiques et naturelles (solaire + volcans) au forçage radiatif effectif. Il est important de noter que les valeurs affichées pour chaque variable dans cette figure sont des moyennes globales pouvant masquer des différences très marquées au niveau local. Les effets albédo en moyennes globales sont faibles. Néanmoins, des effets albédo très forts ou ayant les mêmes magnitudes que les GES peuvent être observés localement selon les changements d'occupation et d'utilisation des sols (Forster et al., 2023). 4

Figure 3. Les 3 principes de l'agriculture de conservation (FAO, 2015). 6

Figure 4. Le cadre de gauche montre les processus biogéochimiques impactant le climat qui correspondent aux composantes du bilan carbone et aux émissions de gaz à effet de serre. Dans le cadre de droite les processus biogéophysiques au sein et à l'interface avec les agroécosystèmes qui correspondent aux flux radiatifs de courte et longue longueur d'ondes et aux flux d'énergie non radiatifs avec λE correspondant au flux de chaleur latente, H représente le flux de chaleur sensible, et G au flux de chaleur dans le sol par conduction (adapté de Ceschia et al., 2017). 8

Figure 5. Signatures spectrales de différentes composantes dans le visible, proche infrarouge et dans infrarouge moyen (Begue et al., 2016). 11

Figure 6. Représentativité des sols étudiés en Afrique. Les Lixisols et les Ferralsols sont très représentatifs en Afrique subsaharienne en se référant (Fisher et al., 2008) 20

Figure 7. La figure (A) correspond au site situé à Domboshawa (DTC) et installé sur un sol sableux de type Lixisol, et la figure (B) correspond au site du CIMMYT (UZF) installé sur un sol plus argileux de type xanthic Ferralsol. 21

Figure 8. Protocole de mesure du PAI. 1A est la mesure prise au-dessus du couvert avec A comme "above", 1,2,3,4B avec B comme "below" sont les mesures prises en dessous du couvert. Les lignes discontinues vertes en diagonales représentent les transectes sur lesquelles les mesures ont été prises. 24

Figure 9. Protocole de mesure du taux de couverture. Les carrés verts représentent les photos prises sur les zones cibles pour mesurer le taux de couverture du sol par de la végétation verte avec l'application mobile Canopeo. 24

Figure 10. Radiomètre à 4 composantes. LWin représente le rayonnement grande longueur d'ondes entrant et LWout le rayonnement grande longueur d'onde sortant. SWin correspond au rayonnement courte longueur d'onde incident et SWout le rayonnement courte longueur d'onde réfléchi. Les capteurs mesurant les rayonnements courtes longueurs d'ondes sont les pyranomètres et ceux qui mesurent les rayonnement

grandes longueurs d'ondes sont les pyrgéomètres. 25

Figure 11. A gauche la station météo (METER group) pour mesurer la température de l'air, l'humidité de l'air, la vitesse du vent à 2 m de hauteur et la précipitation. A droite, les sondes pour mesurer en continu la température et l'humidité du sol à 1, 10 et 20 cm de profondeur. 26

Figure 12. Représentation de la relation entre l'albédo de surface et le contenu en sol de la couche superficielle (Beaudoin et al., 2023) 28

Figure I-1. Daily temperatures, shortwave incoming solar radiation and rainfall over two cropping years at the DTC and UZF sites. 36

Figure I-2. (A, C) The dynamics of the top (1 cm depth) soil moisture (SM) divided by 250 to fit at the same y-Axis as the surface albedo (dashed lines) and the surface albedo (solid lines) at UZF (Ferralsol, dark-coloured) and DTC (Lixisol, light-coloured),) for three treatments: conventional tillage (CT, salmon); no-tillage (NT, green); and no-tillage with mulch (NTM, blue) during the 1st (2021/22) and 2nd (2022/23) cropping years in Zimbabwe. (B, D) Plant area index (PAI) dynamics at UZF and DTC, respectively. The error bars represent the standard deviations (N=6). The light blue bars represent daily rainfall. The vertical green dashed lines represent the maize sowing dates, the red dashed lines represent the harvest dates, and the black dashed lines represent the application of mulch after harvest. S: Sowing, H: Harvest, and M: Mulching. The solid vertical dark lines represent the end of the first cropping year and the beginning of the second cropping year. Tillage and mulching in the first cropping year were performed before the start of the measurements. Tillage and the 1st mulch application during the second cropping year were performed at maize sowing. In year 2, mulch was also applied after harvest 46

Figure I-3. Dynamics of the surface albedo as a function of the plant area index (PAI). The solid lines correspond to the maize growing phase with only the green PAI (labelled "GPAI"), and the dashed lines correspond to the senescence phase, during which the leaves have both green and yellow tissues (labelled "GPAI + YPAI" with YPAI standing for yellow PAI). The green colour represents the 2021/22 season, and the light khaki colour represents the 2022/23 season. 49

Figure I-4. Correlations between topsoil moisture (1 cm soil depth) and surface albedo on a xanthic Ferralsol (top, University of Zimbabwe farm (UZF)) and on an abruptic Lixisol (top, Domboshawa training center (DTC)) and for CT: conventional tillage, NT: no-tillage, NT: no-tillage and mulch. The data are shown for the periods between soil preparation for sowing and emergence and after harvest until the next soil preparation of the following cropping season. 51

Figure I-5. Daily instantaneous radiative forcing (iRF) of no-tillage (NT, grey triangles) and no-tillage with mulch (NTM, black triangles) systems compared with conventional tillage (CT) systems. Interpolated dots represent the dynamics of the plant area index (PAI) in the three treatments: CT in salmon, NT in green, and NTM in blue. The green and red vertical dashed lines represent the sowing (S) and harvest (H) dates, respectively. The black dashed line represents the mulch (M) application date. The solid vertical dark line

represents the end of the first cropping year and the beginning of the second cropping year. Tillage and mulching in the first cropping year were completed before the beginning of the measurements. Tillage and the 1st mulch application during the second cropping year were completed at maize sowing. In the 2nd cropping year, mulch was also applied after maize harvest.....53

Figure I-6. Dynamics of outgoing longwave radiation dynamics (LWout) (A and C) between no-tillage (NT) and conventional tillage (CT) (green lines) and between no-tillage with mulch (NTM) and CT (blue lines) at the UZF and DTC sites. Topsoil temperatures (1 cm) during two cropping years (2021/22 and 2022/23) between NT and CT (green lines) and between NTM and CT (blue lines). The green and red dashed lines represent the sowing (S) and harvest (H) dates, respectively. The black dashed line represents the mulch (M) application date. The solid vertical dark line represents the end of the first cropping year and the beginning of the second cropping year. Tillage and mulching in the first cropping year were performed before the beginning of the measurement. Tillage and 1st mulch application during the second cropping year were performed at sowing. Mulch was also applied after harvest. 56

Figure I-S1. Kinetic decomposition of crop residues (mulch) on an abruptic Lixisol (DTC) and on a xanthic Ferralsol (UZF) during the growing season 2022/23. 65

Figure I-S2. PAI and GFCC dynamics during 2021/22 and 2022/23 growing seasons at DTC and UZF sites for CT: Conventional tillage, NT: No-tillage, NTM: No-tillage and mulch. 66

Figure I-S3. Soil temperature difference between NT and NTM compared to CT at 1, 10 and 20 cm depth during 2021/22 and 2022/23 on an abruptic Lixisol (DTC) and on a xanthic Ferralsol (UZF). CT: Conventional tillage, NT: No-tillage, NTM: No-tillage and mulch. The vertical green dashed line is the sowing date and the red dashed line is the harvest date and black dashed line represents the application of mulch after harvest for each cropping year and site. S: Sowing, H: Harvest, M: Mulching. The solid vertical dark line is the end of the first cropping year and the beginning of the second. Tillage and mulching in the first cropping year is done before the beginning of measurement. Tillage and 1st mulch application during the second cropping year is done at sowing. In 2022/23, mulch was also applied after harvest and was present during the fallow period.67

Figure I-S4. Daily soil moisture difference between NT and NTM compared to CT at 1, 10 and 20 cm depth during 2021/22 and 2022/23 on an abruptic Lixisol (DTC) and on a xanthic Ferralsol (UZF). CT: Conventional tillage, NT: No-tillage, NTM: No-tillage and mulch. The vertical green dashed line is the sowing date and the red dashed line is the harvest date and black dashed line represents the application of mulch after harvest for each cropping year and site. S: Sowing, H: Harvest, M: Mulching. The solid vertical dark line is the end of the first cropping year and the beginning of the second. Tillage and mulching in the first cropping year is done before the beginning of measurement. Tillage and 1st mulch application during the second cropping year is done at sowing. In year 2, mulch was also applied after harvest and was present during the fallow period.....68

Figure II-1. Soil organic carbon stocks (0-30 cm) simulated by the ICBM model for no-tillage (NT, green) and no-tillage with mulch (NTM with mulch, blue) relative to the reference conventional tillage (CT, red). Dots represents SOC measured 8 years after the start of the trials.....79

Figure II-2. Change in global mean temperature due to change in SOC stock (red line), N2O emissions (green line) and surface albedo (blue line) under no-tillage (NT on the left) and no-tillage and mulch (NTM, on the right) compared to conventional tillage (CT) on a light-coloured sandy Lixisol (DTC, up) and on a dark-coloured clayey Ferralsol (UZF, bottom). The net climate effect (purple line) includes effects of changes in surface albedo, N2O emissions and SOC sequestration. Dashed lines represent the scenario with temporary mulch cover (scenario 1) and solid lines represent the scenario with permanent mulch cover (scenario 2). 81

Figure II-3. Climate impact due to SOC sequestration, N2O emissions and surface albedo changes expressed as GWP (Mg CO2 eq ha-1 yr-1) considering 20 and 100 years time horizons under no-tillage (NT) and no-tillage with mulch (NT) compared to conventional tillage (CT) on a light-coloured sandy soil Lixisol (DTC) and on a dark-coloured clayey Ferralsol (UZF). Scenario 1 represents temporary mulch cover and scenario 2 represents permanent mulch cover. 83

Figure II-S1. Change in global mean temperature due to change in SOC stock (red line), N2O emissions (green line) and surface albedo (blue line) under no-tillage (NT on the left) and no-tillage and mulch (NTM, on the right) compared to conventional tillage (CT) on a light-coloured sandy Lixisol (DTC, up) and on a dark-coloured clayey Ferralsol (UZF, bottom) over 10. 30. 50 and 100 years of practice of no-tillage (NT) and no-tillage with mulch (NTM). The net climate effect (purple line) includes effects of changes in surface albedo, N2O emissions and SOC sequestration. Dashed lines represent the scenario with temporary mulch cover (scenario 1) and solid lines represent the scenario with permanent mulch cover (scenario 2). 92

Figure III-1. Leaf Area Index (LAI) dynamics observed (red dots) and simulations (black lines) during (A) 2021/22 (B) and 2022/23 cropping years for Conventional tillage (CT), No-tillage (NT) and No-tillage with mulch (NTM) at DTC and UZF sites. 106

Figure III-2. Observations vs STICS simulations of (A) Leaf Area Index (LAI), (B) Total Aboveground Biomass (AGB), and (C) grain yield of maize. at DTC and UZF sites under Conventional-tillage CT (red dots), NT (green dots) and NTM (blue dots) treatments during 2021/22 and 2022/23 cropping years. 107

Figure III-3. Soil water content (SWC) 0-105 cm observation (red dots) and simulations with the current soil evaporation formalism (black lines, Evap1) and with the new soil evaporation formalism (grey lines, Evap2) at DTC (left) and UZF (right) sites. Measurements were done during the 2020/21 cropping year by using neutron probe. 108

Figure III-4. Topsoil moisture (0-1 cm) observation (red lines) and and simulations with the current soil evaporation formalism (black lines, Evap1) and with the new soil evaporation formalism (grey lines, Evap2) at DTC (left) and UZF (right) sites. Measurements were conducted during the (A) 2021/22 and 2022/23 (B) cropping years. 109

Figure III-5. Surface albedo observed (red line) and simulated (dark line) using the current formalism of surface albedo (Albedo 1) by the STICS soil-crop model during the (A, top) 2021/22 and (B, bottom) 2022/23 cropping years at DTC and UZF. CT = conventional tillage, NT = no-tillage and NTM = no-tillage with mulch. S: Sowing,

VP: Vegetative period, BS: Beginning of senescence, SP: Senescence period, FP: Fallow period 110

Figure III-6. Surface albedo observed (red line) and simulated (dark line) using the new formalism of surface albedo (Albedo 2) by the STICS soil-crop model during the (A, top) 2021/22 and (B, bottom) 2022/23 cropping years at DTC and UZF. CT = conventional tillage, NT = no-tillage and NTM = no-tillage with mulch. S: Sowing, VP: Vegetative period, BS: Beginning of senescence, SP: Senescence period, FP: Fallow period 112

Figure III-7. Surface albedo observed (red line) and simulated (dark line) combining the current formalism of surface albedo (Albedo 1) and new formalism of soil evaporation (Evap 2) by the STICS soil-crop model during the (A, top) 2021/22 and (B, bottom) 2022/23 cropping years at DTC and UZF. CT = conventional tillage, NT = no-tillage and NTM = no-tillage with mulch. S: Sowing, VP: Vegetative period, BS: Beginning of senescence, SP: Senescence period, FP: Fallow period 114

Figure III-S1. STICS-soil crop model performances on calibrated variables pooled together : HR_1 = Soil water content (0-1 cm depth), idrps = anthesis, imats = physiological maturity, lai_n = Leaf Area Index (LAI), mafruit = grain yield, masec_n = dry aboveground biomass, resmes = soil water content in the profile (0-105 cm depth). Evap1 is the calibration using the actual formalism of soil evaporation and Evap2 is the calibration using the new soil evaporation formalism. During 2021/22 and 2022/23 cropping years..... 119

Figure III-S2. Crop phenology calibration. Here two stages were calibrated anthesis (circles) and physiological maturity (cones) at DTC (red dots) and UZF (blue dots) expressed as days after planting (DAP). 119

Figure III-S3. Senescence LAI observed (red dots) and simulated (blue lines) dynamics at DTC (top) and UZF (bottom) sites under conventional tillage (CT) no-tillage (NT) and no-tillage with mulch (NTM)..... 120

Annexe 3 : Liste des tables

Table 1 : Description générale des deux sites ; coordonnées, traitements, types et propriétés de sols, moyennes annuelles mesurées sur chaque site. Les abréviations des traitements sont respectivement CT: Conventional tillage, NT : no-tillage, NTM: no-tillage with mulch. 33

Table I-1. Mean surface albedo values during the growing seasons (i.e. from maize emergence to harvest); the fallow periods (i.e. the dry seasons, when the soil is bare or covered by only crop residues) and the cropping years (i.e. the whole period from October to the following October, including both the growing and bare fallow periods). 56

Table I-2. Maximum PAI (± standard deviation, N=6) and green fractional canopy cover (± standard deviation, N = 4) during 2 successive cropping years at the Domboshawa training center (DTC) and University of Zimbabwe farm (UZF). CT: Conventional tillage, NT: No-tillage, NTM: No-tillage and mulch. 59

Table I-S1. Gap filling equations for albedo based on the relationship between bare soil surface albedo and soil moisture. 75

Table I-S2. Mean (±standard deviation N = 5) surface albedo of dry soil 5 days before and after key land management activities on an abruptic lixisol and a xanthic Ferralsol. CT: Conventional tillage, NT: No-tillage, NT: No-tillage and mulch. In 2022/23, mulch was also applied after harvest and was present during the fallow period. *Corresponds to albedo values measured under wet conditions. 76

Table II-S1. Parametrization of ICBM carbon model 100

Table II-S2. Surface albedo difference of No-tillage (NT) and No-tillage with mulch (NTM) relative to Conventional-tillage (CT). 100

Table II-S3. Climate impact including albedo change using ΔT(K ha-1). 101

Table II-S4. Climate impact including albedo change using GWP express in Mg CO2 ha-1 yr-1. 102

Table III-1. Model performances of surface albedo simulated during senescence phase using the current (Evap 1) and the new (Evap 2) formalism of soil evaporation combined to the actual (Albedo 1) and the new (Albedo 2) formalism of surface albedo under Conventional tillage (CT), No-tillage (NT) and No-tillage with mulch (NTM) at DTC and UZF sites. 122

Table III-2. Model performances of surface albedo simulated over the two cropping years (2021/22 and 2022/23) using the current (Evap 1) and the new (Evap 2) formalism of soil evaporation combined to the actual (Albedo 1) and the new (Albedo 2) formalism of surface albedo under Conventional tillage (CT), No-tillage (NT) and No-tillage with mulch (NTM) at DTC and UZF sites. 124

Table III-S1. Soil parameters defined in the STICS crop model for experiments on an Abruptic Lixisol (DTC) and on a Xanthic Ferralsol (UZF) in Zimbabwe subhumid.* represents new parameters of the new soil evaporation module 131